Doctoral Dissertation

Development of coelenterazine derivatives for monitoring of biological phenomena

Eric Jorgen Lindberg

October 2013

Laboratory of Chemical Biology

Division of Advanced Science and Biotechnology

Department of Material and Life Science

Graduate School of Engineering,

Osaka University

Contents

General Introduction

Molecular imaging allows for the visualization and quantification of biological processes at the cellular and subcellular levels within intact living organisms. This biomedical research discipline is gaining great interest to address frontier issues related to pathology and physiology.[1] Several common imaging techniques have been developed for such applications including: computer tomography (CT), magnetic resonance imaging (MRI), positron emission tomography (PET), single photon emission computer tomography (SPECT), ultrasound, photoacoustic imaging, and novel optical small animal imaging techniques such as fluorescence imaging (FLI) and , bioluminescence imaging (BLI).[2] The main area of utility of bioluminescence used to be in *in vitro* gene-reporter assay measurements, however significant leaps in the development of more sensitive CCD-camera technology has diversified the use of BLI in the life sciences. The use of bioluminescence imaging and analysis have some distinctive advantages such as low background, high signal-to-noise (S/N) ratio profiles, generally wider range of signals, flexible in the molecular design, allows for extended period of measurement, and also highly suitable for imaging of small animal models.[3,4] The relative sensitivity will depend on the emission wavelength of the light emitted and also the sensitivity of the camera system. Examples of applications of BLI include: monitoring of protein-protein interactions[5], *in vivo* and *in vitro* drug screening[6], sensing bioactive small molecules[7], assessing protein stability and function[8], *in vivo* imaging of animal models[9], imaging of organs[10] , imaging of disease progression such as cancer and their metastasis[11], and 3D BLI of cerebral ischemia[12] to name a few.

Bioluminescence is the product of certain photoproteins (luciferases) which catalyze oxidation of small molecular substrates (luciferins), which results in the generation of light in the form of bioluminescence. Bioluminescent species can be found across many phyla such as insects, marine organisms, and prokaryotes. Although a number of luciferase-luciferin pairs have been discovered in nature, only a selected few have been sufficiently characterized for use as tools in chemical biology (Table 1.). The bioluminescence system based on firefly and beetle luciferases together with D-luciferin has been the most reported system. Especially in studies involving *in vivo* imaging because of the emission spectra of firefly and beetle luciferases (~560-610 nm)[13]. The D-luciferin is relatively stable and can diffuse between tissues. The reaction between D-luciferin and its luciferases requires ATP and magnesium ions, which limits its use to intracellular monitoring. The other commonly used luciferases all utilize various luciferin substrates which all share a imidazopyrazinone core structure (Table 1). Unlike

Table 1. Characteristics of luciferase-luciferin pairs commonly used in BLI
Adapted from (19) and (20).

Luciferase	Luciferin (substrate)	Peak emission (nm)	Size (kDa)	Comments	Reference
North American firefly (FLuc)	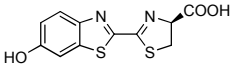 **D-Luciferin**	565	61	Requires ATP and Mg^{2+} Codon optimized	13
Renilla reniformis (native RLuc)	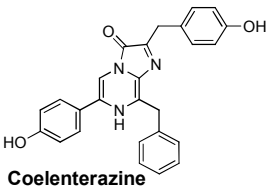 **Coelenterazine**	480	36	Can be used in extracellular environments, codon-optimized	14
Gaussia princeps (GLuc)		480	20	Naturally secreted enzyme cell-anchored versions available	15
Gaussia princeps (Monsta)		503	20	Mutant enzyme with red-shifted emission spectrum	16
Oplophorus gracilirostris (NanoLuc)	 **Furimazine**	460	20	Stabile mutant enzyme with increased light output	17
Cypridina noctiluca (CLuc)	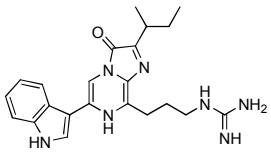 ***Cypridina* luciferin**	465	62	Naturally secreted enzyme	18

D-luciferin, these luciferases do not require any other co-factor other than molecular oxygen, which allows for extracellular as well as intracellular applications. The general emission spectrum with imidazopyrazinone compounds range from ~460-480 nm, limiting their use in *in vivo* imaging due to poor penetration. However, red-shifted mutants have been developed[16, 21], and also it is possible to obtain a red-shifted emission by utilizing bioluminescence resonance energy transfer (BRET).[22] In addition coelenterate luciferases such as *Gaussia* luciferase (GLuc) has been shown to have over 1000-fold stronger signal output over firefly luciferase (FLuc)[15a], whilst the recent NanoLuc has been shown to have 100-fold stronger signal than FLuc. As each substrate is quite specific for its respective luciferase enzyme it has been possible to monitor multiple parameters by utilizing a combination of up to 3 luciferases in *in vitro* and *in vivo* monitoring of cellular processes.[23]

Derivatization and functionalization of luciferin substrates

The three most common types of derivatization studies of D-luciferin substrates have been focused on: 1) increasing the luminescence output; 2) red-shifted emission

spectrum, and 3) activatable-luciferins. Several improved and red-shifted analogues of D-luciferin and aminoluciferin have been reported. [24] In addition, red-shifted aminoluciferin-BRET acceptor conjugates have also been reported. [25] Several D-luciferin derivatives for the specific monitoring of enzyme and bioactive small molecules have been reported (Figure 1.)[26] For coelenterate luciferin substrates, most studies have focused on modification of coelenterazine to obtain an improved luminescence output.[27]In most cases any modification of coelenterazine will result in a significant decrease in bioluminescence output. However, in two instances an improvement in signal output was observed[17, 27a]. Unlike the D-luciferin substrates, modification of coelenterazine greatly affects its stability, thus in addition to retaining the luminescence output; the overall stability of the molecule also has to be taken into account.[27c] Therefore it is not surprising that D-luciferin has been favored due to the high substrate specificity of coelenterate luciferases together with its stability issues.

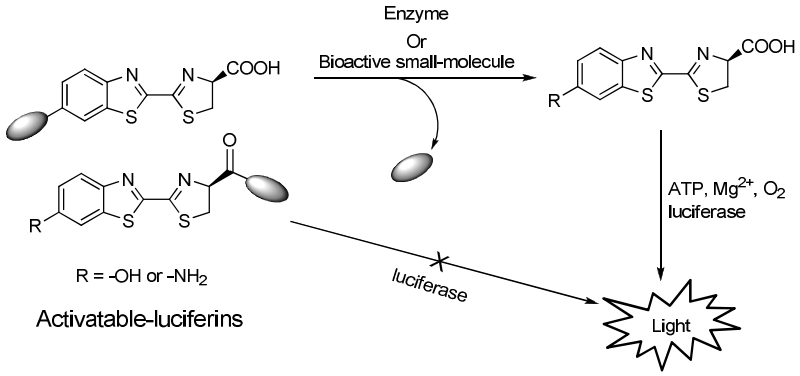

Figure 1. Concept behind activatable-luciferins. Adopted from (26).

Purpose of research

The work presented herein is based around the synthetic modification of coelenterazine together with the use of *Gaussia* luciferase, due to its much higher luminescence output over other luciferases such as that of *Renilla reniformis*. The immediate difficulty however is related to the ability to predict the impact on luminescence output based on the position of modification on coelenterazine. There are several reasons for this: i) high substrate specificity of GLuc[27c]; ii) little to no homology with other coelenterate luciferases; iii) no existing x-ray crystal structure of GLuc; and iv) probably cooperativity between proposed two catalytic sites GLuc.[28] As this dissertation is divided into two major chapters the detailed research aim of each respective differ in the type of modification of coelenterazine. In chapter 1 the major concern is loss in luminescence output, whilst in chapter 2 the focus is more on stability.

References

1. Massoud, T. F.; Gambhir, S. S. *Gene* **2003**, *17*, 545-580.
2. Weissleder, R.; Pittet, M. J. *Nature* **2008**, *452*, 580-589.
3. Ozawa, T.; Yoshimura, H.; Kim, S. B. *Anal. Chem.* **2013**, *85*, 590-609.
4. Keyaerts, M.; Caveliers, V.; Lahoutte, T. *Trends Mol. Med.* **2012**, *18*, 164-172.
5. Ozawa, T.; Kaihara, A.; Sato, M.; Tachihara, K.; Umezawa, Y. *Anal. Chem.* **2001**, *73*, 2516-2521.
6. (a) Kelkar, M.; De, A. *Curr. Opin. Pharmacol.* **2012**, *12*, 592-600. (b) Bacart, J.; Corbel, C.; Jockers, R.; Bach, S.; Couturier, C. *Biotechnol. J.* **2008**, *3*, 311-324.
7. Paulmurugan, R.; Gambhir, S. S. *Proc. Natl. Acad. Sci. U.S.A.* **2006**, *103*, 15883-15888.
8. Banaszynski, L. A.; Sellmyer, M. A.; Contag, C. H.; Wandless, T. J.; Thorne, S. H. *Nat. Med.* **2008**, *14*, 1123-1127.
9. Dothager, R. S.; Flentie, K.; Moss, B.; Pan, M-H.; Kesarwala, A.; Piwnica-Worms, D. *Curr. Opin. Biotechnol.* **2009**, *20*, 45-53.
10. (a) de Heredia, L. L.; Gengatharan, A.; Foster, J.; Mather, S.; Magoulas, C. *Neurosci. Lett.* **2011**, *497*, 134-138. (b) Ozaki, M.; Haga, S.; Ozawa, T. *Theranostics* **2012**, *2*, 207-214. (c) Hong, H,; Zhang, Y.; Severin, G. W.; Yang, Y. N.; Engle, J. W.; Niu, G.; Nickles, R. J.; Chen, X. Y.; Leigh, B. R.; Barnhart, T. E.; Cai, W. B. *Mol. Pharmaceut.* **2012**, *9*, 2339-2349.
11. (a) Xie, X.; Xia, W.; Li, Z.; Kuo, H. P.; Liu, Y.; Li, Z.; Ding, Q.; Zhang, S.; Spohn, B.; Yang, Y.; Wei, Y.; Lang, J. Y.; Evans, D. B.; Chiao, P. J.; Abbruzzese, J. L.; Hung, M. C. *Cancer Cell* **2007**, *12*, 52-65. (b) Chi, X.; Huang, D.; Zhao, Z.; Zhou, Z.; Yin, Z.; Gao, J. *Biomaterials* **2012**, *33*, 189-206.
12. Cordeau, P.; Kriz, J. *Methods in Enzymology* **2012**, *506*, 117-131.
13. (a) Zhao, H.; Doyle, T. C.; Coquoz, O.; Kalish, F.; Rice, B. W.; Contag, C. H. *J. Biomed. Opt.* **2002**, *10*, 41210. (b) Miloud, T.; Henrich, C.; Hammerling, G. *J. Biomed. Opt.* **2007**, *12*, 054018.
14. Bhaumik, S.; Gambhir, S. S.; *Proc. Natl. Acad. Sci. U.S.A.* **2002**, *99*, 377-382.
15. (a) Tannous, B. A.; Kim, D. E.; Fernandez, J. L.; Weissleder, R.; Breakefield, X. O. *Mol. Ther.* **2005**, *11*, 435-443. (b) Santos, E. B.; Yeh, R.; Lee, J.; Nikhamin, Y.; Punzalan, B.; Punzalan, B.; La Perle, K.; Larson, S. M.; Sadelain, M.; Brentjens, R. J. *Nat. Med.* **2009**, *15*, 338-344.
16. Kim, S. B.; Suzuki, H.; Sato, M.; Tao, H. *Anal. Chem.* **2011**, *83*, 8732-8740.
17. M. P. Hall, J. Unch, B. F. Binkowski, M. P. Valley, B. L. Butler, M.G. Wood, P.

Otto, K. Zimmerman, G. Vidugiris, T. Machleidt, M. B. Robers, H. A. Benink, C. T. Eggers, M. R. Slater, P. L. Meisenheimer, D. H. Klaubert, F. Fan, L. P. Encell, K. V. Wood, *ACS Chem. Biol.* **2012**, *7*, 1848-1857.

18. Nakajima, Y.; Kobayashi, K.; Yamagishi, K.; Enomoto, T.; Ohmiya, Y. *Biosci. Biotechnol. Biochem.* **2004**, *68*, 565-570
19. Prescher, J. A.; Contag, C. H. *Curr. Opin. Chem. Biol.* **2010**, *14*, 80-89.
20. Luker, K. E.; Luker, G. D. *Antiviral Res.* **2008**, *78*, 179-187.
21. Loening, A. M.; Wu, A. M.; Gambhir, S. S. *Nat. Methods.* **2007**, *4*, 641-643.
22. Xia, Z.; Rao, J. *Curr. Opin. Biotechnol.* **2009**, *20*, 37-44.
23. (a) Maguire, C. A.; Bovenberg, M. S.; Crommentuijn, M. H. W.; Niers, J. M.; Kerami, M.; Teng, J.; Sena-Esteves, M.; Badr, C. E.; Tannous, B. A. *Mol. Ther. Nucleic Acids* **2013**, *2*, e99. (b) Heise, K.; Oppermann, H.; Meixensberger, J.; Gebhardt, R.; Gaunitz, F. *Assay and Drug Development Technologies* **2013**, *11*, 244-252.
24. (a) Takaura, H.; Sasakura, K.; Ueno, T.; Urano, Y.; Terai, T.; Hanaoka, K.; Tsuboi, T.; Nagano, T. *Chem. Asian J.* **2010**, *5*, 2053-2061. (b) Conley, N. R.; Dragulescu-Andrasi, A.; Rao, J.; Moerner, W. E. *Angew. Chem. Int. Ed. 51*, 3350-3353.
25. (a) Takaura, H.; Kojima, R.; Urano, Y.; Terai, T.; Hanaoka, K.; Nagano, T. *Chem. Asian J.* **2011**, *6*, 1800-1810. (b) Kojima, R.; Takakura, H.; Ozawa, T.; Tada, Y.; Nagano, T.; Urano, Y. *Angew. Chem. Int. Ed.* **2012**, *51*, 1-6.
26. Li, J.; Chen, L.; Du, L.; Li, M. *Chem. Soc. Rev.* **2013**, *42*, 662-676.
27. (a) Inouye, S.; Shimomura, O. *Biochem. Biophys. Res. Commun.* **1997**, *233*, 349-353. (b)Wu, C.; Nakamura, H.; Murai, A.; Shimomura, O. *Tet. Lett.* **2001**, *42*, 2997-3000. (c) Inouye, S.; Sahara-Miura, Y.; Sato, J-I.; Iimori, R.; Yoshida, S.; Hosoya, T. **2013**, *88*, 150-156.
28. Tzertzinis, G.; Schildkraut, E.; Schildkraut, I. *PLoS ONE* **2012**, *7*, e40099.

Chapter 1 Development of Cell-Impermeable Coelenterazine Derivatives

Gaussia luciferase (GLuc) is the brightest among all reported luciferases and displays a flash-type luminescence profile.[1] These lucifereases have mostly been used as a reporter to monitor dynamic changes in gene expression and transcription.[2] Monitoring of single exocytotic events in living cells has mostly employed methods such as total internal reflection fluorescence (TIRF), and two-photon laser scanning microscopy.[3-6] However, these methods are confined to monitoring a limited section of the cells and the use of fluorogenic dyes for accurate localization can be difficult due to diffusion. In addition, fluorescence methods require continuous irradiation, causing cell damage and photobleaching. Moreover due to their temporal resolution properties, confocal and twophoton laser scanning microscopies are more suitable when monitoring membrane fusion of vesicles with slower kinetics.[7]

BLI can offer distinct advantages over fluorescence imaging in monitoring of protein secretion and other exocytotic events in living cells. Visualization of luciferase secretion in living mammalian cells was first realized with *Cypridina* luciferase (CLuc) in CHO cells,[8] and in live mouse embryos to monitor transcriptional activation of genes.[9] CLuc was also utilized for imaging of neurotransmitter release.[10] Recently secretion of the brighter GLuc in PC12D cells was monitored in real-time.[11] However, in general BLI has suffered from poor resolution due to low luminescence intensity. Using an electron multiplying charge coupled device (EM-CCD) camera, video-rate BLI was employed in the studying of secretory dynamics of MMP-2 with GLuc at much improved resolutions.[12] In another study, the same group also demonstrated that video-rate BLI could be used for quantitative analysis of insulin oscillations in pancreatic MIN6 β cells, which could have potential drugscreening applications.[13]

Recently, in an effort to monitor exocytosis in synaptic boutons via BLI, a mutant GLuc with enhanced luminescence output was fused to the part of a vesicle-associated membrane protein (VAMP) located within the interior of the synaptic vesicle (unpublished data). Hence, when the vesicle fuses with the cell membrane undergoing exocytosis the luciferase would react with its substrate coelenterazine, generating a bioluminescent response. However, a very poor signal-to-noise was observed which was attributed to the high cell-membrane permeability of coelenterazine, *i.e.* coelenterazine could diffuse across the synaptic and vesicle membranes and react with the luciferase before the exocytotic event, giving rise to high background luminescence

(Figure 1a). Miesenbock *et al.* also observed a similar issue with *Cypridina* luciferin when imaging patterns of synaptic activity in hippocampal neuronal cells.[10] Therefore a modified coelenterazine substrate with decreased cell-membrane permeability is desired (Figure 1b–1c). However modifying the bioluminogenic substrate without having a negative impact on the bioluminescence activity is very difficult. This is especially true in the case of GLuc, which has very high substrate specificity. Hence, even the smallest modification of the coelenterazine substrate will result in a significant drop in bioluminescence activity.[14-16] Therefore it is not surprising that only one coelenterazine derivative (s-CTZ) with improved bioluminescence activity with GLuc has been reported.[17] The compound structure has yet to be published, however, the published data strongly implies that s-CTZ is highly cell-permeable. Hence we sought to design and synthesize a cell-membrane impermeable coelenterazine derivative with retained bioluminescence activity.

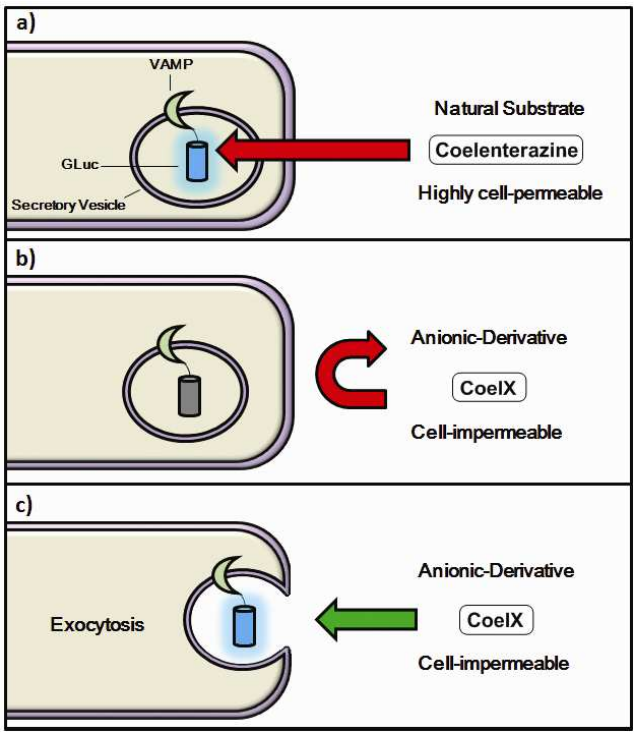

Figure 1. Monitoring membrane fusion events via BLI; Concept (a) coelenterazine readily penetrates the cell-membrane, giving rise to background noise prior to fusion taking place; (b) coelenterazine derivative CoelX has a negative charge, making it highly cell-impermeable and unable to react with GLuc; (c) following fusion of the secretory vesicle with the cell-membrane CoelX can react with GLuc, generating a bioluminescence signal.

Results and Discussion: Design and Synthesis of 2-BnO-TEG-CTZ and 6-BnOTEG-CTZ

When conceiving of a proper rational substrate design strategy, it is very useful to perform docking simulations of substrate derivatives before undertaking actual experimental work. Urano *et al.* constructed near-infrared-emitting firefly luciferins by initially performing docking simulations with luciferase from *Photinus pyralis*.[18] However, as there is no existing x-ray crystal structure of *Gaussia* luciferase (GLuc), lack of homology with other coelenterate luciferases, for which crystal-structures are available, rational design and modification of coelenterazine remains a difficult task in terms of being able to predict the effect of any modification of the coelenterazine substrate on bioluminescence activity. Modification of the coelenterazine substrate has mostly been focused on increasing light output, redshifting the emission spectrum of coelenterazine and increasing the stability of coelenterazine to decrease autoluminescence background noise. [19-24] As mentioned above coelenterate luciferases share very little homology and hence any modification of coelenterazine, that might have an advantageous impact on the luminesence output of one luciferase, might have the reverse effect on another. This is especially true for GLuc which has been shown to have an extremely narrow substrate specificity.[14-16] In order to construct a cell-impermeable derivative of coelenterazine, we decided to attach a flexible linker with a terminal anionic phosphonate group. Initially we synthesized two coelenterazine derivatives with a highly flexible polyethylene glycol (PEG) linker with terminal benzyl-protecting groups installed at the 2 and 6 positions of coelenterazine (Scheme 1) to investigate the effect on bioluminescence activity of GLuc. We prepared **11** from

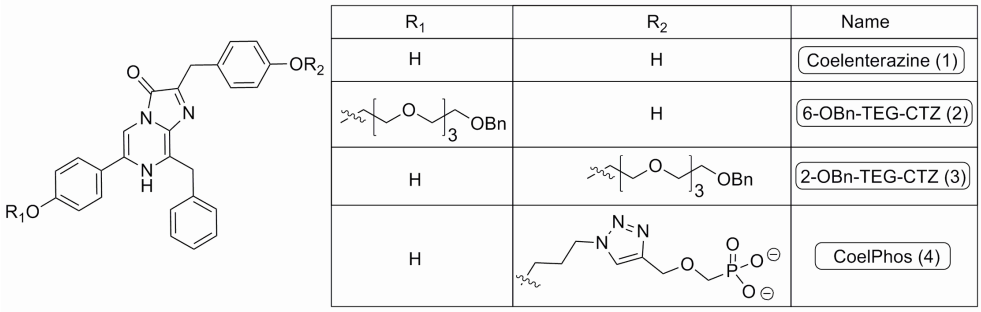

Figure 2. Structures of native coelenterazine and synthesized derivatives.

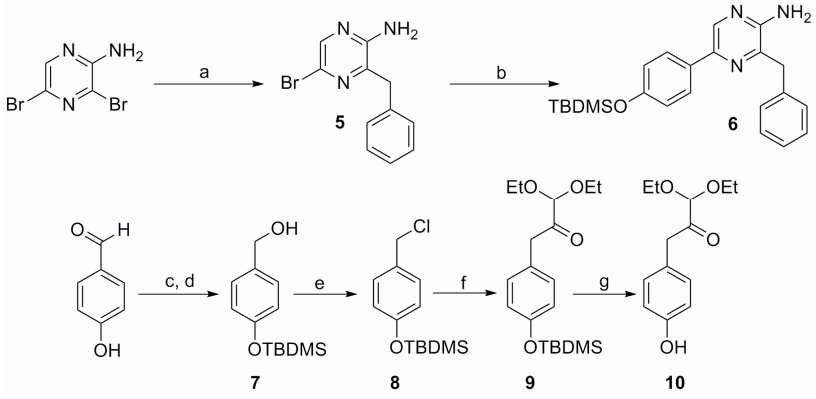

Scheme 1. (a) $PhCH_2MgCl$, $ZnCl_2$, $Pd(PPh_3)_2Cl_2$, THF, rt, 72 h, 83%; (b) 4-(TBDMS-O)Ph-$B(OH)_2$, bddp, $(C_6H_5CN)_2PdCl_2$, Na_2CO_3 (1M (aq)), EtOH, Toluene, reflux, 24 h, 83%; (c) TBDMSCl, imidazole, DMF, rt, 12 h; (d) $NaBH_4$, MeOH, 0 °C, 2 h, 86% over 2 steps; (e) $SOCl_2$, CH_2Cl_2, 0°, 2 h, 81%; (f) Mg, $EtBr_2$, THF, sonication; ethyl diethoxyacetate, THF, -78°C, 6 h, 47%; (g) Bu_4NF, THF, 0 °C, 30 min, 93%.

tetraethylene glycol (TEG) by mono-benzylation with benzyl bromide, followed by were synthesized as previously described (Scheme S1).[25-26] **13** was synthesized via bromination to **12** via the Apple reaction (Scheme S2). Synthetic intermediates **6** and **10** standard alkylation of coelenteramine **6** with **12**. Following acid-catalyzed condensation reaction of **13** and the α-ketoacetal **9** under reflux the desired compound 6-BnO-TEG-CTZ (**2**) was synthesized (Figure 2). Synthesis of 2-BnO-TEG-CTZ (**3**) was accomplished by initial alkylation of deprotected α-ketoacetal **10** with the TEG linker **12** to give **14**. Acid-catalyzed condensation reaction between **6** and **14** under reflux generated the desired product, 2-BnO-TEG-CTZ (**3**).

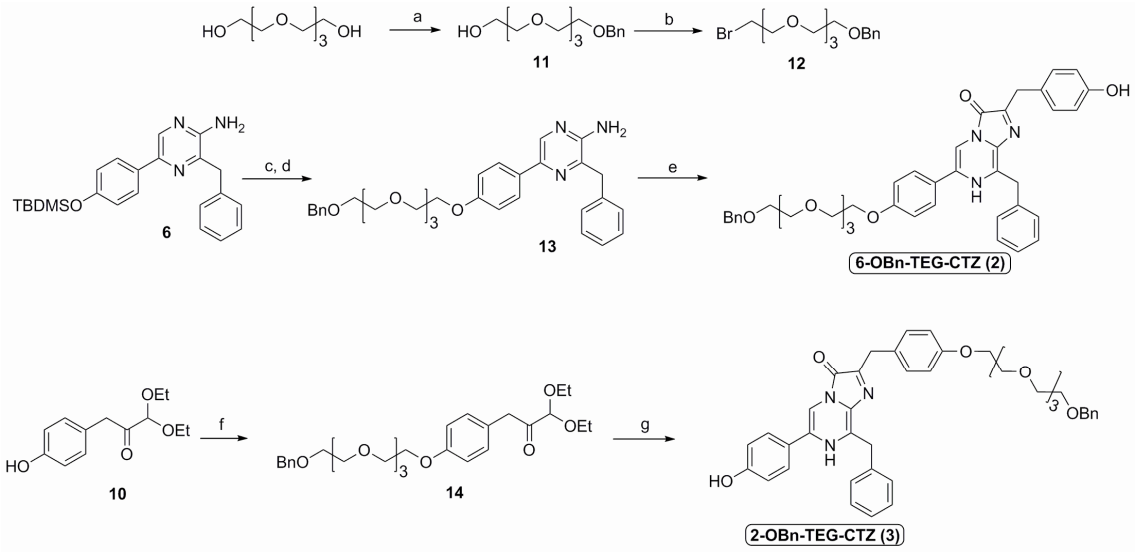

Scheme 2. Synthesis of 6-OBn-TEG-CTZ and 2-OBn-TEG-CTZ. (a) NaH, BnBr, THF/DMF, 0 °C to rt. 5 h, 67%; (b) PPh_3, CBr_4, CH_2Cl_2, reflux, 12 h, 91%; (c) Bu_4NF, THF, 0 °C, 2 h; (d) **12,** NaH, DMF, 0 °C, 5 h, 55% over 2 steps, (e) **9**, 1,4-dioxane / 6N HCl (10:1), 24 h, 49%; f) **12**, Cs_2CO_3, MeCN, reflux, 3 h, 73%; (g) **6**, 1,4-dioxane / 6N HCl (10:1), reflux, 14 h, 17%

Next the luminescent properties of 2- and 6-BnO-TEG-CTZ were evaluated with GLuc in comparison with native coelenterazine. Both substrates 2-BnO-TEG-CTZ and 6-BnOTEG-CTZ showed more than 200- and 950-fold reduction in total bioluminescence activity, respectively (Table 1). Interestingly, Urano *et al.* observed similarly poor bioluminescence activity when attaching flexible PEG linkers to aminoluciferin.[18] Installing rigid alkyl linkers also resulted in a low bioluminescence output. The poor observed activity was attributed to that these linkers may be linear and adopt conformations that hinder access of the luciferin substrate to the active site of the luciferase enzyme. Hence, it was concluded that long PEG linkers conjugated near the luminophore are unsuitable. This conclusion also seems to be valid in the case of installing PEG linkers on coelenterazine as well.

Table 1. Relative and maximum luminescence of 2- and 6-BnO-TEG-CTZ, and CoelPhos.

Compound	*Gaussia* luciferase	
	I_{Total} (%)[a]	I_{Max} (%)[b]
Coelenterazine (**1**)	100	100
2-BnO-TEG-CTZ (**2**)	0.45	0.17
6-BnO-TEG-CTZ (**3**)	0.10	0.14
CoelPhos (**4**)	3.23	2.70

[a] I_{Total}: total luminescence integrating for 60 s in 1 s intervals.

[b] I_{Max}: maximum observed intensity at any 1 s interval.

Design and Synthesis of CoelPhos

Due to detrimental effect on bioluminescence activity of PEGmodified coelenterazines we decided to change to more rigid alkyl linkers. Although our initial results suggested that both 2- and 6-positions of coelenterazine were both sensitive to modification, we decided to focus on modification of the 2- position of coelenterazine. We synthesized a phosphonate alkyne, dimethyl(prop-2-ynyloxy)methylphospho-nate **16** in two steps (Scheme S3). Alkylation of **10** with 1,3-dibromopropane resulted in formation of **17**, which was converted into the propyl azide **18**. Copper(I)-catalyzed azide-alkyne Huisgen cycloaddition[26] gave the desired 1,2,3-triazole **19**. In the final step acid-catalyzed condensation reaction of **6** and **19** was conducted, generating the desired product CoelPhos (Figure 2) (See supporting information for further description and details). Next, we evaluated the luminescent properties of CoelPhos with GLuc (Table 1) and *Renilla* luciferase (RLuc) comparison with coelenterazine (Table 2). CoelPhos yielded a much stronger luminescence with GLuc than RLuc and also a significant improvement in bioluminescence activity compared with both 2- and 6-BnO-TEG-CTZ, although CoelPhos still showed about a 30-fold reduction in luminescence intensity in comparison with coelenterazine. With the exception of s-CTZ,[17] the highest reported bioluminescence activity of any coelenterazine derivative with GLuc was that of *MeO*-CTZ (methylation of the 2-hydroxy group) (13.6%) and *3iso*-CTZ (replacement of 2-hydroxy group with 3-isopropylbenzene), (14.3%).[16]

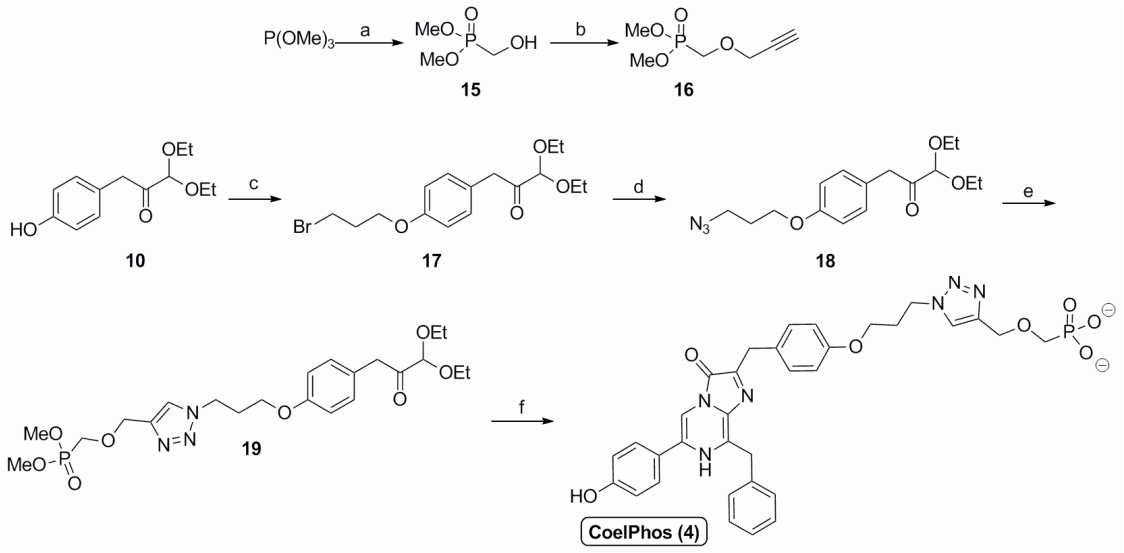

Scheme 3. Synthesis of CoelPhos. (a) paraformaldehyde, TEA, 130 °C, 3 h. 12%; (b) propargyl bromide, NaH, THF, -70 °C. 35%; (c) 1,3-dibromopropane, Cs_2CO_3, MeCN, reflux, 3 h. 35%; (d) NaN_3, DMF, 50 °C, 12 h, 76%; (e) **16**, $CuSO_4$, Sodium Ascorbate, H_2O/CH_2Cl_2(1:1), rt, 12 h, 88%; (f) **6**, 1,4-dioxane/6N HCl (10:1), 110 °C, 5-6 h, 9%.

Table 2. Relative and maximum luminescence of CoelPhos with *Renilla* luciferase cell lysate.

Compound	*Renilla* luciferase	
	I_{Total} (%)[a]	I_{Max} (%)[b]
Coelenterazine	100	100
CoelPhos	0.14	0.09

[a] I_{Total}: total luminescence integrating for 20 s in 1 s intervals.

[b] I_{Max}: maximum observed intensity at any 1 s interval.

2.3 Bioluminescence Imaging with CoelPhos

Recently GLuc mutants with improved luminescence output and stable luminescence profiles have been reported.[28,29] We utilized a recently developed mutant GLuc (GLucM23) with roughly 10-fold improvement in luminescence intensity in living cells, and a glow-type kinetic profile (Figure). We evaluated CoelPhos by measuring bioluminescence activity with a charge-coupled device (CCD) camera in

HeLa cells expressing outer-membrane localized wild-type GLuc or GLucM23 ($GLucM23_{Mem}$) to determine if the improved mutant GLuc had a negative or positive impact on the luminescence intensity of CoelPhos (Figure 3). We determined the relative intensities of coelenterazine and CoelPhos by comparing the relative mKO fluorescence and luminescence intensities of 5 cells (Figure 4). CoelPhos showed similar relative bioluminescence activity with the mutant GLucM23 in comparison with the wild-type GLuc relative to coelenterazine (~ 3–4 %). Hence the GLuc mutant did not affect the bioluminescence activity of CoelPhos relative to coelenterazine. The contrast observed in HeLa cells expressing outer membrane bound GLuc was very poor in comparison with GLucM23. This is related to the flash-type luminescence of GLuc, together with the luminescence sensitivity of our imaging system. The stable glow-type luminescence of GLucM23 and its higher luminescence output makes it more suitable for BLI in living cells. This was especially true for our derivative CoelPhos which could

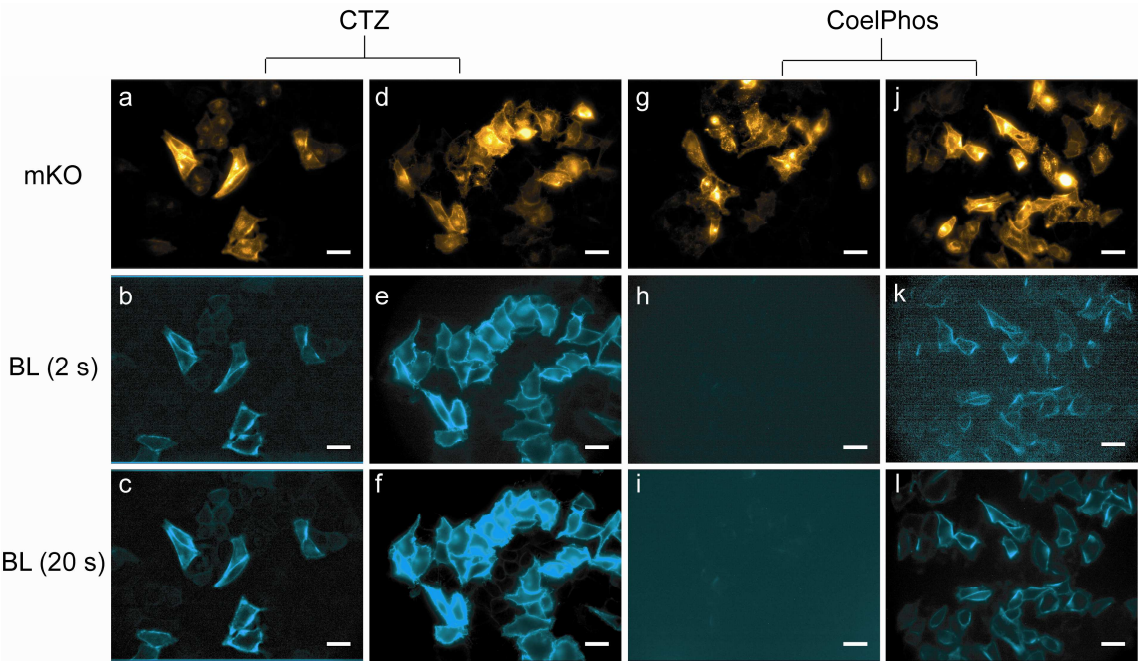

Figure 3. Bioluminescence imaging with coelenterazine (CTZ) and CoelPhos in HeLa cells expressing outer-membrane bound GLuc or GLucM23. (a, d, g, j) Fluorescence images of mKO (λ_{ex} = 548 nm / λ_{em} = 559 nm; 200 ms) before addition of bioluminogenic substrate. CTZ with $GLuc_{Mem}$, exposure time: 2 s (b) and 20 s (c); CTZ with $GLucM23_{MeM}$, exposure time: 2 s (e) and 20 s (f); CoelPhos with $GLuc_{Mem}$, exposure time: 2 s; (h), 20 s (i) CoelPhos with $GLucM23_{Mem}$, exposure time: 2 s (k) and 20 s (l). Concentration of CTZ and CoelPhos: 22.7 μM. Objective lens: 60×. Scale bar: 40 μm.

be imaged with much improved signal-to-noise with GLucM23Mem (Figure 3k, 3l) over $GLuc_{Mem}$ (Figure 3h, 3i).

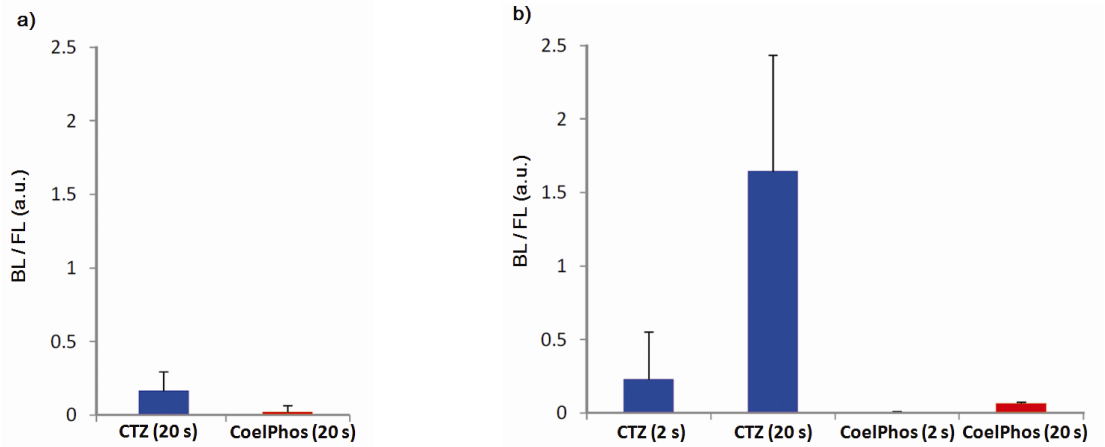

Figure 4. Relative activity of CoelPhos with GLuc and GLucM23 versus Coelenterazine (CTZ) in HeLa cells. (a) CTZ and CoelPhos with GLuc; (b) CTZ and CoelPhos with GLucM23. (n = 5 cells); Signal was quantified using ImageJ. (2 or 20 s) = exposure time.

Finally, we evaluated the relative cell-membrane permeability of our probe CoelPhos in comparison with coelenterazine. We transfected HeLa cells with an endoplasmic reticulum (ER)-localizing GLuc construct ($GLuc_{ER}$). The construct also contained Venus fluorescent protein as a control for expression levels as well as confirmation of localization. We reasoned that whilst coelenterazine would give a strong signal due to its high cell-permeability, CoelPhos would not give any bioluminescence signal due to its inability to cross the cell membrane (Figure 5).

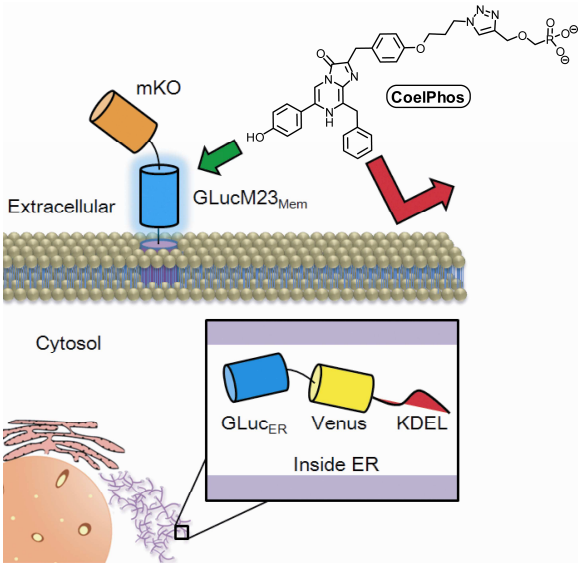

Figure 5. Illustration of cell-permeability of CoelPhos. Because of the attached anionic phosphonate CoelPhos does not penetrate the cell-membrane as readily as native coelenterazine. Therefore a bioluminescent signal will be observed with outer-membrane bound $GLucM23_{Mem}$ but not with intracellularly localized $GLuc_{ER}$.

When coelenterazine was added, strong bioluminescent signals were observed in HeLa cells expressing $GLuc_{ER}$. On the other hand, when CoelPhos was added, no signal could be detected, even after extending the exposure time to 100 s (20-fold) (Figure 6).

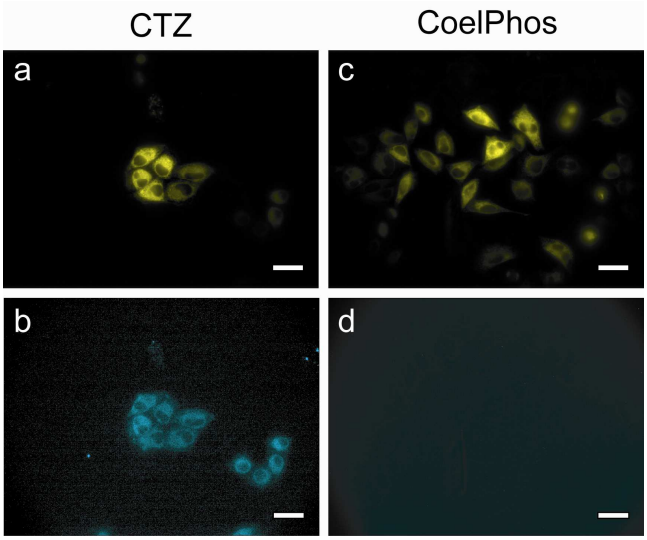

Figure 6. Fluorescence and bioluminescence images of HeLa cells expressing $GLuc_{ER}$ with coelenterazine (CTZ) and CoelPhos. (a) Venus FL; (b) CTZ (22.7 μM); exposure time: 5 s; (c) Venus FL; (d) CoelPhos (22.7 μM); exposure time: 100 s. Objective lens: 60 ×. Scale bar: 40 μm.

The observed data seem to suggest that attachment of a terminal phosphonate moiety is enough to significantly decrease cell-membrane permeability of the coelenterate substrate. It has been shown that GLuc produces 1000-fold higher BL signal than RLuc or FLuc in mammalian cells.1,30 GLucM23 has roughly 10 times higher BL intensity over wild-type GLuc in mammalian cells, suggesting that this novel mutant GLuc could have 10000-fold higher BL signal over RLuc and FLuc in mammalian cells. Although there was over 30-fold decrease in BL activity of CoelPhos with GLuc and GLucM23 in comparison with native coelenterazine, it seems reasonable to assume that CoelPhos together with GLucM23 would show stronger BL intensity over RLuc with coelenterazine. Further investigation is required however, in order to be able to make a direct comparison. Not only does the substrate specificity of GLuc differ from other coelenterate luciferases such as *Renilla* and *Oplophorus* luciferase. GLuc has been shown to contain two catalytic domains; both with similarly narrow substrate specificities.[30] Significant differences are also observed in the kinetic properties. Unlike other marine luciferases (RLuc, CLuc) which respond to their respective coelenterate luciferin concentration in a linear non-cooperative manner, it was recently shown that GLuc operates in a cooperative manner, possibly via an allosteric mechanism.[31] Previous studies utilizing bioluminescence imaging for monitoring of real-time protein secretion showed the importance of the type of camera used. Exocytotic events of native GLuc in CHO-K1 cells were visualized in real time with a time resolution of 10 s. However, the resolution of luminescence spots was low, which made if difficult to

identify single exocytotic spots of luminescence due to the low luminescence sensitivity of the camera used.[12] In more recent studies the same group utilized a more powerful EM-CCD which resulted in a 60-fold increase in sensitivity which allowed for the real-time monitoring of localization and dynamics of proteins on the surface of cells with millisecond temporal resolution.[13,14] Notwithstanding the fact that the CCD camera employed in our imaging studies was inferior to cameras utilized in the above references in terms of quantum efficiency and signal-to-noise, we were able to visualize CoelPhos with GLucM23Mem at a sampling rate of 2 s. Hence it is plausible to venture that utilization of EM-CCD cameras with improved sensitivity will allow for bioluminescence imaging of CoelPhos with much improved temporal resolution and luminescence sensitivity.

3 Conclusions

In conclusion, we have developed a cell-membrane impermeable coelenterazine derivative, CoelPhos, as a potential tool for monitoring membrane fusion events in living cells. The derivative was constructed by alkylating the phenolic hydroxyl group at the 2-position of coelenterazine with an alkyl linker containing a terminal phosphonate group. While displaying 30-fold less activity with GLuc compared with native coelenterazine, CoelPhos showed a high specificity for GLuc over RLuc with a 30-fold higher activity. By utilizing a new mutant GLuc, GLucM23, we were able to image membrane-localized GLucM23 despite the lower luminescence intensity of CoelPhos. We demonstrated that CoelPhos has decreased cell-membrane permeability in comparison with native coelenterazine. Our probe, CoelPhos, has the potential to be used as a cell-impermeable bioluminescent tool for monitoring of exocytotic events.

Experimental

Materials and Instruments

General reagents and chemicals were purchased from Sigma-Aldrich Chemical Co. (St. Louse, MO), Tokyo Chemical Industries (Tokyo, Japan), and Wako Pure Chemical (Osaka, Japan) and were used without further purification. Silica gel chromatography was performed using BW-300 (Fuji Silisia Chemical Ltd., Greenville, NC). pcDNA4™/TO/myc-His/lacZ was purchased from Life Technologies Corporation (Japan) NMR spectra were recorded on a JEOL JNM-AL400 instrument at 400 MHz for ^{1}H and 100.4 MHz for ^{13}C NMR, using tetramethylsilane as an internal standard. Mass

spectra were measured on a Waters LCT-Premier XE mass spectrometer for ESI or on a JEOL JMS-700 for FAB. UV-visible absorbance spectra were measured using a Shimadzu UV1650PC spectrometer. High pressure liquid chromatography (HPLC) analysis was performed with an Inertsil ODS3 column (4.6 × 250 mm, GL Science, Inc. Torrance, CA) using an HPLC system that comprised a pump (PU2080, JASCO) and a detector (MD2010 and FP2020, JASCO). Preparative HPLC was performed with an Inertsil ODS3 column (10.0 × 250 mm)(GL Sciences Inc.) using an HPLC system with a pump (PU-2087, JASCO) and a detector (UV-2075, JASCO). Bioluminescence was measured in 96-optiplate multiwell plates (PerkinElmer Co., Ltd.) using a Wallac ARVO mx / light 1420 Multilabel / Luminescence counter with an auto-injector (PerkinElmer Co., Ltd.). Bioluminescence imaging was performed utilizing an Olympus DP30 Cooled Monochrome CCD Microscope Camera with a 60 × objective lens. Coelenterazine was synthesized as previously described and stored as 10 mM MeOH/HCl (<1%) solution aliquotes in sealed glass ampulles at -80°C.[25,26]

Mutant GLuc

The cDNA for *Gaussia* luciferase (GLuc) was purchased from New England BioLabs Inc. The DNA sequence coding for GLuc without sequence for signal peptide (dspGLuc, aa18-) was amplified by PCR with primers containing the sequence encoding NdeI site, a bacterial periplasm localization signal (pelB) and XhoI site at the 5′ end and PstI site at the 3′ end. The entire cDNA of pelB-dspGLuc was cloned into NdeI and PstI sites of $pRSET_B$ (Invitrogen), yielding pRSET-pelB-dspGLuc. For mutant GLuc, The sequences corresponding to dspGLuc were randomly mutated by error-prone PCR, The sequence for dspGLuc in pRSET-pelB-dspGLuc was replaced with those PCR products containing mutant dspGLuc. These plasmids were transformed into JM109(DE3) competent cells, then, spread on LB ampicillin plates. After each bacterial colony was visible, each colony was picked and transferred to two new LB ampicillin plates, sequentially. After colonies were grown, we poured 50 μM coelenterazine containing PBS solution on top of the plate. The colonies which showed bright luminescence were picked and and evaluated by sequencing analysis. We obtained two mutants that showed bright luminescence. Mut1 contained K50E, M60L, M127I mutations, and Mut2 contained A36V, V113D mutations. We analyzed each of these mutations and found these mutations showed additive effects. A combination of these mutations resulted in an even brighter GLuc mutant, which had K50E, M60L, V113D, M127I and G184D mutations (GLucM23).

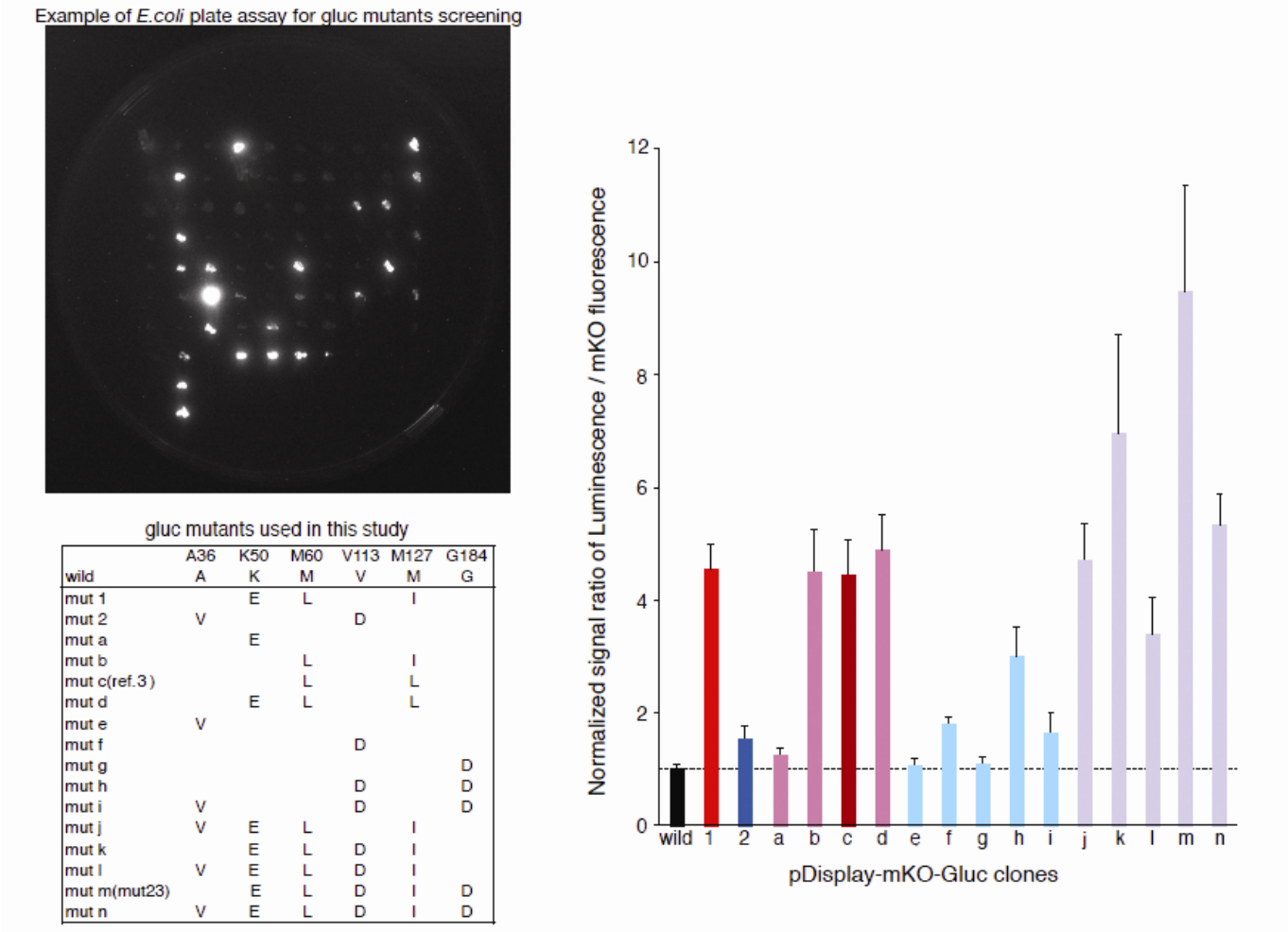

	A36	K50	M60	V113	M127	G184
wild	A	K	M	V	M	G
mut 1		E	L		I	
mut 2	V			D		
mut a		E				
mut b			L		I	
mut c(ref.3)			L		L	
mut d		E	L		L	
mut e	V					
mut f				D		
mut g						D
mut h				D		D
mut i	V			D		D
mut j	V	E	L		I	
mut k		E	L	D	I	
mut l	V	E	L	D	I	
mut m(mut23)		E	L	D	I	D
mut n	V	E	L	D	I	D

Figure S1. Displaying types of mutant variations of GLuc generated and their respective activities.

Mammalian cell expression constructs

To make pCDNA3- GLuc-Venus-KDEL, the entire sequence of GLuc was amplified by PCR with primers containing BamHI site, kozak sequence (ccacc) before start codon at the 5′ end and BspEI site, KDEL for endoplasmic reticulum localization signal sequence, stop codon and EcoRI site at the 3′ end. This PCR product was cloned into BamHI and EcoRI site of pcDNA3 vector (Invitrogen). This plasmid was then cut by BspEI and the cDNA of Venus fluorescent protein containing 5′ BspEI site and 3′ AgeI site was inserted. To make pDisplay-mKO-GLucM23, the entire sequence of mKusabira-Orange (mKO) was amplified by PCR with primer containing BamHI site at the 5′ end and BglII site at the 3′ end. The sequence of dspGLucM23 was also amplified

by PCR with primers containing BglII site at the 5' end and PstI site at the 3' end. Two PCR products were ligated and cloned into BglII and PstI sites of pDisplay vector (Invitrogen). pDisplay-mKO-GLuc was constructed in a similar fashion.

General experimental details for cell-cultures

HeLaS3 cells were maintained in Dulbecco's Modified Eagle Medium (DMEM) (Invitrogen), supplemented with 10% fetal bovine serum (FBS) at 37°C under 5% CO_2. *Transfection*: Optimem (Invitrogen) solutions containing lipofectamine 2000 (Invitrogen) and plasmid DNA were added to HeLaS3 cell cultures and incubated at 37°C under 5% CO_2 for 24 h. Cells were then washed three times with PBS, trypsinized, washed with Leibovitz's L-15 medium, then resuspended in black 96-well optiplates (PerkinElmer) and incubated at 37 °C in luminometer (PerkinElmer).

Preparation of secreted *Gaussia* luciferase

HEK293T cells maintained in DMEM (no phenol red) supplemented with 10% FBS and transfected with pCM-GLuc (New England Biolabs) were incubated at 37 °C under 5% CO_2 for 24 h. The cell-medium was carefully transferred to a separate tube, and centrifuged. The supernatant was aliquoted and stored at −80 °C.

Preparation of *Renilla* luciferase cell lysate

HEK293T cells transfected with pRL-TK at 37 °C under 5% CO_2 for 24 h were washed with PBS (0.1 M, pH 7.4). 800 μL lysate buffer (20 mM Tris buffer (pH 7.4) 150 mM NaCl), containing a mixture of protease inhibitors (PSMF (1 mM), Leupeptin (~ 1 μg / ml), and Pepstatin (~ 1 μg / ml). The suspension was frozen in liquid nitrogen and dethawed 3 times, followed by centrifugation at 15000 rpm at 4 °C for 30 min. Protein concentration was determined by Bradford assay; 41.67 μg / mL.

Determination of Relative and Maximum Luminescence of Coelenterazine Derivatives with GLuc

To a solution of 10 μL GLuc in 90 μL PBS (pH 7.4, 20 mM EDTA, 0.02% Tween20) was added a buffer solution of coelenterate substrate (100 μL, 10 μM) via auto-injector (Final concentration 5 μM). Luminescence was measured for 60 s at 1 s intervals.

Determination of Relative and Maximum Luminescence of Coelenterazine Derivatives with RLuc

To a solution of Rluc (12.5 μg / mL) in 100 μL Tris buffer (20 mM , pH 7.6), 10 mM

EDTA) was added a buffer solution of coelenterate substrate (100 μL, 10 μM) via auto-injector (Final concentration 5 μM). Luminescence was measured for 20 s at 1 s intervals.

Bioluminescence Imaging

HeLaS3 cells in glass-bottom dishes were transfected with pDisplay-mKO-GLuc, pDisplay-mKO-GlucM23, or pcDNA3-GLuc-Venus-KDEL and incubated at 37°C under 5% CO_2 for 20 h. Cells were washed with Hank's balanced salt solution (HBSS) and suspended in 100 μL HBSS (covering the central glass bottom part of the dish). Coelenterazine or CoelPhos in HBSS (1000 μL, 25 μM) was added to the glass-bottom dish (final concentration 22.7 μM) and luminescence was recorded at set exposure times. Fluorescence microscopic images were obtained before addition of coelenterate substrate (mKO: ex/em: 548/561; 200 ms; Venus Ex/Em: 515/528; 300 ms).

2. Syntheses of Compounds

1. Synthesis of coelenteramine and α-ketoacetal.

3-benzyl-5-bromo-2-pyrazinamine (5)

To a solution of benzylmagnesium chloride (2.0 M, 2.6 mL, 5.20 mmol) in THF (10 mL) was added zinc chloride in Et_2O (1.0 M, 5.7 mL, 5.70 mmol) at room temperature under argon. The resulting turbid mixture was stirred for 30 min, after which bis(triphenyl phosphine)palladium (II) dichloride (83 mg, 0.12 mmol) and 2-amino-3,5-dibromo-pyrazine (600 mg, 2.37 mmol) was added. The reaction was stirred for 3 days at room temperature. The reaction mixture was poured into water and extracted with EtOAc. The combined organic layer was washed with brine, dried over anhydrous sodium sulfate, and concentrated *in vacuo*. Purification by silica gel chromatography (25% EtOAc / hexane) afforded 525 mg (1.99 mmol, 84%) of 3-benzyl-5-bromo -2-pyrazinamine (**5**). ^{1}H-NMR (400 MHz, DMSO-d_6) δ 7.96 (s, 1H) 7.26-7.14 (m, 5H) 4.01 (s, 2H) ESI-MS: calc: 264.02; found: 264.00 $[M+H]^+$.

3-benzyl-5-(4-*tert*-butyldimethylsilyloxyphenyl)-2-pyrazinamine (6)

To a suspension of bis(benzonitrile)dichloro palladium (44 mg, 0.11 mmol) in toluene (5 mL) was added 1,4-bis(diphenyl- phosphino)butane (53 mg, 0.12 mmol) and the mixture was stirred for 30 min under argon at room temperature. 5-benzyl-5-bromo-2-pyrazinamine (**5**)(519 mg, 1.97 mmol), 4-(*tert*-butyldimethylsilyloxy)-

phenylboronic acid (656 mg, 2.60 mmol), toluene (10 mL), ethanol (1 mL), and aqueous sodium carbonate (1 M) were added sequentially and the mixture was refluxed for 24 h. After cooling down to room temperature the reaction mixture was poured into water and extracted with EtOAc. The combined organic layer was washed with brine, dried over anhydrous sodium sulfate, and concentrated *in vacuo*. Purification by silica gel chromatography (20-30% EtOAc / hexane) afforded 639 mg (1.63 mmol, 83%) 3-benzyl-5-(4-*tert*-butyldimethyl- silyloxyphenyl)-2-pyrazinamine (**6)** as a pale yellow solid. ^{1}H-NMR (400 MHz, $(CD_3)_2CO$) δ 8.36 (s, 1H) 7.88 (d, ^{3}J = 8.0 Hz, 2H) 7.35 (d, ^{3}J = 8.0 Hz, 1H) 7.28 (m, 2H) 7.20 (dd, ^{3}J = 8.0 Hz, 2H) 6.93 (d, ^{3}J = 8.0 Hz, 2H) 4.16 (s, 2H) 1.00 (s, 9H) 0.23 (s, 6H); ESI-MS: calc: 392.22; found: 392.18 $[M+H]^{+}$.

4-(*tert*-butyldimethylsilyloxy)phenylmethanol (7)

To a solution of 4-hydroxybenzaldehyde (5.75 g, 47.1 mmol) and imidazole (6.45 g, 94.8 mmol) in anhydrous CH_2Cl_2 (60 mL) was added TBDMSCl (7.88 g, 52.28 mmol) and was stirred overnight at room temperature under an argon atmosphere. The reaction mixture was poured into water washed with water and brine. The organic layer was dried over anhydrous sodium sulfate and the solvent was removed *in vacuo* and the residue was dried over night. To a solution of the crude 4-(*tert*-butyldimethylsilyloxy)benzaldehyde in methanol was added sodium borohydride (2.24 g, 59.1 mmol) at 0 °C. The ice-bath was removed and the solution was stirred under argon for 2 h. Reaction was quenched by addition of brine. MeOH was evaporated and water was added. The aqueous layer was extracted with EtOAc. The organic layer was washed with brine, dried over sodium sulfate and concentrated *in vacuo,* followed by purification by silica gel chromatography (30% EtOAc / hexane) to afford 9.709 g (86% for 2 steps) of 4-(*tert*-butyldimethylsilyloxy)phenylmethanol (**7**) as a pale yellow viscous oil. ^{1}H-NMR (400 MHz,$CDCl_3$) δ 7.22 (d, ^{3}J = 8.6 Hz, 2H) 6.82 (d, ^{3}J = 8.6 Hz, 2H) 4.60 (s, 2H) 0.99 (s, 9H) 0.20 (s, 6H).

4-(*tert*-butyldimethylsilyloxy)benzyl chloride (8)

To solution of 4-(*tert*-butyldimethylsilyloxy)phenylmethanol (**7**)(10.6 g, 41.3 mmol) in CH_2Cl_2 (~50 mL) at 0 °C under argon was added thionyl chloride (4.6 mL, 63.0 mmol) dropwise. The reaction mixture was stirred for 2 h and poured into water. The organic layer was washed with water ample times, followed by brine. The organic layer was dried over sodium sulfate and evaporated *in vacuo*. Purification by silica gel chromatography (10% EtOAc / hexane) to afford 8.60 g (81 %) of 4-(*tert*-butyl-dimethylsilyloxy)benzyl chloride (**8**). ^{1}H-NMR (400 MHz,$CDCl_3$) δ 7.26 (d, ^{3}J = 8.6 Hz,

2H) 6.83 (d, ^{3}J = 8.6 Hz, 2H) 4.57 (s, 2H) 1.00 (s, 9H) 0.22 (s, 6H). ^{13}C-NMR (100 MHz, $CDCl_3$) δ 155.89, 130.29, 129.96, 120.26, 46.29, 25.64, 18.19, -4.44.

3-(4-(*tert*-butyldimethylsilyloxy)phenyl)-1,1-diethoxyacetone (9)

To magnesium turnings (4.29 g, 176.5 mmol) (vigorously stirred under argon for 3 days) was added 4-(*tert*-butyldimethyl- silyloxy)benzyl chloride (**8**)(8.60 g, 33.5 mmol) in anhydrous THF, followed by additional THF (~ 50 mL), and 1,2-dibromo- ethane (50 μL, 0.58 mmol). The reaction mixture was sonicated for 5 mins, and heated at 50 °C for 1 h. The dark grey reaction mixture was allowed to cool to room temperature. To a separate reaction flask was added ethyl diethoxyacetate (8.0 mL, 44.7 mmol) and THF (~10 mL) and cooled to -78 °C (dry ice / acetone) under argon. The Grignard reagent was added via syringe over 30 mins and the reaction mixture was allowed to stir for 6 h, followed by addition of water (25 mL) and the reaction mixture allowed to warm to room temperature. Additional water was added and extracted with EtOAc. The organic layer was washed with brine, dried over sodium sulfate, and concentrated *in vacuo*. The crude pale yellow oil was purified by silica gel chromatography (10% EtOAc / hexane) to afford 5.54 g (15.7 mmol, 47%) of 3-(4-(*tert*-butyldimethylsilyloxy)-phenyl)-1,1-diethoxy acetone (**9**) as a pale yellow oil. ^{1}H-NMR (400 MHz, $CDCl_3$) δ 7.07 (d, ^{3}J = 8.0 Hz, 2H) 6.78(d, ^{3}J = 8.0 Hz, 2H) 4.62 (s, 1H) 3.80 (s, 2H) 3.70-3.51 (m, 2 x 2H) 1.24 (t, ^{3}J = 7.0 Hz, 6H) 0.97 (s, 9H) 0.18 (s, 6H); ^{13}C-NMR (100 MHz, $CDCl_3$) δ 203.6, 154.5, 130.7, 126.3, 120.1, 102.1, 63.3, 43.1, 25.7, 18.2, 15.1, -4.5. ESI-MS: calc: 370.2408; found: 370.3069 $[M+NH_4]^+$.

3-(4-hydroxyphenyl)-1,1-diethoxyacetone (10)

To 0 °C cooled solution of 3-(4-(*tert*-butyldimethylsilyloxy)phenyl)-1,1- diethoxy acetone (**9**)(1.50 g, 4.25 mmol) in THF (10 mL) under argon was added tetra-*n*-butylammonium fluoride (1.0 M in THF, 2.2 mL, 2.2 mmol). After 30 min, the reaction was quenched with saturated aqueous sodium chloride and extracted with CH_2Cl_2. The combined organic layer was dried over anhydrous sodium sulfate and concentrated *in vacuo*. Purification by silica gel chromatography afforded 944 mg, (3.96 mmol, 93%) of 3-(4-hydroxyphenyl)-1,1-diethoxyacetone. ^{1}H-NMR (400 MHz, $CDCl_3$) δ 7.26 (d, ^{3}J = 8.0 Hz, 2H) 6.78 (d, ^{3}J = 8.0 Hz, 2H) 4.69 (s, 1H) 4.63 (s, 2H) 3.82 (s, 2H) 3.72-3.53 (m, 2 x 2H) 1.25 (t, 6H). ESI-MS: calc: 256.1543; found: 256.1663 $[M+NH_4]^+$.

2. Synthesis of 2 and 6-OBn-TEG-CTZ.

.13-bromo-1-phenyl-2,5,8,11-tetraoxatridecane (12)

Sodium hydride (60% in mineral oil)(839 mg, 20.98 mmol) was added to a cooled reaction flask containing anhydrous DMF under argon. The mixture was stirred for 10 minutes, after which the ice-bath was removed and the mixture was stirred at rt for another 15 min. The mixture was cooled with an icebath, followed by dropwise addition of benzyl bromide (2.3 mL, 19.34 mmol). Reaction mixture was concentrated *in vacuo*, followed by silica gel chromatographyEtOAc to afford **11** (3.34 g, 11.61 mmol, 67%) as a colorless oil. To a solution of triphenylphosphine (856 mg, 3.26 mmol) and carbon tetrabromide (1088 mg, 3.28 mmol) in anhydrous CH_2Cl_2 under argon was added **7** (592 mg, 2.08 mmol). The reaction mixture was refluxed for 18 h. Reaction mixture was concentrated *in vacuo*. silica gel chromatography ((1:1) EtOAc / hexane) to afford **12** (483 mg, 15.7 mmol, 79% over two steps) as a colorless oil. 1H-NMR (400 MHz, $CDCl_3$) δ 7.35-7.34 (m, 5H) 4.57 (s, 2H) 3.72-3.59 (m, 16H). FAB: Calculated: 540.0879; Found: 540.0887 $[M+Na]^+$. ESI-MS: Calculated: 540.0879; Found: 540.1243$[M+Na]^+$.

3-benzyl-5-(4-(1-phenyl-2,5,8,11-tetraoxatridecan-13-yloxy)phenyl)pyrazin-2-amine (13)

To an ice-cooled solution of 3-benzyl-5-(4-*tert*-butyldimethylsilyloxyphenyl)-2-pyrazinamine (**6**) (80 mg, 0.20 mmol) in anhydrous THF under argon was added tetrabutylammonium fluoride (160 μL, 0.16 mmol) in THF. After 1 stirring for 1 h the reaction was quenced with brine, poured into water and extracted with EtOAc. The combined organic layer was washed with brine, dried over anhydrous sodium sulfate, and concentrated *in vacuo*. The resulting residue was subjected to silica gel chromatography ((1:1) EtOAc / Hexane), affording crude coelenteramine (~56 mg, 0.2 mmol). To a ice-cooled solution of sodium hydride (60% in mineral oil)(18 mg, 0.45 mmol) in anhydrous DMF (5 mL) was added coelenteramine (55 mg, 0.2 mmol) and the reaction mixture was stirred for 30 min. 12-bromo-1-benzyl-tetraethylene glycol (170 mg, 0.49 mmol) in DMF (5 mL) was added dropwise. The ice-bath was removed and the reaction mixture was stirred at rt for 4.5 h, after which the reaction was quenched with 20% NH_4Cl. The reaction mixture was diluted with water and extracted with EtOAc. The combined organic layers were washed with brine, dried over anhydrous sodium sulfate, and concentrated *in vacuo*. The resulting residue was subjected to silica column chromatography (2% MeOH / CH_2Cl_2) to afford the desired product **13** (58 mg, 55% over two steps). ^{1}H-NMR (400

MHz, $CDCl_3$) δ 8.31(s, 1H) 7.85 (d, 2H, ^3J = 8.0 Hz) 7.33-7.25 (m, 10H) 6.98 (d, ^3J = 8.0 Hz, 2H) 4.55 (s, 2H) 4.46 (s, 2H) 3.86 (t, 2H) 3.74-3.61 (m, 14H). ^{13}C-NMR (100 MHz, $CDCl_3$) δ 158.90, 151.29, 142.38, 140.40, 138.22, 136.82, 136.75, 130.10, 128.91 128.55, 128.32, 127.71, 127.56, 126.96, 126.90, 114.87, 73.18, 70.81, 70.61, 69.68, 69.39, 67.44, 41.15. ESI-MS: Calculated: 544.2806; Found: 544.2834 $[M+H]^+$. FAB: Calculated: 543.2733; Found: 543.2722 $[M]^+$.

1,1-diethoxy-3-(4-(1-phenyl-2,5,8,11-tetraoxatridecan-13-yloxy)phenyl)propan-2-one (14)

A solution of 3-(4-hydroxyphenyl)1,1-diethoxyacetone (**10**) (100 mg, 0.42 mmol), Cs_2CO_3 (202 mg, 0.62 mmol), and **12** (217 mg, 0.62 mmol) in anhydrous MeCN (5 mL) was refluxed under argon for 3 h. The reaction mixture was poured into water and extracted with EtOAc. The combined organic layer was washed with brine and dried over anhydrous sodium sulfate. The mixture was concentrated *in vacuo*, followed by purification by silica gel chromatography (40% EtOAc / Hexane) to yield **14** (154 mg, 0.31 mmol, 73%). ^{1}H-NMR (400 MHz, $CDCl_3$) δ 7.34-7.33 (m, 5H) 7.11 (d, ^3J = 8.4 Hz, 2H) 6.85 (d, ^3J = 8.4 Hz, 2H) 4.62 (s, 1H) 4.56 (s, 2H) 4.10 (t, 2H) 3.83 (t, 2H) 3.81 (s, 2H) 3.73-3.67 (m, 12H) 3.68-3.52 (m, 4H) 1.24 (t, ^3J = 7.2 Hz, 6H). ^{13}C-NMR (100 MHz,$CDCl_3$) δ 203.47, 157.69, 138.21, 130.65, 128.30, 127.68, 127.52, 125.83, 114.60, 102.14, 73.16, 70.75, 70.59, 69.66, 69.37, 67.13, 63.26, 42.80, 15.11. ESI-MS: Calculated: 522.3061; Found: 522.2361 $[M+NH_4]^+$.

6-OBn-TEG-CTZ (2)

A solution of **13** (55 mg, 0.10 mmol) and **9** (73 mg, 0.21 mmol) in 1,4-dioxane (5 mL) and 6N HCl (0.5 mL) was refluxed under argon for 24 h. The reaction was allowed to cool to rt and concentrated *in vacuo*. Silica gel chromatography, (3-6 % MeOH / CH_2Cl_2) afforded the desired product **6-OBn-TEG-CTZ (2)** as a dark red solid (14 mg, 0.02 mmol, 20 %). ^{1}H-NMR (400 MHz, CD_3OD) δ 7.67 (s, 1H) 7.38 (m, 2H) 7.31-7.15 (m, 10H) 6.78 (d, ^3J = 8.4 Hz, 2H) 6.72 (d, ^3J = 8.0 Hz, 2H) 4.52 (s, 2H) 4.41 (s, 2H) 4.13 (m, 2H+2H) 3.85 (t, 2H) 3.70-3.61 (m, 12H). ^{13}C-NMR (100 MHz, $CDCl_3$) δ 160.77, 156.27, 138.76, 136.92, 131.35, 130.90, 130.45, 129.85, 129.48, 129.33, 128.93, 128.81, 128.44, 128.28, 127.81, 125.91, 115.87, 115.64, 73.78, 73.12, 71.29, 71.11, 70.25, 70.05, 68.18, 61.78, 30.25. ESI-MS: Calculated: 690.3174; Found: 690.3279 $[M+H]^+$.

2-OBn-TEG-CTZ (3)

A solution of **2** (51 mg, 0.13 mmol) and **10** (124 mg, 0.25 mmol) in 1,4-dioxane (5 mL) and 6N HCl (0.5 mL) was refluxed under argon for 14 h. The reaction was allowed to cool to rt and concentrated *in vacuo*. Silica gel chromatography, (5-10 % MeOH / CH_2Cl_2) afforded the crude desired product (38.5 mg). The residue was further purified via RP-HPLC (H_2O (0.1 % formic acid) / MeCN (0.1 % formic acid) ; 60:40 → 70:30, 4.7 mL/min; column: ODS-3). The combined fractions were lyophilized, yielding the desired product **2-OBn-TEG-CTZ (3)** as a red solid (15 mg, 0.02 mmol, 17%). ^{1}H-NMR (400 MHz, $CDCl_3$) δ 7.64 (s, 1H) 7.32 (m, 2H) 7.25-7.07 (m, 10H) 6.98 (d, 2H, ^3J = 8.4 Hz) 6.72 (d, ^3J = 8.0 Hz, 2H) 4.54 (s, 2H) 4.41 (s, 2H) 4.02 (m, 2H + 2H) 3.84 (t, 2H) 3.68-3.58 (m, 12H) ^{13}C-NMR (100 MHz, $CDCl_3$) δ 158.77, 155.35, 137.56, 134.92, 129.64, 130.40, 130.25, 129.85, 129.68, 129.26 128.73, 128.51, 128.34, 128.26, 127.14, 125.68, 115.41, 114.55, 73.67, 73.08, 71.24, 71.01, 70.04, 70.01, 68.28, 60.75, 30.15. ESI-MS: Calculated:690.3174; Found: 690.2411 $[M+H]^+$. FAB: Calculated: 689.3101; Found: 689.3088 $[M]^+$.

3. Synthesis of CoelPhos

Comment: Initially installing of a propylphosphonate at the 2-position of coelenterazine was perceived as a suitable candidate compound. However, alkylation of the α-ketoacetal **10** with 3-bromopropylphosphonate proved difficult with formation of several side products (data not shown). Interestingly alkylation of **10** with 1,3-dibromopropane gave **17** which could be separated from the undesired side products more easily. Alkylation of **10** with ethyl 4-bromobutyrate has been reported previously,[1] which also resulted in a poor yield. On the other hand, alkylation of **10** with PEG linker **12** gave **14** in a satisfactory yield, suggesting stereochemistry to be an important factor in the general alkylation of **10**.. Hence we modified our synthetic route by considering converting the propyl bromide **17** into the propyl azide **18**, which would allow for diversification via copper(I)-catalyzed azide-alkyne Huisgen cycloaddition. In our initial attempt to form the 1,2,3-triazole between **16** and **18**, we utilized the common solvent system H_2O/*t*BuOH (1:1),[4] however in our hands hardly any product was formed. When we applied a two-phase solvent system (H_2O/CH_2Cl_2 (1:1)), which has been shown to improve reaction kinetics,[5] gave the desired 1,2,3-triazole **19** in very good yield.

Dimethyl hydroxymethylphosphonate (15)

To a solution of paraformaldehyde (1.27 g, 42.4 mmol) in trimethyl phosphite (5 mL, 42.3 mmol) was added triethylamine (0.6 mL, 4.30 mmol) under argon and was

refluxed at 130 °C for 3 h. Volatiles were removed *in vacuo*. The crude residue was purified by silica gel chromatography (4-5% MeOH / EtOAc) to afford 697 mg (4.98 mmol, 12%) of dimethyl hydroxyl- methylphophonate (**15**). ^{1}H-NMR (400 MHz,$CDCl_3$) δ 3.96 (m, 2H) 3.81 (d, ^{3}J = 8 Hz, 6H); ^{13}C-NMR (100 MHz, $CDCl_3$) δ 56.4 (d, J = 162.1 Hz) 53.1 (d, J = 6.6 Hz); ^{31}P-NMR (162 MHz, $CDCl_3$) single peak. ESI-MS: calc: 141.0311, found: 141.0473 $[M+H]^+$.

Dimethyl (prop-2-ynyloxy)methylphosphonate (16)

To -78 °C cooled solution of dimethyl hydroxymethylphosphonate (**15**)(172 mg, 1.23 mmol) in THF (2 mL) was added sodium hydride (96 mg, 2.40 mmol) and allowed to stir for 1.5 h. A solution of propargyl bromide (0.2 mL, 1.85 mmol) in THF (1 mL) was added dropwise via syringe. The reaction was left stirring for 14 h. The reaction was quenched with ammonium chloride and the solvent was evaporated. Water was added and extracted with CH_2Cl_2. The combined organic layer was washed with brine, dried over anhydrous sodium sulfate, and concentrated *in vacuo*. Purification by silica gel chromatography (3-4% MeOH / EtOAc) afforded 76 mg (0.43 mmol, 35%) of dimethyl (prop-2-ynyloxy)methylphosphonate (**16**) as a colorless oil. ^{1}H-NMR (400 MHz, $CDCl_3$) δ 4.28 (m, 2H) 3.92 (d, ^{2}J = 12Hz, 2H) 3.82 (d, ^{3}J = 8 Hz, 6H) 2.51 (m, 1H); ^{13}C-NMR (100 MHz, $CDCl_3$) δ 78.1, 76.0, 63.2 (d, J = 167.1 Hz) 60.1 (d, J = 14.9 Hz) 53.1 (d, J = 6.5 Hz); ^{31}P-NMR (162 MHz, $CDCl_3$) single peak. ESI-MS: calc: 179.0468, found: 179.0625 $[M+H]^+$.

3-(4-(3-bromopropoxy)phenyl)-1,1-diethoxyacetone (17)

To a solution of 3-(4-hydroxyphenyl)-1,1-diethoxyacetone (**10**) (952 mg, 4.00 mmol) and Cs_2CO_3 (1411 mg, 4.33 mmol) in anhydrous acetonitrile (20 mL) under argon was added 1,3-dibromopropane (2 mL, 19.7 mmol) by syringe. The solution was heated at 100 °C for 3 h. After cooling to room temperature the reaction mixture was filtered and washed with EtOAc and evaporated to dryness. The resulting residue was partitioned between water and EtOAc and the aqueous layer was extracted with EtOAc. The combined organic layer was washed with brine, dried over anhydrous sodium sulfate and concentrate *in vacuo*. Purification by gradual silica gel chromatography (5-10% EtOAc / hexane) afforded 510 mg (1.42 mmol, 35%) of 3-(4-(3-bromopropoxy)phenyl)-1,1-diethoxyacetone (**17**) as a pale yellow oil. ^{1}H-NMR (400 MHz, $CDCl_3$) δ 7.12 (d, ^{3}J = 8.0 Hz, 2H) 6.86 (d, ^{3}J = 8.0 Hz, 2H) 4.63 (s, 1H) 4.09 (t, ^{3}J = 8.0 Hz, 2H) 3.83 (s, 2H) 3.70 (m, 2H) 3.60 (m, 2H) 3.55 (m, 2H) 2.31 (m, 2H) 1.25 (t, ^{3}J = 8.0 Hz, 6H); ^{13}C-NMR (100 MHz, $CDCl_3$) δ 203.5, 157.6, 130.8, 126.0, 114.6,

102.3, 65.2, 63.4, 42.8, 32.4, 30.1, 15.2.

3-(4-(3-azidopropoxy)phenyl)-1,1-diethoxyacetone (18)

To a solution of 3-(4-(3- bromopropoxy)phenyl)-1,1-diethoxyacetone (**17**) (268 mg, 0.75 mmol) in anhydrous DMF, (~2 mL) was added sodium azide (78 mg, 1.20 mmol) and the reaction was heated at 50 °C for 12 h. The reaction was allowed to cool to room temperature, poured into water, and extracted with EtOAc. The combined organic layer was washed with brine and dried over anhydrous sodium sulfate, and concentrated *in vacuo*. Purification by silica gel chromatography (10% EtOAc / hexane) afforded 187 mg (0.58 mmol, 76%) of 3-(4-(3-azidopropoxy)phenyl)-1,1-diethoxyacetone (**18**). ^{1}H-NMR (400 MHz,$CDCl_3$) δ 7.12 (d, ^{3}J = 8.0 Hz, 2H) 6.85 (d, ^{3}J = 8.0 Hz, 2H) 4.62 (s, 1H) 4.03 (s, 2H) 3.70 (t, ^{3}J = 7.2 Hz, 2H) 3.54 (m, 4H) 2.04 (t, ^{3}J = 5.6 Hz, 2H) 1.25 (t, ^{3}J = 6.6 Hz, 6H). ^{13}C-NMR (100 MHz, $CDCl_3$) δ 203.5, 157.6, 130.8, 126.0, 114.6, 102.3, 64.5, 63.4, 48.3, 42.8, 28.8, 15.2. ESI-MS: calc: 339.2027; found: 339.2164 $[M+NH_4]^+$.

Dimethyl((1-(3-(4-(3,3-diethoxy-2-oxopropyl)phenoxy)propyl)-1H-1,2,3-triazol-4-yl)methoxy)methylphosphonate (19)

To a solution of 3-(4-(3-azidopropoxy)phenyl)-1,1-diethoxyacetone (**18**) (94 mg, 0.29 mmol), dimethyl (prop-2-ynyloxy) methylphosphonate (**16**) (61 mg, 0.34 mmol) in water (1 mL) and dichloromethane (1 mL) was added copper (II) sulfate (2.8 mg, 0.02 mmol), and sodium ascorbate (13.6 mg, 0.09 mmol). The reaction mixture was vigorously stirred for 12 h, poured into water and extracted with dichloromethane, dried over sodium sulfate, and concentrated *in vacuo*. Purification by silica gel chromatography afforded 129 mg (0.26 mmol, 88%) of dimethyl ((1-(3-(4-(3,3-diethoxy-2-oxopropyl)phenoxy)propyl)-1H- 1,2,3-triazol-4-yl)methoxy)methylphosphonate (**19**) as a viscous oil. ^{1}H-NMR (400 MHz, $CDCl_3$) δ 7.60 (s, 1H) 7.12 (d, ^{3}J = 8.4 Hz, 2H) 6.83 (d, ^{3}J = 8.4 Hz, 2H) 4.75 (s, 2H) 4.63 (s, 1H) 4.58 (t, ^{3}J = 7.2 Hz, 2H) 3.96 (t, ^{3}J = 5.6 Hz, 2H) 3.88-3.83 (m, 4H) 3.78 (d, ^{3}J = 10.8 Hz, 6H) 3.71 (m, 2H) 3.56 (m, 2H) 2.39 (m, 2H) 1.25 (t, ^{3}J = 6.8 Hz, 6H); ^{13}C-NMR (100 MHz, $CDCl_3$) δ 203.4, 157.3, 143.8, 130.9, 126.3, 123.5, 102.33, 66.2, 63.2 (d, ^{3}J = 167.0 Hz) 63.9, 63.4, 53.0, 47.1, 42.6, 29.9, 15.1. ^{31}P-NMR (162 MHz, $CDCl_3$) single peak. ESI-MS: calc: 500.2156; found: 500.1754 $[M+H]^+$.

((1-(3-(4-((8-benzyl-6-(4-hydroxyphenyl)-3-oxo-3,7-dihydroimidazo[1,2-a]pyrazin-2-yl)methyl)phenoxy)propyl)-1H-1,2,3-triazol-4-yl)methoxy)methylphosphonate

CoelPhos

To a solution of **19** (80 mg, 0.16 mmol) in 1,4-dioxane (1 mL) was added **6** (63 mg, 0.16 mmol). To this mixture was added 6 N $HCl_{(aq)}$ (100 µL) and the solution was thoroughly flushed and kept under an argon atmosphere. The reaction mixture was then heated to 110 °C and stirred for 5-6 h. The dark mixture was allowed to cool to room temperature and the solvent was evaporated. Reaction mixture was purified by reverse-phase HPLC (100 mM triethylammonium acetate / acetonitrile; 90:10 → 40:60, 4.7 mL/min; column: ODS-3). Collected fractions were concentrated, combined, and lyophilized to give product **CoelPhos** as the triethylammonium salt (11 mg, 9% yield). ^{1}H-NMR (400 MHz, CD_3OD) δ 7.94 (s, 1H) 7.70 (s, 1H) 7.50 (d, ^{3}J = 8.8 Hz, 2H) 7.35 (d, ^{3}J = 7.6 Hz, 2H) 7.23-7.11 (m, 7H) 6.82 (d, ^{3}J = 8.8 Hz, 2H) 6.75 (d, ^{3}J = 9.0 Hz, 2H) 4.62 (s, 2H) 4.53 (t, ^{3}J = 7.0 Hz, 2H) 4.34 (s, 2H) 4.04 (s, 2H) 3.89 (t, ^{3}J = 6.0 Hz, 2H) 3.56 (d, ^{3}J = 9.6 Hz, 2H) 2.28 (m, 2H). ^{13}C-NMR (100 MHz, CD_3OD) δ 159.52, 158.50, 146.07, 139.17, 133.63, 130.82, 129.85, 129.50, 129.14, 128.57, 127.73, 125.44, 125.40, 116.84, 115.45, 108.48, 69.43, 67.85, 66.68, 66.54, 65.57, 47.53, 36.71, 33.02, 31.09, 29.43, 23.85, 9.26. HRMS:ESI-MS: calc: 657.2221; found: 657.3062 $[M+H]^{+}$. ^{31}P NMR (162 MHz, CD_3OD, single peak. H-H COSY (400 MHz, CD_3OD)(Figure S2)

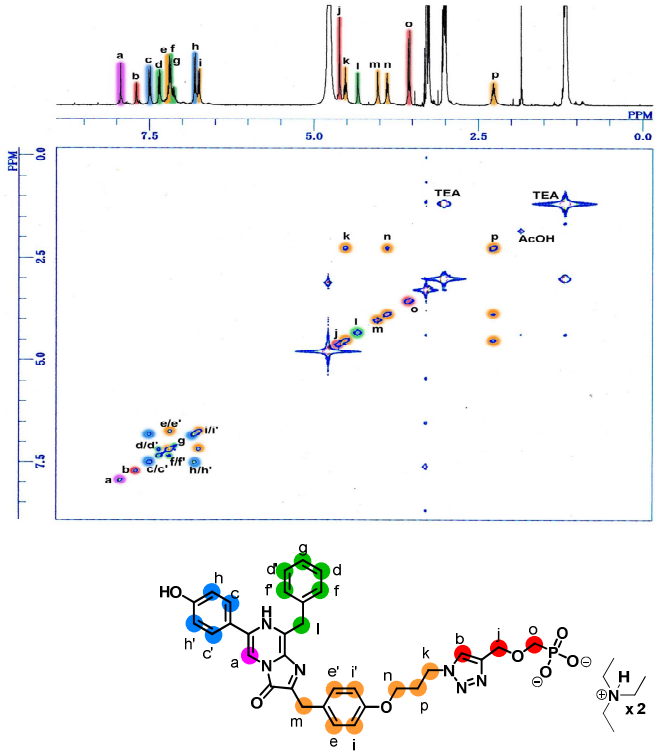

Figure S2. H-H-COSY diagram of CoelPhos

References

(1) Tannous, B. A.; Kim, D. -E.; Fernandez, J. L.; Weissleder, R.; Breakefield, X.O. *Mol. Ther.* **2005**, *11*, 435-443.

(2) Ozawa, T.; Yoshimura, H.; Kim, S. B.; *Anal. Chem.* **2013**, *85*, 590-609.

(3) Akopova, I.; Tatur, S.; Grygorczyk, M.; Luchowski, R.; Gryczynski, I.; Boredjo, J.; Grygorczyk, R. *Puriner. Signal.* **2012**, *8*, 59-70.

(4) Burchfield, J. G.; Lopez, J. A.; Mele, K.; Vallotton, P.; Hughes, W. E. *Traffic* **2010**, *11*, 429-439.

(5) Takahashi, N.; Kasai, H. *Endocrine J.* **2007**, *54*, 337-346.

(6) Oshima, A.; Kojima, T.; Dejima, K.; Hisa, Y.; Kasai, H.; Nemoto, T. *Cell Calcium* **2005**, *37*, 349-357.

(7) Matsuzaki, M.; Ellis-Davies, G. C. R.; Nemoto, T.; Miyashita, Y.; Iino, M.; Kasai, H. *Nat. Neurosci.* **2001**, *4*, 1086-1092.

(8) Inouye, S.; Ohmiya, Y.; Toya, Y.; Tsuji, F. *Proc. Natl. Acad. Sci. USA* **1992**, *89*, 9584-9587.

(9) Thompson, E. M.; Adenot, P.; Tsuji, F.; Renard, J-P. *Proc. Natl. Acad. Sci. USA* **1995**, *92*, 1317-1321.

(10) Miesenbock, G.; Rothman, J. E. *Proc. Natl. Acad. Sci. USA* **1997**, *94*, 3402-3407.

(11) Suzuki, T.; Usuda, S.; Ichinose, H.; Inouye, S. *FEBS Lett.* **2007**, *581*, 4551-4556.

(12) Suzuki, T.; Kondo, C.; Kanamori, T.; Inouye, S. *Anal. Biochem.* **2011**, *415*, 182-189.

(13) Suzuki, T.; Kondo, C.; Kanamori, T.; Inouye, S. *PLos ONE* **2011**, *6*, e25243.

(14) Inouye, S.; Sahara, Y. *Biochem. Biophys. Res. Commun.* **2008**, *365*, 96-101.

(15) Kimura, T.; Hiraoka, K.; Kasahara, N.; Logg, C. R. *J. Gene. Med.* **2010**, *12*, 528-537.

(16) Inouye, S.; Sahara-Miura, Y.; Sato, J-I.; Iimori, R.; Yoshida, S.; Hosoya, T. *Prot. Exp. Pur.* **2013**, *88*, 150-156.

(17) Morse, D.; Tannous, B. A.; *Mol. Ther.* **2012**, *20*, 692-693.

(18) Kojima, R.; Takakura, H.; Ozawa, T.; Tada, Y.; Nagano, T.; Urano, Y. *Angew. Chem. Int. Ed.* **2012**, *51*, 1-6.

(19) Shimomura, O.; Musick, B.; Kishi, Y. *Biochem. J.* **1988**, *251*, 405-410.

(20) Shimomura, O.; Musick, B.; Kishi, Y. *Biochem. J.* **1989**, *261*, 913-920.

(21) Qi, C. F.; Gomi, Y.; Hirano, T.; Ohashi, M.; Ohmiya, Y.; Tsuji, F. *J. Chem. Soc. Perkin Trans. 1* **1992**, 1607-1611.

(22) Inouye, S.; Shimomura, O. *Biochem. Biophys. Res. Commun.* **1997**, *233*, 349-353.

(23) Wu, C.; Nakamura, H.; Murai, A.; Shimomura, O. **2001**, *42*, 2997-3000.
(24) Hall, M. P.; Unch, J.; Binkowski, B. F.; Valley, M. P.; Butler, B. L. Wood, M. G.; Otto, P.; Zimmerman, K.; Vidugiris, G.; Machleidt, T.; Robers, M. B.; Benink, H. A.; Eggers, C. T.; Slater, M. R.; Meisenheimer, P. L.; Klaubert, D. H.; Fan, F.; Encell, L. P.; Wood, K. V. *ACS Chem. Biol.* **2012**, *7*, 1848-1857.
(25) Adamczyk, M.; Johnson, D. D.; Mattingly, P. G.; Pan, Y.; Reddy, R. E. *Org. Prep. Proc. Int.* **2001**, *33*, 477-485.
(26) Adamczyk, M.; Akireddy, S. R.; Johnson, D. D.; Mattingly, P. G.; Pan, Y.; Reddy, R. E. *Tetrahedron* **2003**, *59*, 8129-8142.
(27) Rostovtsev, V. V.; Green, L. G.; Fokin, V. V.; Sharpless, K. B. *Angew. Chem. Int. Ed.* **2002**, *41*, 2596-2599.
(28) Kim, S. B.; Suzuki, H.; Sato, M.; Tao, H. *Anal. Chem.* **2011**, *83*, 8732-8740.
(29) Degeling, M. H.; Bovenberg, M. S. S.; Lewandrowski, G. K.; de Gooijer, M. C.; Vleggeert-Lankamp, C. L. A.; Tannous, M., Maguire, C. A.; Tannous, B. A. *Anal. Chem.* **2013**, *85*, 3006-3012.
(30) Inouye, S.; Sahara, Y. *Biochem. Biophys. Res. Commun.* **2008**, *365*, 96-101.
(31) Tzertzinis, G.; Schildkraut, E.; Schildkraut, I. *PLoS ONE* **2012**, *7*, e40099.

Chapter 2.1. Development of Luminescent Coelenterazine Derivatives Activatable by β-Galactosidase for Monitoring Dual Gene Expression

(*Chem. Eur. J.* **2013**)

BLI with coelenterate substrates suffers from several drawbacks, including a blue-shifted emission spectrum which is unfavorable for whole animal imaging due to light attenuation by tissues. In addition it has been shown that MDR1 P-glycoprotein can actively transport coelenterazine out of cells.[1] Coelenterazine is also very unstable,[2] with a half-life of 15 min at 37 °C.[3] Its utility is further compromised by its proneness to bind to serum albumin and other intrinsic proteins, which have been shown to catalyze the oxidation of coelenterazine, giving rise to background noise, BLI with cellular assays.[4]

It has been shown that the substituent at the C2-position of coelenterazine plays a major role in its stability and auto-oxidation. [5,6] Introduction of $–CF_3$ at the para position of the C2-benzyl group increased the stability of coelenterazine against auto-oxidation, but also resulted in a significant decrease in bioluminescence activity.[7] Coelenterazine can also be stabilized by introducing protecting groups at the 3-carbonyl position of the imidazpyrazinone ring of coelenterazine.[8,9] The protecting groups are then cleaved by intracellular esterases and lipases resulting in a longer half-life and a lower rate of auto-oxidation. However, it has been suggested that different cell lines may give different results as the type and level of esterases vary with each cell line, thus leading to a lower or higher light output.[9] In addition, as cellular esterases are ubiquitous in most cells, undesired non-selective cleavage of the ester groups in non-targeted cells could lead to background noise.

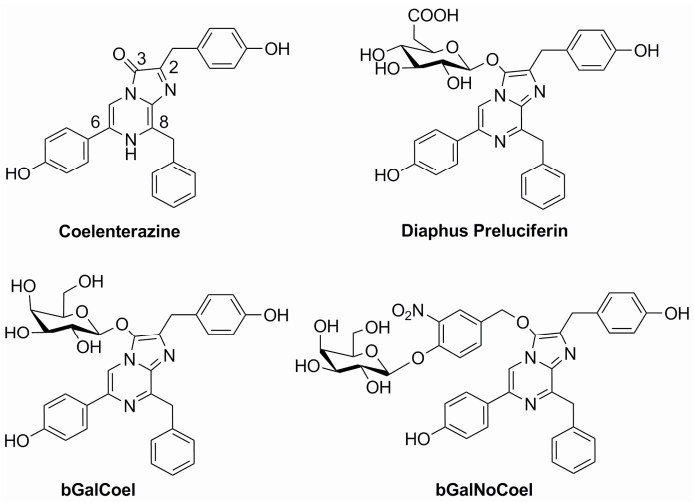

Figure 1. Chemical structures of coelenterazine, Diaphus Preluciferin and the two galactose-conjugated coelenterazine derivatives reported herein.

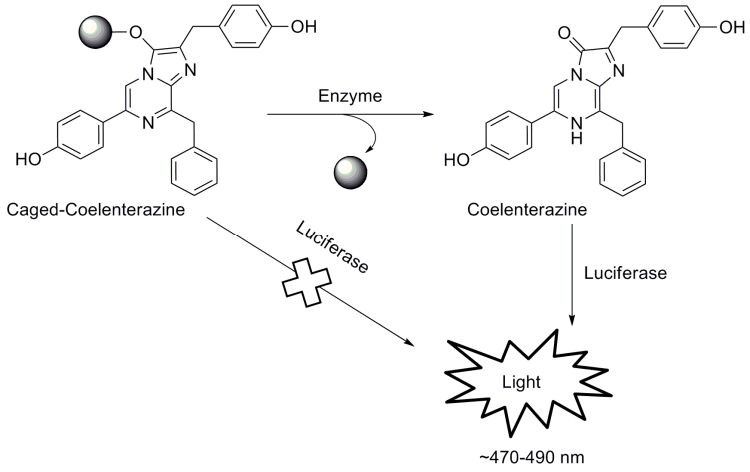

Scheme 1. The concept of Sequential Reporter-enzyme Luminescence (SRL) applied to coelenterazine. SRL allows monitoring the activity of a separate enzyme by making the luminescence generated from the oxidation of coelenterazine by its luciferase dependent on the activity of that enzyme. By installing a caging group on coelenterazine it cannot react with its luciferase, but in the presence of separate enzyme, the caging group can be cleaved and free coelenterazine is generated, which is subsequently oxidized by its luciferase to generate light.

To capitalize on the advantages of coelenterate luciferases, while addressing their limitations, we adopted sequential reporter-enzyme luminescence (SRL) imaging technology.[10] SRL allows imaging of another enzyme by making luminescence dependent on the activity of that enzyme thorugh the use of a caged luciferin substrate

(Scheme 1). SRL has been used to image ß-galactosidase (ß-Gal) activity, a widely used reporter enzyme, using the D-luciferin-ß-galactose derivative, Lugal.[11] Herein we report two new coelenterazine-ß-galactose conjugates as new potential tools for wide array of applications including monitoring of dual-gene expression, enzyme activity, and high-throughput screening. It has also been suggested that SRL could enable applications in toxicology, pharmacology, and in organ and tissue physiology and pathology.[12]

Design, Synthesis and Properties of bGalCoel

Initial probe design strategy was based on the previously reported natural Diaphus Preluciferin (3-enol glucuronide from fish)[13] by conjugating a β-galactose molecule to coelenterazine at the 3-position. bGalCoel was synthesized in four steps from coelenterazine (Scheme 2). Following per-acetylation of coelenterazine, selective deacetylation at the 3-position of the Imidazo pyrazinone ring was accomplished by addition of 1% NH_3 in MeOH to **2** in CH_2Cl_2 at 0 °C.[14] Subsequently, 2,3,4,6-tetra-*O*-acetyl-α-D-galactopyranosyl bromide was added to **3** in DMF to give **4** as the main product. After standard deacetylation with sodium methoxide in MeOH, bGalCoel was purified via reverse phase-HPLC.

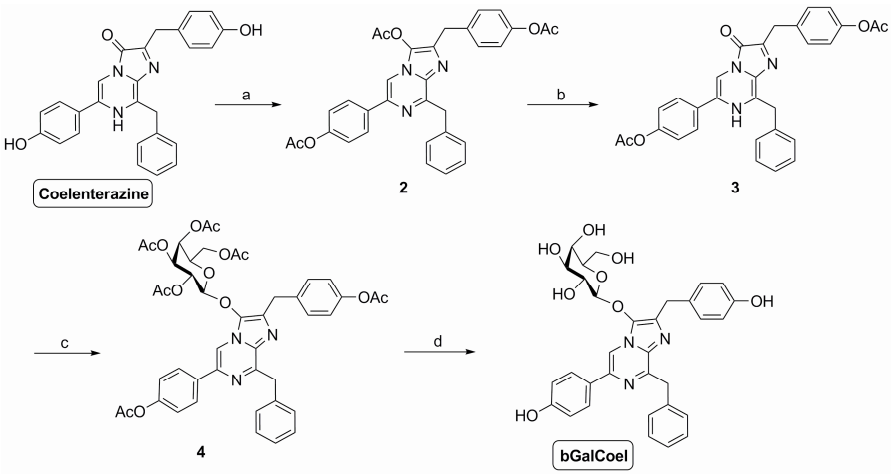

Scheme 2. Synthesis of bGalCoel. a) Ac_2O, DMAP, 76%; b) 1% NH_3 in MeOH, CH_2Cl_2, quant.; c) 2,3,4,6-tetra-*O*-acetyl-α-D-galactopyranosyl bromide, Cs_2CO_3, DMF, 48%; d) NaOMe, MeOH, 44%.

Next, the luminescent properties of bGalCoel were evaluated in comparison with native coelenterazine. bGalCoel displayed glow-type kinetics in presence of β-Gal and GLuc (Figure 2a) with an average signal half-life of 77 min (Figure 3). GLuc is known to exhibit flash-type kinetics with coelenterazine, with a half-life of only a few

seconds.[15] The luminescent signal of bGalCoel did not return to basal levels even after 3 h, making a direct comparison with native coelenterazine very difficult in terms of relative signal output. Relative bioluminescence activity of bGalCoel was 11% of that of coelenterazine after a photoncount of ~10 min using a luminometer (Figure 2c). The observed glow-type luminescence of bGalCoel suggested slow cleavage kinetics of β-galactosidase. HPLC studies further showed that the cleavage reaction of β-galactosidase with bGalCoel was very slow, with most of the substrate remaining intact even after 8 h (Figure 4).

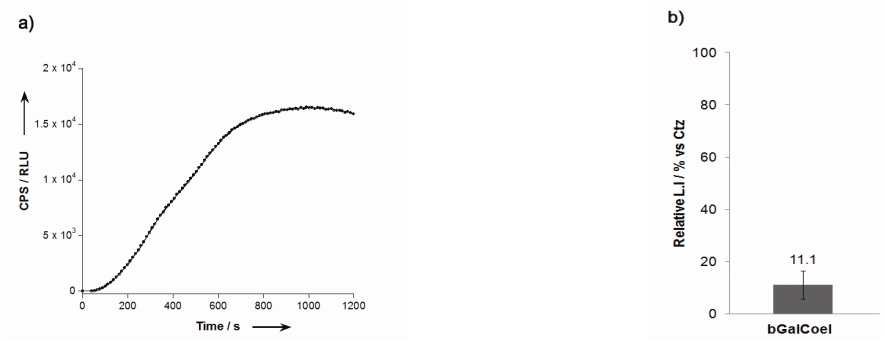

Figure 2. Kinetic profile and relative bioluminescence activity of bGalCoel (a) cleavage by β-galactosidase measured by light output of *Gaussia* luciferase; Reaction conditions: 5 µM bGalCoel, 2 U β-galactosidase, 3 mM $MgCl_2$, *Gaussia* luciferase, 0.1 M PBS (pH 7.4); Total light output measured in luminometer (12 s × 100). (b) Relative light output of bGalCoel versus native coelenterazine (CTZ).

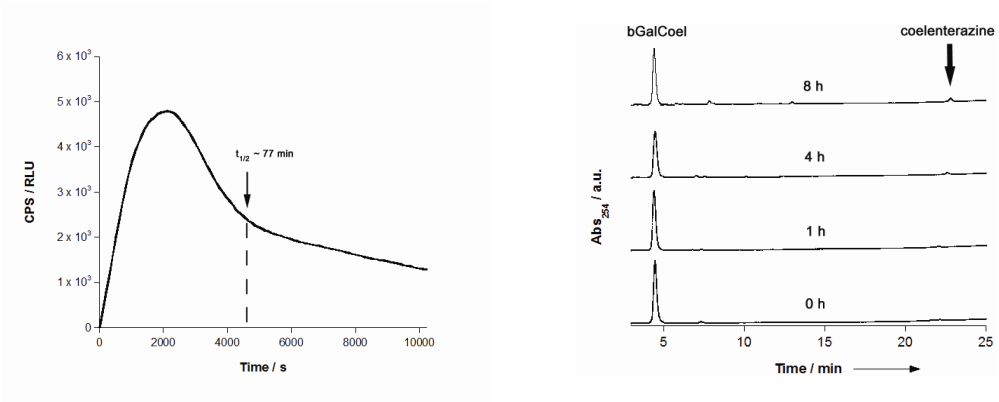

Figure 3. **(Left)** Extended kinetic luminescence profile of bGalCoel; cleavage by ß-galactosidase measured by light output of *GLuc* (left); Reaction conditions: 5 µM bGalCoel, 2U ß-gal, 3 mM $MgCl_2$, *Gaussia* luciferase, 0.1 M PBS (pH 7.4); Total light output measured in luminometer (100 s for 100 repeats). **(Right)** Cleavage reaction of bGalCoel with ß-gal, monitored by HPLC. Reaction conditions: 100 µM bGalCoel, 8U ß-gal, 3 mM $MgCl_2$, 1% DMSO in PBS buffer (0.02% Tween) (pH 7.4) at 37°C.

Design, Synthesis and Properties of bGalNoCoel

Due to slow kinetics in the cleavage of bGalCoel with β-Gal we re-designed our substrate by incorporating a self-immolative nitrobenzyl linker between the coelenterazine and β-galactose moiety as previously described (Scheme 3).[15]

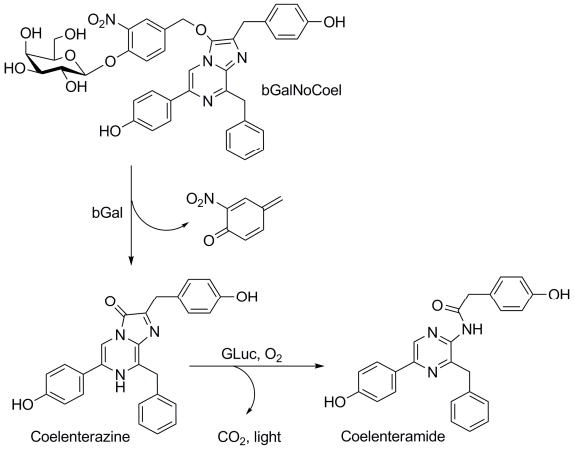

Scheme 3. Cleavage of bGalNoCoel by β-galactosidase generates free coelenterazine that is oxidized by *Gaussia* luciferase in a light producing reaction.

We named this new substrate as bGalNoCoel (Figure 1). bGalNoCoel was synthesized in 6 steps (Scheme 4). Initially, compound **8** was synthesized from 4-hydroxy-3-nitrobenzaldehyde and 2,3,4,6-tetra-*O*-acetyl-α-D- galactopyranosyl bromide (Scheme S2). The primary alcohol was then reacted with thionyl chloride to give **9**, followed by alkylation with **3** to give the per-*O*-acetylated galactonitrobenzylcoelenterazine derivative **10**. Deacetylation of **10** with sodium methoxide in methanol, followed by purification via reverse phase-HPLC gave bGalNoCoel.

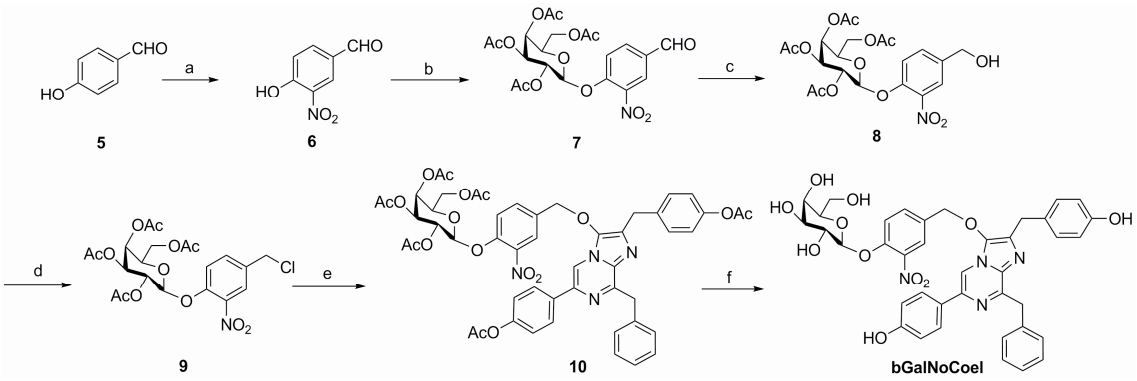

Scheme 4 Synthesis of bGalNoCoel. a) HNO_3, AcOH, MeCN, 90%; b) 2,3,4,6-tetra-O-acetyl-α-D-galactopyranosyl bromide, Ag_2O, MeCN, 66%; c) $NaBH_4$, MeOH, 78%; d) $SOCl_2$, DMAP, CH_2Cl_2, 85%; e) **3**, K_2CO_3, KI, MeCN, 29%; f) NaOMe, MeOH, 20%.

Evaluation of the luminescent properties of bGalNoCoel showed a much faster response than bGalCoel (Figure 4a) and comparable luminescence output to that of native coelenterazine, 78% (Figure 4b). Unlike bGalCoel, bGalNoCoel displayed flash-kinetics with a signal half-life of less than 30 s (Figure 4a).

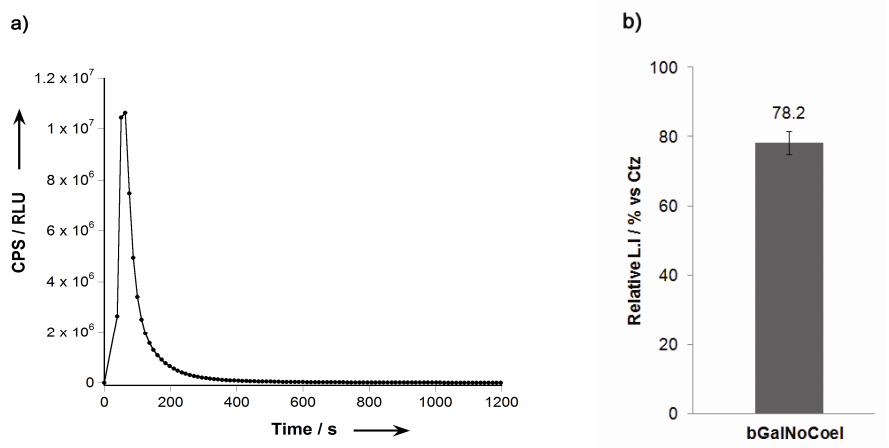

Figure 4. Kinetic profile and relative bioluminescence activity of bGalNoCoel (a) cleavage by β-galactosidase measured by light output of *Gaussia* luciferase; Reaction conditions: 5 μM bGalNoCoel, 2 U β-galactosidase, 3 mM $MgCl_2$, *Gaussia* luciferase, 0.1 M PBS (pH 7.4); Total light output measured in luminometer (12 s × 100). (b) Relative light output of bGalNoCoel versus native coelenterazine (CTZ).

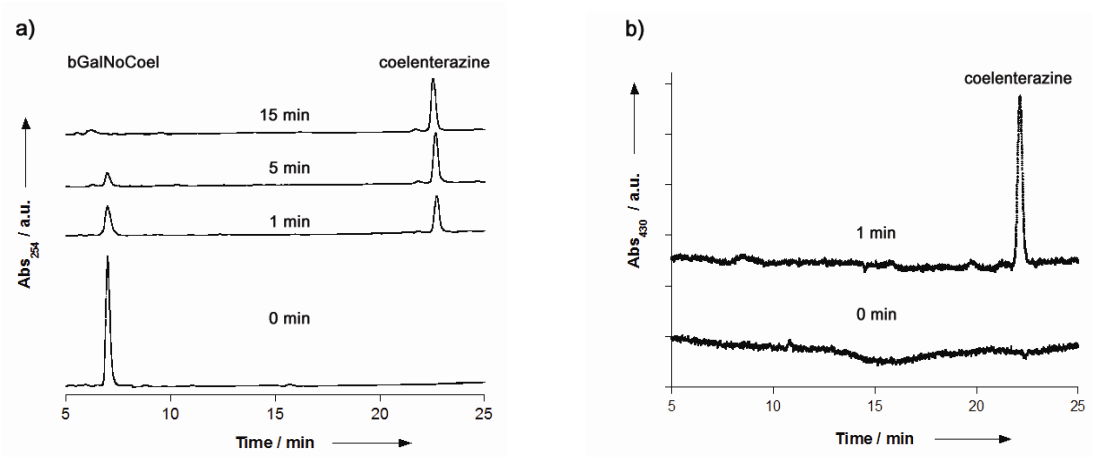

Figure 5. Cleavage reaction of bGalNoCoel with β-galactosidase, monitored by HPLC. Reaction conditions: 100 μM bGalNoCoel, 8U β-galactosidase, 3 mM $MgCl_2$, 1% DMSO in PBS buffer (0.02% Tween) (pH 7.4) at 37°C**.** Eluent: (A) H_2O (0.1% TFA); (B) acetonitrile (0.1% TFA). The percentage of A decreased linearly from 60% at 0 min to 30% at 15 min, followed by a decrease to 10% at 30 min. The flow rate was 1.0 ml/min and was monitored at 254 (a) and 430 nm (b) absorbance.

Monitoring via HPLC indicated a very fast cleavage reaction with the majority of the substrate cleaved after 5 min (Figure 5). No intermediates were detected in the HPLC cleavage reaction. This suggested that the cleavage of the β-galactoside bond was the slowest step in the enzyme-catalyzed hydrolysis cascade.

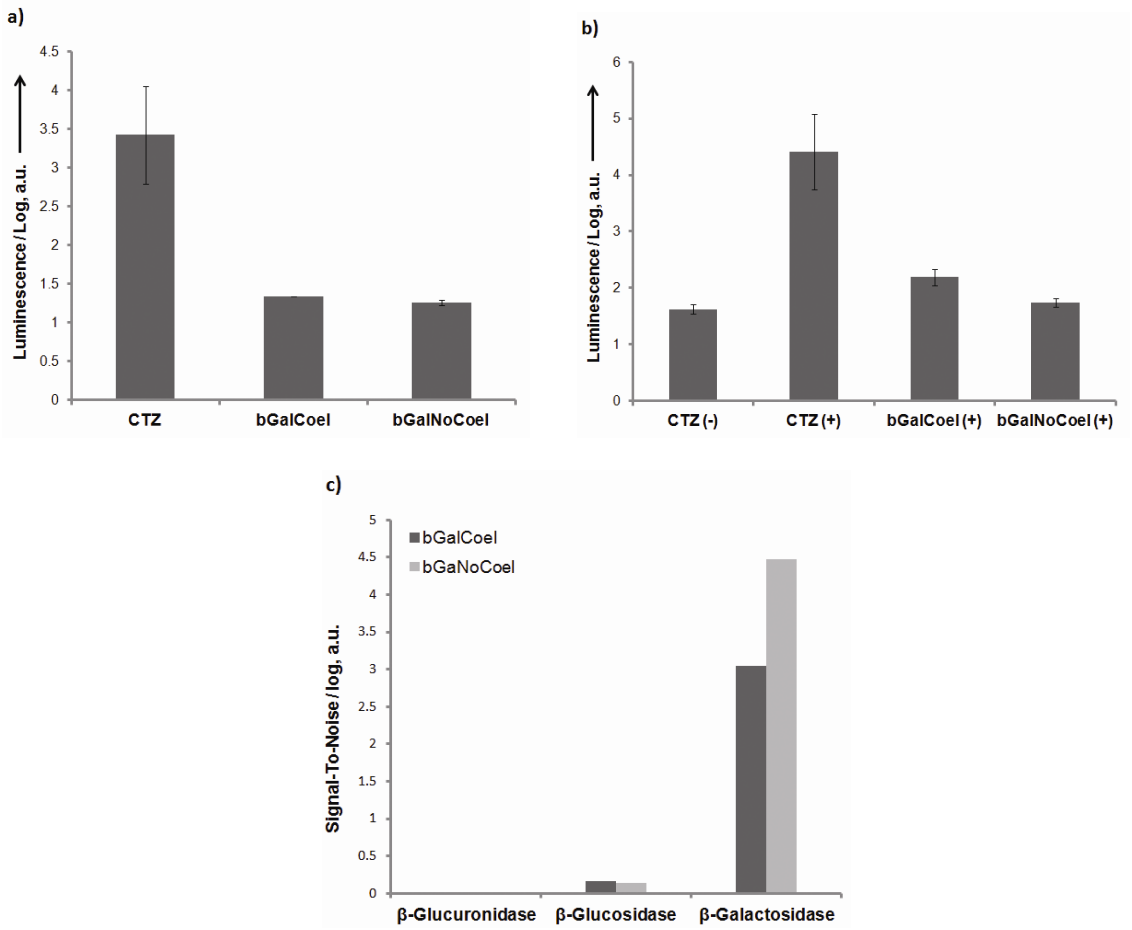

Figure 6. Stability and enzyme specificity of bGalCoel and bGalNoCoel. a) Substrate stability in 2 × 10^4 non-transfected HEK293T cell cultures. Stability was evaluated by directly adding substrate (15 μM) and the resulting light output was measured for 10 min at 37 °C. Experiments were performed in triplicate. b) Substrate stability in presence of BSA. Substrate (final concentration 20 μM) was added to wells containing BSA (final concentration 2% *w*/*v*) in 50 mM HEPES buffer (pH 7.5); c) Relative enzyme specificity of bGalCoel and bGalNoCoel with 3 different glycoside hydrolases. Reaction conditions: bGalCoel or bGalNoCoel (final concentration 5 μM) was added to a well containing *Gaussia* luciferase and 2 U of β-galactosidase, β-glucosidase or β-glucuronidase in 0.1 M PBS (pH 7.4) and the light output was measured for 30 min. Each experiment was repeated three times.

Stability of bGalNoCoel and bGalCoel in non-transfected HEK293T cells was evaluated in comparison with coelenterazine by addition of bGalNoCoel, bGalCoel or coelenterazine to HEK293T cell-cultures, followed by measurement of autoluminescence for 10 min (Figure 6a). Both substrates showed very low levels of autoluminescence under these conditions. It has also been reported that coelenterazine is extremely unstable in presence of serum albumin by acting as a mono-oxygenase that catalyzes the oxidation of coelenterazine, giving rise to background chemiluminescence.

Thus we evaluated the relative stability of bGalNoCoel and bGalCoel against coelenterazine by measuring the autoluminescence levels for 2 min after addition of bGalNoCoel, bGalCoel or coelenterazine to solutions containing bovine serum albumin (BSA)(Figure 6b). Both bGalNoCoel bGalCoel were found to be highly stable in the presence of BSA, whilst coelenterazine displayed high levels of autoluminescence, which agrees with previous publications.[4]

The relative substrate specificity of bGalNoCoel and bGalCoel to β-Gal was compared with two other glycoside hydrolases, β-glucosidase (β-Glc) and β-glucuronidase (β-Glu). Relative cleavage was measured as total luminescence over 30 min in the presence of GLuc. bGalNoCoel and bGalCoel showed over 20000 and 1000-fold higher selectivity towards β-Gal respectively. (Figure 6c).

Next, we evaluated the relative bioluminescence activity in 2×10^4 living HEK293T cells expressing a mutant GLuc (GLucM23) with a KDEL, endoplasmic reticulum localization peptide sequence (GLucM23er). GLucM23 does not display the same flash-type kinetics, rather a more stable glow-type signal. In addition, GLucM23 has roughly 10 times higher luminescence output over the wild-type luciferase in the context of BLI with living cells. bGalCoel or bGalNoCoel was added to cells expressing GLucM23er and β-Gal or just the luciferase (Figure 4a). Maximum luminescence signal intensity was obtained approximately 2 min after addition of bGalNoCoel. bGalNoCoel showed a high signal-to-noise ratio (S/N = 524)(Figure 7a). The bioluminescent emission from cells expressing β-Gal and GLucM23er was proportionally dependent on the cell numbers, and as few as ~300 intact cells were detected in the presence of 25 μM bGalNoCoel (Figure 7b). The observed contrast (signal-to-noise ratio) was also proportionally dependent on the cell numbers (Figure 7c). These results demonstrate that bGalNoCoel is cell-permeable and able to detect the β-galactosidase activity in living mammalian cells. bGalCoel on the other hand showed very poor relative bioluminescence activity compared with coelenterazine, with a 100-fold weaker output. Initially this was attributed to poor cell-membrane permeability of the substrate.

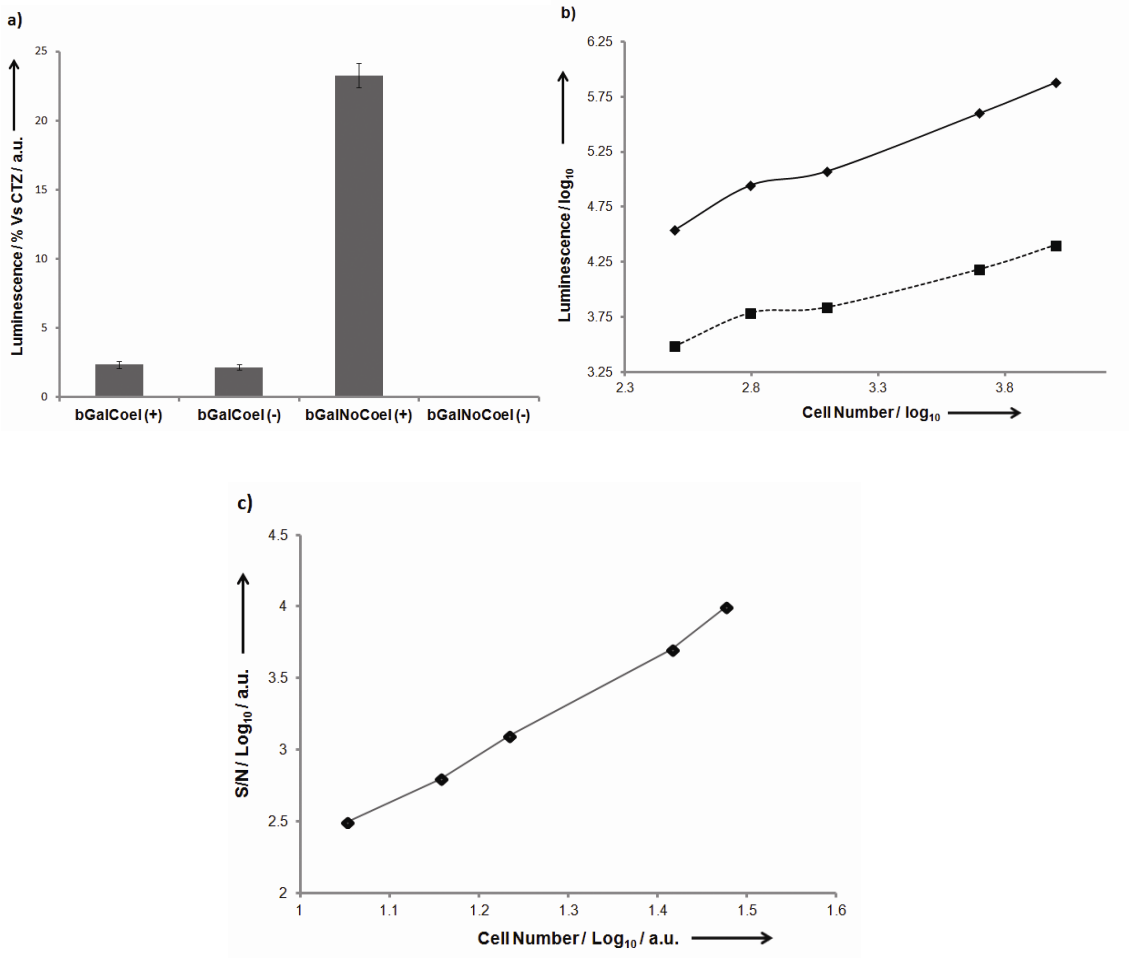

Figure 7. Bioluminescence assays of HEK293T cells transfected with GLucM23 with bGalCoel and bGalNoCoel a) Relative bioluminescence of bGalCoel and bGalNoCoel versus native coelenterazine (CTZ) in ~ 2 × 10^4 HEK293T cells transfected with GLucM23-Venus-KDEL and in the presence (+) and in the absence (-) of β-Gal. b) Bioluminescence output dependence on cell number with bGalNoCoel in the presence (◆) and in the absence (■) of β-Gal and $GLucM23_{ER}$ c) Dependence of contrast (S/N) on cell number with bGalNoCoel. Reaction conditions: 25 μM substrates, 37 °C; total light output measured in luminometer every 10 s for 100 repeats.

However, significant luminescence was also observed in the absence of β-Gal which suggested that free coelenterazine was generated from bGalCoel independently of the expression of β-Gal. The relative signal-to-noise ratio (S/N) was just above 1. In a separate experiment, we evaluated the relative bioluminescent activity of bGalCoel with

HEK293T cells expressing *Renilla* luciferase, another commonly used coelenterate luciferase. In this case the signal-to-noise ratio was even lower (data not shown). Hence the instability of bGalCoel itself seemed to be related to the expression of GLucM23 itself. However, as bGalCoel was shown to be stable in the presence of secreted GLuc under cell-free assay conditions, with a signal-to-noise ratio of over 2300, the non-specific luminescence of bGalCoel does not seem to be related to the luciferase itself. Interestingly it was also shown that bGalCoel was highly stable in non-transfected HEK293T cell cultures (Figure 6a). In addition, we also investigated whether the nature of the transfection agent could have any influence on the stability of bGalCoel. Luminescence was measured after addition of bGalCoel to solutions containing GLuc and one of the following transfection agents: Lipofectamine 2000™, Lipofectamine LTX™, FuGene™, and Xtreme Gene™. No significant difference could be observed between the experimental or control groups (Figure 8). Therefore, we are currently uncertain about the cause of the observed instability of bGalCoel in luciferase-expressing cells. From the available data, it seems to suggest that the poor bioluminescence response of bGalCoel observed in living cells is the result of several factors including slow cleavage kinetics, poor cell-membrane permeability and auto-cleavage due to instability of the substrate.

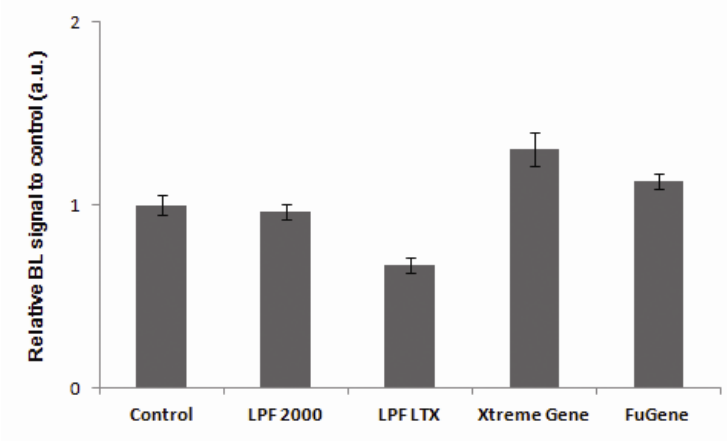

Figure 8. Showing influence of various transfection agents on stability of bGalCoel. Reaction conditions: 5 µM bGalCoel, GLuc, 0.1 M PBS (pH 7.4), with of without 1 µl transfection agent.

Dual Gene-Reporter Assay

Finally we investigated whether coelenterazine, generated after cleavage of bGalNoCoel by β-Gal-expressing cells, would readily diffuse out of the cells or be

retained inside. We excluded bGalCoel on the premise that it was earlier shown to have poor S/N in living cells (Figure 7a). In addition to the *lacZ* gene, we also utilized two different GLucM23-expressing plasmid vectors, localizing GLucM23 to cell membrane surface (mem) or endoplasmic reticulum (er) respectively (Figure 8). The luminescence profiles of HEK293T cells expressing the luciferase together with β-Gal were compared against the luciferase and β-Gal being independently expressed and combined before addition of bGalNoCoel. We combined 2 sets of 1×10^4 cells where GlucM23 and β-Gal expressed seperately, giving a cell ratio of 1:1. If coelenterazine could freely diffuse out of cells, we hypothesized that the average time to reach maximum luminescence (T_{Lmax}) should be related to the relative distance between the sites of expression of the luciferase and β-Gal, *i.e.* the shortest distance would be the set of cells co-expressing GLucM23er/β-Gal whilst the longest distance would be between the set of cells independently expressing GLucM23er + β-Gal. Therefore, the following trend in terms

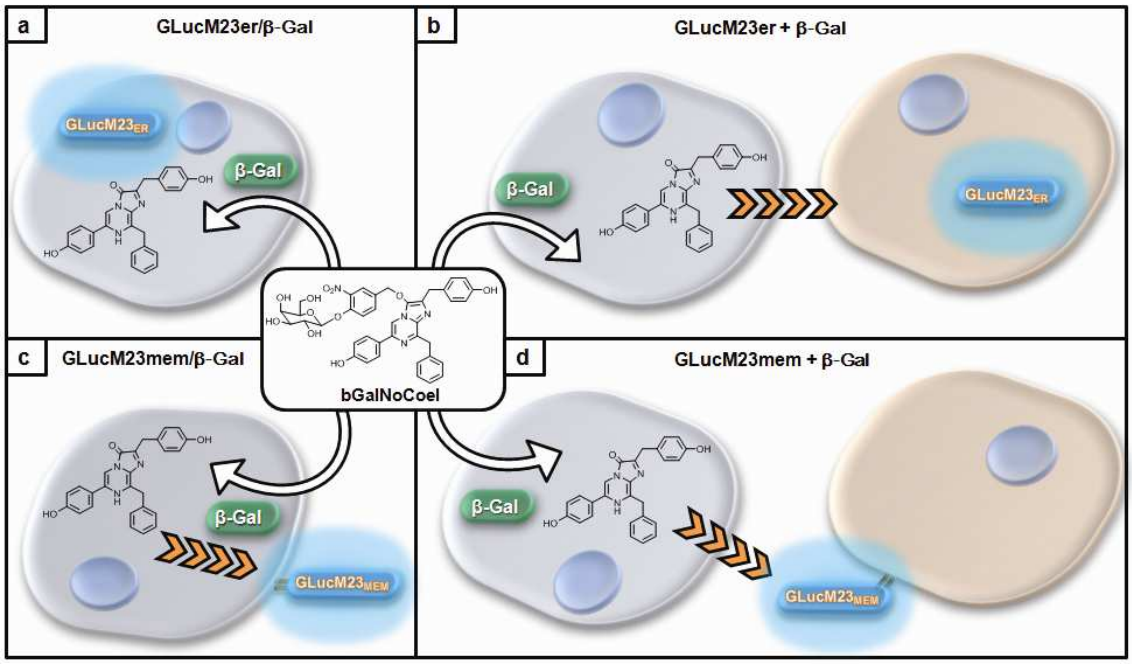

Figure 8. Showing the concept of dual-gene reporter assay of GLucM23 and β-Gal with bGalNoCoel in living cells. bGalNoCoel diffuses into cells and gets cleaved by β-Gal. The generated coelenterazine will readily diffuse and become oxidized by GLucM23 to generate luminescence: a) Cells co-expressing $\mathrm{GLucM2_{ER}}$ and β-Gal; b) Mixture of 2 cell populations expressing $\mathrm{GLucM2_{ER}}$ and β-Gal separately; c) Cells co-expressing $\mathrm{GLucM23_{MEM}}$ and β-Gal; Mixture of 2 cell populations expressing $\mathrm{GLucM2_{MEM}}$ and β-Gal separately. Orange broken arrows indicates extracellular diffusion of coelenterazine.

of T_{Lmax} would be expected: GLucM23er/β-Gal < GLucM23mem/β-Gal < GLucM23mem + β-Gal < GLucM23er + β-Gal. Statistical analysis of the observed data however, indicated the following trend: GLucM23er/β-Gal < GLucM23mem/β-Gal << GLucM23mem + β-Gal = GLucM23er + β-Gal (Figure 6). We could not observe a significant difference between the means of GLucM23mem + β-Gal and GLucM23er + β-Gal. However we could show from our data that after the β-galactose moiety of bGalNoCoel gets cleaved by β-Gal, the resulting coelenterazine diffused from the cytosol to the extracellular environment. Hence bGalNoCoel could potentially function as a dual-gene reporter in two different cell-populations, where the β-Gal-expressing cells could be thought of as 'producers' of coelenterazine from bGalNoCoel, whilst the GLucM23- expressing cells could be labeled as 'detectors'.

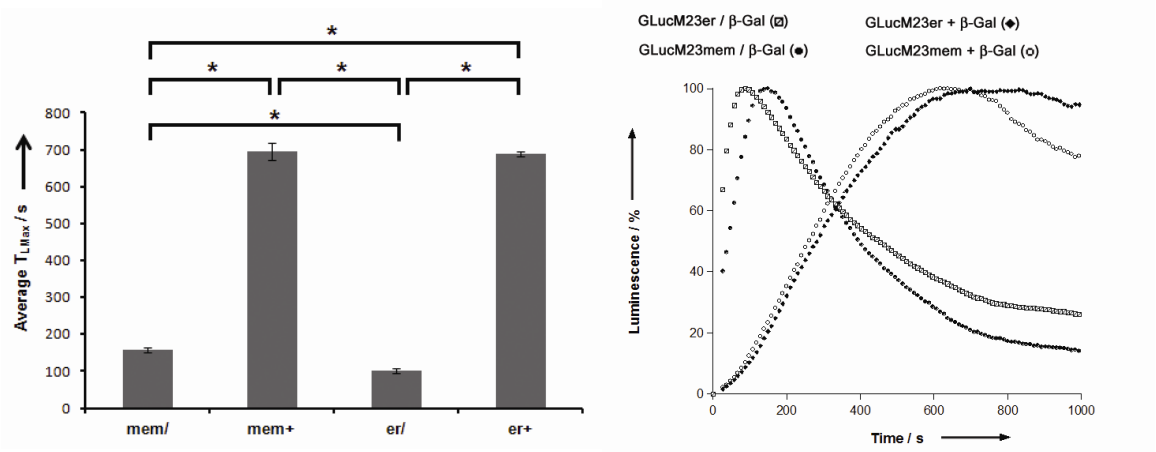

***Figure 9*. (left)** Representative mean T_{LMax} values of bGalNoCoel (25 µM) with 2×10^4 HEK293T cells co-transfected (/) or independently transfected (+) with GLucM23 (mem = surface membrane bound; er = endoplasmic reticulum localization) and β-Gal. Luminescence was measured in luminometer at 37 °C every 10 s for 100 repeats. Statistical analyses were performed with a two-tailed Student's t-test. *P < 0.01 (n=4), and errors bars indicate standard error of mean. **(right)** Representative luminescence profiles of bGalNoCoel (25 µM) with HEK293T cells co-transfected (/) or independently transfected (+) with GLucM23 (mem = surface membrane bound; er = endoplasmic reticulum localization) and β-Gal. Luminescence was measured in luminometer at 37 °C every 10 s for 100 repeats. Note: These curves are not mean values, they are from single experiments that are closest to the mean T_{LMax} shown in Table 1.

Table 1. Average time to reach maximum luminescence for bGalNoCoel in HEK293T cells expressing; GLucM23 (Mem = Membrane bound; ER = Endoplasmic Reticulum localized) and β-Gal. (n = 4)

	$GLuc_{Mem}$/β-Gal	**$GLuc_{Mem}$+β-Gal**	**$GLuc_{ER}$/β-Gal**	**$GLuc_{ER}$+β-Gal**
T_{Lmax} (s) [a]	157.5 (± 7.5 s)	694.25 (± 22.6 s)	101.5 (± 2.7 s)	689 (± 6.1 s)

[a] Time to reach relative maximum luminescence signal.

Conclusions

We have designed and synthesized two caged coelenterazine derivatives, bGalCoel and bGalNoCoel. The probes were cleaved by β-galactosidase to generate free coelenterazine which can then go on to react with *Gaussia* luciferase to generate a bioluminescent signal. Our aim was to create bioluminogenic coelenterate substrates that could detect β-galactose activity. Both substrates showed very low autoluminescence in living cell cultures and high specificity for β-galactosidase over other glycoside hydrolases. However, bGalCoel showed a very slow cleavage reaction profile with β-galactosidase, and poor signal to noise ratio when measuring β-galactosidase activity in living cell cultures. We found that incorporation of a 4-hydroxy-3-nitrobenzyl linker between the β-galactose and the coelenterazine moiety (bGalNoCoel) greatly improved the kinetic profile, overall stability, luminescence output, and signal to noise ratio when detecting β-galactosidase activity in living cells compared with our first generation substrate bGalCoel.

Using bGalNoCoel, we could also show that coelenterazine, generated from β-Gal expressing cells, could readily diffuse to other cells after uncaging by β-galactosidase. Thus bGalNoCoel could be used as a dual-reporter in two different cell-populations where the 'producer' cells, expressing β-galactosidase, generate free coelenterazine by cleavage of bGalNoCoel, the coelenterazine can then diffuse to neigboring 'detector' cells, expressing GLucM23, generating a luminescent reponse.

Existing caged coelenterazine derivatives such as EnduRen™ and ViviRen™ were conceived in part to lower the autoluminescence background signal of the natural substrate and increase the signal-to-noise ratio. However, it has been shown that both of these substrates display similar background signal levels to that of native coelenterazine

in vivo.[2] It is known that reporter gene assays such as Firefly luciferase, used in screening applications can suffer from artifacts due to inhibition by small-molecular weight compounds, many found in typical screening libraries.[16] In a recent study many commonly used reporter gene assays were evaluated against a library of compounds.[17] Reporters such as firefly luciferase, *Renilla* luciferase, and Nanoluc™ all displayed an increase in bioluminescence output caused by inhibitor-based enzyme stabilization. Interestingly few inhibitors were indentified for β-galactosidase and *Gaussia*-Dura (a mutated form of *Gaussia* luciferase). Hence our bGalNoCoel substrate could be a suitable dual-reporter for screening applications. We also hope to further evaluate our dual-reporter substrate for *in vivo* imaging applications in the near future.

Experimental

Materials and Instruments

General reagents and chemicals were purchased from Sigma-Aldrich Chemical Co. (St. Louse, MO), Tokyo Chemical Industries (Tokyo, Japan), and Wako Pure Chemical (Osaka, Japan) and were used without further purification. Silica gel chromatography was performed using BW-300 (Fuji Silisia Chemical Ltd., Greenville, NC). pcDNA4™/TO/myc-His/lacZ was purchased from Life Technologies Corporation (Japan). NMR spectra were recorded on a JEOL JNM-AL400 instrument at 400 MHz for ^{1}H and 100.4 MHz for ^{13}C NMR, using tetramethylsilane as an internal standard. Mass spectra were measured on a Waters LCT-Premier XE mass spectrometer for ESI or on a JEOL JMS-700 for FAB. UV-visible absorbance spectra were measured using a Shimadzu UV1650PC spectrometer. High pressure liquid chromatography (HPLC) analysis was performed with an Inertsil ODS3 column (4.6 × 250 mm, GL Science, Inc. Torrance, CA) using an HPLC system that comprised a pump (PU2080, JASCO) and a detector (MD2010 and FP2020, JASCO). Preparative HPLC was performed with an Inertsil ODS3 column (10.0 × 250 mm)(GL Sciences Inc.) using an HPLC system with a pump (PU-2087, JASCO) and a detector (UV-2075, JASCO). Bioluminescence was measured in 96-optiplate multiwell plates (PerkinElmer Co., Ltd.) using a Wallac ARVO mx / light 1420 Multilabel / Luminescence counter with an auto-injector (PerkinElmer Co., Ltd.). Coelenterazine was synthesized as previously described and stored as 10 mM MeOH/HCl (<1%) solution aliquots in sealed glass ampulles at -80°C.[1,2]

General experimental details for cell-cultures

HEK293T cells were maintained in Dulbecco's Modified Eagle Medium (DMEM)

(Invitrogen), supplemented with 10% fetal bovine serum (FBS) at 37°C under 5% CO_2. *Transfection*: Optimem (Invitrogen) solutions containing lipofectamine 2000 (Invitrogen) and plasmid DNA were added to HEK293T cell cultures and incubated at 37°C under 5% CO_2 for 24 h. Cells were then washed three times with PBS, trypsinized, washed with Leibovitz's L-15 medium, then resuspended in black 96-well optiplates (PerkinElmer) and incubated at 37 °C in luminometer (PerkinElmer).

Preparation of secreted *Gaussia* luciferase

HEK293T cells maintained in DMEM (no phenol red) supplemented with 10% FBS and transfected with pCM-GLuc (New England Biolabs) were incubated at 37 °C under 5% CO_2 for 24 h. The cell-medium was carefully transferred to a separate tube, centrifuged to remove any cells. The supernatant was aliquoted and stored at −80 °C.

1. Synthesis of bGalCoel

Imidazo[1,2-*a*]pyrazin-3-ol,6-[4-(acetyloxy)phenyl]-2-[[4-(acetyloxy)phenyl]methyl]-8-(phenylmethyl)-3-acetate (1). To a solution of coelenterazine (480 mg, 1.13 mmol) in acetic anhydride (5 ml) was added 4-dimethylaminopyridine (367 mg, 3 mmol) and the reaction was stirred at room temperature under argon over night. Excess acetic anhydride was removed *in vacuo* and the remaining residue was subjected to flash column silica chromatography, EtOAc/CH_2Cl_2 (1:9), yielding the product (1) as a dark red sticky solid (323 mg, 76%). ^{1}H NMR (400 MHz, $CDCl_3$**)** δ 2.19, 2.29, 2.32 (s, 3H x 3 (AcO x 3)) 4.16 (s, 2H) 4.18 (s, 2H) 7.02 (d, 2H, ^3J = 8.4 Hz) 7.17 (d, 2H, ^3J = 8.4 Hz) 7.31-7.21 (m, 5H) 7.58 (d, 2H, ^3J = 8.0 Hz) 7.74 (s, 1H) 7.89 (d, 2H, ^3J = 8.0 Hz). ESI-MS $[M+H]^+$ Calc: 550.2045; Found: 550.1038.

Imidazo[1,2-*a*]pyrazin-3(7*H*)-one,6-[4-(acetyloxy)phenyl]-2-[[4-(acetyloxy)phenyl] methyl]-8-(phenylmethyl) (2) (Inoue, S., Sugiura, S., Kakoi, H., Murata, M., Goto, T.. *Tetrahedron Lett.* **1977**, *31*, 2685–2688.) To an ice-cooled solution of Imidazo[1,2-*a*]pyrazin-3(7*H*)-one,6-[4-(acetyloxy)phenyl]-2-[[4-(acetyloxy)phenyl] methyl]-8-(phenylmethyl) (201 mg, 0.37 mmol) in CH_2Cl_2 (3 ml) was added 1% NH_3 in MeOH (3 ml) and the reaction was stirred at 0°C under an argon atmosphere. The reaction was monitored by TLC until no more starting material remained (~ 30 min), after which the solution was evaporated to dryness and dried *in vacuo* and used without further purification.

2-(4-((2-(4-acetoxybenzyl)-6-(4-acetoxyphenyl)-8-benzylimidazo[1,2-a]pyrazin-3-yl oxy)-2,3,4,6-tetra-*O*-acetyl-β-*D*-galactopyranoside (3). To an ice-cooled solution of imidazo[1,2-*a*]pyrazin-3(7*H*)-one,6-[4-(acetyloxy)phenyl]- 2-[[4-(acetyloxy)phenyl] methyl]-8-(phenylmethyl) (50 mg, 0.09 mmol) in CH_2Cl_2 (2 ml) was added 1% NH_3 in MeOH (1 ml) and the reaction was stirred at 0°C under an argon atmosphere for 1 h. The solution was evaporated to dryness and dried *in vacuo* and used without further purification. To a solution of **3** (~0.09 mmol) in anhydrous DMF was added 2,3,4,6-tetra-*O*-acetyl-β-D-galactopyranosyl bromide (106 mg, 0.26 mmol) and Cs_2CO_3 (47 mg, 0.14 mmol). The reaction was degassed by bubbling argon for 30 mins and stirred at room temperature over night. The reaction mixture was filtered and solvent was evaporated *in vacuo*. The residue was extracted with ethyl acetate, and the combined organic layers were washed with brine, dried with Na_2SO_4, filtered, and concentrated *in vacuo*. Silica gel flash chromatography ($MeOH/CH_2Cl_2$; 1:99) gave **3** as a dark red solid (36 mg, 48%).^{1}H NMR (400 MHz, $CDCl_3$**)** δ2.01, 2.04, 2.11. 2.17, 2.30, 2.33 (6s, 18H, AcO x 6) 4.06 ($^3J_{H6a,H5}$ = 6.8, 0.8 Hz) 4.19-4.04 (m, 2H, H5, H6b) 4.26 (dd, $^2J_{H6a,H6b}$ = 11.4, $^3J_{H6a,H5}$ = 6.8 Hz, $^3J_{H1,H2}$, 1H, H6a) 4.24-4.11 (m, 4H, H6a/b, CH_2) 4.58 (s, 2H, CH_2) 4.91 (d, $^3J_{H1,H2}$ = 8.0 Hz, 1H, H1) 5.07 (dd, $^3J_{H3H2}$= 10.4, $^3J_{H3,H4}$ = 3.4 Hz, 1H, H3) 5.44 (d, $^3J_{H4,H3}$ = 3.6,1H, H4) 5.50 (dd, $^3J_{H2,H3}$ = 10.0, $^3J_{H2,H1}$ = 7.6 Hz, 1H, H2) 6.89 (d, 2H, ^3J = 8.0 Hz) 7.01 (d, 2H, ^3J = 8.0 Hz) 7.33-7.16 (m, 5H) 7.76 (d, 2H, ^3J = 8.0 Hz) 7.57 (d, 2H, ^3J = 8.0 Hz) 8.17 (s, 1H) ^{13}C NMR (100 MHz, $CDCl_3$**)** δ 170.43, 170.32, 170.11, 169.91, 169.57, 169.32, 156.91, 152.36, 149.27, 138.75, 137.77, 136.45, 135.05, 133.36, 132.60, 129.62, 129.55, 128.87, 128.22, 127.58, 126.42, 121.74, 115.90, 108.92, 104.41, 90.56, 71.50, 70.49, 68.36, 66.82, 61.10, 39.29, 31.99, 21.03, 20.75, 20.65, 20.61, 20.48, 20.16.ESI-MS [M+H]+ Calc:838.2818; Found: 838.1728.

2-(4-((2-(4-hydroxybenzyl)-6-(4-hydroxyphenyl)-8-benzylimidazo[1,2-a]pyrazin-3-y loxy)-β-*D*-galactopyranoside (bGalCoel) To an ice-chilled solution of **3** (40 mg, 0.048 mmol) in dry MeOH (2 ml) was added a methanolic solution (1 ml) of NaOMe (15 mg, 0.28 mmol) and stirred under argon for 4.5 h. The reaction was quenched with acetic acid (20 µl) and the solution was evaporated to dryness. The residue was dissolved in acetonitrile/water (0.1% HCO_2H) and purified via reverse phase HPLC; acetonitrile/water (30:70 → 70:30). The collected fractions were lyophilized to give bGalCoel as a red/orange solid (12 mg, 44%) ^{1}H NMR (400 MHz, $(CD_3)_2CO$) δ 3.85-3.46 (m, 10H) 4.35 (s, 2H) 4.67 (d, 1H, ^{3}J = 7.6 Hz) 6.62 (d, 2H, ^3J = 8.8 Hz) 6.80 (d, 2H, ^3J = 8.8 Hz) 7.16-7.09 (m, 5H) 8.56 (s, 1H) 7.45 (d, 2H, ^3J = 8.8 Hz) 7.79 (d, 2H, ^3J = 8.8Hz); ^{13}C NMR (100 MHz, $CDCl_3$) δ 159.25, 156.77, 152.75, 140.17, 139.34,

137.30, 135.90, 133.67, 131.64, 130.79, 130.37, 129.49, 129.27, 128.81, 127.45, 116.46, 116.10, 110.84, 108.88, 77.13, 74.74, 72.23, 69.85, 39.78, 32.15. ESI-MS [M+H]+ Calc: 586.2184; Found: 586.1821; FAB $[M+H]^+$ Calc: 586.2184; Found: 586.2174.

2. Synthesis of bGalNoCoel

4-hydroxy-3-nitrobenzaldehyde (6) A solution of 4-hydroxybenzaldehyde (2.46 g, 20.1 mmol) in acetonitrile (40 ml), with acetic acid (20 ml) and concentrated nitric acid (1.5 ml) was refluxed for 3 h. The solution was cooled to room temperature, poured into water, and extracted with EtOAc (x3). The organic layer was washed with brine, dried with sodium sulfate, filtered, and concentrated *in vacuo* to give **4** as a brown solid (3.03 g, 90%), and used without further purification.

1-(4-formyl-2-nitrophenyl)-2,3,4,6-tetra-*O*-acetyl-β-D-galactopyranoside (7) To a solution of 2,3,4,6-tetra-*O*-acetyl-α-D- galactopyranosyl bromide (2.0 g, 4.86 mmol) in dry acetonitrile (40 ml) was added 4-hydroxy-3-nitrobenzaldehyde (0.93 g, 5.54 mmol) and silver oxide (1.32 g, 5.71 mmol). The solution was stirred overnight in the dark at room temperature under argon. The solution was filtered through a pad of celite and concentrated *in vacuo.* The residue was dissolved in ethyl acetate and washed with saturated $NaHCO_3$ and brine. The organic layer was dried under Na_2SO_4, filtered, and concentrated *in vacuo*. Purification by flash chromatography with ethylacetate/hexane (2:3) gave **5** as a white solid (1.61 g, 66%). ^{1}H-NMR (400 MHz, $CDCl_3$) δ 2.03, 2.08, 2.13, 2.20 (4 s, 12H, AcO x 4) 4.29-4.10 (m, 3H, H5, H6) 5.14 (dd, $^3J_{H3,H2}$= 10.2, $^3J_{H3,H4}$= 3.4 Hz, 1H, H3) 5.22 (d, $^3J_{H1,H2}$ = 8.0 Hz, 1H, H1) 5.50 (d, $^3J_{H4,H3}$ = 2.8 Hz, 1H, H4) 5.59 (dd, $^3J_{H2,H3}$ = 10.4, $^3J_{H2,H1}$ = 8.2 Hz, 1H, H2) 7.49 (d, ^3J = 8.4 Hz, 1H, ArH) 8.07 (dd, ^4J = 2.0 Hz ^3J =8.4 Hz, 1H, ArH) 8.31 (d, ^4J = 2.0 Hz,1H, ArH) 9.98 (s, 1H, CHO). ESI(+) $[M+Na]^+$ Calculated: 520.1062; Found: 520.0409.

1-(hydroxymethyl-2-nitrophenyl)-2,3,4,6-tetra-*O*-acetyl-β-D-galactopyranoside (8) To a solution of $NaBH_4$ (100 mg, 2.64 mmol) in $MeOH/CH_2Cl_2$ (1:1, 5 ml) was added 1-(4-formyl-2-nitrophenyl)-2,3,4,6-tetra-*O*-acetyl-β-D-galactopyranoside (650 mg, 1.31 mmol) dropwise over 5 mins at 0°C. The reaction was monitored via TLC and quenched after 2 h with 20% NH_4Cl (3 ml) and evaporated to dryness. The residue was dissolved and extracted with ethyl acetate. The organic layer was washed with brine, dried under Na_2SO_4, filtered, and concentrated *in vacuo*. Purification by flash chromatography, ethyl acetate/hexane (3:2), yielded **6** as a white solid, (509 mg, 78%). ^{1}H-NMR (400 MHz,$CDCl_3$) δ 2.19, 2.13, 2.07, 2.02 (4s, 12H, OAc x 4) 4.19-4.04 (m, 2H, H5, H6b)

4.26 (d, $^{2}J_{H6a,H6b}$ = 11.2, $^{3}J_{H6a,H5}$ = 6.8 Hz, $^{3}J_{H1,H2}$, 1H, H6a) 4.73 (s, 2H, benzylic) 5.06 (d, $^{3}J_{H1,H2}$ = 8.0 Hz, 1H, H1) 5.11 (dd, $^{3}J_{H3H2}$ =10.6, $^{3}J_{H3,H4}$ = 3.4 Hz, 1H, H3) 5.45 (d, $^{3}J_{H4,H3}$ = 3.2Hz, 1H, H4) 5.54 (dd, $^{3}J_{H2,H3}$ = 10.0, $^{3}J_{H2,H1}$ = 7.6 Hz, 1H, H2) 7.36 (d, ^{3}J = 8.4 Hz, 1H, ArH) 7.52 (dd, ^{4}J = 2.2 Hz ^{3}J = 8.6 Hz, 1H, ArH) 7.81 (d, ^{4}J = 2.4 Hz, 1H, ArH). ESI(+) $[M+Na]^{+}$ Calculated: 522.1218; Found: 522.0551.

1-(chloromethyl-2-nitrophenyl)-2,3,4,6-tetra-*O*-acetyl-β-D-galactopyranoside (9) To a solution of 1-(hydroxymethyl-2-nitrophenyl)-2,3,4,6-tetra-*O*-acetyl-β-D-galacto-pyranoside (160 mg, 0.32 mmol) in dry CH_2Cl_2 (5 ml) was added thionyl chloride (50 µl, 0.69 mmol) and a catalytic amount of DMAP (4 mg, 0.03 mmol) at 0°C. The solution was stirred at 0 °C under an argon atmosphere for 5 hrs and poured into water. The organic layer was amply washed with water, followed by brine, drying under Na_2SO_4, filtered, and concentrated *in vacuo*. The product **7**, a white solid (141 mg, 85%) was used without further purification. ^{1}H-NMR (400 MHz, $CDCl_3$) δ 2.02, 2.08, 2.13, 2.19 (4s, 12H, AcO x 4) 4.08 (m, H5) 4.17 (dd, $^{2}J_{H6b,H6a}$= 11.2, $^{3}J_{H6b,H5}$ = 6.0 Hz, 1H, H6b) 4.26 (dd, $^{2}J_{H6a,H6b}$ = 11.4, $^{3}J_{H6a,H5}$ = 6.8 Hz, 1H, H6a) 4.58 (s, 2H, benzylic) 5.06 (d, $^{3}J_{H1,H2}$ = 7.6 Hz, H1) 5.11 (dd, $^{3}J_{H3H2}$ = 10.6, $^{3}J_{H3,H4}$ = 3.4 Hz, 1H, H3) 5.45 (d, $^{3}J_{H4,H3}$ = 3.4Hz, 1.0 Hz, 1H, H4) 5.55 (dd, $^{3}J_{H2,H3}$ = 10.4, $^{3}J_{H2,H1}$ = 7.6 Hz, 1H, H2) 7.37 (d, 1H, ^{3}J = 8.8 Hz, ArH) 7.56 (dd, 1H, ^{3}J = 8.8, Hz, ^{4}J = 2.4 Hz, ArH) 7.84 (d, 1H, ^{4}J = 2.4 Hz, ArH) ^{13}C-NMR (100 MHz, $CDCl_3$) δ20.57, 20.65, 20.68, 44.18, 61.33, 66.68, 67.79, 70.50, 71.50, 100.70, 120.07, 125.24, 133.52, 133.67, 141.18, 149.15, 169.38, 170.13, 170.16, 170.30. ESI(+) $[M+Na]^{+}$ Calculated:540.0879; Found: 540.1243. ESI(-) $[M+HCO_2]^{-}$ Calculated: 562.0969; Found: 562.1071. HRMS (FAB(+)) $[M+Na]^{+}$ Calculated: 540.0879; Found: 540.0887.

2-(4-((2-(4-acetoxybenzyl)-6-(4-acetoxyphenyl)-8-benzylimidazo[1,2-a]pyrazin-3-yl oxy)methyl)-2-nitrophenoxy)-2,3,4,6-tetra-*O*-acety-l-β-D-galactopyranoside (10) To a solution of 2-(4-Hydroxybenzyl)-6-(4-hydroxyphenyl)-8-(phenylmethyl)-imidazo[1,2-a]pyrazin-3(7H)-one (151 mg, 0.30 mmol) in dry acetonitrile (2 ml) was added 1-(chloromethyl-2-nitrophenyl)- 2,3,4,6-tetra-*O*-acetyl-β-D-galactopyranoside (300 mg, 0.58 mmol), potassium carbonate (15 mg, 0.11 mmol), potassium iodide (57 mg, 0.34 mmol). Argon was bubbled through the solution for 30 mins and the solution was stirred at room temperature under argon for 10 h. Water was added and the solution was extracted with ethyl acetate. The organic layer was washed with brine, dried under Na_2SO_4, filtered, and concentrated *in vacuo*. Purification by flash chromatography, 0.1% MeOH – 1% MeOH/CH_2Cl_2, yielded **8** as a red/brown gummy solid (87 mg,

29%).^{1}H-NMR (400 MHz, $CDCl_3$) δ 2.01, 2.04, 2.11. 2.17, 2.30, 2.33 (6s, 18H, AcO x 6) 4.06 ($^{3}J_{H6a,H5}$ = 6.8, 0.8 Hz) 4.19-4.04 (m, 2H, H5, H6b) 4.26 (dd, $^{2}J_{H6a,H6b}$ = 11.4, $^{3}J_{H6a,H5}$ = 6.8 Hz, $^{3}J_{H1,H2}$, 1H, H6a) 4.24-4.11 (m, 4H, H6a/b, CH_2) 4.58 (s, 2H, CH_2) 4.84 (s, 2H, CH_2) 4.91 (d, $^{3}J_{H1,H2}$ = 8.0 Hz, 1H, H1) 5.07 (dd, $^{3}J_{H3H2}$= 10.4, $^{3}J_{H3,H4}$ = 3.4 Hz, 1H, H3) 5.44 (d, $^{3}J_{H4,H3}$ = 3.6,1H, H4) 5.50 (dd, $^{3}J_{H2,H3}$ = 10.0, $^{3}J_{H2,H1}$ = 7.6 Hz, 1H, H2) 7.19 (d, ^{3}J = 8.8 Hz, 2H, ArH) 7.32-7.21 (m, 7H, ArH) 7.58 (d, ^{3}J = 6.4 Hz, 1H, ArH) 7.64 (s, 1H, ArH) 7.77 (s, 1H, ArH) 7.86 (d, ^{3}J = 8.4 Hz, 1H, ArH). ^{13}C-NMR (100 MHz,$CDCl_3$) δ20.57, 20.61, 20.66, 21.11, 21.15, 32.94, 39.99, 61.18, 66.72, 67.73, 70.35, 71.28, 75.10, 75.10, 100.40, 108.63, 119.39, 121.69, 122.05, 124.95, 126.50, 127.24, 128.29, 129.63, 129.67, 131.16, 132.31, 133.26, 133.55, 134.35, 136.36, 136.56, 137.82, 141.03, 149.28, 149.66, 150.98, 152.99, 169.30, 169.49, 169.66, 170.04, 170.17, 170.23. ESI(+) [M+H]+ Calculated: 989.3087; Found: 989.3397. HRMS (FAB(+)) $[M+H]^+$ Calculated: 989.3087; Found: 989.3073.

2-(4-((2-(4-hydroxybenzyl)-6-(4-hydroxyphenyl)-8-benzylimidazo[1,2-a]pyrazin-3-yloxy)methyl)-2-nitrophenoxy)-β-D-galactopyranoside (bGalNoCoel) To a cooled solution of 2-(4-((2-(4-acetoxybenzyl)-6-(4-acetoxyphenyl)-8-benzylimidazo-[1,2-a]pyrazin-3-yloxy)methyl)-2-nitrophenoxy)-2,3,4,6-tetra-*O*-acetyl-β-D-galactopyranoside (69 mg, 0.07 mmol) in dry MeOH (2 ml) was added sodium methoxide in MeOH (0.2 M, 1.4 ml, 4 eq.) and the solution was stirred under argon and monitored via TLC and ESMS and additional sodium methoxide was added until all acetate groups had been cleaved. Dowex 50w H^+ resin was added and the solution was filtered through a cotton plug and evaporated to dryness. The residue was dissolved in acetonitrile/water and purified via reverse phase HPLC; acetonitrile/water (30:70 → 70:30). The collected fractions were lyophilized to give bGalNoCoel as a red sticky solid (10 mg, 20%).^{1}H-NMR (400 MHz, $CDCl_3$) δ3.45 (dd, $^{3}J_{H3H2}$ =10.0, $^{3}J_{H3,H4}$ = 4.0 Hz, 1H, H3) 3.57 (m, 1H, H5) 3.63 (m, 2H, H6a/b) 3.71 (dd, $^{3}J_{H2,H3}$ = 10.0, $^{3}J_{H2,H1}$ = 8.0 Hz, 1H, H2) 3.88 (s, 2H, CH_2) 3.79 (d, $^{3}J_{H4-H3}$ = 4.0 Hz, 1H, H4) 4.37 (s, 2H, CH_2) 4.82 (d, 1H, $^{3}J_{H1-H2}$ = 8.0 Hz, 1H, H1) 4.86 (s, 2H, CH_2) 6.59 (d, ^{3}J = 8.6 Hz, 2H, ArH) 6.74 (d, ^{3}J = 8.4 Hz, 2H ArH) 6.94 (d, ^{3}J = 8.6 Hz, 2H, ArH) 7.15-7.04 (m, 3H, ArH) 7.24 (d, 1H, ^{3}J = 8.8 Hz, ArH) 7.35-7.29 (m, 3H, ArH) 7.59 (d, ^{3}J = 8.4 Hz, 2H, ArH) 7.62 (d, 1H, ^{4}J = 1.2 Hz, ArH) 7.89 (d, 1H, ^{3}J = 1.6 Hz, ArH). ^{13}C-NMR (100 MHz, $CDCl_3$) δ 32.91, 39.75, 62.29, 70.05, 71.90, 74.74, 76.27, 77.30, 103.02, 109.56, 116.34, 116.57, 118.92, 126.54, 127.49, 128.87, 129.13, 129.33, 130.31, 130.66, 130.86, 131.46, 133.22, 135.30, 135.48, 138.00, 139.26, 140.40, 141.80, 152.03, 157.03, 159.31. ESI(+) $[M+H]^+$ Calculated; 737.2453; Found: 737.2450. FAB(+) $[M+H]^+$ Calculated:737.2453;

Found: 737.2406

Determination of relative bioluminescence activity of GLucM23 compared to wild-type GLuc (Figure S1): HeLa cells in glass-bottom dishes, transfected with pDisp-mKO-GLuc or pDisp-mKO-GLucM23 were maintained in Dulbecco's Modified Eagle Medium (DMEM)(Invitrogen), supplemented with 10% fetal bovine serum (FBS) at 37°C under 5% CO_2 for 24 hours. Cells were washed with Hank's balanced salt solution (HBSS) (pH ~ 7.4). 100 µL HBSS was then carefully added. mKO fluorescence was measured ($548_{\lambda ex}/561_{\lambda em}$; 200 ms), after which a solution of HBSS, containing 25 µM of coelenterazine was added. We then measured the luminescence with an Olympus DP30 Cooled Monochrome CCD Microscope Camera; obj. × 60; with an exposure time of 20 seconds at an open filter setting. Obtained images were processed in imageJ. The average BL/FL was obtained from 5 cells from each respective image.

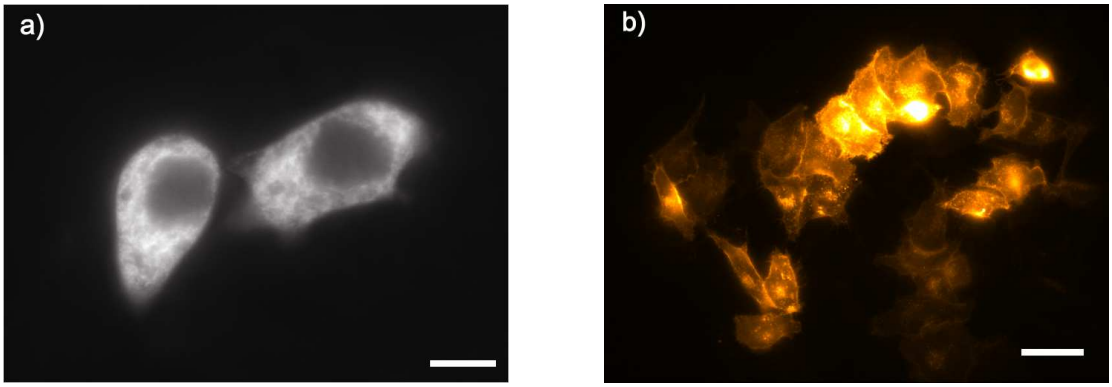

Figure S2. Showing Fluorescence images of GLucM23-Venus-KDEL (a) or mKO-GLucM23 (b) in HeLa cells. (a) Venus localized to endoplasmic reticulum ($515_{\lambda Ex}/528_{\lambda Em}$, 300 ms) Scalebar: 10 µm; (b) mKO localized to outer cell membrane ($548_{\lambda Ex}$ /$561_{\lambda Em}$; 200 ms) Scalebar: 50 µm.

Cleavage reaction of bGalCoel and bGalNoCoel by beta-galactosidase monitored by HPLC. To a solution containing bGalCoel or bGalNoCoel (100 µM), $MgCl_2$, DMSO (1%) in PBS buffer (0.1 M, pH 7.4,Tween 0.02%) was added 8 units of β-galactosidase, and the solution was incubated at 37 °C. Samples were taken at specific time intervals (bGalCoel: 0, 1, 4, and 8 h; (bGalNoCoel: 0, 1, 5, 15, 30, and 60 min.)

diluted with acetonitrile (0.1% TFA), filtered and analyzed by HPLC, or stored in liquid nitrogen until HPLC analysis. Absorbance was monitored at 254 nm.

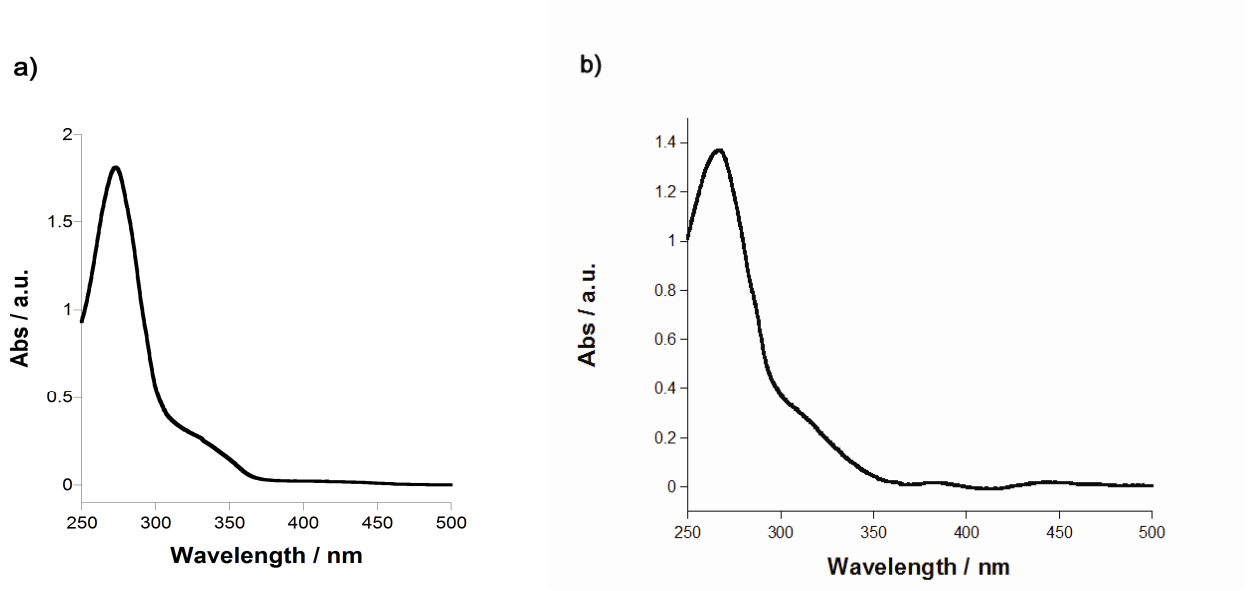

Figure S4 a) Absorbance spectrum of bGalCoel (30 µM in MeOH; b) Absorbance spectrum of bGalNoCoel (50 µM) in MeOH.

References

(1) A. Pichler, J. L. Prior, D. Piwnica-Worms, *Proc. Natl. Acad. Sci.* **2004**, *101*, 1702-1707.

(2) (a) T. Kimura, K. Hiraoka, N. Kasahara, C. R. Logg, *J. Gene Med.* **2010**, *12*, 528. (b) M. K. Wendt, J. Molter, C. A. Flask, W. P. Schiemann, *J. Vis. Exp*. **2011**, *56*, e3245.

(3) E. M. Hawkins in *Bioluminescence & Chemiluminescence: Progress & Current Applications* (Eds.; P.E. Stanley, L.J. Kricka., World Scientific, Singapore, **2002**, pp. 149.

(4) (a) N. Vassel, C. D. Cox, R. Naseem, V. Morse, R.T. Evans, R .L. Power, A. Brancale, K. T. Wann, A. K. Campbell, *Luminescence* **2012**, *27*, 234. (b) M. Keyaerts, C. Heneweer, L. O. Tchouate Gainkam, V. Caveliers, B. J. Beattie, G. A. Martens, C. Vanhove, A. Bossuyt, R. G. Blasberg, T. Lahoutte, *Mol. Imaging Biol.* **2011**, *13*, 59-66.

(5) S. Inouye, Y. Sahara-Miura, J-I. Sato, R. Iimori, S. Yoshida. T. Hosoya, *Prot.Exp.Pur.* **2013**, *88*, 150.

(6) M. P. Hall, J. Unch, B. F. Binkowski, M. P. Valley, B. L. Butler, M.G. Wood, P. Otto, K. Zimmerman, G. Vidugiris, T. Machleidt, M. B. Robers, H. A. Benink, C. T. Eggers, M. R. Slater, P. L. Meisenheimer, D. H. Klaubert, F. Fan, L. P. Encell, K. V. Wood, *ACS Chem. Biol.* **2012**, *7*, 1848-1857.

(7) J. Levi, A. De, Z. Cheng, S. Gambhir, *J. Am. Chem. Soc.* **2007**, *129*, 11900-11901.

(8) Chen, Y.; Chi, Y.; Wen, H.; Lu, Z. *Anal. Chem.* **2007**, *79*, 960–965.

(9) (a) Wehrman, T. S.; von Degenfeld, G.; Krutzik, P. O.; Nolan, G. P.; Blau, H. M. *Nat. Methods* **2006**, *3*, 295-301. (b) Li, J.; Chen, L.; Du, L.; Li, M. *Chem. Soc. Rev.* **2013**, *42*, 662-676.

(10) Geiger, R.; Schneider, E.; Wallenfels, K.; Miska, W. *Biol. Chem. Hoppe-Seyler* **1992**, *373*, 1187-1191.

(11) von Degenfeld, G.; Wehrman, T. S.; Blau, H. M. *Methods Mol. Biol.* **2009**, *574*, 249-259.

(12) Inoue, S.; Okada, K.; Tanino, H.; Kakoi, H. *Chem. Lett.* **1987**, 417-418.

(13) Inoue, S; Sugiura, S.; Kakoi, H.; Hashizume, K.; Goto, T.; Iio, H. *Chem. Lett.* **1975**, 141-144.

(14) Tannous, B. A.: Kim, D-E.; Fernandez, J. L.; Weissleder, R.; Breakefield, X. O. *Mol. Ther.* **2005**, *11*, 435-443.

(15) Ho, N-H.; Weissleder, R.; Tung, C-H. *ChemBioChem* **2007**, *8*, 560-566.

(16) Auld, D. S.; Southall, N. T.; Jadhav, A.; Johnson, R. L.; Diller, D. J.; Simeonov, A.; Austin, C.P.; Inglese, J. *J. Med. Chem.* **2008**, *51*, 2372-2386

(17) Ho, P-I.; Yue, K.; Pandey, P.; Breault, L.; Harbinski, F.; McBride, A. J.; Webb, B.; Narahari, J.; Karassina, N.; Wood, K. V.; Hill, A.; Auld, D. S. *ACS Chem. Biol.* **2013**, *16*, 1848-1857.

Chapter 2.2 Development of Hydrogen Peroxide Activatable Coelenterazine Derivatives

(In preparation)

In chapter 2.1, I demonstrated that blocking of coelenterazine with an enzymatic substrate is a viable strategy to effectively stabilize native coelenterazine. The dual-enzyme substrate, bGalNoCoel, could detect enzyme activity across two separate cell populations. To further expand the scope of activatable-coelenterazines I designed a coelenterazine-boronate derivative that could be activated by hydrogen peroxide, a reactive oxygen species implicated in a variety of physiological phenomena.

Introduction, probe design, and synthesis.

Reactive oxygen species (ROS) like hydrogen peroxide have been implicated in playing a major role in various diseases including cardiovascular disorders[1], diabetes[2] neurodegenerative diseases[3], and cancer[4]. Hydrogen peroxide has also been shown to have significance in events related to inflammation[5], aging[6], post-translational modifications of proteins and various signaling cascades.[7] An large array of various luminescent molecular probes for the detection of hydrogen peroxide has been reported. [8] An ample fraction of these are fluorescent probes utilizing caging boronic acid esters as selective switch for the detection of hydrogen peroxide. Nucleophilic addition of reactive species to electron-deficient boronate probes has prompted their use as effective traps of ROS and RNS in biological systems. Nucleophilic addition of hydrogen peroxide to the boron results in a charged tetrahedral boronate complex, which undergoes a 1,2-insertion featuring a boron to oxygen migration of the ipso-carbon (Scheme 1). The resulting borate ester is then hydrolyzed by water to the phenol.[9]

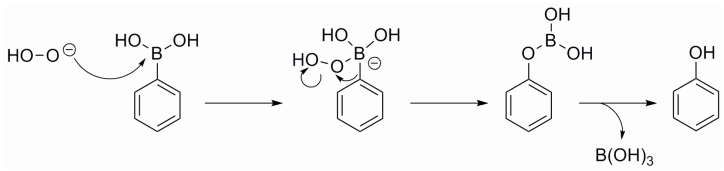

Scheme 1. Reaction mechanism of hydrogen peroxide with boronic acid.

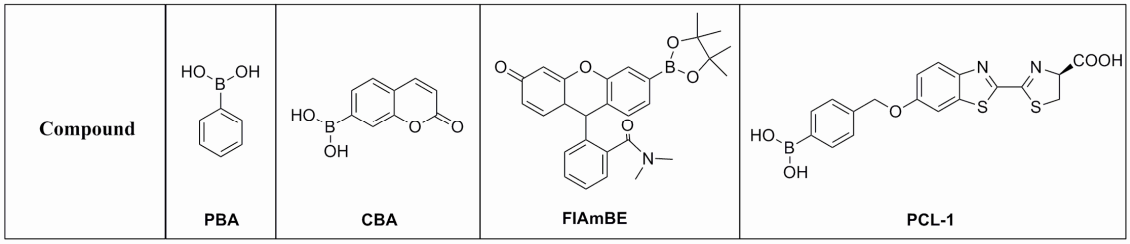

Figure 1. Structures of boronic acid and ester probes. ; adopted from reference [10].

Chang *et al.* created a bioluminescent reporter (PCL-1)(Figure 1), a boronate-D-luciferin conjugate for measuring of H_2O_2 fluxes in living animals.[11] More recently the same group also reported the PCL-2, a pre-bioluminogenic substrate that forms D-luciferin *in situ* and reports on both hydrogen peroxide and caspase activity *in vivo*.[12] In addition to the limitations of using FLuc mentioned in chapter 1 and 2 it was recently reported that FLuc activity can be altered when hydrogen peroxide levels become elevated, which can potentially lead to ambiguous or misleading findings.[13] Interestingly the same study also reported that a variant of *Renilla* luciferase, RLuc8, was far less sensitive to ROS. We reasoned that by utilizing an activatable boronate-coelenterazine probe together with GLuc, the brightest of known luciferases, it would be possible to obtain an even better S/N as the reaction of H_2O_2 with boronic acid is extremely slow (k ~ 1-2 M^{-1} s^{-1}).[10] Hence in a similar vein to that of the design of bGalNoCoel described in Chapter 2.1, we designed a coelenterazine-boronate derivative with a self-immolative benzyl linker, naming it Coel-BeBA (Scheme 2). The phenolic boronic acid group will upon reacting with hydrogen peroxide result in the generation of the phenol, which will trigger the self-elimination of the linker and generation of coelenterazine which can then undergo subsequent reaction with its coelenterate luciferase to give a bioluminescence signal (Scheme 2).

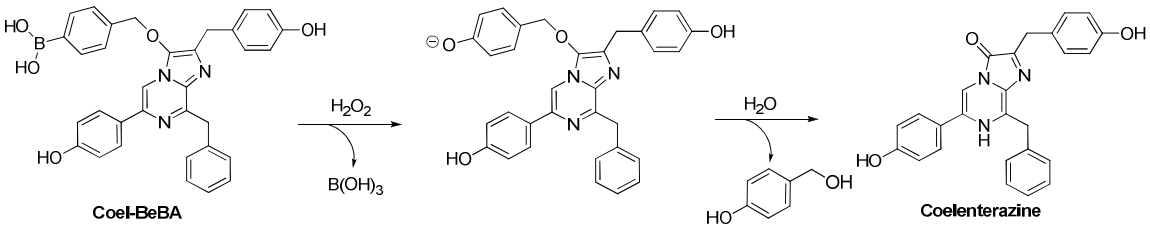

Scheme 2. Design strategy for H_2O_2-mediated release of coelenterazine from Coel-BeBA

Coel-BeBA was synthesized in a similar fashion to bGalNoCoel described in chapter 2. **2** was obtained by halogen-lithium exchange reaction of 4-iodotoluene with bis(pinacolato)diboron as the electrophile, followed by the apple-reaction to generate **3** (Scheme 3.). The di-(CTZ(OAc)$_2$) and tri-acetylated coelenterazine (CTZ(OAc)$_3$) starting materials were prepared as described in chapter 2.1. Alkylation of CTZ(OAc)$_2$ with **3** was conducted in DMF and cesium carbonate in order to minimize C-alkylation at the 2 position of coelenterazine (see appendix).

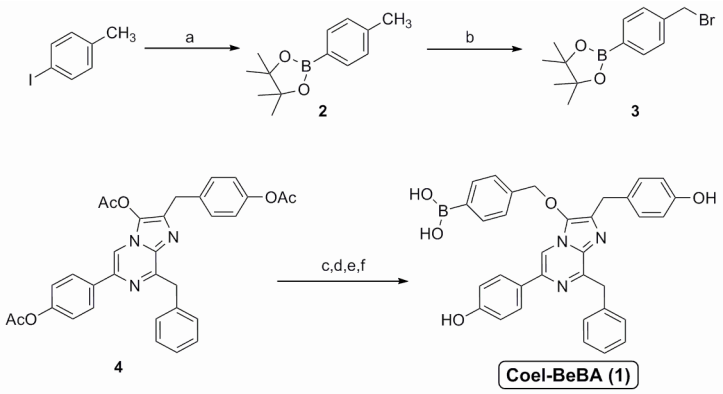

Scheme 3. Synthesis of Coel-BeBA. a) *t*-BuLi, B_2Pin_2, THF, -40 °C, 4.5 h, 40%; b) AIBN, NBS, MeCN, reflux, 20 h, 69%; c) 1% NH_3 in MeOH, CH_2Cl_2, 0 °C, 75 min; d) **3**, Cs_2CO_3, DMF, rt, 12 h; e) NaOMe, MeOH, 0 °C, 4.5 h; f) MeCN / H_2O (0.1 % HCO_2H), 12 h, rt, 9% over 4 steps.

Sensitivity and selectivity of Coel-BeBA for hydrogen peroxide.

First the relative responsiveness of Coel-BeBA to changes in hydrogen peroxide concentrations was evaluated. Coel-BeBA and GLuc were incubated with alternating concentrations of hydrogen peroxide (0-100 µM) and the total photon flux was measured for 1 h (Figure 2.). It was possible to obtain physiologically relevant

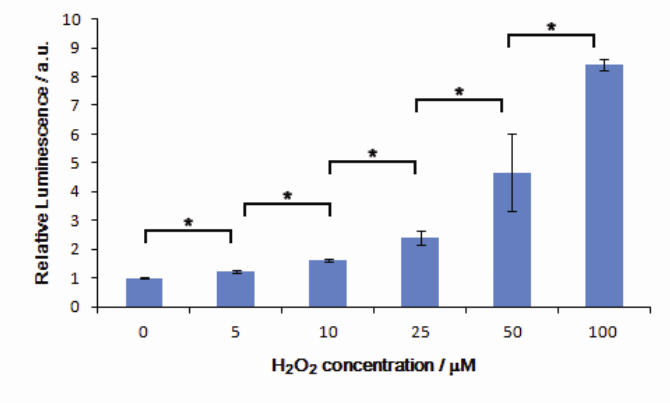

Figure 2. 10 µM Coel-BeBA and GLuc with various concentrations of H_2O_2 in 0.1 M PBS (pH 7.4). Total photon count was measured over 1 h. Statistical analysis was performed with a two-tailed Student's *t*-test. *p < 0.05, and error bars are ±SEM; n = 3.

low-micromolar detection of hydrogen peroxide. Having established that Coel-BeBA could detect changes in H_2O_2 levels in a dose-dependent fashion down to physiologically relevant concentrations we next investigated the selectivity of Coel-BeBA over other ROS (Figure 3). Coel-BeBA and GLuc were incubated with various ROS, including H_2O_2 in the presence and absence of catalase, a H_2O_2-degrading enzyme. Total photon flux was then measured for 1 h. Little to no relative signal increase was observed when Coel-BeBA was reacted with other ROS or H_2O_2 in the presence of catalase.

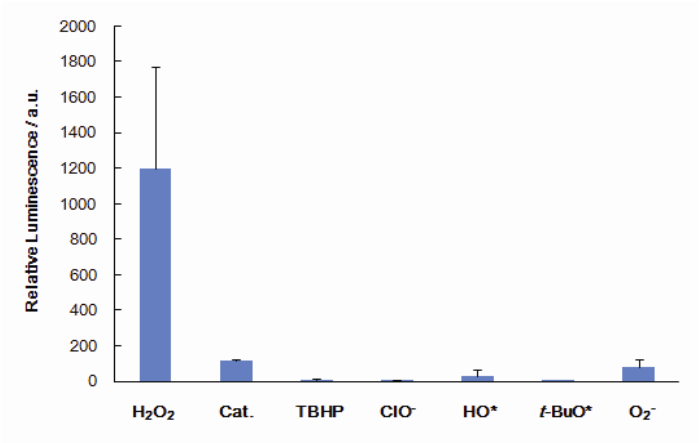

Figure 3. 10 μM Coel-BeBA with various reactive oxygen species (100 μM) and GLuc in 0.1 M PBS (pH 7.4). Total photon count measured over an hour in luminometer. Cat: 0.4 mg / mL catalase. HO* and *t*-BuO* radicals were generated from 1 mM $FeCl_2$ solution and 100 μM H_2O_2 or 100 μM *t*-BuOOH respectively. Solid KO_2 in DMSO (final concentration: 100 μM) was used as a source for O_2^- ; and error bars are ±SEM; n = 3.

Detection of changes in H_2O_2 levels with Coel-BeBA in living cells.

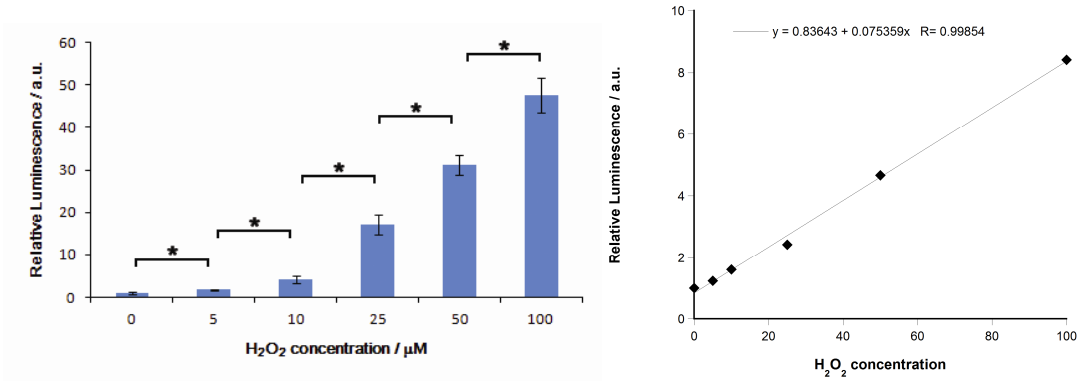

Figure 4. Detection of exogenous H_2O_2 with Coel-BeBA in HEK293T cells expressing GLucM23-Venus-KDEL. Bar graph representation (left). Linear correlation graph (right). Upon addition of Coel-BeBA (25 μM) and H_2O_2 (0-100 μM) total photon flux was measured for 2 h. Statistical analysis was performed with a two-tailed Student's *t*-test. *$p < 0.01$, and error bars are ±SEM; n = 3.

Next it was determined whether the performance of Coel-BeBA could be translated to living cell culture (Figure 4.). Coel-BeBA and various concentrations of H_2O_2 (0-100 µM) were added to HEK293T cells expressing GLucM23-Venus-KDEL (ER-localizing). Photon flux was measured for 2 h. Experiments demonstrated that exogenous addition of H_2O_2 to live-cell assays did not interfere with production of the H_2O_2-dependent bioluminescent signal of Coel-BeBA and demonstrated a linear response to H_2O_2 *in cellulo*. Subsequently we moved on to investigate the possibility to detect endogenously generated H_2O_2 in living cells with Coel-BeBA. RAW264 cells expressing GLucM23-Venus-KDEL were incubated with phorbol 12-myristate 13-acetate (PMA) because PMA activates protein kinase c (PKC) in macrophages which results in the subsequent activation of NADPH-oxidase (NOX) and the generation of H_2O_2.[14] Following incubation with PMA for 1 h, Coel-BeBA was added and after incubation for 10 min the total photon flux was measured for 10 min. (Figure 5.) PMA-treated cells showed statistically significantly ($p < 0.05$) higher bioluminescent signal derived from Coel-BeBA compared to non-stimulated cells. Hence it was possible to detect H_2O_2 generation in living cells with Coel-BeBA, which demonstrates that this probe is sensitive enough to changes in biologically relevant H_2O_2 concentrations.

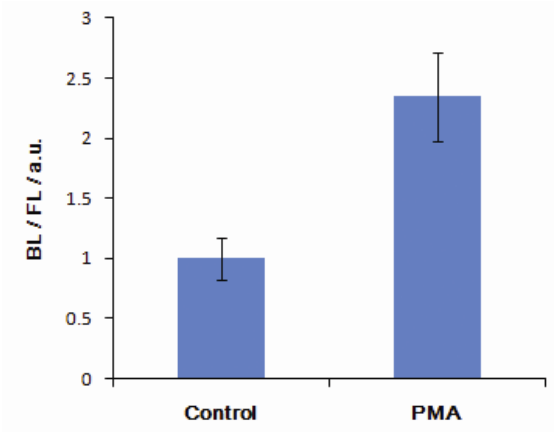

Figure 4. Showing relative bioluminescence and relative bioluminescence/fluorescence (venus) ratio for RAW264 cells transfected with GLucM23-Venus-KDEL and incubated with PMA (3.0 µg / ml) for 1 h. Coel-BeBA was added incubated for 10 min after which total photon count was measured for 10 min. Statistical analysis was performed with a two-tailed Student's *t*-test. *$p < 0.05$, and error bars are ±SEM; n = 4.

Conclusions

A coelenterazine-boronic acid conjugate probe was developed for the selective detection of hydrogen peroxide. In a similar method used to synthesize bGalNoCoel, Coel-BeBA was synthesized with only minor formation of the c-alkylated product (see appendix). It could be established that Coel-BeBA had high specificity for H_2O_2 over other ROS tested. Coel-BeBA, with GLucM23, was able to detect exogenous and endogenous

H_2O_2 in living cells. Thus it was demonstrated that activatable-coelenterazines, in addition to the detection of enzyme activity, can be designed to detect bioactive molecules such as H_2O_2 in living systems. For further improvement it might be appropriate to replace the free boronic acid moiety with a boronate ester. In a recent patent from Promega, detection of H_2O_2 with various D-luciferin-boronic acid and boronate ester derivatives was investigated.[15] It was shown that not only is the reaction between the boronate and H_2O_2 pH-dependent, but also the type of buffer had significant impact on the luminescence output. Interestingly it was also shown that while derivatives containing the free boronic acid had an overall higher luminescence output over the boronate ester derivatives, however, a poorer signal-to-noise profile. Thus similar structure-activity relationships might be observed with coelenterazine-boronate conjugates as well and requires further investigation.

Experimental

Materials and Instruments

General reagents and chemicals were purchased from Sigma-Aldrich Chemical Co. (St. Louse, MO), Tokyo Chemical Industries (Tokyo, Japan), and Wako Pure Chemical (Osaka, Japan) and were used without further purification. Silica gel chromatography was performed using BW-300 (Fuji Silisia Chemical Ltd., Greenville, NC). NMR spectra were recorded on a JEOL JNM-AL400 instrument at 400 MHz for ^{1}H and 100.4 MHz for ^{13}C NMR, using tetramethylsilane as an internal standard. Mass spectra were measured on a Waters LCT-Premier XE mass spectrometer for ESI or on a JEOL JMS-700 for FAB. UV-visible absorbance spectra were measured using a Shimadzu UV1650PC spectrometer. High pressure liquid chromatography (HPLC) analysis was performed with an Inertsil ODS3 column (4.6 × 250 mm, GL Science, Inc. Torrance, CA) using an HPLC system that comprised a pump (PU2080, JASCO) and a detector (MD2010 and FP2020, JASCO). Preparative HPLC was performed with an Inertsil ODS3 column (10.0 × 250 mm)(GL Sciences Inc.) using an HPLC system with a pump (PU-2087, JASCO) and a detector (UV-2075, JASCO). Bioluminescence was measured in 96-optiplate multiwell plates (PerkinElmer Co., Ltd.) using a Wallac ARVO mx / light 1420 Multilabel / Luminescence counter with an auto-injector (PerkinElmer Co., Ltd.) or ImageQuant LAS 4000 mini (GE Healthcare Life Sciences).

In vitro H_2O_2 experiments

To black 96-well plates containing 5 μL Gluc, 180 μL PBS (0.1 M, pH 7.4), 10 μL Coel-BeBA (final concentration 10 μM) was added 5 μL aqueous solution of H_2O_2 (final concentration 0-100 μM). Total luminescence output was recorded for 1 h. The relative luminescence was determined using Image J.

Specificity against other ROS

Fig.10 10 μM Coel-BeBA with various reactive oxygen species (100 μM) and GLuc in 0.1 M PBS (pH 7.4). Total photon count measured over an hour in luminometer. Cat: 0.4 mg / mL catalase. HO* and *t*-BuO* radicals were generated from 1 mM $FeCl_2$ solution and 100 μM H_2O_2 or 100 μM *t*-BuOOH respectively. Solid KO_2 in DMSO (final concentration: 100 μM) was used as a source for O_2^- ; experiments were repeated in triplicate.

Measuring extragenous H_2O_2 in HEK293T cells expressing GLucM23-Venus-KDEL

HEK293T cells grown in Dulbecco's modified Eagle's medium, supplemented with 10% fetal bovine serum, were transfected with pcDNA3-GLucM23-Venus-KDEL and incubated at 37 °C, 5% CO_2 for 24 h. Cells were washed with PBS (0.1 M, pH 7.4), and trypsinized. 2×10^4 cells were suspended in black microplates containing Leibovitz's L15 medium (no phenol red). Coel-BeBA in PBS (final concentration 25 μM) and aqueous solutions of H_2O_2 (0-100 μM) were added. Total luminescence output was recorded for 2 h. The relative luminescence was determined using Image J.

RAW264 with PMA

RAW264 cells were grown in minimum essential medium supplemented with 10% fetal bovine serum and 100 mg / mL non-essential amino acids. Cells were washed with PBS (0.1 M, pH 7.4), trypsinized, and scraped. 1×10^4 cells were suspended in black microplates Leibovitz's L15 medium (no phenol red). Phorbol 12-myristate 13-acetate (PMA)(final concentration 3 μg / μL) in DMSO was added, or DMSO was added and incubated for 1 h (37 °C, 5% CO_2). Coel-BeBA in PBS (final concentration 20 μM) was added and cells were further incubated for 10 min. Venus fluorescence was measured and total luminescence was recorded for 10 min.

Synthesis of Coel-BeBA

4,4,5,5-tetramethyl-2-para-tolyl-1,3,2-dioxaborolane (1)

To a solution of 4-iodotoluene (1 g, 8.06 mmol) in anhydrous THF (10 mL) cooled to -40 C° under an argon atmosphere was added *t*-BuLi (12 mL, 19 mmol). The solution was stirred for 1 h under argon, after which bis(pinacolato)diboron (2.25 g, 8.87 mmol) in anhydrous THF (5 mL). After 3.5 h the reaction was quenched with an aqueous solution of NH_4Cl (20%). The solution was extracted with EtOAc and the combined organic layer was washed with brine, dried over anhydrous Na_2SO_4, and concentrated *in vacuo*. The residue was subjected to silica gel chromatography with EtOAc / Hexane (1:4), yielding **1** (702 mg, 3.2 mmol, 40 %).^{1}H-NMR (400 MHz,$CDCl_3$) δ = 7.70 (d, ^3J = 8.0 Hz, 2H, ArH) 7.18 (d, ^3J = 8.0 Hz, 2H, ArH, b) 2.36 (s, 3H, CH_3) 1.34 (s, 12H, 4 × CH_3). ^{13}C-NMR (100 MHz,$CDCl_3$) δ = 141.30, 134.80, 128.50, 83.60, 24.85, 21.71.

2-(4-bromomethylphenyl)-4,4,5,5-tetramethyl-1,3,2-dioxaborolane (2)

A solution of 4,4,5,5-tetramethyl-2-para-tolyl-1,3,2-dioxaborolane (517 mg, 2.37 mmol), NBS (550 mg, 3.09), and AIBN (19 mg, 0.12 mmol) in anhydrous MeCN (17 mL) was refluxed for 24 h. The reaction mixture was concentrated *in vacuo*, dissolved in EtOAc, filtered and concentrated *in vacuo*. The residue was subjected to a short silica gel plug (5 % EtOAc / Hexane). The combined fractions were combined and concentrated and dried *in vacuo*, yielding **2** as a white powder (488 mg, 1.64 mmol). ^{1}H-NMR (400 MHz, $CDCl_3$) δ = 7.78 (d, ^3J = 8.0 Hz, 2H, ArH) 7.38 (d, ^3J = 8.0 Hz, 2H, ArH) 4.47 (s, 2H, CH_2) 1.33 (s, 12H, 4 × CH_3) ^{13}C-NMR (100 MHz, $CDCl_3$) δ = 140.38, 134.83, 128.03, 125.44, 83.55, 33.04, 24.65.

Coel-BeBA

To a solution of **CTZ(OAc)$_3$** (100 mg, 0.18 mmol) in CH_2Cl_2 (2 mL) was added 1% NH_3 in MeOH (2 mL) at 0 °C under an argon atmosphere. After 75 min the solution was evaporated to dryness and dried *in vacuo*. The dark residue was dissolved in anhydrous DMF and Cs_2CO_3 was added (53 mg, 0.16 mmol). To this solution was added **2** (56 mg, 0.19 mmol) in DMF (1.45 mL) dropwise over 30 min, under argon flush. The reaction was stirred at rt under argon for 24 h. The solution was poured into H_2O and extracted with EtOAc. The organic layer was washed with brine, dried over Na_2SO_4, and concentrated *in vacuo*. The crude residue was dissolved in anhydrous MeOH, cooled in an ice-bath under an argon atmosphere. To this solution was added NaOMe (15 mg, 0.28 mmol) and the solution was stirred at 0 °C for 2 h. Additional NaOMe was added (45 mg, 0.83 mmol) and after 2 h the reaction was quenched with Dowex 50W H^+ resin,

filtered, and concentrated *in vacuo*. The crude residue was dissolved in a solution of MeCN (10 mL) and H_2O (10 mL)(0.1 % formic acid) and stirred at rt for 12 h. The solution was filtered and subjected to preparative reverse-phase HPLC; gradient: 45 to 70 % MeCN (0.1 % formic acid) (0 to 25 min). The combined fractions were lyophilized giving **Coel-BeBA** as a dark sticky red solid (9 mg, 9 % over 4 steps). ^{1}H-NMR (400 MHz, CD_3OD) δ = 7.66 (s, 1H, ArH, a) 7.53-7.38 (m, 6H, ArH) 7.19-7.06 (m, 5H, ArH) 7.06 (d, ^3J = 8.8 Hz, 2H, ArH) 6.76 (d, ^3J = 8.0 Hz, 2H, ArH) 6.66 (d, ^3J = 8.4 Hz, 2H, ArH) 4.86 (s, 2H, CH_2) 4.41 (s, 2H, CH_2) 3.96 (s, 2H, CH_2); ^{13}C-NMR (100 MHz, CD_3OD) δ = 157.14, 154.91, 151.09, 137.19, 133.43, 131.17, 129.12, 128.98, 128.62, 127.57, 127.36, 127.15, 125.75, 114.84, 114.65, 48.00, 37.99, 31.37; ESMS: Calc: 558.2195; found: 558.1752 $[M+H]^+$.

References

(1) Burgoyne, J. R.; Oka, S-I.: Ale-Agha, N.; Eaton, P. *Antioxidants & Redox Signaling*. March 20, **2013**, *18*, 1042-1052.

(2) Gorin, Y.; Block, K. *Clinical Science* **2013**, *125*, 361-382.

(3) Uttara, B.; Singh, A. V.; Zamboni, P.; Mahajan, R. T. *Curr. Neuropharmacol.* **2009**, *7*, 65-74.

(4) Schumacker, P. T. *Cancer Cell* **2006**, *10*, 175-176.

(5) Wittmann, C.; Chockley, P.; Singh, S. K.; Pase, L.; Lieschke, G. J.; Grabher, C. *Adv. Hematology* **2012**, art. No. 541471.

(6) Finkel, T.; Holbrook, N. J. *Nature* **2000**, *408*, 239-247.

(7) (a) Foreman, J.; Demidchik, V.; Bothwell, J. H. F.; Mylona, P.; Miedema, H.; Torres, M. A.; Linstead, P.; Costa, S.; Browniee, C.; Jones, J. D. G.; Davies, J. M.; Dolan, L. *Nature* **2003**, *422*, 442-446. (b) Groeger, G.; Quiney, C.; Cotter, T. G. *Antioxid. Redox Signalling* **2009**, 11, 2655-2671 (c) Lambeth, J. D. *Nat. Rev. Immunol.* **2004**, 4, 181-1.

(8) (a) Schaferling, M.; Grogel, D.B.M.; Schreml, S. *Microchim. Acta* **2011**, 174, 1-18.(b) Lin, V.S.; Dickinson, B.C.; Chang, C.J. *Methods in Enzymology* **2013**, 526, 19-43.(c) Lippert, A. R.; Van De Bittner, G. C.; Chang, C. J. *Acc. Chem. Res.* **2011**, 44, 793-804. (d) Tsien, R. Y. *Nat. Rev. Cell. Biol.* **2003**, 4, SS16-SS21. (e) Meade, T. J.; Aime, S. *Acc. Chem. Res.* **2009**, 42, 821. (f) Hildebrand, S. A.; Weissleder, R. *Curr. Opin. Chem. Biol.* **2010**, 14, 71-79. (g) Ueno, T.; Nagano, T. *Nat. Methods* **2011**, 8, 642-645. (h) Pittet, M. J.; Weissleder, R. *Cell*, **2011**, 147, 983-991. (i) James, M. L.; Gambhir, S. S. *Physiol. Rev.* **2012**, 92, 897-965.

(9) (a) Kuivila, H.G. (1954) J. Am. Chem. Soc. 76 , 870 – 874. (b) Kuivila, H.G. and Armour, A.G. (1957) J. Am. Chem. Soc.79, 5659–5662.

(10) Kalyanaraman, B.; Darley-Usmar, V.; Davies, K. J. A.; Dennery, P. A.; Forman, H. J.; Grisham, M. B.; Mann, G. E.; Moore, K.; Roberts II, L. J.; Ischiropoulos, H. *Free Rad. Biol. Med.* **2012**, *52*, 1-6..

(11) Van de Bittner, G. C.; Dubikovskaya, E. A.; Bertozzi, C. R.; Chang, C. J. *Proc. Natl. Acad. Sci. U.S.A.* **2010**, 107, 21316-21321.

(12) Van de Bittner, G. C.; Bertozzi, C. R.; Chang, C. J. *J. Am. Chem. Soc.* **2013**, 135, 1783-1795.

(13) Czupryna, J.; Tsourkas, A. *PLoS ONE* **2011**, 6, e20073.

(14) (a) Karlsson, A.; Nixon, J. B.; McPhail, L. C. *J. Leukoc. Biol.* **2000**, 67, 396-404; (b) Bellavite, P. *Free Rad. Biol. Med.* **1988**, 4, 225-261.

(15) Klaubert, D.; Shultz, J.; Valley, M. P.; Wang, H.; Zhou, W. Detection of Hydrogen Peroxide. US patent WO2013/025885A1, February 21, 2013.

Conclusions and Perspective

This thesis has described development of cell-impermeable coelenterazine derivatives for monitoring of exocytotic events and the development of activatable coelenterazine derivatives.

In the first chapter I demonstrated that coelenterazine can be modified with a flexible linker, containing a terminal phosphonic acid, by alkylating the phenol in the 2-position of coelenterazine (CoelPhos). CoelPhos showed higher activity with GLuc over RLuc. Despite CoelPhos having lower luminescence output compared to native coelenterazine with GLuc it was possible to visualize membrane bound GLucM23 mutant in HeLa cells with CoelPhos. The derivative CoelPhos also showed low cell-membrane permeability, which was demonstrated in cells expressing ER-localized GLuc. These results indicated that CoelPhos could be potentially used as a bioluminescent tool for the monitoring of exocytotic events in real-time. It should be emphasized that improvements in luminescence output by optimizing the linker composition and length are expected. Thus further exploration of the chemical space is desired. Notwithstanding, employing CCD-cameras with high luminescence sensitivity should also facilitate improvements in the applicability of CoelPhos.

In Chapter 2, I designed and synthesized activatable coelenterazine derivatives for specific detection of enzyme or bioactive small-molecule activity, and stabilization of the coelenterazine substrate. I expected that blocking of the 3-position of the imidazopyrazinone ring would effectively stabilize coelenterazine. In subchapter 2.1 I designed and synthesized two probes, bGalCoel, a β-galactose-coelenterazine hybrid, and bGalNoCoel, a β-galactose-nitrobenzyl-coelenterazine derivative. Both probes showed high stability and specificity however bGalNoCoel greatly outperformed bGalNoCoel in cell assays and I demonstrated that bGalNoCoel could be used to detect enzyme activity in two separate cell populations. I was also able to demonstrate for the first time that coelenterazine readily diffuses out of cells. In subchapter 2.2 I described the design and synthesis of a boronic acid-coelenterazine derivative for the selective detection of hydrogen peroxide in living cells; Coel-BeBA. This probe had adequate sensitivity and selectivity for hydrogen peroxide. In addition I could show that this probe could be used to detect endogenously generated hydrogen peroxide in macrophage cells. Having demonstrated that in both cases, blocking of the 3-position leads to a stabilization of the coelenterazine substrate is seems very straightforward

what the future holds for this type of technology. My concept can easily be expanded to incorporate many other types of enzymes and bioactive small-molecules, especially with the recent availability of coelenterate luciferases which display more glow-type luminescence profiles (GLucM23, NanoLuc). Combining this technology with BRET, protein-fragment complementation assays etc a wide range of applications are possible. Thus I venture that overall my work has helped expanding the bioluminescence toolbox.

Appendix

Modification of the 2- and 3-positions of the imidazopyrazinone ring of coelenterazine

In chapter 2.1 and 2.2 I described the synthesis of bGalNoCoel and CoelBeBA. Both of these compounds were obtained by O-alkylation of the carbonyl at the 3-position of the imidazopyrazinone ring of $CTZ(OAc)_2$. However, I discovered that under certain conditions a certain amount of C-alkylation at the 2-position also took place (Scheme 1). C-alkylation of coelenterazine has not been reported in the literature thus far.

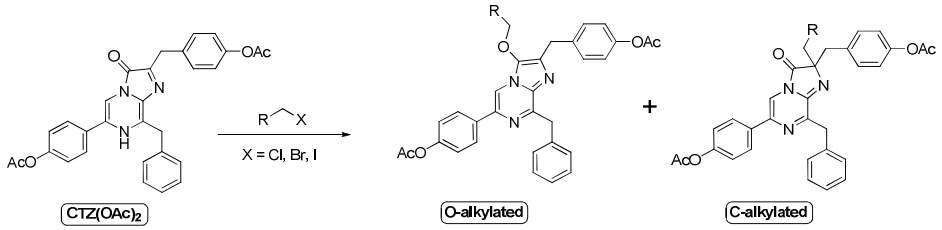

Scheme 1.

This was first observed during the synthesis of bGalNoCoel where a significant amount of the c-alkylated product was also obtained (scheme 2). Attempted deacetylation of Per-OAc-bGalNoCoel(C) with sodium methoxide, lithium hydroxide among others resulted in nucleophilic addition to the 3-carbonyl group.

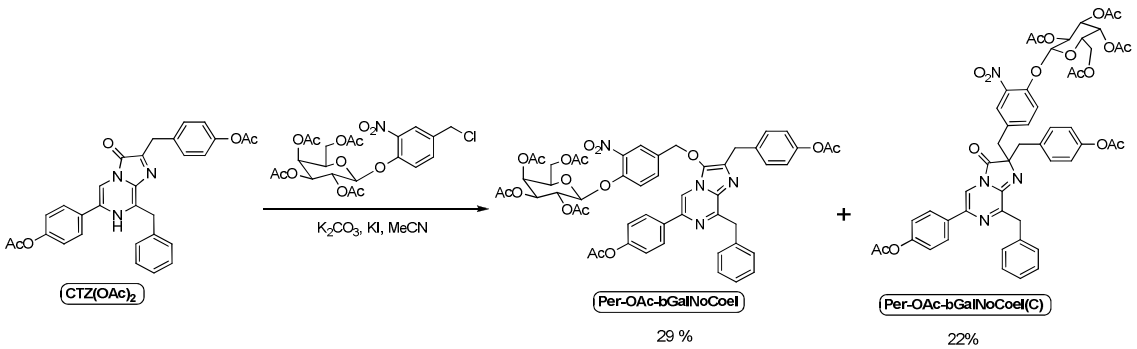

Scheme 2. Showing the relative yields of O- and C-alkylation respectively in the synthesis of bGalNoCoel.

Interestingly in the synthesis of Coel-BeBA O-alkylation was almost exclusively obtained (Chapter 2.2). It is common knowledge that O- and C-alkylation is largely

influenced by reaction conditions such that aprotic solvents, bases with large counter-ions, and hard leaving groups tend to favor O-alkylation whilst conducting reactions with protic solvents, bases with small counter-ions, and soft leaving groups tends to favor C-alkylation.

In another instance I attempted to synthesize a coelenterazine probe, Coel-BePA for the monitoring of alkaline phosphatase (Scheme 3). By changing the conditions as to favor C-alkylation a slightly higher proportion of C-alkylated product (Pro-Coel-BeBA(C)) was observed. Separation of the O- and C- alkylated products is highly difficult with very similar rf values, despite extensive flash silica gel chromatography (Figure 1).

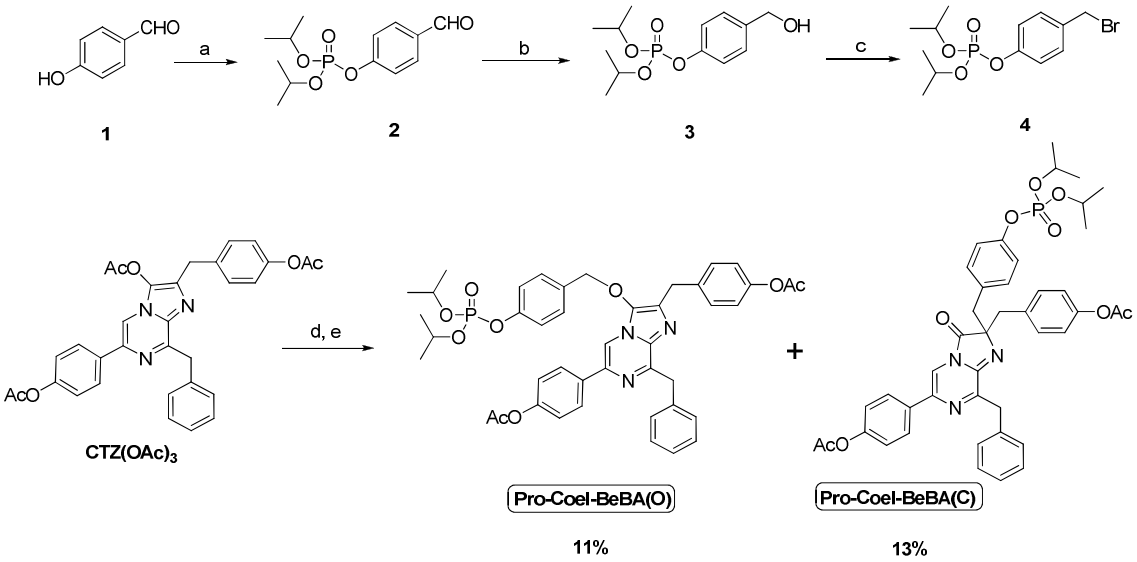

Scheme 3. Synthesis of bGalCoel. a), CBr_4, Et_3N, THF, 80%; b) $NaBH_4$, MeOH, 87%; c) CBr_4, PPh_3, CH_2Cl_2, 90%; d) 1% NH_3 in MeOH / CH_2Cl_2; e) **5**, Na_2CO_3, NaI, THF.

It became clear that the C-alkylated coelenterazines are highly unstable in the presence of base and readily decomposes to coelenterazine, whilst being more stable under acidic conditions. The opposite is true for the O-alkylated coelenterazines. Only one method for selective deprotection of the 3-carbonyl has been reported, selective deacetylation.[1,2] However, in order to obtain C-alkylated coelenterazines it would be more suitable to utilize protecting groups which can easily be cleaved under acidic conditions. This area of research is seriously lacking and needs to be explored further. Although, other substrates such as bisdeoxycoelenterazine (BDC), which does not have any phenolic groups, does not suffer from this problem. Even if deprotected C-alkylated

coelenterazines could be readily obtained, it remains to be seen how stable they are under biological conditions in the presence of natural nucleophiles such as glutathione.

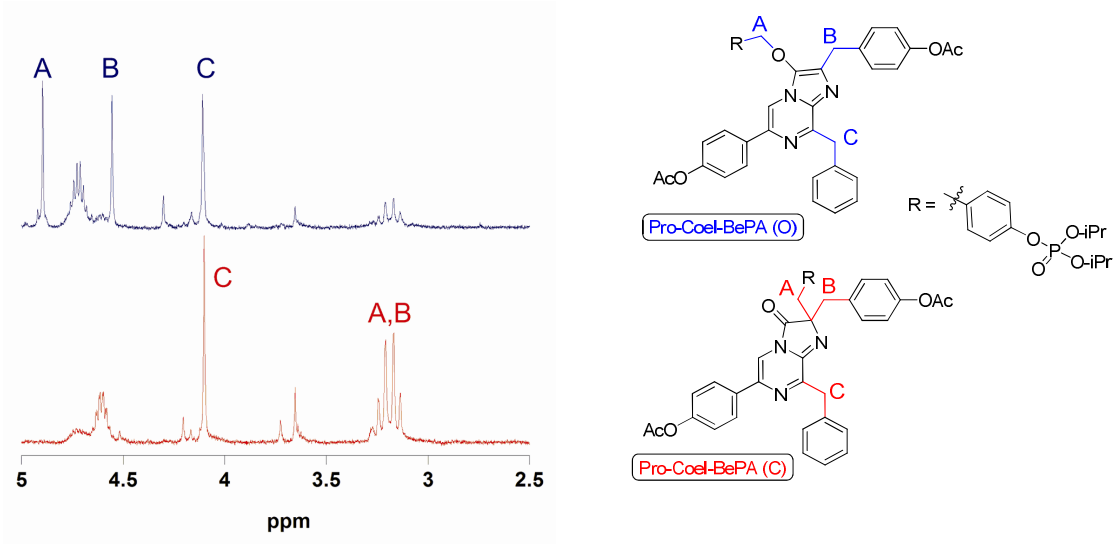

Figure 1. Showing comparison of ^{1}H-NMR of O-alkylated (blue) vs C-alkylated (red)

Experimental

Materials and Instruments

General reagents and chemicals were purchased from Sigma-Aldrich Chemical Co. (St. Louse, MO), Tokyo Chemical Industries (Tokyo, Japan), and Wako Pure Chemical (Osaka, Japan) and were used without further purification. Silica gel chromatography was performed using BW-300 (Fuji Silysia Chemical Ltd., Greenville, NC). NMR spectra were recorded on a JEOL JNM-AL400 instrument at 400 MHz for ^{1}H and 100.4 MHz for ^{13}C NMR, using tetramethylsilane as an internal standard. Mass spectra were measured on a Waters LCT-Premier XE mass spectrometer for ESI or on a JEOL JMS-700 for FAB.

Synthesis

4-formylphenyl diisopropyl phosphate (2)

To an ice-cooled solution of 4-hydroxybenzaldehyde (**1**) (123 mg, 1.01 mmol) and carbon tetrabromide (998 mg, 3.01 mmol) in anhydrous THF (10-11 mL) under an argon atmosphere was added anhydrous Et_3N (0.42 mL, 3.01 mmol), followed by

dropwise addition of diisopropylphosphite (0.33 mL, 1.99 mmol). After 5 min the ice-bath was removed and the reaction was stirred at rt for 24 h. The reaction was quenched with water. The aqueous solution was extracted with EtOAc, washed with brine, dried under Na_2SO_4, filtered, and concentrated *in vacuo*. Purification by flash chromatography (EtOAc / Hexane; 1:1) yielded the desired product (2) as a clear yellow oil (231 mg, 0.81, 80%). ^{1}H-NMR (400 MHz,$CDCl_3$)δ 9.97 (s, 1H, CHO) 7.89 (d, ^3J = 8.0 Hz, 2H, ArH) 7.39 (d, ^3J = 8.0 Hz, 2H, ArH) 4.78 (m, 2H, 2 × CH) 1.38 (d, ^3J = 6.2 Hz, 6H, 2 × CH_3) 1.34 (d, ^3J = 6.2 Hz, 6H, 2 × CH_3); ^{13}C-NMR (100 MHz,$CDCl_3$) δ 190.76, 155.67, 133.02, 131.56, 120.43, 100.54, 73.98, 23.61, 23.56, 23.51, 23.45; ESI-MS: calc: 287.1043; found: 287.1467 $[M+H]^+$.

4-(hydroxymethyl)phenyl diisopropyl phosphate (3)

To an ice-cooled solution of **2** in MeOH (2 mL) was added sodium borohydride (53 mg, 1.40 mmol). After 1 h the reaction mixture was poured into water and extracted with EtOAc, washed with brine, dried under Na_2SO_4, filtered and concentrated and dried *in vacuo*. Purification by flash chromatography gave the desired product **3** as a clear oil (198 mg, 0.69 mmol, 87%). ^{1}H-NMR (400 MHz,$CDCl_3$) δ 7.12 (d, ^3J = 8.0 Hz, 2H, ArH) 6.96 (d, ^3J = 8.0 Hz, 2H, ArH) 4.52 (m, 2H, 2 × CH) 4.38 (s, 2H, CH_2) 1.16 (d, ^3J = 6.0 Hz, 6H, 2 × CH_3) 1.11 (d, ^3J = 6.0 Hz, 6H, 2 × CH_3); ^{13}C-NMR (100 MHz, $CDCl_3$) δ 149.18, 137.74, 127.37, 119.06, 72.82, 62.91, 22.78, 22.73, 22.70, 22.64; ESI-MS: calc: 289.1199; found: 289.1836 $[M+H]^+$

4-(bromomethyl)phenyl diisopropyl phosphate (4)

To an ice-cooled solution of **3** (197 mg, 0.68 mmol) in anhydrous CH_2Cl_2 was added carbon tetrabromide (345 mg, 1.04 mmol) and triphenyl phosphine (284 mg, 1.08 mmol) under argon. The reaction was stirred at rt for 20 h. The reaction mixture was concentrated *in vacuo*. The residue was dissolved in a minimal amount of CH_2Cl_2 and loaded onto a silica gel column. Flash chromatography (EtOAc / Hexane; 1:1) yielded the desired product **4** as a colorless liquid (214 mg, 90%). ^{1}H-NMR (400 MHz,$CDCl_3$) δ 7.35 (d, ^3J = 8.0 Hz, 2H, ArH) 7.19 (d, ^3J = 8.0 Hz, 2H, ArH) 4.73 (m, 2H, 2 × CH) 4.45 (s, 2H, CH_2, d) 1.32-1.24 (m, 12H, 6 × CH_3); ^{13}C-NMR (100 MHz,$CDCl_3$) δ 150.32, 133.96, 130.08, 119.98, 73.23, 32.39, 23.22.

Prot-Coel-BeBA(O)/(C)

To an ice-cooled solution of $CTZ(OAc)_3$ (56 mg, 0.10 mmol) in CH_2Cl_2 (1 mL) under

an argon atmosphere was added 1% NH_3 in MeOH (1 mL) and the solution was stirred for 2.5 h. The reaction mixture was concentrated and dried *in vacuo* and used without further purification. The residue was dissolved in anhydrous THF (5 mL) under an argon atmosphere. To this solution was added Na_2CO_3 (4.5 mg, 0.04) NaI (15 mg, 0.10), and **4** (47 mg, 0.13) in anhydrous THF. The reaction was bubbled with argon gas for 30 min. The reaction was stirred over night at rt. The reaction was diluted with water and extracted with CH_2Cl_2. The organic layer was washed with water, brine, dried under Na_2SO_4, filtered, and concentrated *in vacuo*. Purification via flash chromatography (0 $\rightarrow$ 3% MeOH / CH_2Cl_2) yielded two major products: The O-alkylated product (**6**) (8.6 mg, 0.011 mmol, 11%) and the C-alkylated product (**7**) (9.8 mg, 0.013 mmol, 13%)

Prot-Coel-BeBA(O)

^{1}H-NMR (400 MHz,$CDCl_3$) δ 7.84-7.79 (m, 3H, ArH) 7.56 (d, ^3J = 8.0 Hz, 2H, ArH) 7.33-7.15 (m, 11H, ArH) 7.01 (d, ^3J = 8.0 Hz, 2H, ArH) 4.90 (s, 2H, CH_2) 4.72 (m, 2H, 2xCH) 4.56 (s, 2H, CH_2) 4.11 (s, 2H, CH_2) 2.31 (s, 3H, CH_3CO) 2.27 (s, 3H, CH_3CO) 1.34 (d, ^3J = 6.4 Hz, 6H, 2×CH_3) 1.27 (d, ^3J = 6.4 Hz, 6H, 2×CH_3); ^{13}C-NMR (100 MHz,$CDCl_3$) δ169.42, 169.29, 152.69, 151.59, 151.52, 150.83, 149.18, 137.90, 137.68, 137.07, 136.55, 134.58, 133.14, 132.26, 131.96, 130.05, 129.66, 129.64, 128.17, 127.24, 126.36, 121.84, 121.47, 120.39, 120.35, 108.93, 73.64, 39.31, 32.79, 23.57, 23.52, 23.46, 23.41, 21.08, 21.04. ESIMS: Calc: 779.2961; found: 779.1447 $[M+2H]^+$

List of Publications

1. Full Paper: Development of Luminescent Coelenterazine Derivatives Activatable by β-Galactosidase for Monitoring Dual Gene Expression
   Lindberg, E.; Mizukami, S.; Ibata, K.; Miyawaki, A.; Kikuchi, K.
   Chem. Eur. J. **2013***, in press*

2. Full Paper: Development of Cell-Impermeable Coelenterazine Derivatives
   Lindberg, E.; Mizukami, S.; Ibata, K.; Fukano, T.; Miyawaki, A.; Kikuchi, K.
   Chem. Sci. **2013**, *in press*

3. Communication: Development of Hydrogen Peroxide Activatable Coelenterazine Derivatives
   Lindberg, E.; Mizukami, S.; Kikuchi, K.
   In preparation.

Presentations at International Conferences

1. Poster: Development of Cell-Impermeable Coelenterazine Derivatives
   Lindberg, E.; Mizukami, S.; Kikuchi, K.
   Catalysis and Sensing for Health (CASH 2011) Bath, United Kingdom, February, 2011

2. Poster: Development of Cell-Impermeable Coelenterazine Derivatives
   Lindberg, E.; Mizukami,; Kikuchi, K.
   RIKEN Chemical Biology Symposium "Next Generation Tools for Molecular Target Discovery", Saitama, Japan, 2011

3. Oral: Development of Cell-Impermeable Coelenterazine Derivatives
   Lindberg, E.; Mizukami, S.; Kikuchi, K.
   The 92th Spring Meeting of the Chemical Society of Japan, Kanagawa, Japan, March 2012

Acknowledgements

The author would like to express gratitude to Professor Kazuya Kikuchi for his continuous guidance, support, and encouragement throughout this study. The author expresses his sincere thanks to Dr. Shin Mizukami for his valuable guidance and discussion. The author also expresses his cordial thanks to Dr. Yuichiro Hori for his kind help and useful suggestion.

The author is deeply grateful to Dr. Miyawaki and Dr. Fukano at RIKEN, Saitama and Dr. Ibata at Keio University for their help and support with bioluminescence imaging experiments. Deep thanks also go out to all the members of the Kikuchi laboratory group for their kind help, teaching, and friendship.

The author acknowledges financial support from the Japanese government, MEXT.

Finally, the author appreciates the tremendous support and continuous encouragement from his family and friends.

Osaka, Japan
October, 2013

Eric LINDBERG

Division of Advanced Science and Biotechnology
Department of Material and Life Science
Graduate School of Engineering, Osaka University

Doctoral Dissertation

Development of coelenterazine derivatives for monitoring of biological phenomena

Eric Jorgen Lindberg

October 2013

Laboratory of Chemical Biology

Division of Advanced Science and Biotechnology

Department of Material and Life Science

Graduate School of Engineering,

Osaka University

Contents

General Introduction

Molecular imaging allows for the visualization and quantification of biological processes at the cellular and subcellular levels within intact living organisms. This biomedical research discipline is gaining great interest to address frontier issues related to pathology and physiology.[1] Several common imaging techniques have been developed for such applications including: computer tomography (CT), magnetic resonance imaging (MRI), positron emission tomography (PET), single photon emission computer tomography (SPECT), ultrasound, photoacoustic imaging, and novel optical small animal imaging techniques such as fluorescence imaging (FLI) and , bioluminescence imaging (BLI).[2] The main area of utility of bioluminescence used to be in *in vitro* gene-reporter assay measurements, however significant leaps in the development of more sensitive CCD-camera technology has diversified the use of BLI in the life sciences. The use of bioluminescence imaging and analysis have some distinctive advantages such as low background, high signal-to-noise (S/N) ratio profiles, generally wider range of signals, flexible in the molecular design, allows for extended period of measurement, and also highly suitable for imaging of small animal models.[3,4] The relative sensitivity will depend on the emission wavelength of the light emitted and also the sensitivity of the camera system. Examples of applications of BLI include: monitoring of protein-protein interactions[5], *in vivo* and *in vitro* drug screening[6], sensing bioactive small molecules[7], assessing protein stability and function[8], *in vivo* imaging of animal models[9], imaging of organs[10] , imaging of disease progression such as cancer and their metastasis[11], and 3D BLI of cerebral ischemia[12] to name a few.

Bioluminescence is the product of certain photoproteins (luciferases) which catalyze oxidation of small molecular substrates (luciferins), which results in the generation of light in the form of bioluminescence. Bioluminescent species can be found across many phyla such as insects, marine organisms, and prokaryotes. Although a number of luciferase-luciferin pairs have been discovered in nature, only a selected few have been sufficiently characterized for use as tools in chemical biology (Table 1.). The bioluminescence system based on firefly and beetle luciferases together with D-luciferin has been the most reported system. Especially in studies involving *in vivo* imaging because of the emission spectra of firefly and beetle luciferases (~560-610 nm)[13]. The D-luciferin is relatively stable and can diffuse between tissues. The reaction between D-luciferin and its luciferases requires ATP and magnesium ions, which limits its use to intracellular monitoring. The other commonly used luciferases all utilize various luciferin substrates which all share a imidazopyrazinone core structure (Table 1). Unlike

Table 1. Characteristics of luciferase-luciferin pairs commonly used in BLI
Adapted from (19) and (20).

Luciferase	Luciferin (substrate)	Peak emission (nm)	Size (kDa)	Comments	Reference
North American firefly (FLuc)	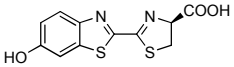 **D-Luciferin**	565	61	Requires ATP and Mg^{2+} Codon optimized	13
Renilla reniformis (native RLuc)	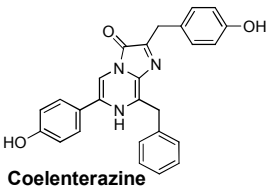 **Coelenterazine**	480	36	Can be used in extracellular environments, codon-optimized	14
Gaussia princeps (GLuc)		480	20	Naturally secreted enzyme cell-anchored versions available	15
Gaussia princeps (Monsta)		503	20	Mutant enzyme with red-shifted emission spectrum	16
Oplophorus gracilirostris (NanoLuc)	 **Furimazine**	460	20	Stabile mutant enzyme with increased light output	17
Cypridina noctiluca (CLuc)	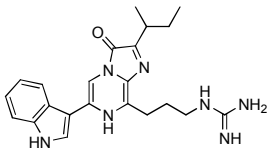 ***Cypridina* luciferin**	465	62	Naturally secreted enzyme	18

D-luciferin, these luciferases do not require any other co-factor other than molecular oxygen, which allows for extracellular as well as intracellular applications. The general emission spectrum with imidazopyrazinone compounds range from ~460-480 nm, limiting their use in *in vivo* imaging due to poor penetration. However, red-shifted mutants have been developed[16, 21], and also it is possible to obtain a red-shifted emission by utilizing bioluminescence resonance energy transfer (BRET).[22] In addition coelenterate luciferases such as *Gaussia* luciferase (GLuc) has been shown to have over 1000-fold stronger signal output over firefly luciferase (FLuc)[15a], whilst the recent NanoLuc has been shown to have 100-fold stronger signal than FLuc. As each substrate is quite specific for its respective luciferase enzyme it has been possible to monitor multiple parameters by utilizing a combination of up to 3 luciferases in *in vitro* and *in vivo* monitoring of cellular processes.[23]

Derivatization and functionalization of luciferin substrates

The three most common types of derivatization studies of D-luciferin substrates have been focused on: 1) increasing the luminescence output; 2) red-shifted emission

spectrum, and 3) activatable-luciferins. Several improved and red-shifted analogues of D-luciferin and aminoluciferin have been reported. [24] In addition, red-shifted aminoluciferin-BRET acceptor conjugates have also been reported. [25] Several D-luciferin derivatives for the specific monitoring of enzyme and bioactive small molecules have been reported (Figure 1.)[26] For coelenterate luciferin substrates, most studies have focused on modification of coelenterazine to obtain an improved luminescence output.[27]In most cases any modification of coelenterazine will result in a significant decrease in bioluminescence output. However, in two instances an improvement in signal output was observed[17, 27a]. Unlike the D-luciferin substrates, modification of coelenterazine greatly affects its stability, thus in addition to retaining the luminescence output; the overall stability of the molecule also has to be taken into account.[27c] Therefore it is not surprising that D-luciferin has been favored due to the high substrate specificity of coelenterate luciferases together with its stability issues.

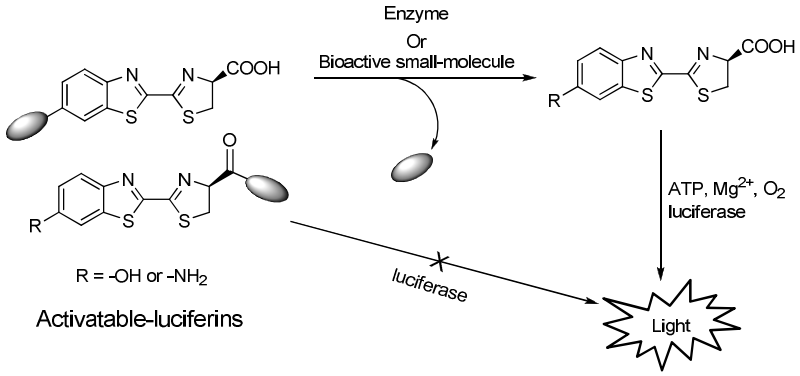

Figure 1. Concept behind activatable-luciferins. Adopted from (26).

Purpose of research

The work presented herein is based around the synthetic modification of coelenterazine together with the use of *Gaussia* luciferase, due to its much higher luminescence output over other luciferases such as that of *Renilla reniformis*. The immediate difficulty however is related to the ability to predict the impact on luminescence output based on the position of modification on coelenterazine. There are several reasons for this: i) high substrate specificity of GLuc[27c]; ii) little to no homology with other coelenterate luciferases; iii) no existing x-ray crystal structure of GLuc; and iv) probably cooperativity between proposed two catalytic sites GLuc.[28] As this dissertation is divided into two major chapters the detailed research aim of each respective differ in the type of modification of coelenterazine. In chapter 1 the major concern is loss in luminescence output, whilst in chapter 2 the focus is more on stability.

References

1. Massoud, T. F.; Gambhir, S. S. *Gene* **2003**, *17*, 545-580.
2. Weissleder, R.; Pittet, M. J. *Nature* **2008**, *452*, 580-589.
3. Ozawa, T.; Yoshimura, H.; Kim, S. B. *Anal. Chem.* **2013**, *85*, 590-609.
4. Keyaerts, M.; Caveliers, V.; Lahoutte, T. *Trends Mol. Med.* **2012**, *18*, 164-172.
5. Ozawa, T.; Kaihara, A.; Sato, M.; Tachihara, K.; Umezawa, Y. *Anal. Chem.* **2001**, *73*, 2516-2521.
6. (a) Kelkar, M.; De, A. *Curr. Opin. Pharmacol.* **2012**, *12*, 592-600. (b) Bacart, J.; Corbel, C.; Jockers, R.; Bach, S.; Couturier, C. *Biotechnol. J.* **2008**, *3*, 311-324.
7. Paulmurugan, R.; Gambhir, S. S. *Proc. Natl. Acad. Sci. U.S.A.* **2006**, *103*, 15883-15888.
8. Banaszynski, L. A.; Sellmyer, M. A.; Contag, C. H.; Wandless, T. J.; Thorne, S. H. *Nat. Med.* **2008**, *14*, 1123-1127.
9. Dothager, R. S.; Flentie, K.; Moss, B.; Pan, M-H.; Kesarwala, A.; Piwnica-Worms, D. *Curr. Opin. Biotechnol.* **2009**, *20*, 45-53.
10. (a) de Heredia, L. L.; Gengatharan, A.; Foster, J.; Mather, S.; Magoulas, C. *Neurosci. Lett.* **2011**, *497*, 134-138. (b) Ozaki, M.; Haga, S.; Ozawa, T. *Theranostics* **2012**, *2*, 207-214. (c) Hong, H,; Zhang, Y.; Severin, G. W.; Yang, Y. N.; Engle, J. W.; Niu, G.; Nickles, R. J.; Chen, X. Y.; Leigh, B. R.; Barnhart, T. E.; Cai, W. B. *Mol. Pharmaceut.* **2012**, *9*, 2339-2349.
11. (a) Xie, X.; Xia, W.; Li, Z.; Kuo, H. P.; Liu, Y.; Li, Z.; Ding, Q.; Zhang, S.; Spohn, B.; Yang, Y.; Wei, Y.; Lang, J. Y.; Evans, D. B.; Chiao, P. J.; Abbruzzese, J. L.; Hung, M. C. *Cancer Cell* **2007**, *12*, 52-65. (b) Chi, X.; Huang, D.; Zhao, Z.; Zhou, Z.; Yin, Z.; Gao, J. *Biomaterials* **2012**, *33*, 189-206.
12. Cordeau, P.; Kriz, J. *Methods in Enzymology* **2012**, *506*, 117-131.
13. (a) Zhao, H.; Doyle, T. C.; Coquoz, O.; Kalish, F.; Rice, B. W.; Contag, C. H. *J. Biomed. Opt.* **2002**, *10*, 41210. (b) Miloud, T.; Henrich, C.; Hammerling, G. *J. Biomed. Opt.* **2007**, *12*, 054018.
14. Bhaumik, S.; Gambhir, S. S.; *Proc. Natl. Acad. Sci. U.S.A.* **2002**, *99*, 377-382.
15. (a) Tannous, B. A.; Kim, D. E.; Fernandez, J. L.; Weissleder, R.; Breakefield, X. O. *Mol. Ther.* **2005**, *11*, 435-443. (b) Santos, E. B.; Yeh, R.; Lee, J.; Nikhamin, Y.; Punzalan, B.; Punzalan, B.; La Perle, K.; Larson, S. M.; Sadelain, M.; Brentjens, R. J. *Nat. Med.* **2009**, *15*, 338-344.
16. Kim, S. B.; Suzuki, H.; Sato, M.; Tao, H. *Anal. Chem.* **2011**, *83*, 8732-8740.
17. M. P. Hall, J. Unch, B. F. Binkowski, M. P. Valley, B. L. Butler, M.G. Wood, P.

Otto, K. Zimmerman, G. Vidugiris, T. Machleidt, M. B. Robers, H. A. Benink, C. T. Eggers, M. R. Slater, P. L. Meisenheimer, D. H. Klaubert, F. Fan, L. P. Encell, K. V. Wood, *ACS Chem. Biol.* **2012**, *7*, 1848-1857.

18. Nakajima, Y.; Kobayashi, K.; Yamagishi, K.; Enomoto, T.; Ohmiya, Y. *Biosci. Biotechnol. Biochem.* **2004**, *68*, 565-570
19. Prescher, J. A.; Contag, C. H. *Curr. Opin. Chem. Biol.* **2010**, *14*, 80-89.
20. Luker, K. E.; Luker, G. D. *Antiviral Res.* **2008**, *78*, 179-187.
21. Loening, A. M.; Wu, A. M.; Gambhir, S. S. *Nat. Methods.* **2007**, *4*, 641-643.
22. Xia, Z.; Rao, J. *Curr. Opin. Biotechnol.* **2009**, *20*, 37-44.
23. (a) Maguire, C. A.; Bovenberg, M. S.; Crommentuijn, M. H. W.; Niers, J. M.; Kerami, M.; Teng, J.; Sena-Esteves, M.; Badr, C. E.; Tannous, B. A. *Mol. Ther. Nucleic Acids* **2013**, *2*, e99. (b) Heise, K.; Oppermann, H.; Meixensberger, J.; Gebhardt, R.; Gaunitz, F. *Assay and Drug Development Technologies* **2013**, *11*, 244-252.
24. (a) Takaura, H.; Sasakura, K.; Ueno, T.; Urano, Y.; Terai, T.; Hanaoka, K.; Tsuboi, T.; Nagano, T. *Chem. Asian J.* **2010**, *5*, 2053-2061. (b) Conley, N. R.; Dragulescu-Andrasi, A.; Rao, J.; Moerner, W. E. *Angew. Chem. Int. Ed. 51*, 3350-3353.
25. (a) Takaura, H.; Kojima, R.; Urano, Y.; Terai, T.; Hanaoka, K.; Nagano, T. *Chem. Asian J.* **2011**, *6*, 1800-1810. (b) Kojima, R.; Takakura, H.; Ozawa, T.; Tada, Y.; Nagano, T.; Urano, Y. *Angew. Chem. Int. Ed.* **2012**, *51*, 1-6.
26. Li, J.; Chen, L.; Du, L.; Li, M. *Chem. Soc. Rev.* **2013**, *42*, 662-676.
27. (a) Inouye, S.; Shimomura, O. *Biochem. Biophys. Res. Commun.* **1997**, *233*, 349-353. (b)Wu, C.; Nakamura, H.; Murai, A.; Shimomura, O. *Tet. Lett.* **2001**, *42*, 2997-3000. (c) Inouye, S.; Sahara-Miura, Y.; Sato, J-I.; Iimori, R.; Yoshida, S.; Hosoya, T. **2013**, *88*, 150-156.
28. Tzertzinis, G.; Schildkraut, E.; Schildkraut, I. *PLoS ONE* **2012**, *7*, e40099.

Chapter 1 Development of Cell-Impermeable Coelenterazine Derivatives

Gaussia luciferase (GLuc) is the brightest among all reported luciferases and displays a flash-type luminescence profile.[1] These lucifereases have mostly been used as a reporter to monitor dynamic changes in gene expression and transcription.[2] Monitoring of single exocytotic events in living cells has mostly employed methods such as total internal reflection fluorescence (TIRF), and two-photon laser scanning microscopy.[3-6] However, these methods are confined to monitoring a limited section of the cells and the use of fluorogenic dyes for accurate localization can be difficult due to diffusion. In addition, fluorescence methods require continuous irradiation, causing cell damage and photobleaching. Moreover due to their temporal resolution properties, confocal and twophoton laser scanning microscopies are more suitable when monitoring membrane fusion of vesicles with slower kinetics.[7]

BLI can offer distinct advantages over fluorescence imaging in monitoring of protein secretion and other exocytotic events in living cells. Visualization of luciferase secretion in living mammalian cells was first realized with *Cypridina* luciferase (CLuc) in CHO cells,[8] and in live mouse embryos to monitor transcriptional activation of genes.[9] CLuc was also utilized for imaging of neurotransmitter release.[10] Recently secretion of the brighter GLuc in PC12D cells was monitored in real-time.[11] However, in general BLI has suffered from poor resolution due to low luminescence intensity. Using an electron multiplying charge coupled device (EM-CCD) camera, video-rate BLI was employed in the studying of secretory dynamics of MMP-2 with GLuc at much improved resolutions.[12] In another study, the same group also demonstrated that video-rate BLI could be used for quantitative analysis of insulin oscillations in pancreatic MIN6 β cells, which could have potential drugscreening applications.[13]

Recently, in an effort to monitor exocytosis in synaptic boutons via BLI, a mutant GLuc with enhanced luminescence output was fused to the part of a vesicle-associated membrane protein (VAMP) located within the interior of the synaptic vesicle (unpublished data). Hence, when the vesicle fuses with the cell membrane undergoing exocytosis the luciferase would react with its substrate coelenterazine, generating a bioluminescent response. However, a very poor signal-to-noise was observed which was attributed to the high cell-membrane permeability of coelenterazine, *i.e.* coelenterazine could diffuse across the synaptic and vesicle membranes and react with the luciferase before the exocytotic event, giving rise to high background luminescence

(Figure 1a). Miesenbock *et al.* also observed a similar issue with *Cypridina* luciferin when imaging patterns of synaptic activity in hippocampal neuronal cells.[10] Therefore a modified coelenterazine substrate with decreased cell-membrane permeability is desired (Figure 1b–1c). However modifying the bioluminogenic substrate without having a negative impact on the bioluminescence activity is very difficult. This is especially true in the case of GLuc, which has very high substrate specificity. Hence, even the smallest modification of the coelenterazine substrate will result in a significant drop in bioluminescence activity.[14-16] Therefore it is not surprising that only one coelenterazine derivative (s-CTZ) with improved bioluminescence activity with GLuc has been reported.[17] The compound structure has yet to be published, however, the published data strongly implies that s-CTZ is highly cell-permeable. Hence we sought to design and synthesize a cell-membrane impermeable coelenterazine derivative with retained bioluminescence activity.

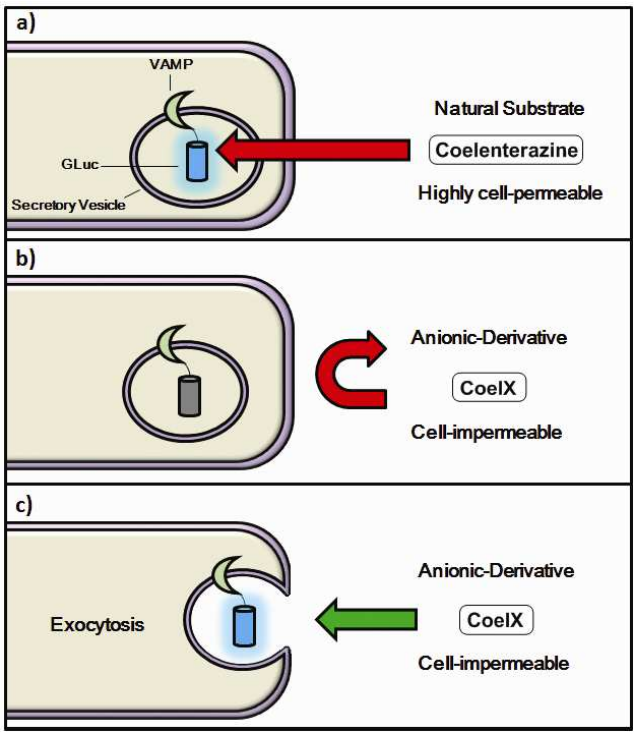

Figure 1. Monitoring membrane fusion events via BLI; Concept (a) coelenterazine readily penetrates the cell-membrane, giving rise to background noise prior to fusion taking place; (b) coelenterazine derivative CoelX has a negative charge, making it highly cell-impermeable and unable to react with GLuc; (c) following fusion of the secretory vesicle with the cell-membrane CoelX can react with GLuc, generating a bioluminescence signal.

Results and Discussion: Design and Synthesis of 2-BnO-TEG-CTZ and 6-BnOTEG-CTZ

When conceiving of a proper rational substrate design strategy, it is very useful to perform docking simulations of substrate derivatives before undertaking actual experimental work. Urano *et al.* constructed near-infrared-emitting firefly luciferins by initially performing docking simulations with luciferase from *Photinus pyralis*.[18] However, as there is no existing x-ray crystal structure of *Gaussia* luciferase (GLuc), lack of homology with other coelenterate luciferases, for which crystal-structures are available, rational design and modification of coelenterazine remains a difficult task in terms of being able to predict the effect of any modification of the coelenterazine substrate on bioluminescence activity. Modification of the coelenterazine substrate has mostly been focused on increasing light output, redshifting the emission spectrum of coelenterazine and increasing the stability of coelenterazine to decrease autoluminescence background noise. [19-24] As mentioned above coelenterate luciferases share very little homology and hence any modification of coelenterazine, that might have an advantageous impact on the luminesence output of one luciferase, might have the reverse effect on another. This is especially true for GLuc which has been shown to have an extremely narrow substrate specificity.[14-16] In order to construct a cell-impermeable derivative of coelenterazine, we decided to attach a flexible linker with a terminal anionic phosphonate group. Initially we synthesized two coelenterazine derivatives with a highly flexible polyethylene glycol (PEG) linker with terminal benzyl-protecting groups installed at the 2 and 6 positions of coelenterazine (Scheme 1) to investigate the effect on bioluminescence activity of GLuc. We prepared **11** from

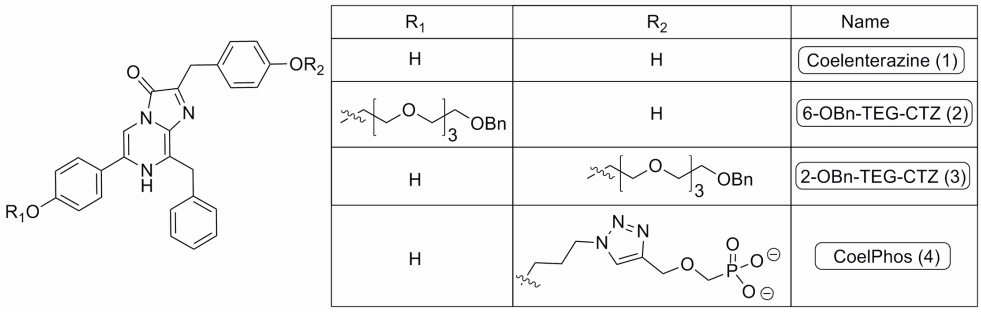

Figure 2. Structures of native coelenterazine and synthesized derivatives.

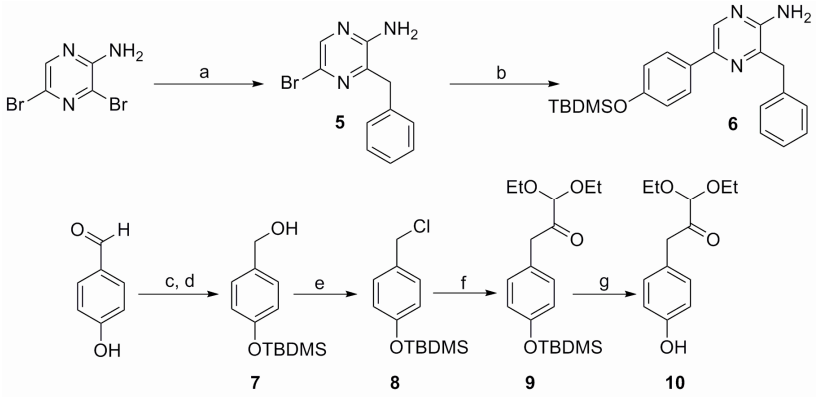

Scheme 1. (a) $PhCH_2MgCl$, $ZnCl_2$, $Pd(PPh_3)_2Cl_2$, THF, rt, 72 h, 83%; (b) 4-(TBDMS-O)Ph-$B(OH)_2$, bddp, $(C_6H_5CN)_2PdCl_2$, Na_2CO_3 (1M (aq)), EtOH, Toluene, reflux, 24 h, 83%; (c) TBDMSCl, imidazole, DMF, rt, 12 h; (d) $NaBH_4$, MeOH, 0 °C, 2 h, 86% over 2 steps; (e) $SOCl_2$, CH_2Cl_2, 0°, 2 h, 81%; (f) Mg, $EtBr_2$, THF, sonication; ethyl diethoxyacetate, THF, -78°C, 6 h, 47%; (g) Bu_4NF, THF, 0 °C, 30 min, 93%.

tetraethylene glycol (TEG) by mono-benzylation with benzyl bromide, followed by were synthesized as previously described (Scheme S1).[25-26] **13** was synthesized via bromination to **12** via the Apple reaction (Scheme S2). Synthetic intermediates **6** and **10** standard alkylation of coelenteramine **6** with **12**. Following acid-catalyzed condensation reaction of **13** and the α-ketoacetal **9** under reflux the desired compound 6-BnO-TEG-CTZ (**2**) was synthesized (Figure 2). Synthesis of 2-BnO-TEG-CTZ (**3**) was accomplished by initial alkylation of deprotected α-ketoacetal **10** with the TEG linker **12** to give **14**. Acid-catalyzed condensation reaction between **6** and **14** under reflux generated the desired product, 2-BnO-TEG-CTZ (**3**).

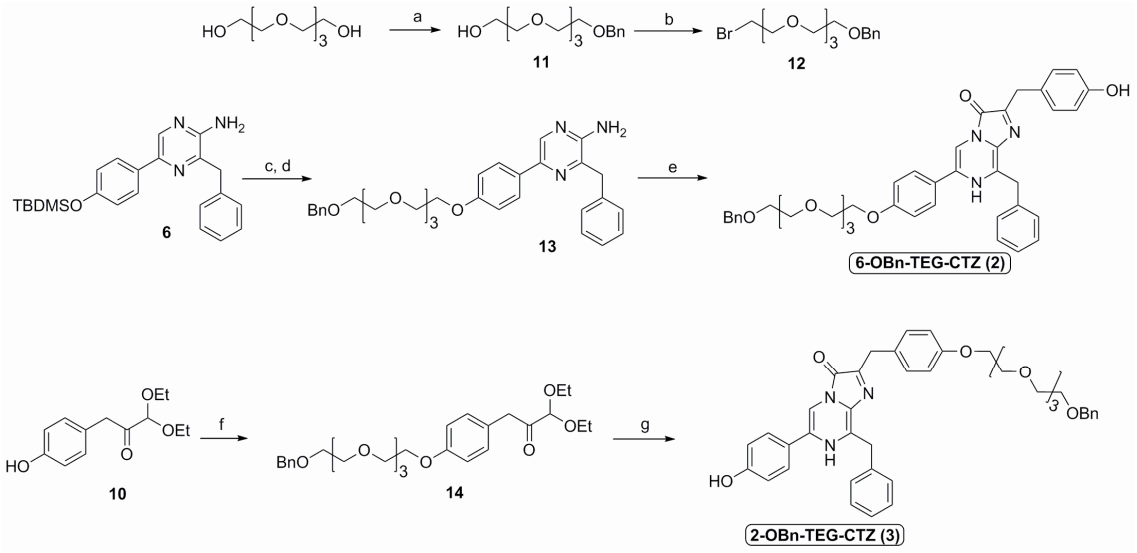

Scheme 2. Synthesis of 6-OBn-TEG-CTZ and 2-OBn-TEG-CTZ. (a) NaH, BnBr, THF/DMF, 0 °C to rt. 5 h, 67%; (b) PPh_3, CBr_4, CH_2Cl_2, reflux, 12 h, 91%; (c) Bu_4NF, THF, 0 °C, 2 h; (d) **12,** NaH, DMF, 0 °C, 5 h, 55% over 2 steps, (e) **9**, 1,4-dioxane / 6N HCl (10:1), 24 h, 49%; f) **12**, Cs_2CO_3, MeCN, reflux, 3 h, 73%; (g) **6**, 1,4-dioxane / 6N HCl (10:1), reflux, 14 h, 17%

Next the luminescent properties of 2- and 6-BnO-TEG-CTZ were evaluated with GLuc in comparison with native coelenterazine. Both substrates 2-BnO-TEG-CTZ and 6-BnOTEG-CTZ showed more than 200- and 950-fold reduction in total bioluminescence activity, respectively (Table 1). Interestingly, Urano *et al.* observed similarly poor bioluminescence activity when attaching flexible PEG linkers to aminoluciferin.[18] Installing rigid alkyl linkers also resulted in a low bioluminescence output. The poor observed activity was attributed to that these linkers may be linear and adopt conformations that hinder access of the luciferin substrate to the active site of the luciferase enzyme. Hence, it was concluded that long PEG linkers conjugated near the luminophore are unsuitable. This conclusion also seems to be valid in the case of installing PEG linkers on coelenterazine as well.

Table 1. Relative and maximum luminescence of 2- and 6-BnO-TEG-CTZ, and CoelPhos.

Compound	*Gaussia* luciferase	
	I_{Total} (%)[a]	I_{Max} (%)[b]
Coelenterazine (**1**)	100	100
2-BnO-TEG-CTZ (**2**)	0.45	0.17
6-BnO-TEG-CTZ (**3**)	0.10	0.14
CoelPhos (**4**)	3.23	2.70

[a] I_{Total}: total luminescence integrating for 60 s in 1 s intervals.

[b] I_{Max}: maximum observed intensity at any 1 s interval.

Design and Synthesis of CoelPhos

Due to detrimental effect on bioluminescence activity of PEGmodified coelenterazines we decided to change to more rigid alkyl linkers. Although our initial results suggested that both 2- and 6-positions of coelenterazine were both sensitive to modification, we decided to focus on modification of the 2- position of coelenterazine. We synthesized a phosphonate alkyne, dimethyl(prop-2-ynyloxy)methylphospho-nate **16** in two steps (Scheme S3). Alkylation of **10** with 1,3-dibromopropane resulted in formation of **17**, which was converted into the propyl azide **18**. Copper(I)-catalyzed azide-alkyne Huisgen cycloaddition[26] gave the desired 1,2,3-triazole **19**. In the final step acid-catalyzed condensation reaction of **6** and **19** was conducted, generating the desired product CoelPhos (Figure 2) (See supporting information for further description and details). Next, we evaluated the luminescent properties of CoelPhos with GLuc (Table 1) and *Renilla* luciferase (RLuc) comparison with coelenterazine (Table 2). CoelPhos yielded a much stronger luminescence with GLuc than RLuc and also a significant improvement in bioluminescence activity compared with both 2- and 6-BnO-TEG-CTZ, although CoelPhos still showed about a 30-fold reduction in luminescence intensity in comparison with coelenterazine. With the exception of s-CTZ,[17] the highest reported bioluminescence activity of any coelenterazine derivative with GLuc was that of *MeO*-CTZ (methylation of the 2-hydroxy group) (13.6%) and *3iso*-CTZ (replacement of 2-hydroxy group with 3-isopropylbenzene), (14.3%).[16]

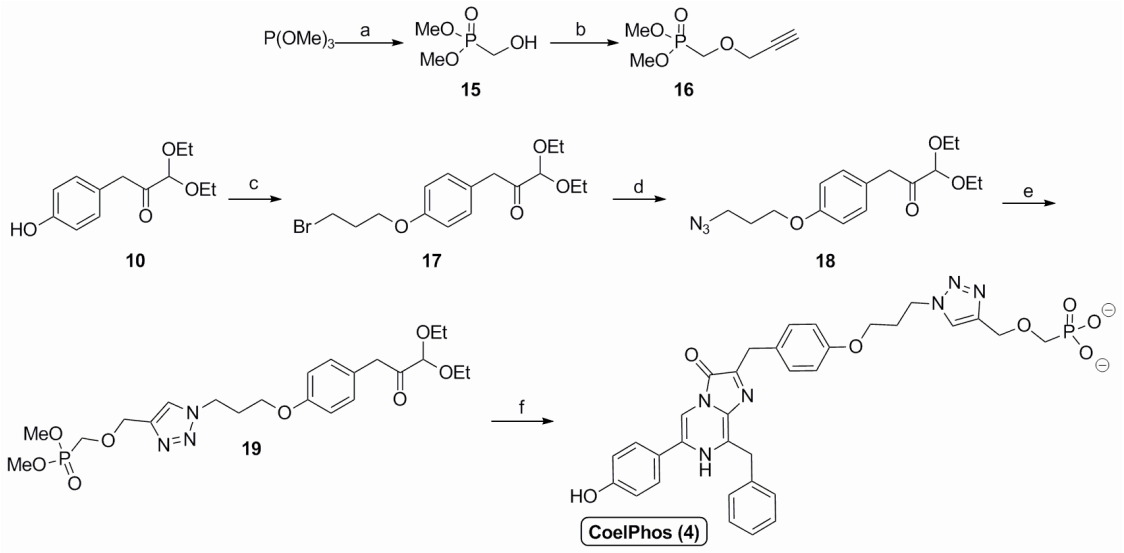

Scheme 3. Synthesis of CoelPhos. (a) paraformaldehyde, TEA, 130 °C, 3 h. 12%; (b) propargyl bromide, NaH, THF, -70 °C. 35%; (c) 1,3-dibromopropane, Cs_2CO_3, MeCN, reflux, 3 h. 35%; (d) NaN_3, DMF, 50 °C, 12 h, 76%; (e) **16**, $CuSO_4$, Sodium Ascorbate, H_2O/CH_2Cl_2(1:1), rt, 12 h, 88%; (f) **6**, 1,4-dioxane/6N HCl (10:1), 110 °C, 5-6 h, 9%.

Table 2. Relative and maximum luminescence of CoelPhos with *Renilla* luciferase cell lysate.

Compound	*Renilla* luciferase	
	I_{Total} (%)[a]	I_{Max} (%)[b]
Coelenterazine	100	100
CoelPhos	0.14	0.09

[a] I_{Total}: total luminescence integrating for 20 s in 1 s intervals.

[b] I_{Max}: maximum observed intensity at any 1 s interval.

2.3 Bioluminescence Imaging with CoelPhos

Recently GLuc mutants with improved luminescence output and stable luminescence profiles have been reported.[28,29] We utilized a recently developed mutant GLuc (GLucM23) with roughly 10-fold improvement in luminescence intensity in living cells, and a glow-type kinetic profile (Figure). We evaluated CoelPhos by measuring bioluminescence activity with a charge-coupled device (CCD) camera in

HeLa cells expressing outer-membrane localized wild-type GLuc or GLucM23 ($GLucM23_{Mem}$) to determine if the improved mutant GLuc had a negative or positive impact on the luminescence intensity of CoelPhos (Figure 3). We determined the relative intensities of coelenterazine and CoelPhos by comparing the relative mKO fluorescence and luminescence intensities of 5 cells (Figure 4). CoelPhos showed similar relative bioluminescence activity with the mutant GLucM23 in comparison with the wild-type GLuc relative to coelenterazine (~ 3–4 %). Hence the GLuc mutant did not affect the bioluminescence activity of CoelPhos relative to coelenterazine. The contrast observed in HeLa cells expressing outer membrane bound GLuc was very poor in comparison with GLucM23. This is related to the flash-type luminescence of GLuc, together with the luminescence sensitivity of our imaging system. The stable glow-type luminescence of GLucM23 and its higher luminescence output makes it more suitable for BLI in living cells. This was especially true for our derivative CoelPhos which could

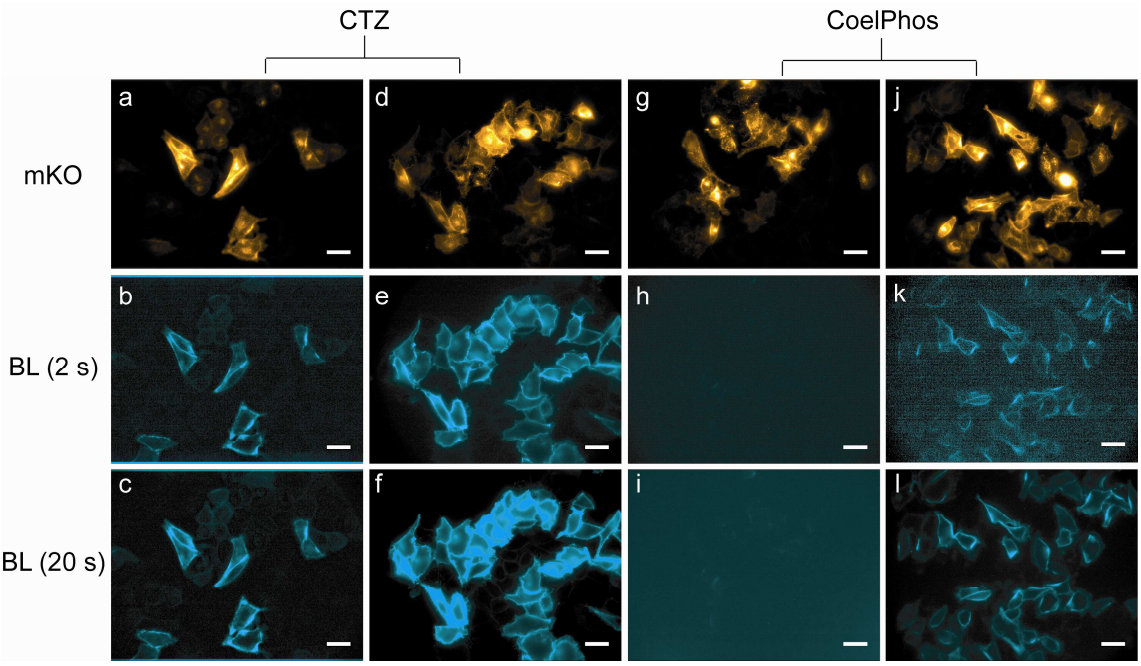

Figure 3. Bioluminescence imaging with coelenterazine (CTZ) and CoelPhos in HeLa cells expressing outer-membrane bound GLuc or GLucM23. (a, d, g, j) Fluorescence images of mKO (λ_{ex} = 548 nm / λ_{em} = 559 nm; 200 ms) before addition of bioluminogenic substrate. CTZ with $GLuc_{Mem}$, exposure time: 2 s (b) and 20 s (c); CTZ with $GLucM23_{MeM}$, exposure time: 2 s (e) and 20 s (f); CoelPhos with $GLuc_{Mem}$, exposure time: 2 s; (h), 20 s (i) CoelPhos with $GLucM23_{Mem}$, exposure time: 2 s (k) and 20 s (l). Concentration of CTZ and CoelPhos: 22.7 μM. Objective lens: 60×. Scale bar: 40 μm.

be imaged with much improved signal-to-noise with GLucM23Mem (Figure 3k, 3l) over $GLuc_{Mem}$ (Figure 3h, 3i).

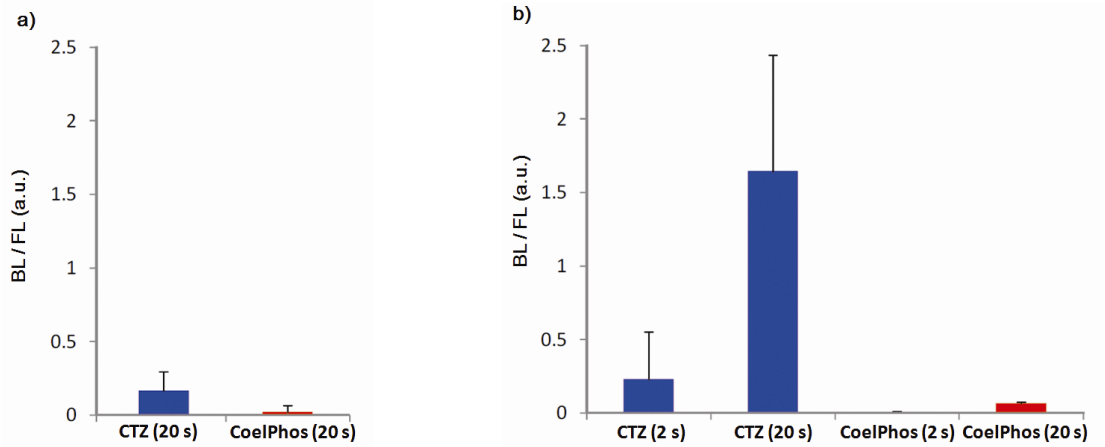

Figure 4. Relative activity of CoelPhos with GLuc and GLucM23 versus Coelenterazine (CTZ) in HeLa cells. (a) CTZ and CoelPhos with GLuc; (b) CTZ and CoelPhos with GLucM23. (n = 5 cells); Signal was quantified using ImageJ. (2 or 20 s) = exposure time.

Finally, we evaluated the relative cell-membrane permeability of our probe CoelPhos in comparison with coelenterazine. We transfected HeLa cells with an endoplasmic reticulum (ER)-localizing GLuc construct ($GLuc_{ER}$). The construct also contained Venus fluorescent protein as a control for expression levels as well as confirmation of localization. We reasoned that whilst coelenterazine would give a strong signal due to its high cell-permeability, CoelPhos would not give any bioluminescence signal due to its inability to cross the cell membrane (Figure 5).

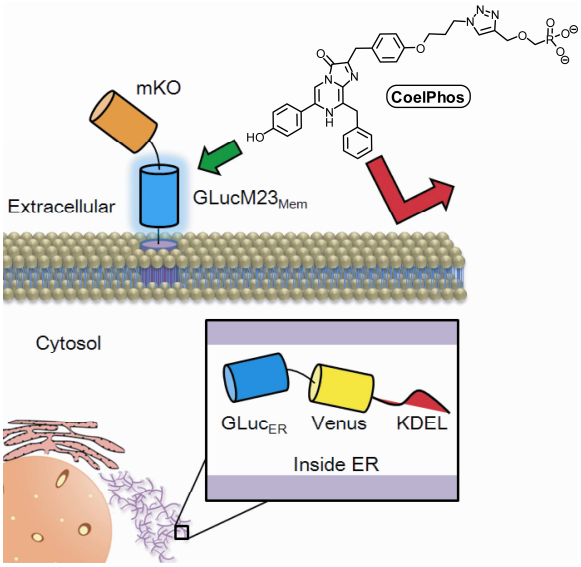

Figure 5. Illustration of cell-permeability of CoelPhos. Because of the attached anionic phosphonate CoelPhos does not penetrate the cell-membrane as readily as native coelenterazine. Therefore a bioluminescent signal will be observed with outer-membrane bound $GLucM23_{Mem}$ but not with intracellularly localized $GLuc_{ER}$.

When coelenterazine was added, strong bioluminescent signals were observed in HeLa cells expressing $GLuc_{ER}$. On the other hand, when CoelPhos was added, no signal could be detected, even after extending the exposure time to 100 s (20-fold) (Figure 6).

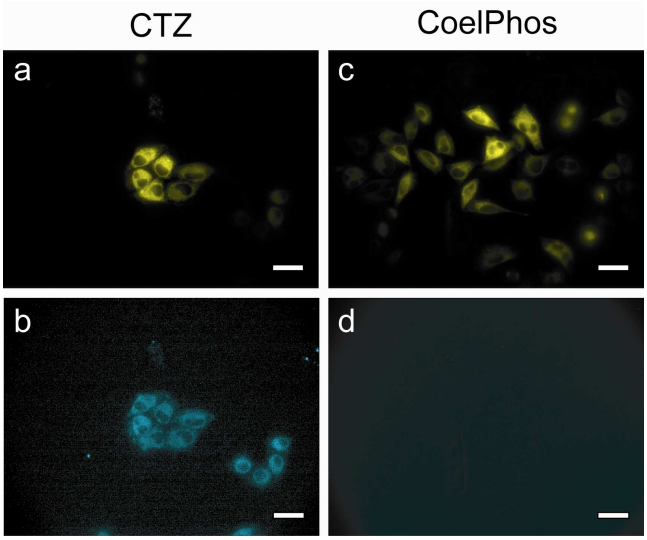

Figure 6. Fluorescence and bioluminescence images of HeLa cells expressing $GLuc_{ER}$ with coelenterazine (CTZ) and CoelPhos. (a) Venus FL; (b) CTZ (22.7 μM); exposure time: 5 s; (c) Venus FL; (d) CoelPhos (22.7 μM); exposure time: 100 s. Objective lens: 60 ×. Scale bar: 40 μm.

The observed data seem to suggest that attachment of a terminal phosphonate moiety is enough to significantly decrease cell-membrane permeability of the coelenterate substrate. It has been shown that GLuc produces 1000-fold higher BL signal than RLuc or FLuc in mammalian cells.1,30 GLucM23 has roughly 10 times higher BL intensity over wild-type GLuc in mammalian cells, suggesting that this novel mutant GLuc could have 10000-fold higher BL signal over RLuc and FLuc in mammalian cells. Although there was over 30-fold decrease in BL activity of CoelPhos with GLuc and GLucM23 in comparison with native coelenterazine, it seems reasonable to assume that CoelPhos together with GLucM23 would show stronger BL intensity over RLuc with coelenterazine. Further investigation is required however, in order to be able to make a direct comparison. Not only does the substrate specificity of GLuc differ from other coelenterate luciferases such as *Renilla* and *Oplophorus* luciferase. GLuc has been shown to contain two catalytic domains; both with similarly narrow substrate specificities.[30] Significant differences are also observed in the kinetic properties. Unlike other marine luciferases (RLuc, CLuc) which respond to their respective coelenterate luciferin concentration in a linear non-cooperative manner, it was recently shown that GLuc operates in a cooperative manner, possibly via an allosteric mechanism.[31] Previous studies utilizing bioluminescence imaging for monitoring of real-time protein secretion showed the importance of the type of camera used. Exocytotic events of native GLuc in CHO-K1 cells were visualized in real time with a time resolution of 10 s. However, the resolution of luminescence spots was low, which made if difficult to

identify single exocytotic spots of luminescence due to the low luminescence sensitivity of the camera used.[12] In more recent studies the same group utilized a more powerful EM-CCD which resulted in a 60-fold increase in sensitivity which allowed for the real-time monitoring of localization and dynamics of proteins on the surface of cells with millisecond temporal resolution.[13,14] Notwithstanding the fact that the CCD camera employed in our imaging studies was inferior to cameras utilized in the above references in terms of quantum efficiency and signal-to-noise, we were able to visualize CoelPhos with GLucM23Mem at a sampling rate of 2 s. Hence it is plausible to venture that utilization of EM-CCD cameras with improved sensitivity will allow for bioluminescence imaging of CoelPhos with much improved temporal resolution and luminescence sensitivity.

3 Conclusions

In conclusion, we have developed a cell-membrane impermeable coelenterazine derivative, CoelPhos, as a potential tool for monitoring membrane fusion events in living cells. The derivative was constructed by alkylating the phenolic hydroxyl group at the 2-position of coelenterazine with an alkyl linker containing a terminal phosphonate group. While displaying 30-fold less activity with GLuc compared with native coelenterazine, CoelPhos showed a high specificity for GLuc over RLuc with a 30-fold higher activity. By utilizing a new mutant GLuc, GLucM23, we were able to image membrane-localized GLucM23 despite the lower luminescence intensity of CoelPhos. We demonstrated that CoelPhos has decreased cell-membrane permeability in comparison with native coelenterazine. Our probe, CoelPhos, has the potential to be used as a cell-impermeable bioluminescent tool for monitoring of exocytotic events.

Experimental

Materials and Instruments

General reagents and chemicals were purchased from Sigma-Aldrich Chemical Co. (St. Louse, MO), Tokyo Chemical Industries (Tokyo, Japan), and Wako Pure Chemical (Osaka, Japan) and were used without further purification. Silica gel chromatography was performed using BW-300 (Fuji Silisia Chemical Ltd., Greenville, NC). pcDNA4™/TO/myc-His/lacZ was purchased from Life Technologies Corporation (Japan) NMR spectra were recorded on a JEOL JNM-AL400 instrument at 400 MHz for ^{1}H and 100.4 MHz for ^{13}C NMR, using tetramethylsilane as an internal standard. Mass

spectra were measured on a Waters LCT-Premier XE mass spectrometer for ESI or on a JEOL JMS-700 for FAB. UV-visible absorbance spectra were measured using a Shimadzu UV1650PC spectrometer. High pressure liquid chromatography (HPLC) analysis was performed with an Inertsil ODS3 column (4.6 × 250 mm, GL Science, Inc. Torrance, CA) using an HPLC system that comprised a pump (PU2080, JASCO) and a detector (MD2010 and FP2020, JASCO). Preparative HPLC was performed with an Inertsil ODS3 column (10.0 × 250 mm)(GL Sciences Inc.) using an HPLC system with a pump (PU-2087, JASCO) and a detector (UV-2075, JASCO). Bioluminescence was measured in 96-optiplate multiwell plates (PerkinElmer Co., Ltd.) using a Wallac ARVO mx / light 1420 Multilabel / Luminescence counter with an auto-injector (PerkinElmer Co., Ltd.). Bioluminescence imaging was performed utilizing an Olympus DP30 Cooled Monochrome CCD Microscope Camera with a 60 × objective lens. Coelenterazine was synthesized as previously described and stored as 10 mM MeOH/HCl (<1%) solution aliquotes in sealed glass ampulles at -80°C.[25,26]

Mutant GLuc

The cDNA for *Gaussia* luciferase (GLuc) was purchased from New England BioLabs Inc. The DNA sequence coding for GLuc without sequence for signal peptide (dspGLuc, aa18-) was amplified by PCR with primers containing the sequence encoding NdeI site, a bacterial periplasm localization signal (pelB) and XhoI site at the 5′ end and PstI site at the 3′ end. The entire cDNA of pelB-dspGLuc was cloned into NdeI and PstI sites of $pRSET_B$ (Invitrogen), yielding pRSET-pelB-dspGLuc. For mutant GLuc, The sequences corresponding to dspGLuc were randomly mutated by error-prone PCR, The sequence for dspGLuc in pRSET-pelB-dspGLuc was replaced with those PCR products containing mutant dspGLuc. These plasmids were transformed into JM109(DE3) competent cells, then, spread on LB ampicillin plates. After each bacterial colony was visible, each colony was picked and transferred to two new LB ampicillin plates, sequentially. After colonies were grown, we poured 50 μM coelenterazine containing PBS solution on top of the plate. The colonies which showed bright luminescence were picked and and evaluated by sequencing analysis. We obtained two mutants that showed bright luminescence. Mut1 contained K50E, M60L, M127I mutations, and Mut2 contained A36V, V113D mutations. We analyzed each of these mutations and found these mutations showed additive effects. A combination of these mutations resulted in an even brighter GLuc mutant, which had K50E, M60L, V113D, M127I and G184D mutations (GLucM23).

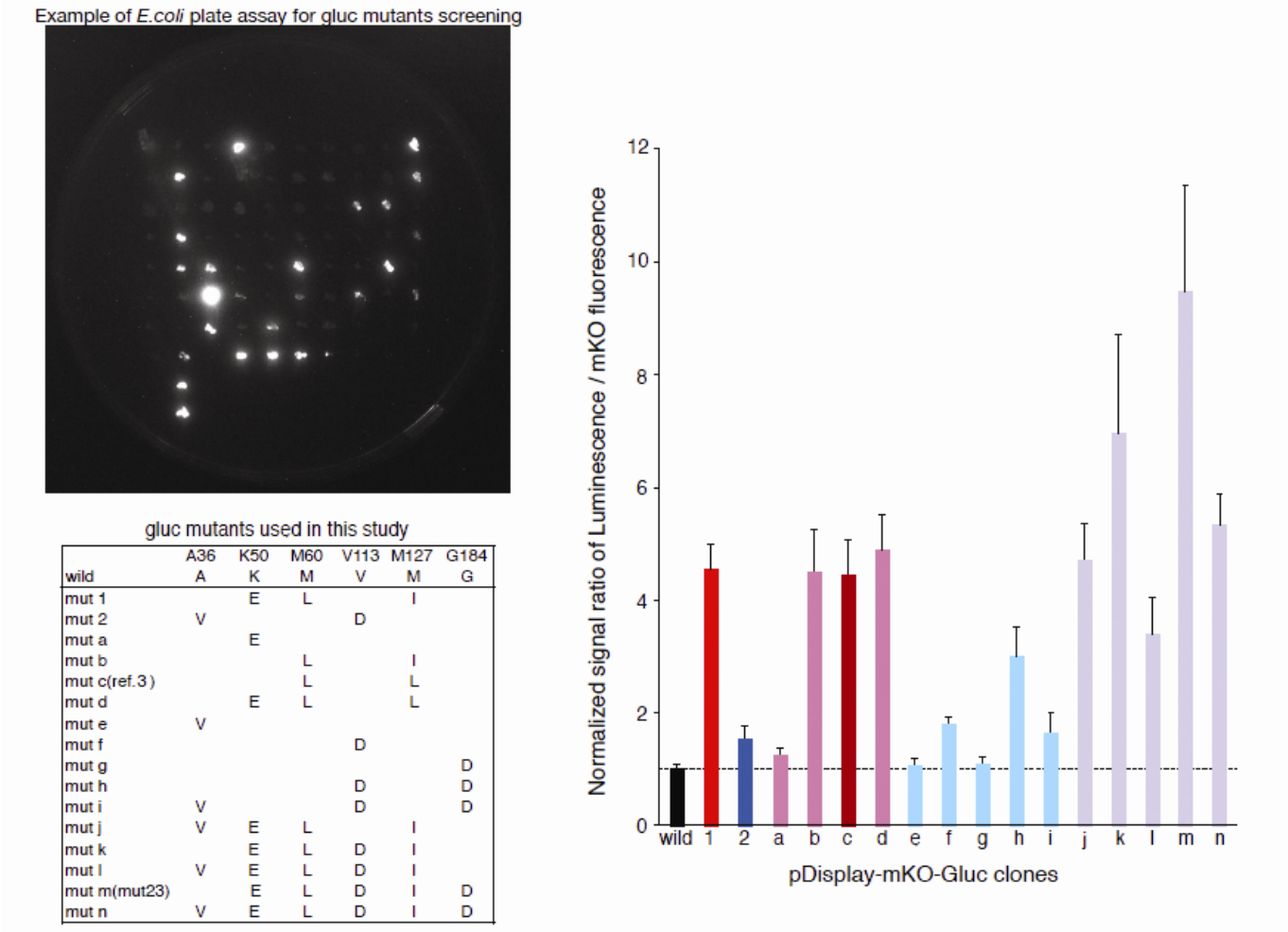

	A36	K50	M60	V113	M127	G184
wild	A	K	M	V	M	G
mut 1		E	L		I	
mut 2	V			D		
mut a		E				
mut b			L		I	
mut c(ref.3)			L		L	
mut d		E	L		L	
mut e	V					
mut f				D		
mut g						D
mut h				D		D
mut i	V			D		D
mut j	V	E	L		I	
mut k		E	L	D	I	
mut l	V	E	L	D	I	
mut m(mut23)		E	L	D	I	D
mut n	V	E	L	D	I	D

Figure S1. Displaying types of mutant variations of GLuc generated and their respective activities.

Mammalian cell expression constructs

To make pCDNA3- GLuc-Venus-KDEL, the entire sequence of GLuc was amplified by PCR with primers containing BamHI site, kozak sequence (ccacc) before start codon at the 5′ end and BspEI site, KDEL for endoplasmic reticulum localization signal sequence, stop codon and EcoRI site at the 3′ end. This PCR product was cloned into BamHI and EcoRI site of pcDNA3 vector (Invitrogen). This plasmid was then cut by BspEI and the cDNA of Venus fluorescent protein containing 5′ BspEI site and 3′ AgeI site was inserted. To make pDisplay-mKO-GLucM23, the entire sequence of mKusabira-Orange (mKO) was amplified by PCR with primer containing BamHI site at the 5′ end and BglII site at the 3′ end. The sequence of dspGLucM23 was also amplified

by PCR with primers containing BglII site at the 5' end and PstI site at the 3' end. Two PCR products were ligated and cloned into BglII and PstI sites of pDisplay vector (Invitrogen). pDisplay-mKO-GLuc was constructed in a similar fashion.

General experimental details for cell-cultures

HeLaS3 cells were maintained in Dulbecco's Modified Eagle Medium (DMEM) (Invitrogen), supplemented with 10% fetal bovine serum (FBS) at 37°C under 5% CO_2. *Transfection*: Optimem (Invitrogen) solutions containing lipofectamine 2000 (Invitrogen) and plasmid DNA were added to HeLaS3 cell cultures and incubated at 37°C under 5% CO_2 for 24 h. Cells were then washed three times with PBS, trypsinized, washed with Leibovitz's L-15 medium, then resuspended in black 96-well optiplates (PerkinElmer) and incubated at 37 °C in luminometer (PerkinElmer).

Preparation of secreted *Gaussia* luciferase

HEK293T cells maintained in DMEM (no phenol red) supplemented with 10% FBS and transfected with pCM-GLuc (New England Biolabs) were incubated at 37 °C under 5% CO_2 for 24 h. The cell-medium was carefully transferred to a separate tube, and centrifuged. The supernatant was aliquoted and stored at −80 °C.

Preparation of *Renilla* luciferase cell lysate

HEK293T cells transfected with pRL-TK at 37 °C under 5% CO_2 for 24 h were washed with PBS (0.1 M, pH 7.4). 800 μL lysate buffer (20 mM Tris buffer (pH 7.4) 150 mM NaCl), containing a mixture of protease inhibitors (PSMF (1 mM), Leupeptin (~ 1 μg / ml), and Pepstatin (~ 1 μg / ml). The suspension was frozen in liquid nitrogen and dethawed 3 times, followed by centrifugation at 15000 rpm at 4 °C for 30 min. Protein concentration was determined by Bradford assay; 41.67 μg / mL.

Determination of Relative and Maximum Luminescence of Coelenterazine Derivatives with GLuc

To a solution of 10 μL GLuc in 90 μL PBS (pH 7.4, 20 mM EDTA, 0.02% Tween20) was added a buffer solution of coelenterate substrate (100 μL, 10 μM) via auto-injector (Final concentration 5 μM). Luminescence was measured for 60 s at 1 s intervals.

Determination of Relative and Maximum Luminescence of Coelenterazine Derivatives with RLuc

To a solution of Rluc (12.5 μg / mL) in 100 μL Tris buffer (20 mM , pH 7.6), 10 mM

EDTA) was added a buffer solution of coelenterate substrate (100 μL, 10 μM) via auto-injector (Final concentration 5 μM). Luminescence was measured for 20 s at 1 s intervals.

Bioluminescence Imaging

HeLaS3 cells in glass-bottom dishes were transfected with pDisplay-mKO-GLuc, pDisplay-mKO-GlucM23, or pcDNA3-GLuc-Venus-KDEL and incubated at 37°C under 5% CO_2 for 20 h. Cells were washed with Hank's balanced salt solution (HBSS) and suspended in 100 μL HBSS (covering the central glass bottom part of the dish). Coelenterazine or CoelPhos in HBSS (1000 μL, 25 μM) was added to the glass-bottom dish (final concentration 22.7 μM) and luminescence was recorded at set exposure times. Fluorescence microscopic images were obtained before addition of coelenterate substrate (mKO: ex/em: 548/561; 200 ms; Venus Ex/Em: 515/528; 300 ms).

2. Syntheses of Compounds

1. Synthesis of coelenteramine and α-ketoacetal.

3-benzyl-5-bromo-2-pyrazinamine (5)

To a solution of benzylmagnesium chloride (2.0 M, 2.6 mL, 5.20 mmol) in THF (10 mL) was added zinc chloride in Et_2O (1.0 M, 5.7 mL, 5.70 mmol) at room temperature under argon. The resulting turbid mixture was stirred for 30 min, after which bis(triphenyl phosphine)palladium (II) dichloride (83 mg, 0.12 mmol) and 2-amino-3,5-dibromo-pyrazine (600 mg, 2.37 mmol) was added. The reaction was stirred for 3 days at room temperature. The reaction mixture was poured into water and extracted with EtOAc. The combined organic layer was washed with brine, dried over anhydrous sodium sulfate, and concentrated *in vacuo*. Purification by silica gel chromatography (25% EtOAc / hexane) afforded 525 mg (1.99 mmol, 84%) of 3-benzyl-5-bromo -2-pyrazinamine (**5**). ^{1}H-NMR (400 MHz, DMSO-d_6) δ 7.96 (s, 1H) 7.26-7.14 (m, 5H) 4.01 (s, 2H) ESI-MS: calc: 264.02; found: 264.00 $[M+H]^+$.

3-benzyl-5-(4-*tert*-butyldimethylsilyloxyphenyl)-2-pyrazinamine (6)

To a suspension of bis(benzonitrile)dichloro palladium (44 mg, 0.11 mmol) in toluene (5 mL) was added 1,4-bis(diphenyl- phosphino)butane (53 mg, 0.12 mmol) and the mixture was stirred for 30 min under argon at room temperature. 5-benzyl-5-bromo-2-pyrazinamine (**5**)(519 mg, 1.97 mmol), 4-(*tert*-butyldimethylsilyloxy)-

phenylboronic acid (656 mg, 2.60 mmol), toluene (10 mL), ethanol (1 mL), and aqueous sodium carbonate (1 M) were added sequentially and the mixture was refluxed for 24 h. After cooling down to room temperature the reaction mixture was poured into water and extracted with EtOAc. The combined organic layer was washed with brine, dried over anhydrous sodium sulfate, and concentrated *in vacuo*. Purification by silica gel chromatography (20-30% EtOAc / hexane) afforded 639 mg (1.63 mmol, 83%) 3-benzyl-5-(4-*tert*-butyldimethyl- silyloxyphenyl)-2-pyrazinamine (**6)** as a pale yellow solid. ^{1}H-NMR (400 MHz, $(CD_3)_2CO$) δ 8.36 (s, 1H) 7.88 (d, ^{3}J = 8.0 Hz, 2H) 7.35 (d, ^{3}J = 8.0 Hz, 1H) 7.28 (m, 2H) 7.20 (dd, ^{3}J = 8.0 Hz, 2H) 6.93 (d, ^{3}J = 8.0 Hz, 2H) 4.16 (s, 2H) 1.00 (s, 9H) 0.23 (s, 6H); ESI-MS: calc: 392.22; found: 392.18 $[M+H]^{+}$.

4-(*tert*-butyldimethylsilyloxy)phenylmethanol (7)

To a solution of 4-hydroxybenzaldehyde (5.75 g, 47.1 mmol) and imidazole (6.45 g, 94.8 mmol) in anhydrous CH_2Cl_2 (60 mL) was added TBDMSCl (7.88 g, 52.28 mmol) and was stirred overnight at room temperature under an argon atmosphere. The reaction mixture was poured into water washed with water and brine. The organic layer was dried over anhydrous sodium sulfate and the solvent was removed *in vacuo* and the residue was dried over night. To a solution of the crude 4-(*tert*-butyldimethylsilyloxy)benzaldehyde in methanol was added sodium borohydride (2.24 g, 59.1 mmol) at 0 °C. The ice-bath was removed and the solution was stirred under argon for 2 h. Reaction was quenched by addition of brine. MeOH was evaporated and water was added. The aqueous layer was extracted with EtOAc. The organic layer was washed with brine, dried over sodium sulfate and concentrated *in vacuo,* followed by purification by silica gel chromatography (30% EtOAc / hexane) to afford 9.709 g (86% for 2 steps) of 4-(*tert*-butyldimethylsilyloxy)phenylmethanol (**7**) as a pale yellow viscous oil. ^{1}H-NMR (400 MHz,$CDCl_3$) δ 7.22 (d, ^{3}J = 8.6 Hz, 2H) 6.82 (d, ^{3}J = 8.6 Hz, 2H) 4.60 (s, 2H) 0.99 (s, 9H) 0.20 (s, 6H).

4-(*tert*-butyldimethylsilyloxy)benzyl chloride (8)

To solution of 4-(*tert*-butyldimethylsilyloxy)phenylmethanol (**7**)(10.6 g, 41.3 mmol) in CH_2Cl_2 (~50 mL) at 0 °C under argon was added thionyl chloride (4.6 mL, 63.0 mmol) dropwise. The reaction mixture was stirred for 2 h and poured into water. The organic layer was washed with water ample times, followed by brine. The organic layer was dried over sodium sulfate and evaporated *in vacuo*. Purification by silica gel chromatography (10% EtOAc / hexane) to afford 8.60 g (81 %) of 4-(*tert*-butyl-dimethylsilyloxy)benzyl chloride (**8**). ^{1}H-NMR (400 MHz,$CDCl_3$) δ 7.26 (d, ^{3}J = 8.6 Hz,

2H) 6.83 (d, ^{3}J = 8.6 Hz, 2H) 4.57 (s, 2H) 1.00 (s, 9H) 0.22 (s, 6H). ^{13}C-NMR (100 MHz, $CDCl_3$) δ 155.89, 130.29, 129.96, 120.26, 46.29, 25.64, 18.19, -4.44.

3-(4-(*tert*-butyldimethylsilyloxy)phenyl)-1,1-diethoxyacetone (9)

To magnesium turnings (4.29 g, 176.5 mmol) (vigorously stirred under argon for 3 days) was added 4-(*tert*-butyldimethyl- silyloxy)benzyl chloride (**8**)(8.60 g, 33.5 mmol) in anhydrous THF, followed by additional THF (~ 50 mL), and 1,2-dibromo- ethane (50 μL, 0.58 mmol). The reaction mixture was sonicated for 5 mins, and heated at 50 °C for 1 h. The dark grey reaction mixture was allowed to cool to room temperature. To a separate reaction flask was added ethyl diethoxyacetate (8.0 mL, 44.7 mmol) and THF (~10 mL) and cooled to -78 °C (dry ice / acetone) under argon. The Grignard reagent was added via syringe over 30 mins and the reaction mixture was allowed to stir for 6 h, followed by addition of water (25 mL) and the reaction mixture allowed to warm to room temperature. Additional water was added and extracted with EtOAc. The organic layer was washed with brine, dried over sodium sulfate, and concentrated *in vacuo*. The crude pale yellow oil was purified by silica gel chromatography (10% EtOAc / hexane) to afford 5.54 g (15.7 mmol, 47%) of 3-(4-(*tert*-butyldimethylsilyloxy)-phenyl)-1,1-diethoxy acetone (**9**) as a pale yellow oil. ^{1}H-NMR (400 MHz, $CDCl_3$) δ 7.07 (d, ^{3}J = 8.0 Hz, 2H) 6.78(d, ^{3}J = 8.0 Hz, 2H) 4.62 (s, 1H) 3.80 (s, 2H) 3.70-3.51 (m, 2 x 2H) 1.24 (t, ^{3}J = 7.0 Hz, 6H) 0.97 (s, 9H) 0.18 (s, 6H); ^{13}C-NMR (100 MHz, $CDCl_3$) δ 203.6, 154.5, 130.7, 126.3, 120.1, 102.1, 63.3, 43.1, 25.7, 18.2, 15.1, -4.5. ESI-MS: calc: 370.2408; found: 370.3069 $[M+NH_4]^+$.

3-(4-hydroxyphenyl)-1,1-diethoxyacetone (10)

To 0 °C cooled solution of 3-(4-(*tert*-butyldimethylsilyloxy)phenyl)-1,1- diethoxy acetone (**9**)(1.50 g, 4.25 mmol) in THF (10 mL) under argon was added tetra-*n*-butylammonium fluoride (1.0 M in THF, 2.2 mL, 2.2 mmol). After 30 min, the reaction was quenched with saturated aqueous sodium chloride and extracted with CH_2Cl_2. The combined organic layer was dried over anhydrous sodium sulfate and concentrated *in vacuo*. Purification by silica gel chromatography afforded 944 mg, (3.96 mmol, 93%) of 3-(4-hydroxyphenyl)-1,1-diethoxyacetone. ^{1}H-NMR (400 MHz, $CDCl_3$) δ 7.26 (d, ^{3}J = 8.0 Hz, 2H) 6.78 (d, ^{3}J = 8.0 Hz, 2H) 4.69 (s, 1H) 4.63 (s, 2H) 3.82 (s, 2H) 3.72-3.53 (m, 2 x 2H) 1.25 (t, 6H). ESI-MS: calc: 256.1543; found: 256.1663 $[M+NH_4]^+$.

2. Synthesis of 2 and 6-OBn-TEG-CTZ.

.13-bromo-1-phenyl-2,5,8,11-tetraoxatridecane (12)

Sodium hydride (60% in mineral oil)(839 mg, 20.98 mmol) was added to a cooled reaction flask containing anhydrous DMF under argon. The mixture was stirred for 10 minutes, after which the ice-bath was removed and the mixture was stirred at rt for another 15 min. The mixture was cooled with an icebath, followed by dropwise addition of benzyl bromide (2.3 mL, 19.34 mmol). Reaction mixture was concentrated *in vacuo*, followed by silica gel chromatographyEtOAc to afford **11** (3.34 g, 11.61 mmol, 67%) as a colorless oil. To a solution of triphenylphosphine (856 mg, 3.26 mmol) and carbon tetrabromide (1088 mg, 3.28 mmol) in anhydrous CH_2Cl_2 under argon was added **7** (592 mg, 2.08 mmol). The reaction mixture was refluxed for 18 h. Reaction mixture was concentrated *in vacuo*. silica gel chromatography ((1:1) EtOAc / hexane) to afford **12** (483 mg, 15.7 mmol, 79% over two steps) as a colorless oil. 1H-NMR (400 MHz, $CDCl_3$) δ 7.35-7.34 (m, 5H) 4.57 (s, 2H) 3.72-3.59 (m, 16H). FAB: Calculated: 540.0879; Found: 540.0887 $[M+Na]^+$. ESI-MS: Calculated: 540.0879; Found: 540.1243$[M+Na]^+$.

3-benzyl-5-(4-(1-phenyl-2,5,8,11-tetraoxatridecan-13-yloxy)phenyl)pyrazin-2-amine (13)

To an ice-cooled solution of 3-benzyl-5-(4-*tert*-butyldimethylsilyloxyphenyl)-2-pyrazinamine (**6**) (80 mg, 0.20 mmol) in anhydrous THF under argon was added tetrabutylammonium fluoride (160 μL, 0.16 mmol) in THF. After 1 stirring for 1 h the reaction was quenced with brine, poured into water and extracted with EtOAc. The combined organic layer was washed with brine, dried over anhydrous sodium sulfate, and concentrated *in vacuo*. The resulting residue was subjected to silica gel chromatography ((1:1) EtOAc / Hexane), affording crude coelenteramine (~56 mg, 0.2 mmol). To a ice-cooled solution of sodium hydride (60% in mineral oil)(18 mg, 0.45 mmol) in anhydrous DMF (5 mL) was added coelenteramine (55 mg, 0.2 mmol) and the reaction mixture was stirred for 30 min. 12-bromo-1-benzyl-tetraethylene glycol (170 mg, 0.49 mmol) in DMF (5 mL) was added dropwise. The ice-bath was removed and the reaction mixture was stirred at rt for 4.5 h, after which the reaction was quenched with 20% NH_4Cl. The reaction mixture was diluted with water and extracted with EtOAc. The combined organic layers were washed with brine, dried over anhydrous sodium sulfate, and concentrated *in vacuo*. The resulting residue was subjected to silica column chromatography (2% MeOH / CH_2Cl_2) to afford the desired product **13** (58 mg, 55% over two steps). ^{1}H-NMR (400

MHz, $CDCl_3$) δ 8.31(s, 1H) 7.85 (d, 2H, ^3J = 8.0 Hz) 7.33-7.25 (m, 10H) 6.98 (d, ^3J = 8.0 Hz, 2H) 4.55 (s, 2H) 4.46 (s, 2H) 3.86 (t, 2H) 3.74-3.61 (m, 14H). ^{13}C-NMR (100 MHz, $CDCl_3$) δ 158.90, 151.29, 142.38, 140.40, 138.22, 136.82, 136.75, 130.10, 128.91 128.55, 128.32, 127.71, 127.56, 126.96, 126.90, 114.87, 73.18, 70.81, 70.61, 69.68, 69.39, 67.44, 41.15. ESI-MS: Calculated: 544.2806; Found: 544.2834 $[M+H]^+$. FAB: Calculated: 543.2733; Found: 543.2722 $[M]^+$.

1,1-diethoxy-3-(4-(1-phenyl-2,5,8,11-tetraoxatridecan-13-yloxy)phenyl)propan-2-one (14)

A solution of 3-(4-hydroxyphenyl)1,1-diethoxyacetone (**10**) (100 mg, 0.42 mmol), Cs_2CO_3 (202 mg, 0.62 mmol), and **12** (217 mg, 0.62 mmol) in anhydrous MeCN (5 mL) was refluxed under argon for 3 h. The reaction mixture was poured into water and extracted with EtOAc. The combined organic layer was washed with brine and dried over anhydrous sodium sulfate. The mixture was concentrated *in vacuo*, followed by purification by silica gel chromatography (40% EtOAc / Hexane) to yield **14** (154 mg, 0.31 mmol, 73%). ^{1}H-NMR (400 MHz, $CDCl_3$) δ 7.34-7.33 (m, 5H) 7.11 (d, ^3J = 8.4 Hz, 2H) 6.85 (d, ^3J = 8.4 Hz, 2H) 4.62 (s, 1H) 4.56 (s, 2H) 4.10 (t, 2H) 3.83 (t, 2H) 3.81 (s, 2H) 3.73-3.67 (m, 12H) 3.68-3.52 (m, 4H) 1.24 (t, ^3J = 7.2 Hz, 6H). ^{13}C-NMR (100 MHz,$CDCl_3$) δ 203.47, 157.69, 138.21, 130.65, 128.30, 127.68, 127.52, 125.83, 114.60, 102.14, 73.16, 70.75, 70.59, 69.66, 69.37, 67.13, 63.26, 42.80, 15.11. ESI-MS: Calculated: 522.3061; Found: 522.2361 $[M+NH_4]^+$.

6-OBn-TEG-CTZ (2)

A solution of **13** (55 mg, 0.10 mmol) and **9** (73 mg, 0.21 mmol) in 1,4-dioxane (5 mL) and 6N HCl (0.5 mL) was refluxed under argon for 24 h. The reaction was allowed to cool to rt and concentrated *in vacuo*. Silica gel chromatography, (3-6 % MeOH / CH_2Cl_2) afforded the desired product **6-OBn-TEG-CTZ (2)** as a dark red solid (14 mg, 0.02 mmol, 20 %). ^{1}H-NMR (400 MHz, CD_3OD) δ 7.67 (s, 1H) 7.38 (m, 2H) 7.31-7.15 (m, 10H) 6.78 (d, ^3J = 8.4 Hz, 2H) 6.72 (d, ^3J = 8.0 Hz, 2H) 4.52 (s, 2H) 4.41 (s, 2H) 4.13 (m, 2H+2H) 3.85 (t, 2H) 3.70-3.61 (m, 12H). ^{13}C-NMR (100 MHz, $CDCl_3$) δ 160.77, 156.27, 138.76, 136.92, 131.35, 130.90, 130.45, 129.85, 129.48, 129.33, 128.93, 128.81, 128.44, 128.28, 127.81, 125.91, 115.87, 115.64, 73.78, 73.12, 71.29, 71.11, 70.25, 70.05, 68.18, 61.78, 30.25. ESI-MS: Calculated: 690.3174; Found: 690.3279 $[M+H]^+$.

2-OBn-TEG-CTZ (3)

A solution of **2** (51 mg, 0.13 mmol) and **10** (124 mg, 0.25 mmol) in 1,4-dioxane (5 mL) and 6N HCl (0.5 mL) was refluxed under argon for 14 h. The reaction was allowed to cool to rt and concentrated *in vacuo*. Silica gel chromatography, (5-10 % MeOH / CH_2Cl_2) afforded the crude desired product (38.5 mg). The residue was further purified via RP-HPLC (H_2O (0.1 % formic acid) / MeCN (0.1 % formic acid) ; 60:40 → 70:30, 4.7 mL/min; column: ODS-3). The combined fractions were lyophilized, yielding the desired product **2-OBn-TEG-CTZ (3)** as a red solid (15 mg, 0.02 mmol, 17%). ^{1}H-NMR (400 MHz, $CDCl_3$) δ 7.64 (s, 1H) 7.32 (m, 2H) 7.25-7.07 (m, 10H) 6.98 (d, 2H, ^3J = 8.4 Hz) 6.72 (d, ^3J = 8.0 Hz, 2H) 4.54 (s, 2H) 4.41 (s, 2H) 4.02 (m, 2H + 2H) 3.84 (t, 2H) 3.68-3.58 (m, 12H) ^{13}C-NMR (100 MHz, $CDCl_3$) δ 158.77, 155.35, 137.56, 134.92, 129.64, 130.40, 130.25, 129.85, 129.68, 129.26 128.73, 128.51, 128.34, 128.26, 127.14, 125.68, 115.41, 114.55, 73.67, 73.08, 71.24, 71.01, 70.04, 70.01, 68.28, 60.75, 30.15. ESI-MS: Calculated:690.3174; Found: 690.2411 $[M+H]^+$. FAB: Calculated: 689.3101; Found: 689.3088 $[M]^+$.

3. Synthesis of CoelPhos

Comment: Initially installing of a propylphosphonate at the 2-position of coelenterazine was perceived as a suitable candidate compound. However, alkylation of the α-ketoacetal **10** with 3-bromopropylphosphonate proved difficult with formation of several side products (data not shown). Interestingly alkylation of **10** with 1,3-dibromopropane gave **17** which could be separated from the undesired side products more easily. Alkylation of **10** with ethyl 4-bromobutyrate has been reported previously,[1] which also resulted in a poor yield. On the other hand, alkylation of **10** with PEG linker **12** gave **14** in a satisfactory yield, suggesting stereochemistry to be an important factor in the general alkylation of **10**.. Hence we modified our synthetic route by considering converting the propyl bromide **17** into the propyl azide **18**, which would allow for diversification via copper(I)-catalyzed azide-alkyne Huisgen cycloaddition. In our initial attempt to form the 1,2,3-triazole between **16** and **18**, we utilized the common solvent system H_2O/*t*BuOH (1:1),[4] however in our hands hardly any product was formed. When we applied a two-phase solvent system (H_2O/CH_2Cl_2 (1:1)), which has been shown to improve reaction kinetics,[5] gave the desired 1,2,3-triazole **19** in very good yield.

Dimethyl hydroxymethylphosphonate (15)

To a solution of paraformaldehyde (1.27 g, 42.4 mmol) in trimethyl phosphite (5 mL, 42.3 mmol) was added triethylamine (0.6 mL, 4.30 mmol) under argon and was

refluxed at 130 °C for 3 h. Volatiles were removed *in vacuo*. The crude residue was purified by silica gel chromatography (4-5% MeOH / EtOAc) to afford 697 mg (4.98 mmol, 12%) of dimethyl hydroxyl- methylphophonate (**15**). ^{1}H-NMR (400 MHz,$CDCl_3$) δ 3.96 (m, 2H) 3.81 (d, ^{3}J = 8 Hz, 6H); ^{13}C-NMR (100 MHz, $CDCl_3$) δ 56.4 (d, J = 162.1 Hz) 53.1 (d, J = 6.6 Hz); ^{31}P-NMR (162 MHz, $CDCl_3$) single peak. ESI-MS: calc: 141.0311, found: 141.0473 $[M+H]^+$.

Dimethyl (prop-2-ynyloxy)methylphosphonate (16)

To -78 °C cooled solution of dimethyl hydroxymethylphosphonate (**15**)(172 mg, 1.23 mmol) in THF (2 mL) was added sodium hydride (96 mg, 2.40 mmol) and allowed to stir for 1.5 h. A solution of propargyl bromide (0.2 mL, 1.85 mmol) in THF (1 mL) was added dropwise via syringe. The reaction was left stirring for 14 h. The reaction was quenched with ammonium chloride and the solvent was evaporated. Water was added and extracted with CH_2Cl_2. The combined organic layer was washed with brine, dried over anhydrous sodium sulfate, and concentrated *in vacuo*. Purification by silica gel chromatography (3-4% MeOH / EtOAc) afforded 76 mg (0.43 mmol, 35%) of dimethyl (prop-2-ynyloxy)methylphosphonate (**16**) as a colorless oil. ^{1}H-NMR (400 MHz, $CDCl_3$) δ 4.28 (m, 2H) 3.92 (d, ^{2}J = 12Hz, 2H) 3.82 (d, ^{3}J = 8 Hz, 6H) 2.51 (m, 1H); ^{13}C-NMR (100 MHz, $CDCl_3$) δ 78.1, 76.0, 63.2 (d, J = 167.1 Hz) 60.1 (d, J = 14.9 Hz) 53.1 (d, J = 6.5 Hz); ^{31}P-NMR (162 MHz, $CDCl_3$) single peak. ESI-MS: calc: 179.0468, found: 179.0625 $[M+H]^+$.

3-(4-(3-bromopropoxy)phenyl)-1,1-diethoxyacetone (17)

To a solution of 3-(4-hydroxyphenyl)-1,1-diethoxyacetone (**10**) (952 mg, 4.00 mmol) and Cs_2CO_3 (1411 mg, 4.33 mmol) in anhydrous acetonitrile (20 mL) under argon was added 1,3-dibromopropane (2 mL, 19.7 mmol) by syringe. The solution was heated at 100 °C for 3 h. After cooling to room temperature the reaction mixture was filtered and washed with EtOAc and evaporated to dryness. The resulting residue was partitioned between water and EtOAc and the aqueous layer was extracted with EtOAc. The combined organic layer was washed with brine, dried over anhydrous sodium sulfate and concentrate *in vacuo*. Purification by gradual silica gel chromatography (5-10% EtOAc / hexane) afforded 510 mg (1.42 mmol, 35%) of 3-(4-(3-bromopropoxy)phenyl)-1,1-diethoxyacetone (**17**) as a pale yellow oil. ^{1}H-NMR (400 MHz, $CDCl_3$) δ 7.12 (d, ^{3}J = 8.0 Hz, 2H) 6.86 (d, ^{3}J = 8.0 Hz, 2H) 4.63 (s, 1H) 4.09 (t, ^{3}J = 8.0 Hz, 2H) 3.83 (s, 2H) 3.70 (m, 2H) 3.60 (m, 2H) 3.55 (m, 2H) 2.31 (m, 2H) 1.25 (t, ^{3}J = 8.0 Hz, 6H); ^{13}C-NMR (100 MHz, $CDCl_3$) δ 203.5, 157.6, 130.8, 126.0, 114.6,

102.3, 65.2, 63.4, 42.8, 32.4, 30.1, 15.2.

3-(4-(3-azidopropoxy)phenyl)-1,1-diethoxyacetone (18)

To a solution of 3-(4-(3- bromopropoxy)phenyl)-1,1-diethoxyacetone (**17**) (268 mg, 0.75 mmol) in anhydrous DMF, (~2 mL) was added sodium azide (78 mg, 1.20 mmol) and the reaction was heated at 50 °C for 12 h. The reaction was allowed to cool to room temperature, poured into water, and extracted with EtOAc. The combined organic layer was washed with brine and dried over anhydrous sodium sulfate, and concentrated *in vacuo*. Purification by silica gel chromatography (10% EtOAc / hexane) afforded 187 mg (0.58 mmol, 76%) of 3-(4-(3-azidopropoxy)phenyl)-1,1-diethoxyacetone (**18**). ^{1}H-NMR (400 MHz,$CDCl_3$) δ 7.12 (d, ^{3}J = 8.0 Hz, 2H) 6.85 (d, ^{3}J = 8.0 Hz, 2H) 4.62 (s, 1H) 4.03 (s, 2H) 3.70 (t, ^{3}J = 7.2 Hz, 2H) 3.54 (m, 4H) 2.04 (t, ^{3}J = 5.6 Hz, 2H) 1.25 (t, ^{3}J = 6.6 Hz, 6H). ^{13}C-NMR (100 MHz, $CDCl_3$) δ 203.5, 157.6, 130.8, 126.0, 114.6, 102.3, 64.5, 63.4, 48.3, 42.8, 28.8, 15.2. ESI-MS: calc: 339.2027; found: 339.2164 $[M+NH_4]^+$.

Dimethyl((1-(3-(4-(3,3-diethoxy-2-oxopropyl)phenoxy)propyl)-1H-1,2,3-triazol-4-yl)methoxy)methylphosphonate (19)

To a solution of 3-(4-(3-azidopropoxy)phenyl)-1,1-diethoxyacetone (**18**) (94 mg, 0.29 mmol), dimethyl (prop-2-ynyloxy) methylphosphonate (**16**) (61 mg, 0.34 mmol) in water (1 mL) and dichloromethane (1 mL) was added copper (II) sulfate (2.8 mg, 0.02 mmol), and sodium ascorbate (13.6 mg, 0.09 mmol). The reaction mixture was vigorously stirred for 12 h, poured into water and extracted with dichloromethane, dried over sodium sulfate, and concentrated *in vacuo*. Purification by silica gel chromatography afforded 129 mg (0.26 mmol, 88%) of dimethyl ((1-(3-(4-(3,3-diethoxy-2-oxopropyl)phenoxy)propyl)-1H- 1,2,3-triazol-4-yl)methoxy)methylphosphonate (**19**) as a viscous oil. ^{1}H-NMR (400 MHz, $CDCl_3$) δ 7.60 (s, 1H) 7.12 (d, ^{3}J = 8.4 Hz, 2H) 6.83 (d, ^{3}J = 8.4 Hz, 2H) 4.75 (s, 2H) 4.63 (s, 1H) 4.58 (t, ^{3}J = 7.2 Hz, 2H) 3.96 (t, ^{3}J = 5.6 Hz, 2H) 3.88-3.83 (m, 4H) 3.78 (d, ^{3}J = 10.8 Hz, 6H) 3.71 (m, 2H) 3.56 (m, 2H) 2.39 (m, 2H) 1.25 (t, ^{3}J = 6.8 Hz, 6H); ^{13}C-NMR (100 MHz, $CDCl_3$) δ 203.4, 157.3, 143.8, 130.9, 126.3, 123.5, 102.33, 66.2, 63.2 (d, ^{3}J = 167.0 Hz) 63.9, 63.4, 53.0, 47.1, 42.6, 29.9, 15.1. ^{31}P-NMR (162 MHz, $CDCl_3$) single peak. ESI-MS: calc: 500.2156; found: 500.1754 $[M+H]^+$.

((1-(3-(4-((8-benzyl-6-(4-hydroxyphenyl)-3-oxo-3,7-dihydroimidazo[1,2-a]pyrazin-2-yl)methyl)phenoxy)propyl)-1H-1,2,3-triazol-4-yl)methoxy)methylphosphonate

CoelPhos

To a solution of **19** (80 mg, 0.16 mmol) in 1,4-dioxane (1 mL) was added **6** (63 mg, 0.16 mmol). To this mixture was added 6 N $HCl_{(aq)}$ (100 µL) and the solution was thoroughly flushed and kept under an argon atmosphere. The reaction mixture was then heated to 110 °C and stirred for 5-6 h. The dark mixture was allowed to cool to room temperature and the solvent was evaporated. Reaction mixture was purified by reverse-phase HPLC (100 mM triethylammonium acetate / acetonitrile; 90:10 → 40:60, 4.7 mL/min; column: ODS-3). Collected fractions were concentrated, combined, and lyophilized to give product **CoelPhos** as the triethylammonium salt (11 mg, 9% yield). ^{1}H-NMR (400 MHz, CD_3OD) δ 7.94 (s, 1H) 7.70 (s, 1H) 7.50 (d, ^{3}J = 8.8 Hz, 2H) 7.35 (d, ^{3}J = 7.6 Hz, 2H) 7.23-7.11 (m, 7H) 6.82 (d, ^{3}J = 8.8 Hz, 2H) 6.75 (d, ^{3}J = 9.0 Hz, 2H) 4.62 (s, 2H) 4.53 (t, ^{3}J = 7.0 Hz, 2H) 4.34 (s, 2H) 4.04 (s, 2H) 3.89 (t, ^{3}J = 6.0 Hz, 2H) 3.56 (d, ^{3}J = 9.6 Hz, 2H) 2.28 (m, 2H). ^{13}C-NMR (100 MHz, CD_3OD) δ 159.52, 158.50, 146.07, 139.17, 133.63, 130.82, 129.85, 129.50, 129.14, 128.57, 127.73, 125.44, 125.40, 116.84, 115.45, 108.48, 69.43, 67.85, 66.68, 66.54, 65.57, 47.53, 36.71, 33.02, 31.09, 29.43, 23.85, 9.26. HRMS:ESI-MS: calc: 657.2221; found: 657.3062 $[M+H]^{+}$. ^{31}P NMR (162 MHz, CD_3OD, single peak. H-H COSY (400 MHz, CD_3OD)(Figure S2)

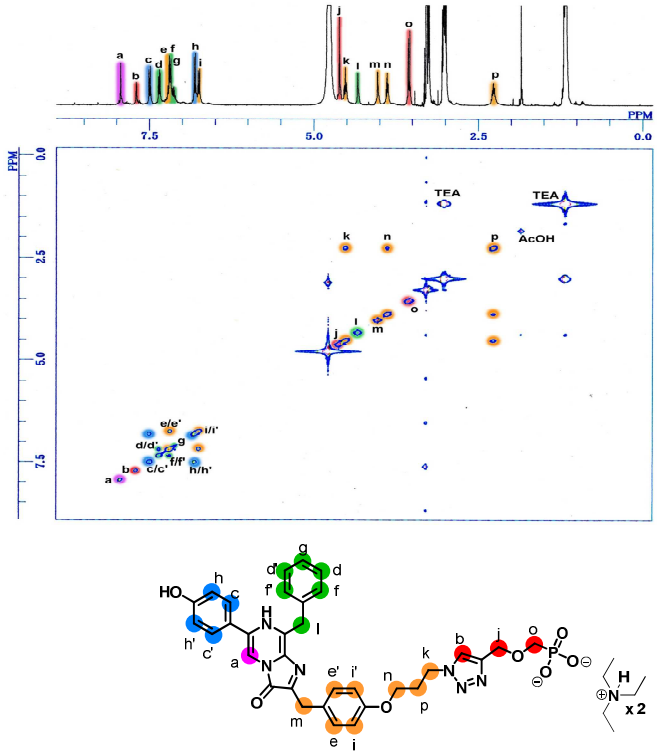

Figure S2. H-H-COSY diagram of CoelPhos

References

(1) Tannous, B. A.; Kim, D. -E.; Fernandez, J. L.; Weissleder, R.; Breakefield, X.O. *Mol. Ther.* **2005**, *11*, 435-443.

(2) Ozawa, T.; Yoshimura, H.; Kim, S. B.; *Anal. Chem.* **2013**, *85*, 590-609.

(3) Akopova, I.; Tatur, S.; Grygorczyk, M.; Luchowski, R.; Gryczynski, I.; Boredjo, J.; Grygorczyk, R. *Puriner. Signal.* **2012**, *8*, 59-70.

(4) Burchfield, J. G.; Lopez, J. A.; Mele, K.; Vallotton, P.; Hughes, W. E. *Traffic* **2010**, *11*, 429-439.

(5) Takahashi, N.; Kasai, H. *Endocrine J.* **2007**, *54*, 337-346.

(6) Oshima, A.; Kojima, T.; Dejima, K.; Hisa, Y.; Kasai, H.; Nemoto, T. *Cell Calcium* **2005**, *37*, 349-357.

(7) Matsuzaki, M.; Ellis-Davies, G. C. R.; Nemoto, T.; Miyashita, Y.; Iino, M.; Kasai, H. *Nat. Neurosci.* **2001**, *4*, 1086-1092.

(8) Inouye, S.; Ohmiya, Y.; Toya, Y.; Tsuji, F. *Proc. Natl. Acad. Sci. USA* **1992**, *89*, 9584-9587.

(9) Thompson, E. M.; Adenot, P.; Tsuji, F.; Renard, J-P. *Proc. Natl. Acad. Sci. USA* **1995**, *92*, 1317-1321.

(10) Miesenbock, G.; Rothman, J. E. *Proc. Natl. Acad. Sci. USA* **1997**, *94*, 3402-3407.

(11) Suzuki, T.; Usuda, S.; Ichinose, H.; Inouye, S. *FEBS Lett.* **2007**, *581*, 4551-4556.

(12) Suzuki, T.; Kondo, C.; Kanamori, T.; Inouye, S. *Anal. Biochem.* **2011**, *415*, 182-189.

(13) Suzuki, T.; Kondo, C.; Kanamori, T.; Inouye, S. *PLos ONE* **2011**, *6*, e25243.

(14) Inouye, S.; Sahara, Y. *Biochem. Biophys. Res. Commun.* **2008**, *365*, 96-101.

(15) Kimura, T.; Hiraoka, K.; Kasahara, N.; Logg, C. R. *J. Gene. Med.* **2010**, *12*, 528-537.

(16) Inouye, S.; Sahara-Miura, Y.; Sato, J-I.; Iimori, R.; Yoshida, S.; Hosoya, T. *Prot. Exp. Pur.* **2013**, *88*, 150-156.

(17) Morse, D.; Tannous, B. A.; *Mol. Ther.* **2012**, *20*, 692-693.

(18) Kojima, R.; Takakura, H.; Ozawa, T.; Tada, Y.; Nagano, T.; Urano, Y. *Angew. Chem. Int. Ed.* **2012**, *51*, 1-6.

(19) Shimomura, O.; Musick, B.; Kishi, Y. *Biochem. J.* **1988**, *251*, 405-410.

(20) Shimomura, O.; Musick, B.; Kishi, Y. *Biochem. J.* **1989**, *261*, 913-920.

(21) Qi, C. F.; Gomi, Y.; Hirano, T.; Ohashi, M.; Ohmiya, Y.; Tsuji, F. *J. Chem. Soc. Perkin Trans. 1* **1992**, 1607-1611.

(22) Inouye, S.; Shimomura, O. *Biochem. Biophys. Res. Commun.* **1997**, *233*, 349-353.

(23) Wu, C.; Nakamura, H.; Murai, A.; Shimomura, O. **2001**, *42*, 2997-3000.
(24) Hall, M. P.; Unch, J.; Binkowski, B. F.; Valley, M. P.; Butler, B. L. Wood, M. G.; Otto, P.; Zimmerman, K.; Vidugiris, G.; Machleidt, T.; Robers, M. B.; Benink, H. A.; Eggers, C. T.; Slater, M. R.; Meisenheimer, P. L.; Klaubert, D. H.; Fan, F.; Encell, L. P.; Wood, K. V. *ACS Chem. Biol.* **2012**, *7*, 1848-1857.
(25) Adamczyk, M.; Johnson, D. D.; Mattingly, P. G.; Pan, Y.; Reddy, R. E. *Org. Prep. Proc. Int.* **2001**, *33*, 477-485.
(26) Adamczyk, M.; Akireddy, S. R.; Johnson, D. D.; Mattingly, P. G.; Pan, Y.; Reddy, R. E. *Tetrahedron* **2003**, *59*, 8129-8142.
(27) Rostovtsev, V. V.; Green, L. G.; Fokin, V. V.; Sharpless, K. B. *Angew. Chem. Int. Ed.* **2002**, *41*, 2596-2599.
(28) Kim, S. B.; Suzuki, H.; Sato, M.; Tao, H. *Anal. Chem.* **2011**, *83*, 8732-8740.
(29) Degeling, M. H.; Bovenberg, M. S. S.; Lewandrowski, G. K.; de Gooijer, M. C.; Vleggeert-Lankamp, C. L. A.; Tannous, M., Maguire, C. A.; Tannous, B. A. *Anal. Chem.* **2013**, *85*, 3006-3012.
(30) Inouye, S.; Sahara, Y. *Biochem. Biophys. Res. Commun.* **2008**, *365*, 96-101.
(31) Tzertzinis, G.; Schildkraut, E.; Schildkraut, I. *PLoS ONE* **2012**, *7*, e40099.

Chapter 2.1. Development of Luminescent Coelenterazine Derivatives Activatable by β-Galactosidase for Monitoring Dual Gene Expression

(*Chem. Eur. J.* **2013**)

BLI with coelenterate substrates suffers from several drawbacks, including a blue-shifted emission spectrum which is unfavorable for whole animal imaging due to light attenuation by tissues. In addition it has been shown that MDR1 P-glycoprotein can actively transport coelenterazine out of cells.[1] Coelenterazine is also very unstable,[2] with a half-life of 15 min at 37 °C.[3] Its utility is further compromised by its proneness to bind to serum albumin and other intrinsic proteins, which have been shown to catalyze the oxidation of coelenterazine, giving rise to background noise, BLI with cellular assays.[4]

It has been shown that the substituent at the C2-position of coelenterazine plays a major role in its stability and auto-oxidation. [5,6] Introduction of $–CF_3$ at the para position of the C2-benzyl group increased the stability of coelenterazine against auto-oxidation, but also resulted in a significant decrease in bioluminescence activity.[7] Coelenterazine can also be stabilized by introducing protecting groups at the 3-carbonyl position of the imidazpyrazinone ring of coelenterazine.[8,9] The protecting groups are then cleaved by intracellular esterases and lipases resulting in a longer half-life and a lower rate of auto-oxidation. However, it has been suggested that different cell lines may give different results as the type and level of esterases vary with each cell line, thus leading to a lower or higher light output.[9] In addition, as cellular esterases are ubiquitous in most cells, undesired non-selective cleavage of the ester groups in non-targeted cells could lead to background noise.

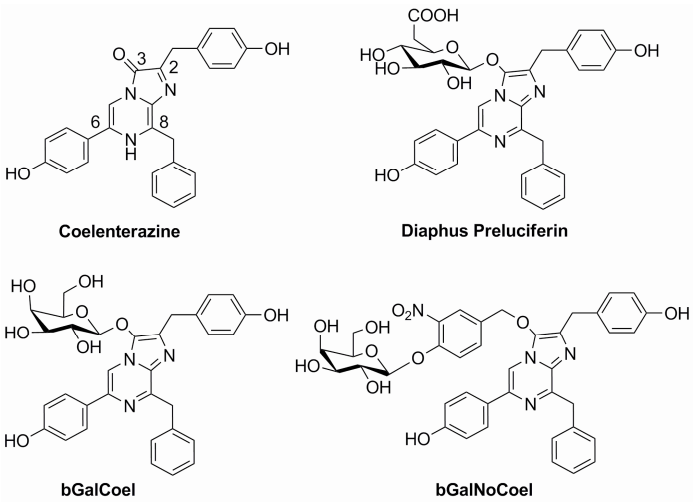

Figure 1. Chemical structures of coelenterazine, Diaphus Preluciferin and the two galactose-conjugated coelenterazine derivatives reported herein.

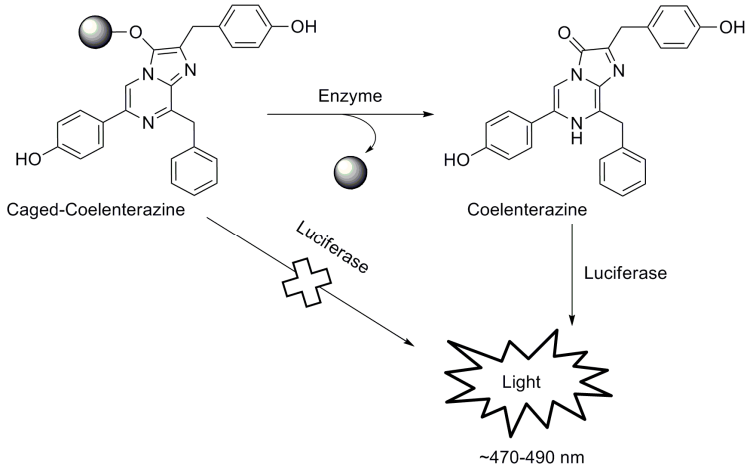

Scheme 1. The concept of Sequential Reporter-enzyme Luminescence (SRL) applied to coelenterazine. SRL allows monitoring the activity of a separate enzyme by making the luminescence generated from the oxidation of coelenterazine by its luciferase dependent on the activity of that enzyme. By installing a caging group on coelenterazine it cannot react with its luciferase, but in the presence of separate enzyme, the caging group can be cleaved and free coelenterazine is generated, which is subsequently oxidized by its luciferase to generate light.

To capitalize on the advantages of coelenterate luciferases, while addressing their limitations, we adopted sequential reporter-enzyme luminescence (SRL) imaging technology.[10] SRL allows imaging of another enzyme by making luminescence dependent on the activity of that enzyme thorugh the use of a caged luciferin substrate

(Scheme 1). SRL has been used to image ß-galactosidase (ß-Gal) activity, a widely used reporter enzyme, using the D-luciferin-ß-galactose derivative, Lugal.[11] Herein we report two new coelenterazine-ß-galactose conjugates as new potential tools for wide array of applications including monitoring of dual-gene expression, enzyme activity, and high-throughput screening. It has also been suggested that SRL could enable applications in toxicology, pharmacology, and in organ and tissue physiology and pathology.[12]

Design, Synthesis and Properties of bGalCoel

Initial probe design strategy was based on the previously reported natural Diaphus Preluciferin (3-enol glucuronide from fish)[13] by conjugating a β-galactose molecule to coelenterazine at the 3-position. bGalCoel was synthesized in four steps from coelenterazine (Scheme 2). Following per-acetylation of coelenterazine, selective deacetylation at the 3-position of the Imidazo pyrazinone ring was accomplished by addition of 1% NH_3 in MeOH to **2** in CH_2Cl_2 at 0 °C.[14] Subsequently, 2,3,4,6-tetra-*O*-acetyl-α-D-galactopyranosyl bromide was added to **3** in DMF to give **4** as the main product. After standard deacetylation with sodium methoxide in MeOH, bGalCoel was purified via reverse phase-HPLC.

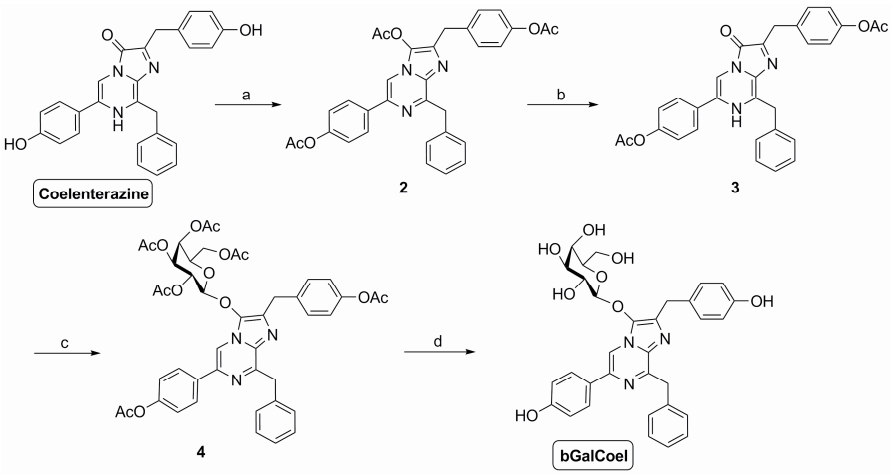

Scheme 2. Synthesis of bGalCoel. a) Ac_2O, DMAP, 76%; b) 1% NH_3 in MeOH, CH_2Cl_2, quant.; c) 2,3,4,6-tetra-*O*-acetyl-α-D-galactopyranosyl bromide, Cs_2CO_3, DMF, 48%; d) NaOMe, MeOH, 44%.

Next, the luminescent properties of bGalCoel were evaluated in comparison with native coelenterazine. bGalCoel displayed glow-type kinetics in presence of β-Gal and GLuc (Figure 2a) with an average signal half-life of 77 min (Figure 3). GLuc is known to exhibit flash-type kinetics with coelenterazine, with a half-life of only a few

seconds.[15] The luminescent signal of bGalCoel did not return to basal levels even after 3 h, making a direct comparison with native coelenterazine very difficult in terms of relative signal output. Relative bioluminescence activity of bGalCoel was 11% of that of coelenterazine after a photoncount of ~10 min using a luminometer (Figure 2c). The observed glow-type luminescence of bGalCoel suggested slow cleavage kinetics of β-galactosidase. HPLC studies further showed that the cleavage reaction of β-galactosidase with bGalCoel was very slow, with most of the substrate remaining intact even after 8 h (Figure 4).

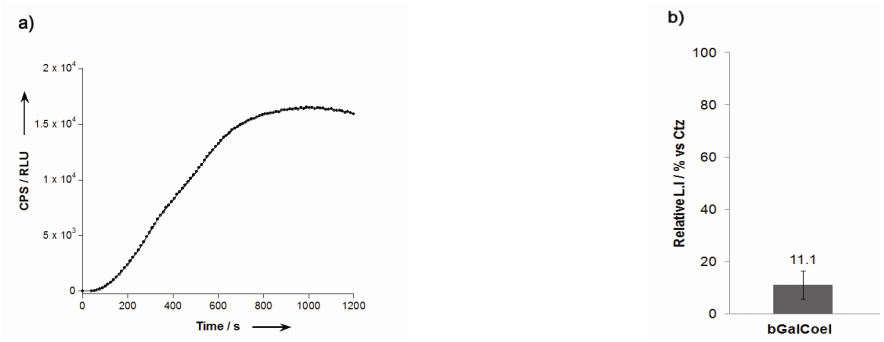

Figure 2. Kinetic profile and relative bioluminescence activity of bGalCoel (a) cleavage by β-galactosidase measured by light output of *Gaussia* luciferase; Reaction conditions: 5 µM bGalCoel, 2 U β-galactosidase, 3 mM $MgCl_2$, *Gaussia* luciferase, 0.1 M PBS (pH 7.4); Total light output measured in luminometer (12 s × 100). (b) Relative light output of bGalCoel versus native coelenterazine (CTZ).

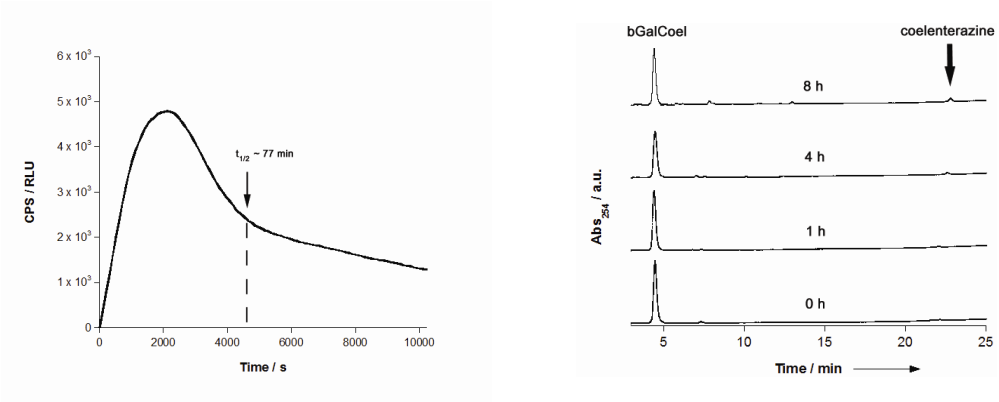

Figure 3. **(Left)** Extended kinetic luminescence profile of bGalCoel; cleavage by ß-galactosidase measured by light output of *GLuc* (left); Reaction conditions: 5 µM bGalCoel, 2U ß-gal, 3 mM $MgCl_2$, *Gaussia* luciferase, 0.1 M PBS (pH 7.4); Total light output measured in luminometer (100 s for 100 repeats). **(Right)** Cleavage reaction of bGalCoel with ß-gal, monitored by HPLC. Reaction conditions: 100 µM bGalCoel, 8U ß-gal, 3 mM $MgCl_2$, 1% DMSO in PBS buffer (0.02% Tween) (pH 7.4) at 37°C.

Design, Synthesis and Properties of bGalNoCoel

Due to slow kinetics in the cleavage of bGalCoel with β-Gal we re-designed our substrate by incorporating a self-immolative nitrobenzyl linker between the coelenterazine and β-galactose moiety as previously described (Scheme 3).[15]

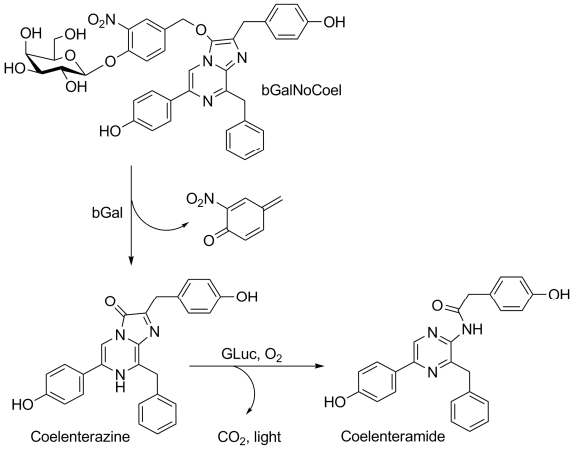

Scheme 3. Cleavage of bGalNoCoel by β-galactosidase generates free coelenterazine that is oxidized by *Gaussia* luciferase in a light producing reaction.

We named this new substrate as bGalNoCoel (Figure 1). bGalNoCoel was synthesized in 6 steps (Scheme 4). Initially, compound **8** was synthesized from 4-hydroxy-3-nitrobenzaldehyde and 2,3,4,6-tetra-*O*-acetyl-α-D- galactopyranosyl bromide (Scheme S2). The primary alcohol was then reacted with thionyl chloride to give **9**, followed by alkylation with **3** to give the per-*O*-acetylated galactonitrobenzylcoelenterazine derivative **10**. Deacetylation of **10** with sodium methoxide in methanol, followed by purification via reverse phase-HPLC gave bGalNoCoel.

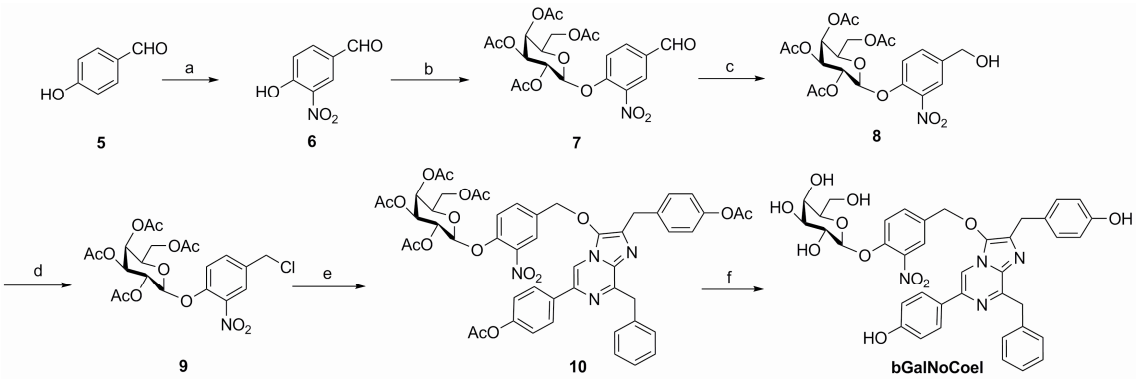

Scheme 4 Synthesis of bGalNoCoel. a) HNO_3, AcOH, MeCN, 90%; b) 2,3,4,6-tetra-O-acetyl-α-D-galactopyranosyl bromide, Ag_2O, MeCN, 66%; c) $NaBH_4$, MeOH, 78%; d) $SOCl_2$, DMAP, CH_2Cl_2, 85%; e) **3**, K_2CO_3, KI, MeCN, 29%; f) NaOMe, MeOH, 20%.

Evaluation of the luminescent properties of bGalNoCoel showed a much faster response than bGalCoel (Figure 4a) and comparable luminescence output to that of native coelenterazine, 78% (Figure 4b). Unlike bGalCoel, bGalNoCoel displayed flash-kinetics with a signal half-life of less than 30 s (Figure 4a).

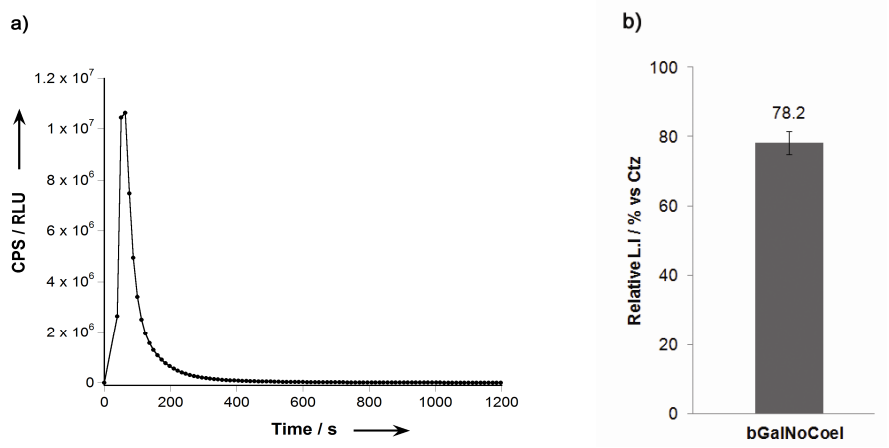

Figure 4. Kinetic profile and relative bioluminescence activity of bGalNoCoel (a) cleavage by β-galactosidase measured by light output of *Gaussia* luciferase; Reaction conditions: 5 μM bGalNoCoel, 2 U β-galactosidase, 3 mM $MgCl_2$, *Gaussia* luciferase, 0.1 M PBS (pH 7.4); Total light output measured in luminometer (12 s × 100). (b) Relative light output of bGalNoCoel versus native coelenterazine (CTZ).

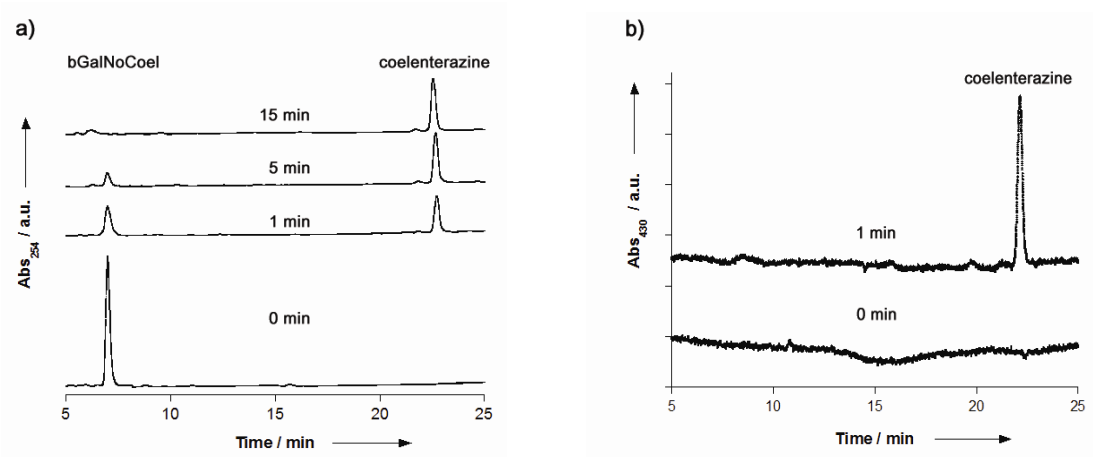

Figure 5. Cleavage reaction of bGalNoCoel with β-galactosidase, monitored by HPLC. Reaction conditions: 100 μM bGalNoCoel, 8U β-galactosidase, 3 mM $MgCl_2$, 1% DMSO in PBS buffer (0.02% Tween) (pH 7.4) at 37°C**.** Eluent: (A) H_2O (0.1% TFA); (B) acetonitrile (0.1% TFA). The percentage of A decreased linearly from 60% at 0 min to 30% at 15 min, followed by a decrease to 10% at 30 min. The flow rate was 1.0 ml/min and was monitored at 254 (a) and 430 nm (b) absorbance.

Monitoring via HPLC indicated a very fast cleavage reaction with the majority of the substrate cleaved after 5 min (Figure 5). No intermediates were detected in the HPLC cleavage reaction. This suggested that the cleavage of the β-galactoside bond was the slowest step in the enzyme-catalyzed hydrolysis cascade.

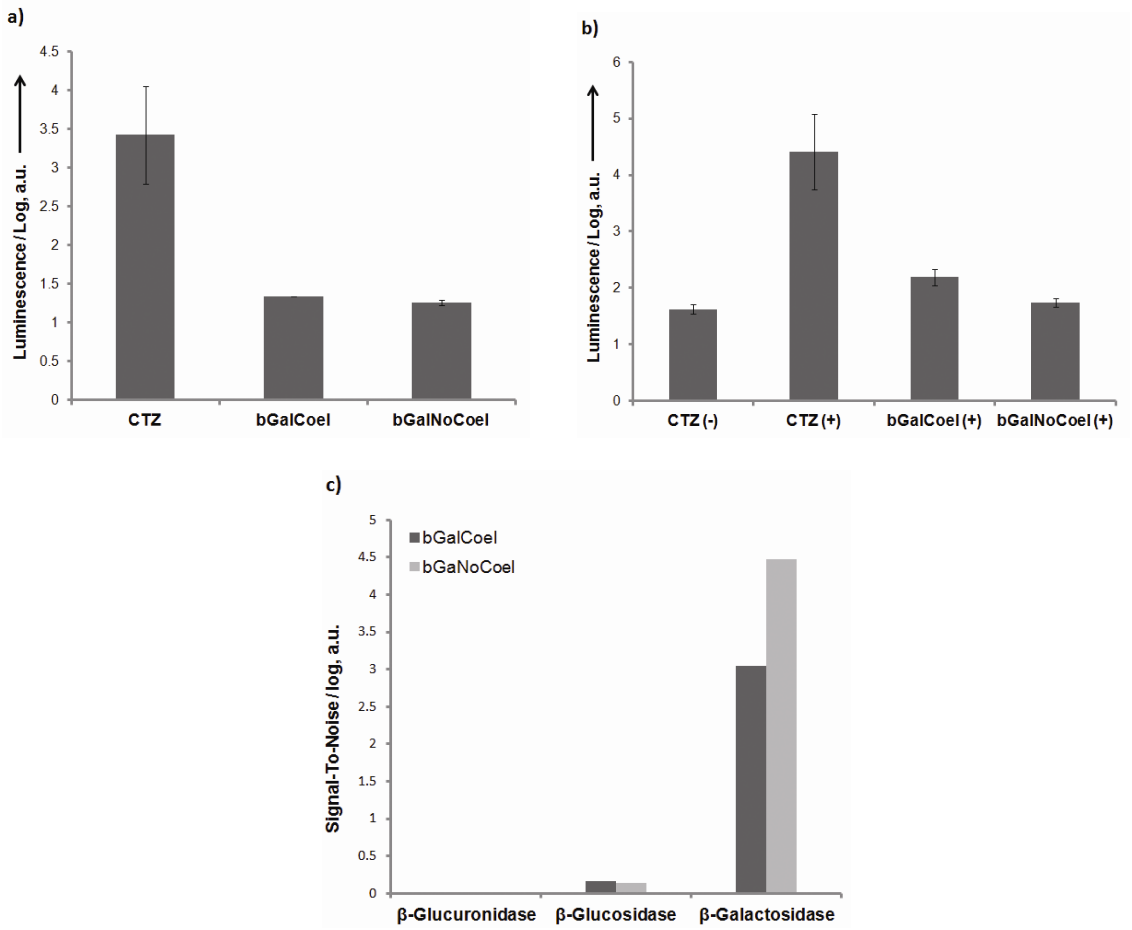

Figure 6. Stability and enzyme specificity of bGalCoel and bGalNoCoel. a) Substrate stability in 2 × 10^4 non-transfected HEK293T cell cultures. Stability was evaluated by directly adding substrate (15 μM) and the resulting light output was measured for 10 min at 37 °C. Experiments were performed in triplicate. b) Substrate stability in presence of BSA. Substrate (final concentration 20 μM) was added to wells containing BSA (final concentration 2% *w*/*v*) in 50 mM HEPES buffer (pH 7.5); c) Relative enzyme specificity of bGalCoel and bGalNoCoel with 3 different glycoside hydrolases. Reaction conditions: bGalCoel or bGalNoCoel (final concentration 5 μM) was added to a well containing *Gaussia* luciferase and 2 U of β-galactosidase, β-glucosidase or β-glucuronidase in 0.1 M PBS (pH 7.4) and the light output was measured for 30 min. Each experiment was repeated three times.

Stability of bGalNoCoel and bGalCoel in non-transfected HEK293T cells was evaluated in comparison with coelenterazine by addition of bGalNoCoel, bGalCoel or coelenterazine to HEK293T cell-cultures, followed by measurement of autoluminescence for 10 min (Figure 6a). Both substrates showed very low levels of autoluminescence under these conditions. It has also been reported that coelenterazine is extremely unstable in presence of serum albumin by acting as a mono-oxygenase that catalyzes the oxidation of coelenterazine, giving rise to background chemiluminescence.

Thus we evaluated the relative stability of bGalNoCoel and bGalCoel against coelenterazine by measuring the autoluminescence levels for 2 min after addition of bGalNoCoel, bGalCoel or coelenterazine to solutions containing bovine serum albumin (BSA)(Figure 6b). Both bGalNoCoel bGalCoel were found to be highly stable in the presence of BSA, whilst coelenterazine displayed high levels of autoluminescence, which agrees with previous publications.[4]

The relative substrate specificity of bGalNoCoel and bGalCoel to β-Gal was compared with two other glycoside hydrolases, β-glucosidase (β-Glc) and β-glucuronidase (β-Glu). Relative cleavage was measured as total luminescence over 30 min in the presence of GLuc. bGalNoCoel and bGalCoel showed over 20000 and 1000-fold higher selectivity towards β-Gal respectively. (Figure 6c).

Next, we evaluated the relative bioluminescence activity in 2×10^4 living HEK293T cells expressing a mutant GLuc (GLucM23) with a KDEL, endoplasmic reticulum localization peptide sequence (GLucM23er). GLucM23 does not display the same flash-type kinetics, rather a more stable glow-type signal. In addition, GLucM23 has roughly 10 times higher luminescence output over the wild-type luciferase in the context of BLI with living cells. bGalCoel or bGalNoCoel was added to cells expressing GLucM23er and β-Gal or just the luciferase (Figure 4a). Maximum luminescence signal intensity was obtained approximately 2 min after addition of bGalNoCoel. bGalNoCoel showed a high signal-to-noise ratio (S/N = 524)(Figure 7a). The bioluminescent emission from cells expressing β-Gal and GLucM23er was proportionally dependent on the cell numbers, and as few as ~300 intact cells were detected in the presence of 25 μM bGalNoCoel (Figure 7b). The observed contrast (signal-to-noise ratio) was also proportionally dependent on the cell numbers (Figure 7c). These results demonstrate that bGalNoCoel is cell-permeable and able to detect the β-galactosidase activity in living mammalian cells. bGalCoel on the other hand showed very poor relative bioluminescence activity compared with coelenterazine, with a 100-fold weaker output. Initially this was attributed to poor cell-membrane permeability of the substrate.

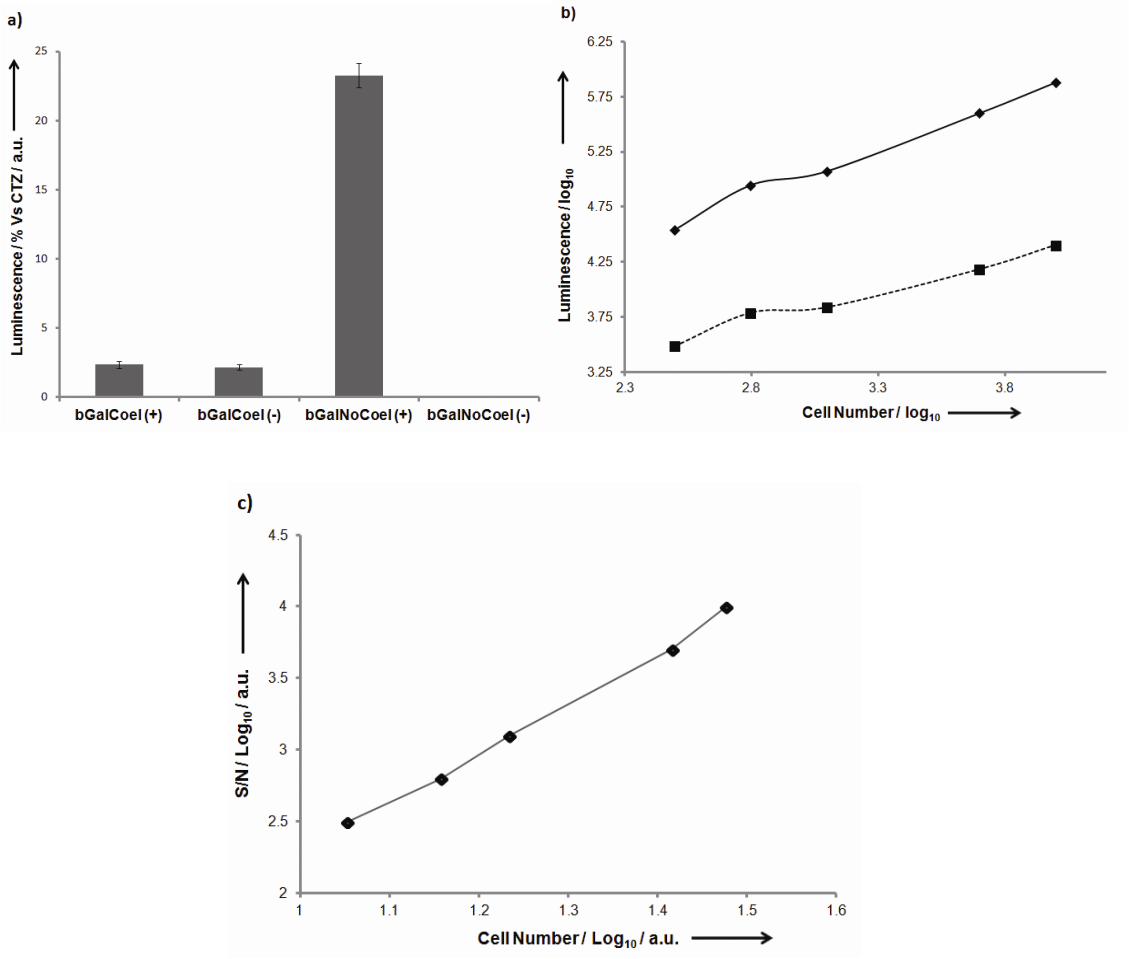

Figure 7. Bioluminescence assays of HEK293T cells transfected with GLucM23 with bGalCoel and bGalNoCoel a) Relative bioluminescence of bGalCoel and bGalNoCoel versus native coelenterazine (CTZ) in ~ 2 × 10^4 HEK293T cells transfected with GLucM23-Venus-KDEL and in the presence (+) and in the absence (-) of β-Gal. b) Bioluminescence output dependence on cell number with bGalNoCoel in the presence (◆) and in the absence (■) of β-Gal and $GLucM23_{ER}$ c) Dependence of contrast (S/N) on cell number with bGalNoCoel. Reaction conditions: 25 μM substrates, 37 °C; total light output measured in luminometer every 10 s for 100 repeats.

However, significant luminescence was also observed in the absence of β-Gal which suggested that free coelenterazine was generated from bGalCoel independently of the expression of β-Gal. The relative signal-to-noise ratio (S/N) was just above 1. In a separate experiment, we evaluated the relative bioluminescent activity of bGalCoel with

HEK293T cells expressing *Renilla* luciferase, another commonly used coelenterate luciferase. In this case the signal-to-noise ratio was even lower (data not shown). Hence the instability of bGalCoel itself seemed to be related to the expression of GLucM23 itself. However, as bGalCoel was shown to be stable in the presence of secreted GLuc under cell-free assay conditions, with a signal-to-noise ratio of over 2300, the non-specific luminescence of bGalCoel does not seem to be related to the luciferase itself. Interestingly it was also shown that bGalCoel was highly stable in non-transfected HEK293T cell cultures (Figure 6a). In addition, we also investigated whether the nature of the transfection agent could have any influence on the stability of bGalCoel. Luminescence was measured after addition of bGalCoel to solutions containing GLuc and one of the following transfection agents: Lipofectamine 2000™, Lipofectamine LTX™, FuGene™, and Xtreme Gene™. No significant difference could be observed between the experimental or control groups (Figure 8). Therefore, we are currently uncertain about the cause of the observed instability of bGalCoel in luciferase-expressing cells. From the available data, it seems to suggest that the poor bioluminescence response of bGalCoel observed in living cells is the result of several factors including slow cleavage kinetics, poor cell-membrane permeability and auto-cleavage due to instability of the substrate.

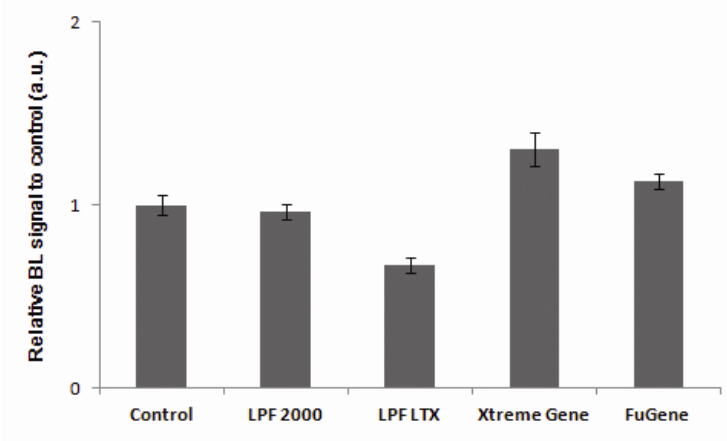

Figure 8. Showing influence of various transfection agents on stability of bGalCoel. Reaction conditions: 5 µM bGalCoel, GLuc, 0.1 M PBS (pH 7.4), with of without 1 µl transfection agent.

Dual Gene-Reporter Assay

Finally we investigated whether coelenterazine, generated after cleavage of bGalNoCoel by β-Gal-expressing cells, would readily diffuse out of the cells or be

retained inside. We excluded bGalCoel on the premise that it was earlier shown to have poor S/N in living cells (Figure 7a). In addition to the *lacZ* gene, we also utilized two different GLucM23-expressing plasmid vectors, localizing GLucM23 to cell membrane surface (mem) or endoplasmic reticulum (er) respectively (Figure 8). The luminescence profiles of HEK293T cells expressing the luciferase together with β-Gal were compared against the luciferase and β-Gal being independently expressed and combined before addition of bGalNoCoel. We combined 2 sets of 1×10^4 cells where GlucM23 and β-Gal expressed seperately, giving a cell ratio of 1:1. If coelenterazine could freely diffuse out of cells, we hypothesized that the average time to reach maximum luminescence (T_{Lmax}) should be related to the relative distance between the sites of expression of the luciferase and β-Gal, *i.e.* the shortest distance would be the set of cells co-expressing GLucM23er/β-Gal whilst the longest distance would be between the set of cells independently expressing GLucM23er + β-Gal. Therefore, the following trend in terms

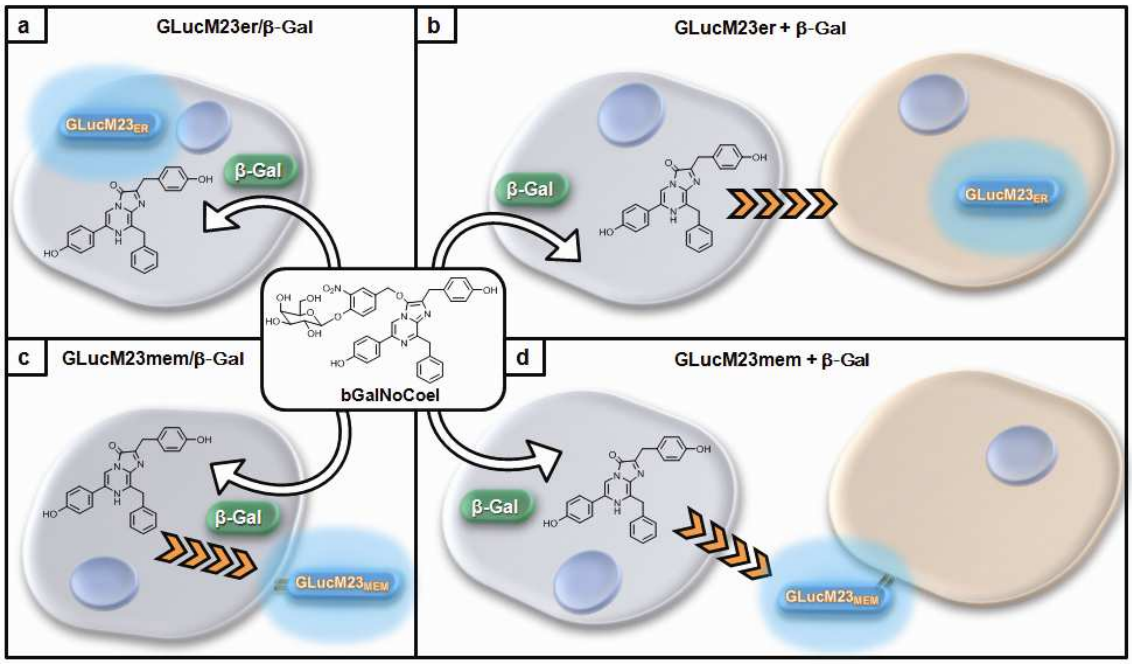

Figure 8. Showing the concept of dual-gene reporter assay of GLucM23 and β-Gal with bGalNoCoel in living cells. bGalNoCoel diffuses into cells and gets cleaved by β-Gal. The generated coelenterazine will readily diffuse and become oxidized by GLucM23 to generate luminescence: a) Cells co-expressing $\mathrm{GLucM2_{ER}}$ and β-Gal; b) Mixture of 2 cell populations expressing $\mathrm{GLucM2_{ER}}$ and β-Gal separately; c) Cells co-expressing $\mathrm{GLucM23_{MEM}}$ and β-Gal; Mixture of 2 cell populations expressing $\mathrm{GLucM2_{MEM}}$ and β-Gal separately. Orange broken arrows indicates extracellular diffusion of coelenterazine.

of T_{Lmax} would be expected: GLucM23er/β-Gal < GLucM23mem/β-Gal < GLucM23mem + β-Gal < GLucM23er + β-Gal. Statistical analysis of the observed data however, indicated the following trend: GLucM23er/β-Gal < GLucM23mem/β-Gal << GLucM23mem + β-Gal = GLucM23er + β-Gal (Figure 6). We could not observe a significant difference between the means of GLucM23mem + β-Gal and GLucM23er + β-Gal. However we could show from our data that after the β-galactose moiety of bGalNoCoel gets cleaved by β-Gal, the resulting coelenterazine diffused from the cytosol to the extracellular environment. Hence bGalNoCoel could potentially function as a dual-gene reporter in two different cell-populations, where the β-Gal-expressing cells could be thought of as 'producers' of coelenterazine from bGalNoCoel, whilst the GLucM23- expressing cells could be labeled as 'detectors'.

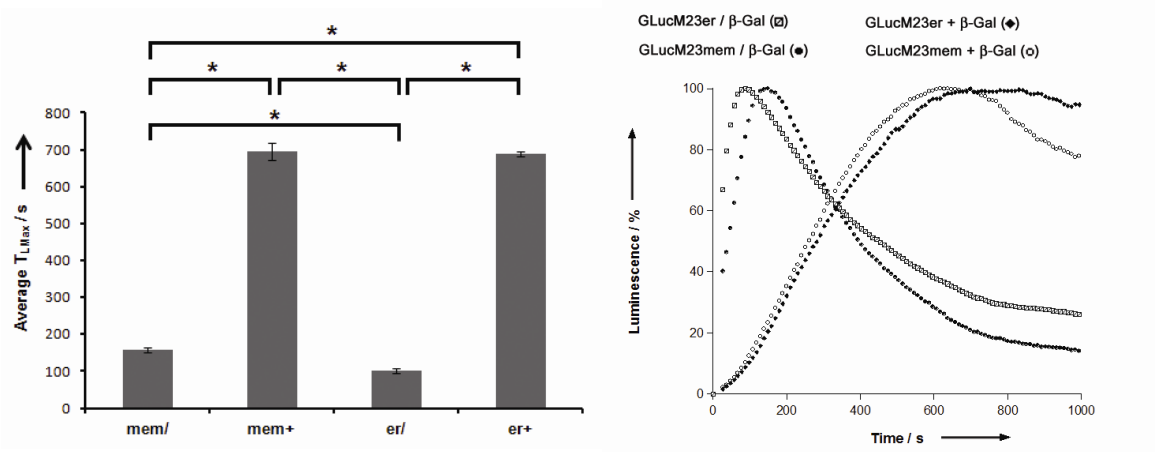

***Figure 9*. (left)** Representative mean T_{LMax} values of bGalNoCoel (25 µM) with 2×10^4 HEK293T cells co-transfected (/) or independently transfected (+) with GLucM23 (mem = surface membrane bound; er = endoplasmic reticulum localization) and β-Gal. Luminescence was measured in luminometer at 37 °C every 10 s for 100 repeats. Statistical analyses were performed with a two-tailed Student's t-test. *P < 0.01 (n=4), and errors bars indicate standard error of mean. **(right)** Representative luminescence profiles of bGalNoCoel (25 µM) with HEK293T cells co-transfected (/) or independently transfected (+) with GLucM23 (mem = surface membrane bound; er = endoplasmic reticulum localization) and β-Gal. Luminescence was measured in luminometer at 37 °C every 10 s for 100 repeats. Note: These curves are not mean values, they are from single experiments that are closest to the mean T_{LMax} shown in Table 1.

Table 1. Average time to reach maximum luminescence for bGalNoCoel in HEK293T cells expressing; GLucM23 (Mem = Membrane bound; ER = Endoplasmic Reticulum localized) and β-Gal. (n = 4)

	$GLuc_{Mem}$/β-Gal	**$GLuc_{Mem}$+β-Gal**	**$GLuc_{ER}$/β-Gal**	**$GLuc_{ER}$+β-Gal**
T_{Lmax} (s) [a]	157.5 (± 7.5 s)	694.25 (± 22.6 s)	101.5 (± 2.7 s)	689 (± 6.1 s)

[a] Time to reach relative maximum luminescence signal.

Conclusions

We have designed and synthesized two caged coelenterazine derivatives, bGalCoel and bGalNoCoel. The probes were cleaved by β-galactosidase to generate free coelenterazine which can then go on to react with *Gaussia* luciferase to generate a bioluminescent signal. Our aim was to create bioluminogenic coelenterate substrates that could detect β-galactose activity. Both substrates showed very low autoluminescence in living cell cultures and high specificity for β-galactosidase over other glycoside hydrolases. However, bGalCoel showed a very slow cleavage reaction profile with β-galactosidase, and poor signal to noise ratio when measuring β-galactosidase activity in living cell cultures. We found that incorporation of a 4-hydroxy-3-nitrobenzyl linker between the β-galactose and the coelenterazine moiety (bGalNoCoel) greatly improved the kinetic profile, overall stability, luminescence output, and signal to noise ratio when detecting β-galactosidase activity in living cells compared with our first generation substrate bGalCoel.

Using bGalNoCoel, we could also show that coelenterazine, generated from β-Gal expressing cells, could readily diffuse to other cells after uncaging by β-galactosidase. Thus bGalNoCoel could be used as a dual-reporter in two different cell-populations where the 'producer' cells, expressing β-galactosidase, generate free coelenterazine by cleavage of bGalNoCoel, the coelenterazine can then diffuse to neigboring 'detector' cells, expressing GLucM23, generating a luminescent reponse.

Existing caged coelenterazine derivatives such as EnduRen™ and ViviRen™ were conceived in part to lower the autoluminescence background signal of the natural substrate and increase the signal-to-noise ratio. However, it has been shown that both of these substrates display similar background signal levels to that of native coelenterazine

in vivo.[2] It is known that reporter gene assays such as Firefly luciferase, used in screening applications can suffer from artifacts due to inhibition by small-molecular weight compounds, many found in typical screening libraries.[16] In a recent study many commonly used reporter gene assays were evaluated against a library of compounds.[17] Reporters such as firefly luciferase, *Renilla* luciferase, and Nanoluc™ all displayed an increase in bioluminescence output caused by inhibitor-based enzyme stabilization. Interestingly few inhibitors were indentified for β-galactosidase and *Gaussia*-Dura (a mutated form of *Gaussia* luciferase). Hence our bGalNoCoel substrate could be a suitable dual-reporter for screening applications. We also hope to further evaluate our dual-reporter substrate for *in vivo* imaging applications in the near future.

Experimental

Materials and Instruments

General reagents and chemicals were purchased from Sigma-Aldrich Chemical Co. (St. Louse, MO), Tokyo Chemical Industries (Tokyo, Japan), and Wako Pure Chemical (Osaka, Japan) and were used without further purification. Silica gel chromatography was performed using BW-300 (Fuji Silisia Chemical Ltd., Greenville, NC). pcDNA4™/TO/myc-His/lacZ was purchased from Life Technologies Corporation (Japan). NMR spectra were recorded on a JEOL JNM-AL400 instrument at 400 MHz for ^{1}H and 100.4 MHz for ^{13}C NMR, using tetramethylsilane as an internal standard. Mass spectra were measured on a Waters LCT-Premier XE mass spectrometer for ESI or on a JEOL JMS-700 for FAB. UV-visible absorbance spectra were measured using a Shimadzu UV1650PC spectrometer. High pressure liquid chromatography (HPLC) analysis was performed with an Inertsil ODS3 column (4.6 × 250 mm, GL Science, Inc. Torrance, CA) using an HPLC system that comprised a pump (PU2080, JASCO) and a detector (MD2010 and FP2020, JASCO). Preparative HPLC was performed with an Inertsil ODS3 column (10.0 × 250 mm)(GL Sciences Inc.) using an HPLC system with a pump (PU-2087, JASCO) and a detector (UV-2075, JASCO). Bioluminescence was measured in 96-optiplate multiwell plates (PerkinElmer Co., Ltd.) using a Wallac ARVO mx / light 1420 Multilabel / Luminescence counter with an auto-injector (PerkinElmer Co., Ltd.). Coelenterazine was synthesized as previously described and stored as 10 mM MeOH/HCl (<1%) solution aliquots in sealed glass ampulles at -80°C.[1,2]

General experimental details for cell-cultures

HEK293T cells were maintained in Dulbecco's Modified Eagle Medium (DMEM)

(Invitrogen), supplemented with 10% fetal bovine serum (FBS) at 37°C under 5% CO_2. *Transfection*: Optimem (Invitrogen) solutions containing lipofectamine 2000 (Invitrogen) and plasmid DNA were added to HEK293T cell cultures and incubated at 37°C under 5% CO_2 for 24 h. Cells were then washed three times with PBS, trypsinized, washed with Leibovitz's L-15 medium, then resuspended in black 96-well optiplates (PerkinElmer) and incubated at 37 °C in luminometer (PerkinElmer).

Preparation of secreted *Gaussia* luciferase

HEK293T cells maintained in DMEM (no phenol red) supplemented with 10% FBS and transfected with pCM-GLuc (New England Biolabs) were incubated at 37 °C under 5% CO_2 for 24 h. The cell-medium was carefully transferred to a separate tube, centrifuged to remove any cells. The supernatant was aliquoted and stored at −80 °C.

1. Synthesis of bGalCoel

Imidazo[1,2-*a*]pyrazin-3-ol,6-[4-(acetyloxy)phenyl]-2-[[4-(acetyloxy)phenyl]methyl]-8-(phenylmethyl)-3-acetate (1). To a solution of coelenterazine (480 mg, 1.13 mmol) in acetic anhydride (5 ml) was added 4-dimethylaminopyridine (367 mg, 3 mmol) and the reaction was stirred at room temperature under argon over night. Excess acetic anhydride was removed *in vacuo* and the remaining residue was subjected to flash column silica chromatography, EtOAc/CH_2Cl_2 (1:9), yielding the product (1) as a dark red sticky solid (323 mg, 76%). ^{1}H NMR (400 MHz, $CDCl_3$**)** δ 2.19, 2.29, 2.32 (s, 3H x 3 (AcO x 3)) 4.16 (s, 2H) 4.18 (s, 2H) 7.02 (d, 2H, ^3J = 8.4 Hz) 7.17 (d, 2H, ^3J = 8.4 Hz) 7.31-7.21 (m, 5H) 7.58 (d, 2H, ^3J = 8.0 Hz) 7.74 (s, 1H) 7.89 (d, 2H, ^3J = 8.0 Hz). ESI-MS $[M+H]^+$ Calc: 550.2045; Found: 550.1038.

Imidazo[1,2-*a*]pyrazin-3(7*H*)-one,6-[4-(acetyloxy)phenyl]-2-[[4-(acetyloxy)phenyl] methyl]-8-(phenylmethyl) (2) (Inoue, S., Sugiura, S., Kakoi, H., Murata, M., Goto, T.. *Tetrahedron Lett.* **1977**, *31*, 2685–2688.) To an ice-cooled solution of Imidazo[1,2-*a*]pyrazin-3(7*H*)-one,6-[4-(acetyloxy)phenyl]-2-[[4-(acetyloxy)phenyl] methyl]-8-(phenylmethyl) (201 mg, 0.37 mmol) in CH_2Cl_2 (3 ml) was added 1% NH_3 in MeOH (3 ml) and the reaction was stirred at 0°C under an argon atmosphere. The reaction was monitored by TLC until no more starting material remained (~ 30 min), after which the solution was evaporated to dryness and dried *in vacuo* and used without further purification.

2-(4-((2-(4-acetoxybenzyl)-6-(4-acetoxyphenyl)-8-benzylimidazo[1,2-a]pyrazin-3-yl oxy)-2,3,4,6-tetra-*O*-acetyl-β-*D*-galactopyranoside (3). To an ice-cooled solution of imidazo[1,2-*a*]pyrazin-3(7*H*)-one,6-[4-(acetyloxy)phenyl]- 2-[[4-(acetyloxy)phenyl] methyl]-8-(phenylmethyl) (50 mg, 0.09 mmol) in CH_2Cl_2 (2 ml) was added 1% NH_3 in MeOH (1 ml) and the reaction was stirred at 0°C under an argon atmosphere for 1 h. The solution was evaporated to dryness and dried *in vacuo* and used without further purification. To a solution of **3** (~0.09 mmol) in anhydrous DMF was added 2,3,4,6-tetra-*O*-acetyl-β-D-galactopyranosyl bromide (106 mg, 0.26 mmol) and Cs_2CO_3 (47 mg, 0.14 mmol). The reaction was degassed by bubbling argon for 30 mins and stirred at room temperature over night. The reaction mixture was filtered and solvent was evaporated *in vacuo*. The residue was extracted with ethyl acetate, and the combined organic layers were washed with brine, dried with Na_2SO_4, filtered, and concentrated *in vacuo*. Silica gel flash chromatography ($MeOH/CH_2Cl_2$; 1:99) gave **3** as a dark red solid (36 mg, 48%).^{1}H NMR (400 MHz, $CDCl_3$**)** δ2.01, 2.04, 2.11. 2.17, 2.30, 2.33 (6s, 18H, AcO x 6) 4.06 ($^3J_{H6a,H5}$ = 6.8, 0.8 Hz) 4.19-4.04 (m, 2H, H5, H6b) 4.26 (dd, $^2J_{H6a,H6b}$ = 11.4, $^3J_{H6a,H5}$ = 6.8 Hz, $^3J_{H1,H2}$, 1H, H6a) 4.24-4.11 (m, 4H, H6a/b, CH_2) 4.58 (s, 2H, CH_2) 4.91 (d, $^3J_{H1,H2}$ = 8.0 Hz, 1H, H1) 5.07 (dd, $^3J_{H3H2}$= 10.4, $^3J_{H3,H4}$ = 3.4 Hz, 1H, H3) 5.44 (d, $^3J_{H4,H3}$ = 3.6,1H, H4) 5.50 (dd, $^3J_{H2,H3}$ = 10.0, $^3J_{H2,H1}$ = 7.6 Hz, 1H, H2) 6.89 (d, 2H, ^3J = 8.0 Hz) 7.01 (d, 2H, ^3J = 8.0 Hz) 7.33-7.16 (m, 5H) 7.76 (d, 2H, ^3J = 8.0 Hz) 7.57 (d, 2H, ^3J = 8.0 Hz) 8.17 (s, 1H) ^{13}C NMR (100 MHz, $CDCl_3$**)** δ 170.43, 170.32, 170.11, 169.91, 169.57, 169.32, 156.91, 152.36, 149.27, 138.75, 137.77, 136.45, 135.05, 133.36, 132.60, 129.62, 129.55, 128.87, 128.22, 127.58, 126.42, 121.74, 115.90, 108.92, 104.41, 90.56, 71.50, 70.49, 68.36, 66.82, 61.10, 39.29, 31.99, 21.03, 20.75, 20.65, 20.61, 20.48, 20.16.ESI-MS [M+H]+ Calc:838.2818; Found: 838.1728.

2-(4-((2-(4-hydroxybenzyl)-6-(4-hydroxyphenyl)-8-benzylimidazo[1,2-a]pyrazin-3-y loxy)-β-*D*-galactopyranoside (bGalCoel) To an ice-chilled solution of **3** (40 mg, 0.048 mmol) in dry MeOH (2 ml) was added a methanolic solution (1 ml) of NaOMe (15 mg, 0.28 mmol) and stirred under argon for 4.5 h. The reaction was quenched with acetic acid (20 µl) and the solution was evaporated to dryness. The residue was dissolved in acetonitrile/water (0.1% HCO_2H) and purified via reverse phase HPLC; acetonitrile/water (30:70 → 70:30). The collected fractions were lyophilized to give bGalCoel as a red/orange solid (12 mg, 44%) ^{1}H NMR (400 MHz, $(CD_3)_2CO$) δ 3.85-3.46 (m, 10H) 4.35 (s, 2H) 4.67 (d, 1H, ^{3}J = 7.6 Hz) 6.62 (d, 2H, ^3J = 8.8 Hz) 6.80 (d, 2H, ^3J = 8.8 Hz) 7.16-7.09 (m, 5H) 8.56 (s, 1H) 7.45 (d, 2H, ^3J = 8.8 Hz) 7.79 (d, 2H, ^3J = 8.8Hz); ^{13}C NMR (100 MHz, $CDCl_3$) δ 159.25, 156.77, 152.75, 140.17, 139.34,

137.30, 135.90, 133.67, 131.64, 130.79, 130.37, 129.49, 129.27, 128.81, 127.45, 116.46, 116.10, 110.84, 108.88, 77.13, 74.74, 72.23, 69.85, 39.78, 32.15. ESI-MS [M+H]+ Calc: 586.2184; Found: 586.1821; FAB $[M+H]^+$ Calc: 586.2184; Found: 586.2174.

2. Synthesis of bGalNoCoel

4-hydroxy-3-nitrobenzaldehyde (6) A solution of 4-hydroxybenzaldehyde (2.46 g, 20.1 mmol) in acetonitrile (40 ml), with acetic acid (20 ml) and concentrated nitric acid (1.5 ml) was refluxed for 3 h. The solution was cooled to room temperature, poured into water, and extracted with EtOAc (x3). The organic layer was washed with brine, dried with sodium sulfate, filtered, and concentrated *in vacuo* to give **4** as a brown solid (3.03 g, 90%), and used without further purification.

1-(4-formyl-2-nitrophenyl)-2,3,4,6-tetra-*O*-acetyl-β-D-galactopyranoside (7) To a solution of 2,3,4,6-tetra-*O*-acetyl-α-D- galactopyranosyl bromide (2.0 g, 4.86 mmol) in dry acetonitrile (40 ml) was added 4-hydroxy-3-nitrobenzaldehyde (0.93 g, 5.54 mmol) and silver oxide (1.32 g, 5.71 mmol). The solution was stirred overnight in the dark at room temperature under argon. The solution was filtered through a pad of celite and concentrated *in vacuo.* The residue was dissolved in ethyl acetate and washed with saturated $NaHCO_3$ and brine. The organic layer was dried under Na_2SO_4, filtered, and concentrated *in vacuo*. Purification by flash chromatography with ethylacetate/hexane (2:3) gave **5** as a white solid (1.61 g, 66%). ^{1}H-NMR (400 MHz, $CDCl_3$) δ 2.03, 2.08, 2.13, 2.20 (4 s, 12H, AcO x 4) 4.29-4.10 (m, 3H, H5, H6) 5.14 (dd, $^3J_{H3,H2}$= 10.2, $^3J_{H3,H4}$= 3.4 Hz, 1H, H3) 5.22 (d, $^3J_{H1,H2}$ = 8.0 Hz, 1H, H1) 5.50 (d, $^3J_{H4,H3}$ = 2.8 Hz, 1H, H4) 5.59 (dd, $^3J_{H2,H3}$ = 10.4, $^3J_{H2,H1}$ = 8.2 Hz, 1H, H2) 7.49 (d, ^3J = 8.4 Hz, 1H, ArH) 8.07 (dd, ^4J = 2.0 Hz ^3J =8.4 Hz, 1H, ArH) 8.31 (d, ^4J = 2.0 Hz,1H, ArH) 9.98 (s, 1H, CHO). ESI(+) $[M+Na]^+$ Calculated: 520.1062; Found: 520.0409.

1-(hydroxymethyl-2-nitrophenyl)-2,3,4,6-tetra-*O*-acetyl-β-D-galactopyranoside (8) To a solution of $NaBH_4$ (100 mg, 2.64 mmol) in $MeOH/CH_2Cl_2$ (1:1, 5 ml) was added 1-(4-formyl-2-nitrophenyl)-2,3,4,6-tetra-*O*-acetyl-β-D-galactopyranoside (650 mg, 1.31 mmol) dropwise over 5 mins at 0°C. The reaction was monitored via TLC and quenched after 2 h with 20% NH_4Cl (3 ml) and evaporated to dryness. The residue was dissolved and extracted with ethyl acetate. The organic layer was washed with brine, dried under Na_2SO_4, filtered, and concentrated *in vacuo*. Purification by flash chromatography, ethyl acetate/hexane (3:2), yielded **6** as a white solid, (509 mg, 78%). ^{1}H-NMR (400 MHz,$CDCl_3$) δ 2.19, 2.13, 2.07, 2.02 (4s, 12H, OAc x 4) 4.19-4.04 (m, 2H, H5, H6b)

4.26 (d, $^{2}J_{H6a,H6b}$ = 11.2, $^{3}J_{H6a,H5}$ = 6.8 Hz, $^{3}J_{H1,H2}$, 1H, H6a) 4.73 (s, 2H, benzylic) 5.06 (d, $^{3}J_{H1,H2}$ = 8.0 Hz, 1H, H1) 5.11 (dd, $^{3}J_{H3H2}$ =10.6, $^{3}J_{H3,H4}$ = 3.4 Hz, 1H, H3) 5.45 (d, $^{3}J_{H4,H3}$ = 3.2Hz, 1H, H4) 5.54 (dd, $^{3}J_{H2,H3}$ = 10.0, $^{3}J_{H2,H1}$ = 7.6 Hz, 1H, H2) 7.36 (d, ^{3}J = 8.4 Hz, 1H, ArH) 7.52 (dd, ^{4}J = 2.2 Hz ^{3}J = 8.6 Hz, 1H, ArH) 7.81 (d, ^{4}J = 2.4 Hz, 1H, ArH). ESI(+) $[M+Na]^{+}$ Calculated: 522.1218; Found: 522.0551.

1-(chloromethyl-2-nitrophenyl)-2,3,4,6-tetra-*O*-acetyl-β-D-galactopyranoside (9) To a solution of 1-(hydroxymethyl-2-nitrophenyl)-2,3,4,6-tetra-*O*-acetyl-β-D-galacto-pyranoside (160 mg, 0.32 mmol) in dry CH_2Cl_2 (5 ml) was added thionyl chloride (50 µl, 0.69 mmol) and a catalytic amount of DMAP (4 mg, 0.03 mmol) at 0°C. The solution was stirred at 0 °C under an argon atmosphere for 5 hrs and poured into water. The organic layer was amply washed with water, followed by brine, drying under Na_2SO_4, filtered, and concentrated *in vacuo*. The product **7**, a white solid (141 mg, 85%) was used without further purification. ^{1}H-NMR (400 MHz, $CDCl_3$) δ 2.02, 2.08, 2.13, 2.19 (4s, 12H, AcO x 4) 4.08 (m, H5) 4.17 (dd, $^{2}J_{H6b,H6a}$= 11.2, $^{3}J_{H6b,H5}$ = 6.0 Hz, 1H, H6b) 4.26 (dd, $^{2}J_{H6a,H6b}$ = 11.4, $^{3}J_{H6a,H5}$ = 6.8 Hz, 1H, H6a) 4.58 (s, 2H, benzylic) 5.06 (d, $^{3}J_{H1,H2}$ = 7.6 Hz, H1) 5.11 (dd, $^{3}J_{H3H2}$ = 10.6, $^{3}J_{H3,H4}$ = 3.4 Hz, 1H, H3) 5.45 (d, $^{3}J_{H4,H3}$ = 3.4Hz, 1.0 Hz, 1H, H4) 5.55 (dd, $^{3}J_{H2,H3}$ = 10.4, $^{3}J_{H2,H1}$ = 7.6 Hz, 1H, H2) 7.37 (d, 1H, ^{3}J = 8.8 Hz, ArH) 7.56 (dd, 1H, ^{3}J = 8.8, Hz, ^{4}J = 2.4 Hz, ArH) 7.84 (d, 1H, ^{4}J = 2.4 Hz, ArH) ^{13}C-NMR (100 MHz, $CDCl_3$) δ20.57, 20.65, 20.68, 44.18, 61.33, 66.68, 67.79, 70.50, 71.50, 100.70, 120.07, 125.24, 133.52, 133.67, 141.18, 149.15, 169.38, 170.13, 170.16, 170.30. ESI(+) $[M+Na]^{+}$ Calculated:540.0879; Found: 540.1243. ESI(-) $[M+HCO_2]^{-}$ Calculated: 562.0969; Found: 562.1071. HRMS (FAB(+)) $[M+Na]^{+}$ Calculated: 540.0879; Found: 540.0887.

2-(4-((2-(4-acetoxybenzyl)-6-(4-acetoxyphenyl)-8-benzylimidazo[1,2-a]pyrazin-3-yl oxy)methyl)-2-nitrophenoxy)-2,3,4,6-tetra-*O*-acety-l-β-D-galactopyranoside (10) To a solution of 2-(4-Hydroxybenzyl)-6-(4-hydroxyphenyl)-8-(phenylmethyl)-imidazo[1,2-a]pyrazin-3(7H)-one (151 mg, 0.30 mmol) in dry acetonitrile (2 ml) was added 1-(chloromethyl-2-nitrophenyl)- 2,3,4,6-tetra-*O*-acetyl-β-D-galactopyranoside (300 mg, 0.58 mmol), potassium carbonate (15 mg, 0.11 mmol), potassium iodide (57 mg, 0.34 mmol). Argon was bubbled through the solution for 30 mins and the solution was stirred at room temperature under argon for 10 h. Water was added and the solution was extracted with ethyl acetate. The organic layer was washed with brine, dried under Na_2SO_4, filtered, and concentrated *in vacuo*. Purification by flash chromatography, 0.1% MeOH – 1% MeOH/CH_2Cl_2, yielded **8** as a red/brown gummy solid (87 mg,

29%).^{1}H-NMR (400 MHz, $CDCl_3$) δ 2.01, 2.04, 2.11. 2.17, 2.30, 2.33 (6s, 18H, AcO x 6) 4.06 ($^{3}J_{H6a,H5}$ = 6.8, 0.8 Hz) 4.19-4.04 (m, 2H, H5, H6b) 4.26 (dd, $^{2}J_{H6a,H6b}$ = 11.4, $^{3}J_{H6a,H5}$ = 6.8 Hz, $^{3}J_{H1,H2}$, 1H, H6a) 4.24-4.11 (m, 4H, H6a/b, CH_2) 4.58 (s, 2H, CH_2) 4.84 (s, 2H, CH_2) 4.91 (d, $^{3}J_{H1,H2}$ = 8.0 Hz, 1H, H1) 5.07 (dd, $^{3}J_{H3H2}$= 10.4, $^{3}J_{H3,H4}$ = 3.4 Hz, 1H, H3) 5.44 (d, $^{3}J_{H4,H3}$ = 3.6,1H, H4) 5.50 (dd, $^{3}J_{H2,H3}$ = 10.0, $^{3}J_{H2,H1}$ = 7.6 Hz, 1H, H2) 7.19 (d, ^{3}J = 8.8 Hz, 2H, ArH) 7.32-7.21 (m, 7H, ArH) 7.58 (d, ^{3}J = 6.4 Hz, 1H, ArH) 7.64 (s, 1H, ArH) 7.77 (s, 1H, ArH) 7.86 (d, ^{3}J = 8.4 Hz, 1H, ArH). ^{13}C-NMR (100 MHz,$CDCl_3$) δ20.57, 20.61, 20.66, 21.11, 21.15, 32.94, 39.99, 61.18, 66.72, 67.73, 70.35, 71.28, 75.10, 75.10, 100.40, 108.63, 119.39, 121.69, 122.05, 124.95, 126.50, 127.24, 128.29, 129.63, 129.67, 131.16, 132.31, 133.26, 133.55, 134.35, 136.36, 136.56, 137.82, 141.03, 149.28, 149.66, 150.98, 152.99, 169.30, 169.49, 169.66, 170.04, 170.17, 170.23. ESI(+) [M+H]+ Calculated: 989.3087; Found: 989.3397. HRMS (FAB(+)) $[M+H]^+$ Calculated: 989.3087; Found: 989.3073.

2-(4-((2-(4-hydroxybenzyl)-6-(4-hydroxyphenyl)-8-benzylimidazo[1,2-a]pyrazin-3-yloxy)methyl)-2-nitrophenoxy)-β-D-galactopyranoside (bGalNoCoel) To a cooled solution of 2-(4-((2-(4-acetoxybenzyl)-6-(4-acetoxyphenyl)-8-benzylimidazo-[1,2-a]pyrazin-3-yloxy)methyl)-2-nitrophenoxy)-2,3,4,6-tetra-*O*-acetyl-β-D-galactopyranoside (69 mg, 0.07 mmol) in dry MeOH (2 ml) was added sodium methoxide in MeOH (0.2 M, 1.4 ml, 4 eq.) and the solution was stirred under argon and monitored via TLC and ESMS and additional sodium methoxide was added until all acetate groups had been cleaved. Dowex 50w H^+ resin was added and the solution was filtered through a cotton plug and evaporated to dryness. The residue was dissolved in acetonitrile/water and purified via reverse phase HPLC; acetonitrile/water (30:70 → 70:30). The collected fractions were lyophilized to give bGalNoCoel as a red sticky solid (10 mg, 20%).^{1}H-NMR (400 MHz, $CDCl_3$) δ3.45 (dd, $^{3}J_{H3H2}$ =10.0, $^{3}J_{H3,H4}$ = 4.0 Hz, 1H, H3) 3.57 (m, 1H, H5) 3.63 (m, 2H, H6a/b) 3.71 (dd, $^{3}J_{H2,H3}$ = 10.0, $^{3}J_{H2,H1}$ = 8.0 Hz, 1H, H2) 3.88 (s, 2H, CH_2) 3.79 (d, $^{3}J_{H4-H3}$ = 4.0 Hz, 1H, H4) 4.37 (s, 2H, CH_2) 4.82 (d, 1H, $^{3}J_{H1-H2}$ = 8.0 Hz, 1H, H1) 4.86 (s, 2H, CH_2) 6.59 (d, ^{3}J = 8.6 Hz, 2H, ArH) 6.74 (d, ^{3}J = 8.4 Hz, 2H ArH) 6.94 (d, ^{3}J = 8.6 Hz, 2H, ArH) 7.15-7.04 (m, 3H, ArH) 7.24 (d, 1H, ^{3}J = 8.8 Hz, ArH) 7.35-7.29 (m, 3H, ArH) 7.59 (d, ^{3}J = 8.4 Hz, 2H, ArH) 7.62 (d, 1H, ^{4}J = 1.2 Hz, ArH) 7.89 (d, 1H, ^{3}J = 1.6 Hz, ArH). ^{13}C-NMR (100 MHz, $CDCl_3$) δ 32.91, 39.75, 62.29, 70.05, 71.90, 74.74, 76.27, 77.30, 103.02, 109.56, 116.34, 116.57, 118.92, 126.54, 127.49, 128.87, 129.13, 129.33, 130.31, 130.66, 130.86, 131.46, 133.22, 135.30, 135.48, 138.00, 139.26, 140.40, 141.80, 152.03, 157.03, 159.31. ESI(+) $[M+H]^+$ Calculated; 737.2453; Found: 737.2450. FAB(+) $[M+H]^+$ Calculated:737.2453;

Found: 737.2406

Determination of relative bioluminescence activity of GLucM23 compared to wild-type GLuc (Figure S1): HeLa cells in glass-bottom dishes, transfected with pDisp-mKO-GLuc or pDisp-mKO-GLucM23 were maintained in Dulbecco's Modified Eagle Medium (DMEM)(Invitrogen), supplemented with 10% fetal bovine serum (FBS) at 37°C under 5% CO_2 for 24 hours. Cells were washed with Hank's balanced salt solution (HBSS) (pH ~ 7.4). 100 µL HBSS was then carefully added. mKO fluorescence was measured ($548_{\lambda ex}/561_{\lambda em}$; 200 ms), after which a solution of HBSS, containing 25 µM of coelenterazine was added. We then measured the luminescence with an Olympus DP30 Cooled Monochrome CCD Microscope Camera; obj. × 60; with an exposure time of 20 seconds at an open filter setting. Obtained images were processed in imageJ. The average BL/FL was obtained from 5 cells from each respective image.

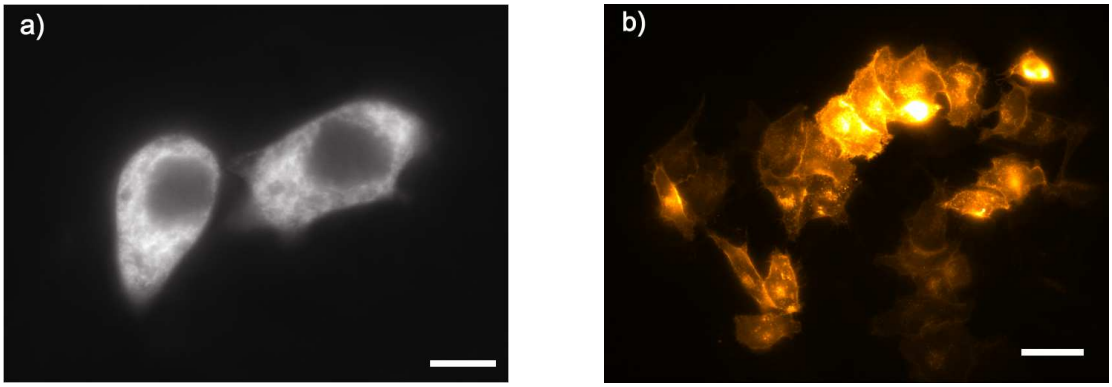

Figure S2. Showing Fluorescence images of GLucM23-Venus-KDEL (a) or mKO-GLucM23 (b) in HeLa cells. (a) Venus localized to endoplasmic reticulum ($515_{\lambda Ex}/528_{\lambda Em}$, 300 ms) Scalebar: 10 µm; (b) mKO localized to outer cell membrane ($548_{\lambda Ex}$ /$561_{\lambda Em}$; 200 ms) Scalebar: 50 µm.

Cleavage reaction of bGalCoel and bGalNoCoel by beta-galactosidase monitored by HPLC. To a solution containing bGalCoel or bGalNoCoel (100 µM), $MgCl_2$, DMSO (1%) in PBS buffer (0.1 M, pH 7.4,Tween 0.02%) was added 8 units of β-galactosidase, and the solution was incubated at 37 °C. Samples were taken at specific time intervals (bGalCoel: 0, 1, 4, and 8 h; (bGalNoCoel: 0, 1, 5, 15, 30, and 60 min.)

diluted with acetonitrile (0.1% TFA), filtered and analyzed by HPLC, or stored in liquid nitrogen until HPLC analysis. Absorbance was monitored at 254 nm.

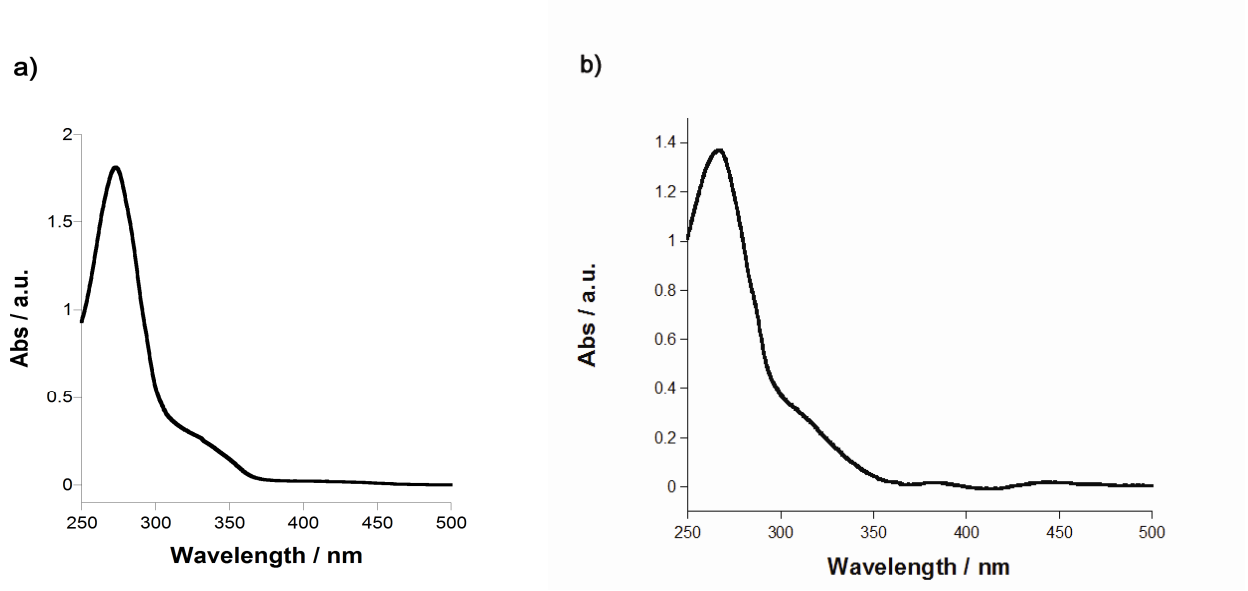

Figure S4 a) Absorbance spectrum of bGalCoel (30 µM in MeOH; b) Absorbance spectrum of bGalNoCoel (50 µM) in MeOH.

References

(1) A. Pichler, J. L. Prior, D. Piwnica-Worms, *Proc. Natl. Acad. Sci.* **2004**, *101*, 1702-1707.

(2) (a) T. Kimura, K. Hiraoka, N. Kasahara, C. R. Logg, *J. Gene Med.* **2010**, *12*, 528. (b) M. K. Wendt, J. Molter, C. A. Flask, W. P. Schiemann, *J. Vis. Exp*. **2011**, *56*, e3245.

(3) E. M. Hawkins in *Bioluminescence & Chemiluminescence: Progress & Current Applications* (Eds.; P.E. Stanley, L.J. Kricka., World Scientific, Singapore, **2002**, pp. 149.

(4) (a) N. Vassel, C. D. Cox, R. Naseem, V. Morse, R.T. Evans, R .L. Power, A. Brancale, K. T. Wann, A. K. Campbell, *Luminescence* **2012**, *27*, 234. (b) M. Keyaerts, C. Heneweer, L. O. Tchouate Gainkam, V. Caveliers, B. J. Beattie, G. A. Martens, C. Vanhove, A. Bossuyt, R. G. Blasberg, T. Lahoutte, *Mol. Imaging Biol.* **2011**, *13*, 59-66.

(5) S. Inouye, Y. Sahara-Miura, J-I. Sato, R. Iimori, S. Yoshida. T. Hosoya, *Prot.Exp.Pur.* **2013**, *88*, 150.

(6) M. P. Hall, J. Unch, B. F. Binkowski, M. P. Valley, B. L. Butler, M.G. Wood, P. Otto, K. Zimmerman, G. Vidugiris, T. Machleidt, M. B. Robers, H. A. Benink, C. T. Eggers, M. R. Slater, P. L. Meisenheimer, D. H. Klaubert, F. Fan, L. P. Encell, K. V. Wood, *ACS Chem. Biol.* **2012**, *7*, 1848-1857.

(7) J. Levi, A. De, Z. Cheng, S. Gambhir, *J. Am. Chem. Soc.* **2007**, *129*, 11900-11901.

(8) Chen, Y.; Chi, Y.; Wen, H.; Lu, Z. *Anal. Chem.* **2007**, *79*, 960–965.

(9) (a) Wehrman, T. S.; von Degenfeld, G.; Krutzik, P. O.; Nolan, G. P.; Blau, H. M. *Nat. Methods* **2006**, *3*, 295-301. (b) Li, J.; Chen, L.; Du, L.; Li, M. *Chem. Soc. Rev.* **2013**, *42*, 662-676.

(10) Geiger, R.; Schneider, E.; Wallenfels, K.; Miska, W. *Biol. Chem. Hoppe-Seyler* **1992**, *373*, 1187-1191.

(11) von Degenfeld, G.; Wehrman, T. S.; Blau, H. M. *Methods Mol. Biol.* **2009**, *574*, 249-259.

(12) Inoue, S.; Okada, K.; Tanino, H.; Kakoi, H. *Chem. Lett.* **1987**, 417-418.

(13) Inoue, S; Sugiura, S.; Kakoi, H.; Hashizume, K.; Goto, T.; Iio, H. *Chem. Lett.* **1975**, 141-144.

(14) Tannous, B. A.: Kim, D-E.; Fernandez, J. L.; Weissleder, R.; Breakefield, X. O. *Mol. Ther.* **2005**, *11*, 435-443.

(15) Ho, N-H.; Weissleder, R.; Tung, C-H. *ChemBioChem* **2007**, *8*, 560-566.

(16) Auld, D. S.; Southall, N. T.; Jadhav, A.; Johnson, R. L.; Diller, D. J.; Simeonov, A.; Austin, C.P.; Inglese, J. *J. Med. Chem.* **2008**, *51*, 2372-2386

(17) Ho, P-I.; Yue, K.; Pandey, P.; Breault, L.; Harbinski, F.; McBride, A. J.; Webb, B.; Narahari, J.; Karassina, N.; Wood, K. V.; Hill, A.; Auld, D. S. *ACS Chem. Biol.* **2013**, *16*, 1848-1857.

Chapter 2.2 Development of Hydrogen Peroxide Activatable Coelenterazine Derivatives

(In preparation)

In chapter 2.1, I demonstrated that blocking of coelenterazine with an enzymatic substrate is a viable strategy to effectively stabilize native coelenterazine. The dual-enzyme substrate, bGalNoCoel, could detect enzyme activity across two separate cell populations. To further expand the scope of activatable-coelenterazines I designed a coelenterazine-boronate derivative that could be activated by hydrogen peroxide, a reactive oxygen species implicated in a variety of physiological phenomena.

Introduction, probe design, and synthesis.

Reactive oxygen species (ROS) like hydrogen peroxide have been implicated in playing a major role in various diseases including cardiovascular disorders[1], diabetes[2] neurodegenerative diseases[3], and cancer[4]. Hydrogen peroxide has also been shown to have significance in events related to inflammation[5], aging[6], post-translational modifications of proteins and various signaling cascades.[7] An large array of various luminescent molecular probes for the detection of hydrogen peroxide has been reported. [8] An ample fraction of these are fluorescent probes utilizing caging boronic acid esters as selective switch for the detection of hydrogen peroxide. Nucleophilic addition of reactive species to electron-deficient boronate probes has prompted their use as effective traps of ROS and RNS in biological systems. Nucleophilic addition of hydrogen peroxide to the boron results in a charged tetrahedral boronate complex, which undergoes a 1,2-insertion featuring a boron to oxygen migration of the ipso-carbon (Scheme 1). The resulting borate ester is then hydrolyzed by water to the phenol.[9]

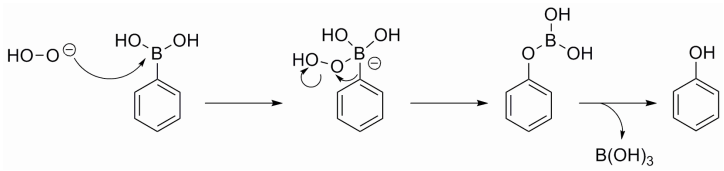

Scheme 1. Reaction mechanism of hydrogen peroxide with boronic acid.

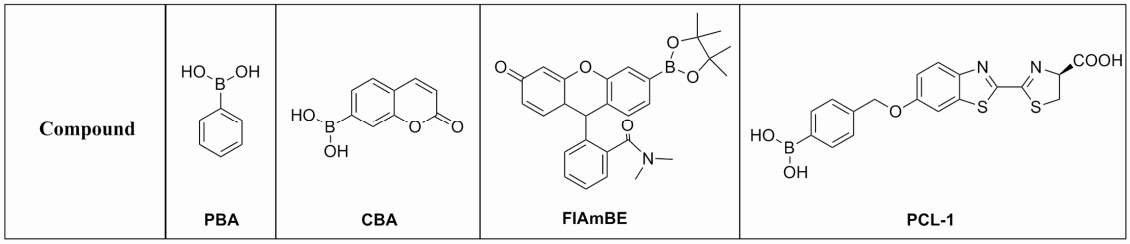

Figure 1. Structures of boronic acid and ester probes. ; adopted from reference [10].

Chang *et al.* created a bioluminescent reporter (PCL-1)(Figure 1), a boronate-D-luciferin conjugate for measuring of H_2O_2 fluxes in living animals.[11] More recently the same group also reported the PCL-2, a pre-bioluminogenic substrate that forms D-luciferin *in situ* and reports on both hydrogen peroxide and caspase activity *in vivo*.[12] In addition to the limitations of using FLuc mentioned in chapter 1 and 2 it was recently reported that FLuc activity can be altered when hydrogen peroxide levels become elevated, which can potentially lead to ambiguous or misleading findings.[13] Interestingly the same study also reported that a variant of *Renilla* luciferase, RLuc8, was far less sensitive to ROS. We reasoned that by utilizing an activatable boronate-coelenterazine probe together with GLuc, the brightest of known luciferases, it would be possible to obtain an even better S/N as the reaction of H_2O_2 with boronic acid is extremely slow (k ~ 1-2 M^{-1} s^{-1}).[10] Hence in a similar vein to that of the design of bGalNoCoel described in Chapter 2.1, we designed a coelenterazine-boronate derivative with a self-immolative benzyl linker, naming it Coel-BeBA (Scheme 2). The phenolic boronic acid group will upon reacting with hydrogen peroxide result in the generation of the phenol, which will trigger the self-elimination of the linker and generation of coelenterazine which can then undergo subsequent reaction with its coelenterate luciferase to give a bioluminescence signal (Scheme 2).

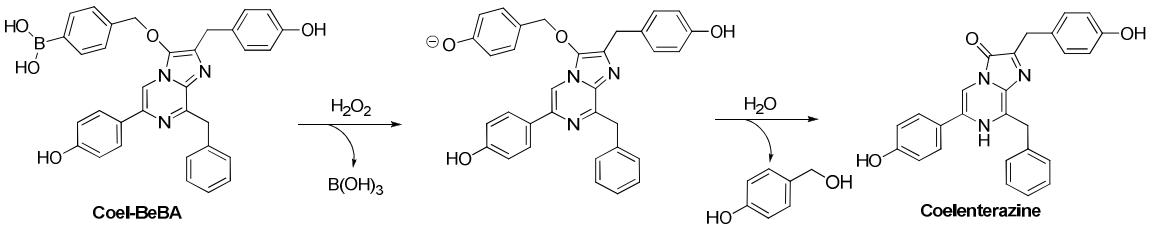

Scheme 2. Design strategy for H_2O_2-mediated release of coelenterazine from Coel-BeBA

Coel-BeBA was synthesized in a similar fashion to bGalNoCoel described in chapter 2. **2** was obtained by halogen-lithium exchange reaction of 4-iodotoluene with bis(pinacolato)diboron as the electrophile, followed by the apple-reaction to generate **3** (Scheme 3.). The di-(CTZ(OAc)$_2$) and tri-acetylated coelenterazine (CTZ(OAc)$_3$) starting materials were prepared as described in chapter 2.1. Alkylation of CTZ(OAc)$_2$ with **3** was conducted in DMF and cesium carbonate in order to minimize C-alkylation at the 2 position of coelenterazine (see appendix).

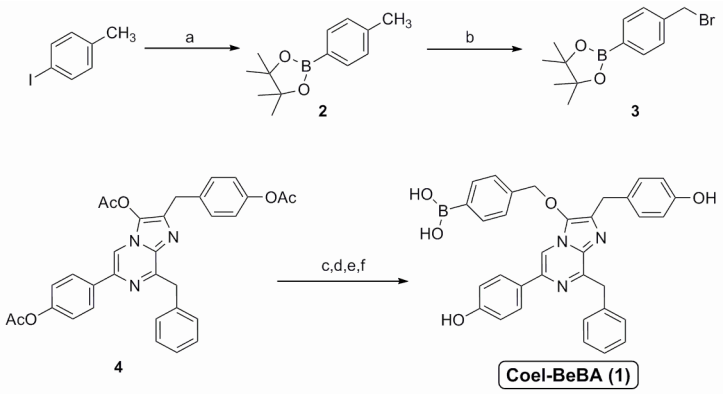

Scheme 3. Synthesis of Coel-BeBA. a) *t*-BuLi, B_2Pin_2, THF, -40 °C, 4.5 h, 40%; b) AIBN, NBS, MeCN, reflux, 20 h, 69%; c) 1% NH_3 in MeOH, CH_2Cl_2, 0 °C, 75 min; d) **3**, Cs_2CO_3, DMF, rt, 12 h; e) NaOMe, MeOH, 0 °C, 4.5 h; f) MeCN / H_2O (0.1 % HCO_2H), 12 h, rt, 9% over 4 steps.

Sensitivity and selectivity of Coel-BeBA for hydrogen peroxide.

First the relative responsiveness of Coel-BeBA to changes in hydrogen peroxide concentrations was evaluated. Coel-BeBA and GLuc were incubated with alternating concentrations of hydrogen peroxide (0-100 µM) and the total photon flux was measured for 1 h (Figure 2.). It was possible to obtain physiologically relevant

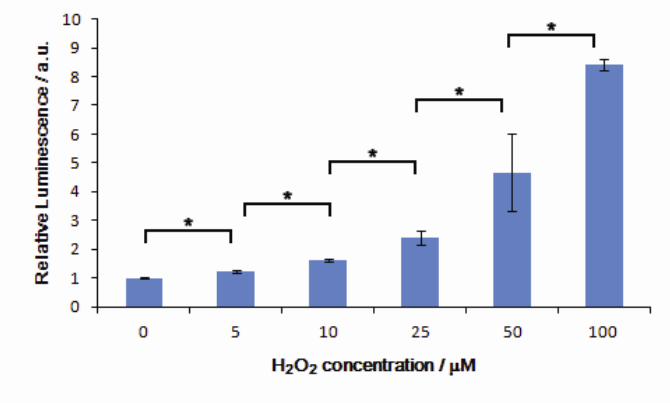

Figure 2. 10 µM Coel-BeBA and GLuc with various concentrations of H_2O_2 in 0.1 M PBS (pH 7.4). Total photon count was measured over 1 h. Statistical analysis was performed with a two-tailed Student's *t*-test. *p < 0.05, and error bars are ±SEM; n = 3.

low-micromolar detection of hydrogen peroxide. Having established that Coel-BeBA could detect changes in H_2O_2 levels in a dose-dependent fashion down to physiologically relevant concentrations we next investigated the selectivity of Coel-BeBA over other ROS (Figure 3). Coel-BeBA and GLuc were incubated with various ROS, including H_2O_2 in the presence and absence of catalase, a H_2O_2-degrading enzyme. Total photon flux was then measured for 1 h. Little to no relative signal increase was observed when Coel-BeBA was reacted with other ROS or H_2O_2 in the presence of catalase.

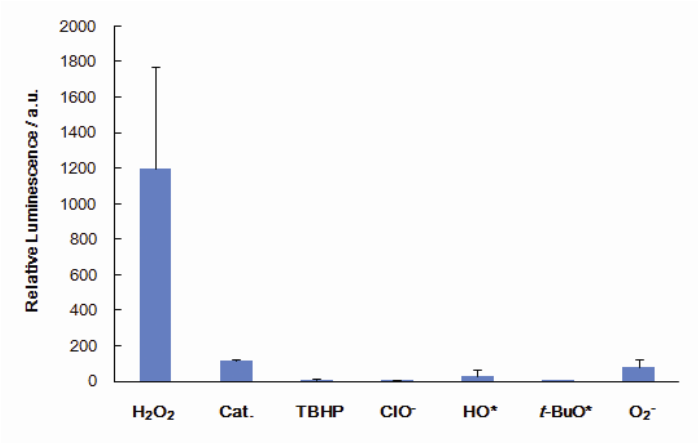

Figure 3. 10 μM Coel-BeBA with various reactive oxygen species (100 μM) and GLuc in 0.1 M PBS (pH 7.4). Total photon count measured over an hour in luminometer. Cat: 0.4 mg / mL catalase. HO* and *t*-BuO* radicals were generated from 1 mM $FeCl_2$ solution and 100 μM H_2O_2 or 100 μM *t*-BuOOH respectively. Solid KO_2 in DMSO (final concentration: 100 μM) was used as a source for O_2^- ; and error bars are ±SEM; n = 3.

Detection of changes in H_2O_2 levels with Coel-BeBA in living cells.

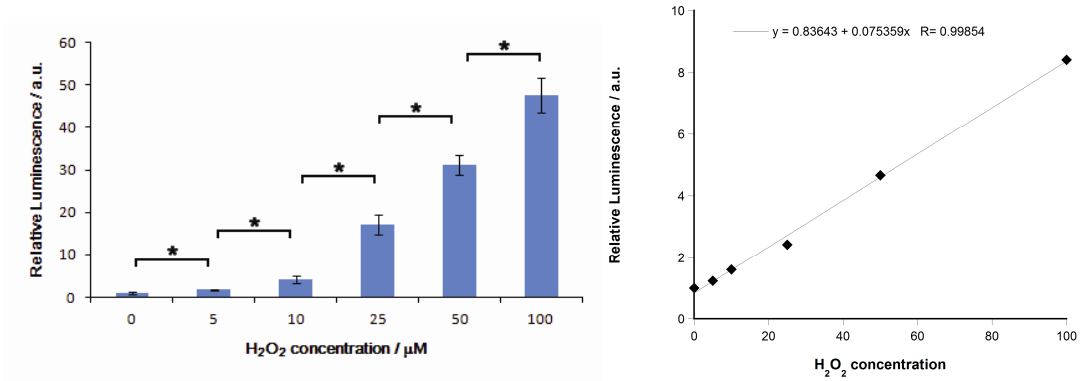

Figure 4. Detection of exogenous H_2O_2 with Coel-BeBA in HEK293T cells expressing GLucM23-Venus-KDEL. Bar graph representation (left). Linear correlation graph (right). Upon addition of Coel-BeBA (25 μM) and H_2O_2 (0-100 μM) total photon flux was measured for 2 h. Statistical analysis was performed with a two-tailed Student's *t*-test. *$p < 0.01$, and error bars are ±SEM; n = 3.

Next it was determined whether the performance of Coel-BeBA could be translated to living cell culture (Figure 4.). Coel-BeBA and various concentrations of H_2O_2 (0-100 µM) were added to HEK293T cells expressing GLucM23-Venus-KDEL (ER-localizing). Photon flux was measured for 2 h. Experiments demonstrated that exogenous addition of H_2O_2 to live-cell assays did not interfere with production of the H_2O_2-dependent bioluminescent signal of Coel-BeBA and demonstrated a linear response to H_2O_2 *in cellulo*. Subsequently we moved on to investigate the possibility to detect endogenously generated H_2O_2 in living cells with Coel-BeBA. RAW264 cells expressing GLucM23-Venus-KDEL were incubated with phorbol 12-myristate 13-acetate (PMA) because PMA activates protein kinase c (PKC) in macrophages which results in the subsequent activation of NADPH-oxidase (NOX) and the generation of H_2O_2.[14] Following incubation with PMA for 1 h, Coel-BeBA was added and after incubation for 10 min the total photon flux was measured for 10 min. (Figure 5.) PMA-treated cells showed statistically significantly ($p < 0.05$) higher bioluminescent signal derived from Coel-BeBA compared to non-stimulated cells. Hence it was possible to detect H_2O_2 generation in living cells with Coel-BeBA, which demonstrates that this probe is sensitive enough to changes in biologically relevant H_2O_2 concentrations.

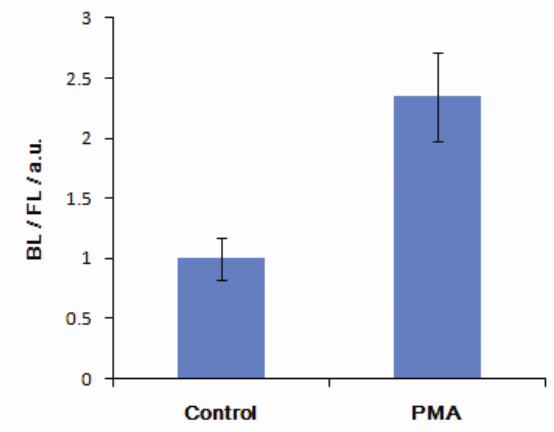

Figure 4. Showing relative bioluminescence and relative bioluminescence/fluorescence (venus) ratio for RAW264 cells transfected with GLucM23-Venus-KDEL and incubated with PMA (3.0 µg / ml) for 1 h. Coel-BeBA was added incubated for 10 min after which total photon count was measured for 10 min. Statistical analysis was performed with a two-tailed Student's *t*-test. *$p < 0.05$, and error bars are ±SEM; n = 4.

Conclusions

A coelenterazine-boronic acid conjugate probe was developed for the selective detection of hydrogen peroxide. In a similar method used to synthesize bGalNoCoel, Coel-BeBA was synthesized with only minor formation of the c-alkylated product (see appendix). It could be established that Coel-BeBA had high specificity for H_2O_2 over other ROS tested. Coel-BeBA, with GLucM23, was able to detect exogenous and endogenous

H_2O_2 in living cells. Thus it was demonstrated that activatable-coelenterazines, in addition to the detection of enzyme activity, can be designed to detect bioactive molecules such as H_2O_2 in living systems. For further improvement it might be appropriate to replace the free boronic acid moiety with a boronate ester. In a recent patent from Promega, detection of H_2O_2 with various D-luciferin-boronic acid and boronate ester derivatives was investigated.[15] It was shown that not only is the reaction between the boronate and H_2O_2 pH-dependent, but also the type of buffer had significant impact on the luminescence output. Interestingly it was also shown that while derivatives containing the free boronic acid had an overall higher luminescence output over the boronate ester derivatives, however, a poorer signal-to-noise profile. Thus similar structure-activity relationships might be observed with coelenterazine-boronate conjugates as well and requires further investigation.

Experimental

Materials and Instruments

General reagents and chemicals were purchased from Sigma-Aldrich Chemical Co. (St. Louse, MO), Tokyo Chemical Industries (Tokyo, Japan), and Wako Pure Chemical (Osaka, Japan) and were used without further purification. Silica gel chromatography was performed using BW-300 (Fuji Silisia Chemical Ltd., Greenville, NC). NMR spectra were recorded on a JEOL JNM-AL400 instrument at 400 MHz for ^{1}H and 100.4 MHz for ^{13}C NMR, using tetramethylsilane as an internal standard. Mass spectra were measured on a Waters LCT-Premier XE mass spectrometer for ESI or on a JEOL JMS-700 for FAB. UV-visible absorbance spectra were measured using a Shimadzu UV1650PC spectrometer. High pressure liquid chromatography (HPLC) analysis was performed with an Inertsil ODS3 column (4.6 × 250 mm, GL Science, Inc. Torrance, CA) using an HPLC system that comprised a pump (PU2080, JASCO) and a detector (MD2010 and FP2020, JASCO). Preparative HPLC was performed with an Inertsil ODS3 column (10.0 × 250 mm)(GL Sciences Inc.) using an HPLC system with a pump (PU-2087, JASCO) and a detector (UV-2075, JASCO). Bioluminescence was measured in 96-optiplate multiwell plates (PerkinElmer Co., Ltd.) using a Wallac ARVO mx / light 1420 Multilabel / Luminescence counter with an auto-injector (PerkinElmer Co., Ltd.) or ImageQuant LAS 4000 mini (GE Healthcare Life Sciences).

In vitro H_2O_2 experiments

To black 96-well plates containing 5 μL Gluc, 180 μL PBS (0.1 M, pH 7.4), 10 μL Coel-BeBA (final concentration 10 μM) was added 5 μL aqueous solution of H_2O_2 (final concentration 0-100 μM). Total luminescence output was recorded for 1 h. The relative luminescence was determined using Image J.

Specificity against other ROS

Fig.10 10 μM Coel-BeBA with various reactive oxygen species (100 μM) and GLuc in 0.1 M PBS (pH 7.4). Total photon count measured over an hour in luminometer. Cat: 0.4 mg / mL catalase. HO* and *t*-BuO* radicals were generated from 1 mM $FeCl_2$ solution and 100 μM H_2O_2 or 100 μM *t*-BuOOH respectively. Solid KO_2 in DMSO (final concentration: 100 μM) was used as a source for O_2^- ; experiments were repeated in triplicate.

Measuring extragenous H_2O_2 in HEK293T cells expressing GLucM23-Venus-KDEL

HEK293T cells grown in Dulbecco's modified Eagle's medium, supplemented with 10% fetal bovine serum, were transfected with pcDNA3-GLucM23-Venus-KDEL and incubated at 37 °C, 5% CO_2 for 24 h. Cells were washed with PBS (0.1 M, pH 7.4), and trypsinized. 2×10^4 cells were suspended in black microplates containing Leibovitz's L15 medium (no phenol red). Coel-BeBA in PBS (final concentration 25 μM) and aqueous solutions of H_2O_2 (0-100 μM) were added. Total luminescence output was recorded for 2 h. The relative luminescence was determined using Image J.

RAW264 with PMA

RAW264 cells were grown in minimum essential medium supplemented with 10% fetal bovine serum and 100 mg / mL non-essential amino acids. Cells were washed with PBS (0.1 M, pH 7.4), trypsinized, and scraped. 1×10^4 cells were suspended in black microplates Leibovitz's L15 medium (no phenol red). Phorbol 12-myristate 13-acetate (PMA)(final concentration 3 μg / μL) in DMSO was added, or DMSO was added and incubated for 1 h (37 °C, 5% CO_2). Coel-BeBA in PBS (final concentration 20 μM) was added and cells were further incubated for 10 min. Venus fluorescence was measured and total luminescence was recorded for 10 min.

Synthesis of Coel-BeBA

4,4,5,5-tetramethyl-2-para-tolyl-1,3,2-dioxaborolane (1)

To a solution of 4-iodotoluene (1 g, 8.06 mmol) in anhydrous THF (10 mL) cooled to -40 C° under an argon atmosphere was added *t*-BuLi (12 mL, 19 mmol). The solution was stirred for 1 h under argon, after which bis(pinacolato)diboron (2.25 g, 8.87 mmol) in anhydrous THF (5 mL). After 3.5 h the reaction was quenched with an aqueous solution of NH_4Cl (20%). The solution was extracted with EtOAc and the combined organic layer was washed with brine, dried over anhydrous Na_2SO_4, and concentrated *in vacuo*. The residue was subjected to silica gel chromatography with EtOAc / Hexane (1:4), yielding **1** (702 mg, 3.2 mmol, 40 %).^{1}H-NMR (400 MHz,$CDCl_3$) δ = 7.70 (d, ^3J = 8.0 Hz, 2H, ArH) 7.18 (d, ^3J = 8.0 Hz, 2H, ArH, b) 2.36 (s, 3H, CH_3) 1.34 (s, 12H, 4 × CH_3). ^{13}C-NMR (100 MHz,$CDCl_3$) δ = 141.30, 134.80, 128.50, 83.60, 24.85, 21.71.

2-(4-bromomethylphenyl)-4,4,5,5-tetramethyl-1,3,2-dioxaborolane (2)

A solution of 4,4,5,5-tetramethyl-2-para-tolyl-1,3,2-dioxaborolane (517 mg, 2.37 mmol), NBS (550 mg, 3.09), and AIBN (19 mg, 0.12 mmol) in anhydrous MeCN (17 mL) was refluxed for 24 h. The reaction mixture was concentrated *in vacuo*, dissolved in EtOAc, filtered and concentrated *in vacuo*. The residue was subjected to a short silica gel plug (5 % EtOAc / Hexane). The combined fractions were combined and concentrated and dried *in vacuo*, yielding **2** as a white powder (488 mg, 1.64 mmol). ^{1}H-NMR (400 MHz, $CDCl_3$) δ = 7.78 (d, ^3J = 8.0 Hz, 2H, ArH) 7.38 (d, ^3J = 8.0 Hz, 2H, ArH) 4.47 (s, 2H, CH_2) 1.33 (s, 12H, 4 × CH_3) ^{13}C-NMR (100 MHz, $CDCl_3$) δ = 140.38, 134.83, 128.03, 125.44, 83.55, 33.04, 24.65.

Coel-BeBA

To a solution of **CTZ(OAc)$_3$** (100 mg, 0.18 mmol) in CH_2Cl_2 (2 mL) was added 1% NH_3 in MeOH (2 mL) at 0 °C under an argon atmosphere. After 75 min the solution was evaporated to dryness and dried *in vacuo*. The dark residue was dissolved in anhydrous DMF and Cs_2CO_3 was added (53 mg, 0.16 mmol). To this solution was added **2** (56 mg, 0.19 mmol) in DMF (1.45 mL) dropwise over 30 min, under argon flush. The reaction was stirred at rt under argon for 24 h. The solution was poured into H_2O and extracted with EtOAc. The organic layer was washed with brine, dried over Na_2SO_4, and concentrated *in vacuo*. The crude residue was dissolved in anhydrous MeOH, cooled in an ice-bath under an argon atmosphere. To this solution was added NaOMe (15 mg, 0.28 mmol) and the solution was stirred at 0 °C for 2 h. Additional NaOMe was added (45 mg, 0.83 mmol) and after 2 h the reaction was quenched with Dowex 50W H^+ resin,

filtered, and concentrated *in vacuo*. The crude residue was dissolved in a solution of MeCN (10 mL) and H_2O (10 mL)(0.1 % formic acid) and stirred at rt for 12 h. The solution was filtered and subjected to preparative reverse-phase HPLC; gradient: 45 to 70 % MeCN (0.1 % formic acid) (0 to 25 min). The combined fractions were lyophilized giving **Coel-BeBA** as a dark sticky red solid (9 mg, 9 % over 4 steps). ^{1}H-NMR (400 MHz, CD_3OD) δ = 7.66 (s, 1H, ArH, a) 7.53-7.38 (m, 6H, ArH) 7.19-7.06 (m, 5H, ArH) 7.06 (d, ^3J = 8.8 Hz, 2H, ArH) 6.76 (d, ^3J = 8.0 Hz, 2H, ArH) 6.66 (d, ^3J = 8.4 Hz, 2H, ArH) 4.86 (s, 2H, CH_2) 4.41 (s, 2H, CH_2) 3.96 (s, 2H, CH_2); ^{13}C-NMR (100 MHz, CD_3OD) δ = 157.14, 154.91, 151.09, 137.19, 133.43, 131.17, 129.12, 128.98, 128.62, 127.57, 127.36, 127.15, 125.75, 114.84, 114.65, 48.00, 37.99, 31.37; ESMS: Calc: 558.2195; found: 558.1752 $[M+H]^+$.

References

(1) Burgoyne, J. R.; Oka, S-I.: Ale-Agha, N.; Eaton, P. *Antioxidants & Redox Signaling*. March 20, **2013**, *18*, 1042-1052.

(2) Gorin, Y.; Block, K. *Clinical Science* **2013**, *125*, 361-382.

(3) Uttara, B.; Singh, A. V.; Zamboni, P.; Mahajan, R. T. *Curr. Neuropharmacol.* **2009**, *7*, 65-74.

(4) Schumacker, P. T. *Cancer Cell* **2006**, *10*, 175-176.

(5) Wittmann, C.; Chockley, P.; Singh, S. K.; Pase, L.; Lieschke, G. J.; Grabher, C. *Adv. Hematology* **2012**, art. No. 541471.

(6) Finkel, T.; Holbrook, N. J. *Nature* **2000**, *408*, 239-247.

(7) (a) Foreman, J.; Demidchik, V.; Bothwell, J. H. F.; Mylona, P.; Miedema, H.; Torres, M. A.; Linstead, P.; Costa, S.; Browniee, C.; Jones, J. D. G.; Davies, J. M.; Dolan, L. *Nature* **2003**, *422*, 442-446. (b) Groeger, G.; Quiney, C.; Cotter, T. G. *Antioxid. Redox Signalling* **2009**, 11, 2655-2671 (c) Lambeth, J. D. *Nat. Rev. Immunol.* **2004**, 4, 181-1.

(8) (a) Schaferling, M.; Grogel, D.B.M.; Schreml, S. *Microchim. Acta* **2011**, 174, 1-18.(b) Lin, V.S.; Dickinson, B.C.; Chang, C.J. *Methods in Enzymology* **2013**, 526, 19-43.(c) Lippert, A. R.; Van De Bittner, G. C.; Chang, C. J. *Acc. Chem. Res.* **2011**, 44, 793-804. (d) Tsien, R. Y. *Nat. Rev. Cell. Biol.* **2003**, 4, SS16-SS21. (e) Meade, T. J.; Aime, S. *Acc. Chem. Res.* **2009**, 42, 821. (f) Hildebrand, S. A.; Weissleder, R. *Curr. Opin. Chem. Biol.* **2010**, 14, 71-79. (g) Ueno, T.; Nagano, T. *Nat. Methods* **2011**, 8, 642-645. (h) Pittet, M. J.; Weissleder, R. *Cell*, **2011**, 147, 983-991. (i) James, M. L.; Gambhir, S. S. *Physiol. Rev.* **2012**, 92, 897-965.

(9) (a) Kuivila, H.G. (1954) J. Am. Chem. Soc. 76 , 870 – 874. (b) Kuivila, H.G. and Armour, A.G. (1957) J. Am. Chem. Soc.79, 5659–5662.

(10) Kalyanaraman, B.; Darley-Usmar, V.; Davies, K. J. A.; Dennery, P. A.; Forman, H. J.; Grisham, M. B.; Mann, G. E.; Moore, K.; Roberts II, L. J.; Ischiropoulos, H. *Free Rad. Biol. Med.* **2012**, *52*, 1-6..

(11) Van de Bittner, G. C.; Dubikovskaya, E. A.; Bertozzi, C. R.; Chang, C. J. *Proc. Natl. Acad. Sci. U.S.A.* **2010**, 107, 21316-21321.

(12) Van de Bittner, G. C.; Bertozzi, C. R.; Chang, C. J. *J. Am. Chem. Soc.* **2013**, 135, 1783-1795.

(13) Czupryna, J.; Tsourkas, A. *PLoS ONE* **2011**, 6, e20073.

(14) (a) Karlsson, A.; Nixon, J. B.; McPhail, L. C. *J. Leukoc. Biol.* **2000**, 67, 396-404; (b) Bellavite, P. *Free Rad. Biol. Med.* **1988**, 4, 225-261.

(15) Klaubert, D.; Shultz, J.; Valley, M. P.; Wang, H.; Zhou, W. Detection of Hydrogen Peroxide. US patent WO2013/025885A1, February 21, 2013.

Conclusions and Perspective

This thesis has described development of cell-impermeable coelenterazine derivatives for monitoring of exocytotic events and the development of activatable coelenterazine derivatives.

In the first chapter I demonstrated that coelenterazine can be modified with a flexible linker, containing a terminal phosphonic acid, by alkylating the phenol in the 2-position of coelenterazine (CoelPhos). CoelPhos showed higher activity with GLuc over RLuc. Despite CoelPhos having lower luminescence output compared to native coelenterazine with GLuc it was possible to visualize membrane bound GLucM23 mutant in HeLa cells with CoelPhos. The derivative CoelPhos also showed low cell-membrane permeability, which was demonstrated in cells expressing ER-localized GLuc. These results indicated that CoelPhos could be potentially used as a bioluminescent tool for the monitoring of exocytotic events in real-time. It should be emphasized that improvements in luminescence output by optimizing the linker composition and length are expected. Thus further exploration of the chemical space is desired. Notwithstanding, employing CCD-cameras with high luminescence sensitivity should also facilitate improvements in the applicability of CoelPhos.

In Chapter 2, I designed and synthesized activatable coelenterazine derivatives for specific detection of enzyme or bioactive small-molecule activity, and stabilization of the coelenterazine substrate. I expected that blocking of the 3-position of the imidazopyrazinone ring would effectively stabilize coelenterazine. In subchapter 2.1 I designed and synthesized two probes, bGalCoel, a β-galactose-coelenterazine hybrid, and bGalNoCoel, a β-galactose-nitrobenzyl-coelenterazine derivative. Both probes showed high stability and specificity however bGalNoCoel greatly outperformed bGalNoCoel in cell assays and I demonstrated that bGalNoCoel could be used to detect enzyme activity in two separate cell populations. I was also able to demonstrate for the first time that coelenterazine readily diffuses out of cells. In subchapter 2.2 I described the design and synthesis of a boronic acid-coelenterazine derivative for the selective detection of hydrogen peroxide in living cells; Coel-BeBA. This probe had adequate sensitivity and selectivity for hydrogen peroxide. In addition I could show that this probe could be used to detect endogenously generated hydrogen peroxide in macrophage cells. Having demonstrated that in both cases, blocking of the 3-position leads to a stabilization of the coelenterazine substrate is seems very straightforward

what the future holds for this type of technology. My concept can easily be expanded to incorporate many other types of enzymes and bioactive small-molecules, especially with the recent availability of coelenterate luciferases which display more glow-type luminescence profiles (GLucM23, NanoLuc). Combining this technology with BRET, protein-fragment complementation assays etc a wide range of applications are possible. Thus I venture that overall my work has helped expanding the bioluminescence toolbox.

Appendix

Modification of the 2- and 3-positions of the imidazopyrazinone ring of coelenterazine

In chapter 2.1 and 2.2 I described the synthesis of bGalNoCoel and CoelBeBA. Both of these compounds were obtained by O-alkylation of the carbonyl at the 3-position of the imidazopyrazinone ring of $CTZ(OAc)_2$. However, I discovered that under certain conditions a certain amount of C-alkylation at the 2-position also took place (Scheme 1). C-alkylation of coelenterazine has not been reported in the literature thus far.

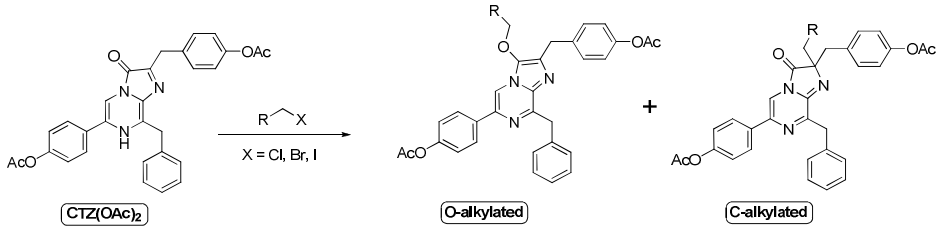

Scheme 1.

This was first observed during the synthesis of bGalNoCoel where a significant amount of the c-alkylated product was also obtained (scheme 2). Attempted deacetylation of Per-OAc-bGalNoCoel(C) with sodium methoxide, lithium hydroxide among others resulted in nucleophilic addition to the 3-carbonyl group.

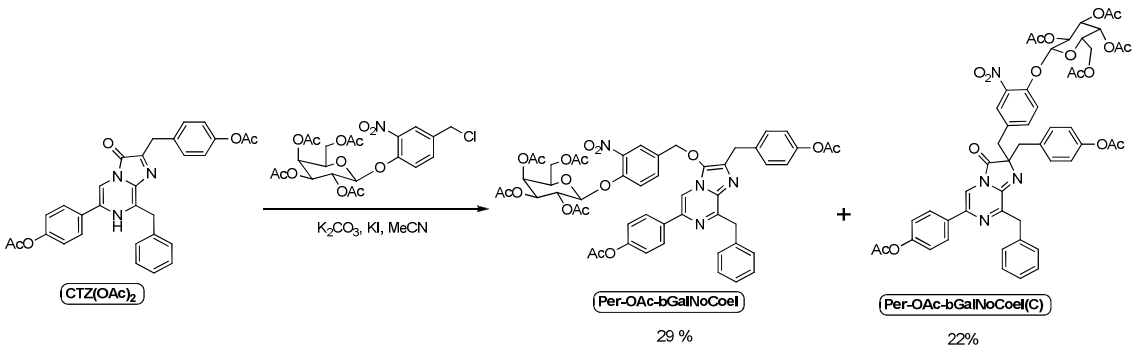

Scheme 2. Showing the relative yields of O- and C-alkylation respectively in the synthesis of bGalNoCoel.

Interestingly in the synthesis of Coel-BeBA O-alkylation was almost exclusively obtained (Chapter 2.2). It is common knowledge that O- and C-alkylation is largely

influenced by reaction conditions such that aprotic solvents, bases with large counter-ions, and hard leaving groups tend to favor O-alkylation whilst conducting reactions with protic solvents, bases with small counter-ions, and soft leaving groups tends to favor C-alkylation.

In another instance I attempted to synthesize a coelenterazine probe, Coel-BePA for the monitoring of alkaline phosphatase (Scheme 3). By changing the conditions as to favor C-alkylation a slightly higher proportion of C-alkylated product (Pro-Coel-BeBA(C)) was observed. Separation of the O- and C- alkylated products is highly difficult with very similar rf values, despite extensive flash silica gel chromatography (Figure 1).

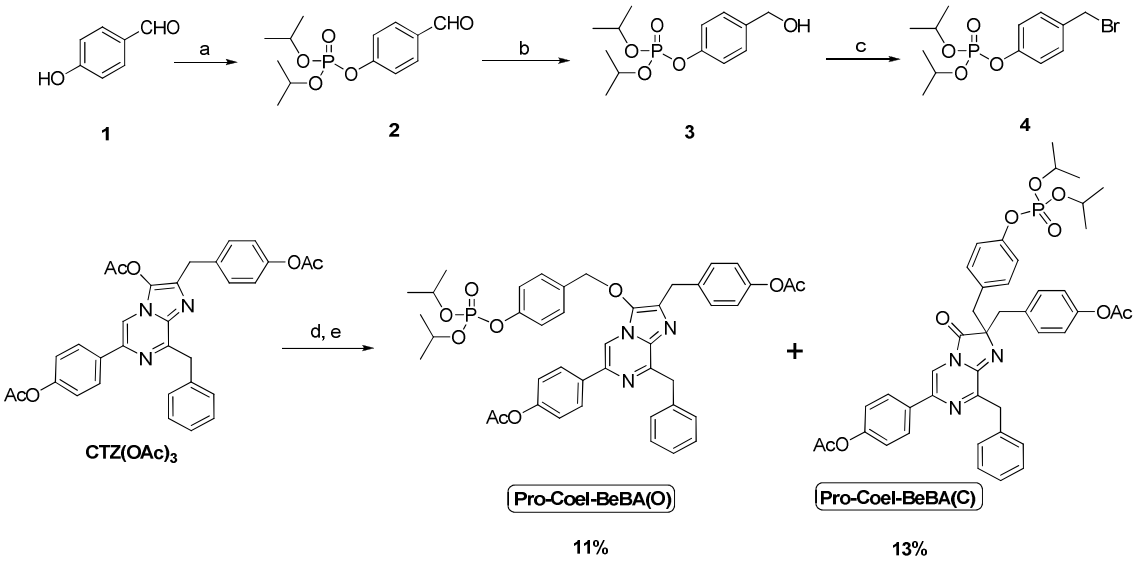

Scheme 3. Synthesis of bGalCoel. a), CBr_4, Et_3N, THF, 80%; b) $NaBH_4$, MeOH, 87%; c) CBr_4, PPh_3, CH_2Cl_2, 90%; d) 1% NH_3 in MeOH / CH_2Cl_2; e) **5**, Na_2CO_3, NaI, THF.

It became clear that the C-alkylated coelenterazines are highly unstable in the presence of base and readily decomposes to coelenterazine, whilst being more stable under acidic conditions. The opposite is true for the O-alkylated coelenterazines. Only one method for selective deprotection of the 3-carbonyl has been reported, selective deacetylation.[1,2] However, in order to obtain C-alkylated coelenterazines it would be more suitable to utilize protecting groups which can easily be cleaved under acidic conditions. This area of research is seriously lacking and needs to be explored further. Although, other substrates such as bisdeoxycoelenterazine (BDC), which does not have any phenolic groups, does not suffer from this problem. Even if deprotected C-alkylated

coelenterazines could be readily obtained, it remains to be seen how stable they are under biological conditions in the presence of natural nucleophiles such as glutathione.

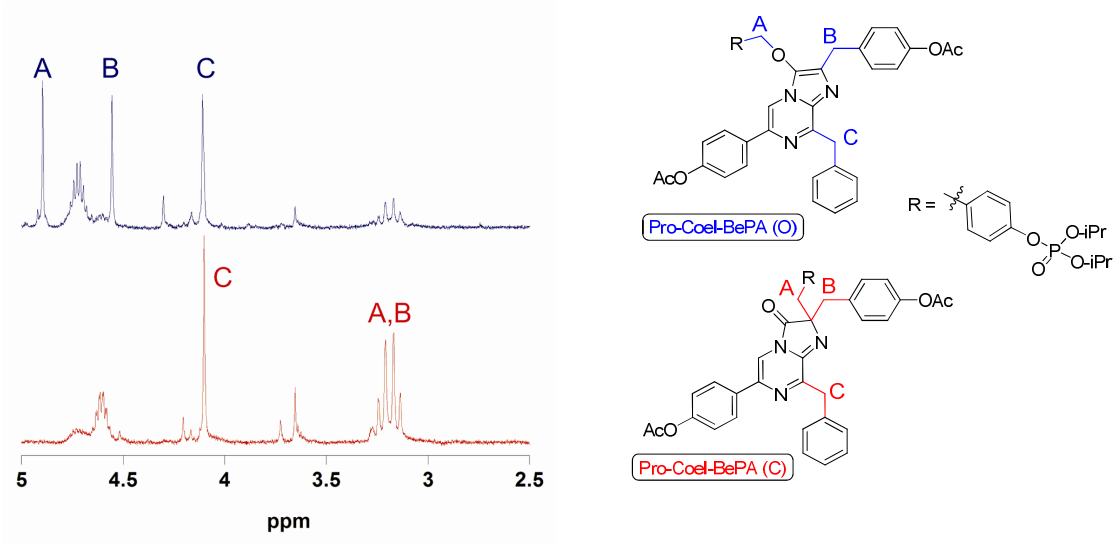

Figure 1. Showing comparison of ^{1}H-NMR of O-alkylated (blue) vs C-alkylated (red)

Experimental

Materials and Instruments

General reagents and chemicals were purchased from Sigma-Aldrich Chemical Co. (St. Louse, MO), Tokyo Chemical Industries (Tokyo, Japan), and Wako Pure Chemical (Osaka, Japan) and were used without further purification. Silica gel chromatography was performed using BW-300 (Fuji Silysia Chemical Ltd., Greenville, NC). NMR spectra were recorded on a JEOL JNM-AL400 instrument at 400 MHz for ^{1}H and 100.4 MHz for ^{13}C NMR, using tetramethylsilane as an internal standard. Mass spectra were measured on a Waters LCT-Premier XE mass spectrometer for ESI or on a JEOL JMS-700 for FAB.

Synthesis

4-formylphenyl diisopropyl phosphate (2)

To an ice-cooled solution of 4-hydroxybenzaldehyde (**1**) (123 mg, 1.01 mmol) and carbon tetrabromide (998 mg, 3.01 mmol) in anhydrous THF (10-11 mL) under an argon atmosphere was added anhydrous Et_3N (0.42 mL, 3.01 mmol), followed by

dropwise addition of diisopropylphosphite (0.33 mL, 1.99 mmol). After 5 min the ice-bath was removed and the reaction was stirred at rt for 24 h. The reaction was quenched with water. The aqueous solution was extracted with EtOAc, washed with brine, dried under Na_2SO_4, filtered, and concentrated *in vacuo*. Purification by flash chromatography (EtOAc / Hexane; 1:1) yielded the desired product (2) as a clear yellow oil (231 mg, 0.81, 80%). ^{1}H-NMR (400 MHz,$CDCl_3$)δ 9.97 (s, 1H, CHO) 7.89 (d, ^3J = 8.0 Hz, 2H, ArH) 7.39 (d, ^3J = 8.0 Hz, 2H, ArH) 4.78 (m, 2H, 2 × CH) 1.38 (d, ^3J = 6.2 Hz, 6H, 2 × CH_3) 1.34 (d, ^3J = 6.2 Hz, 6H, 2 × CH_3); ^{13}C-NMR (100 MHz,$CDCl_3$) δ 190.76, 155.67, 133.02, 131.56, 120.43, 100.54, 73.98, 23.61, 23.56, 23.51, 23.45; ESI-MS: calc: 287.1043; found: 287.1467 $[M+H]^+$.

4-(hydroxymethyl)phenyl diisopropyl phosphate (3)

To an ice-cooled solution of **2** in MeOH (2 mL) was added sodium borohydride (53 mg, 1.40 mmol). After 1 h the reaction mixture was poured into water and extracted with EtOAc, washed with brine, dried under Na_2SO_4, filtered and concentrated and dried *in vacuo*. Purification by flash chromatography gave the desired product **3** as a clear oil (198 mg, 0.69 mmol, 87%). ^{1}H-NMR (400 MHz,$CDCl_3$) δ 7.12 (d, ^3J = 8.0 Hz, 2H, ArH) 6.96 (d, ^3J = 8.0 Hz, 2H, ArH) 4.52 (m, 2H, 2 × CH) 4.38 (s, 2H, CH_2) 1.16 (d, ^3J = 6.0 Hz, 6H, 2 × CH_3) 1.11 (d, ^3J = 6.0 Hz, 6H, 2 × CH_3); ^{13}C-NMR (100 MHz, $CDCl_3$) δ 149.18, 137.74, 127.37, 119.06, 72.82, 62.91, 22.78, 22.73, 22.70, 22.64; ESI-MS: calc: 289.1199; found: 289.1836 $[M+H]^+$

4-(bromomethyl)phenyl diisopropyl phosphate (4)

To an ice-cooled solution of **3** (197 mg, 0.68 mmol) in anhydrous CH_2Cl_2 was added carbon tetrabromide (345 mg, 1.04 mmol) and triphenyl phosphine (284 mg, 1.08 mmol) under argon. The reaction was stirred at rt for 20 h. The reaction mixture was concentrated *in vacuo*. The residue was dissolved in a minimal amount of CH_2Cl_2 and loaded onto a silica gel column. Flash chromatography (EtOAc / Hexane; 1:1) yielded the desired product **4** as a colorless liquid (214 mg, 90%). ^{1}H-NMR (400 MHz,$CDCl_3$) δ 7.35 (d, ^3J = 8.0 Hz, 2H, ArH) 7.19 (d, ^3J = 8.0 Hz, 2H, ArH) 4.73 (m, 2H, 2 × CH) 4.45 (s, 2H, CH_2, d) 1.32-1.24 (m, 12H, 6 × CH_3); ^{13}C-NMR (100 MHz,$CDCl_3$) δ 150.32, 133.96, 130.08, 119.98, 73.23, 32.39, 23.22.

Prot-Coel-BeBA(O)/(C)

To an ice-cooled solution of $CTZ(OAc)_3$ (56 mg, 0.10 mmol) in CH_2Cl_2 (1 mL) under

an argon atmosphere was added 1% NH_3 in MeOH (1 mL) and the solution was stirred for 2.5 h. The reaction mixture was concentrated and dried *in vacuo* and used without further purification. The residue was dissolved in anhydrous THF (5 mL) under an argon atmosphere. To this solution was added Na_2CO_3 (4.5 mg, 0.04) NaI (15 mg, 0.10), and **4** (47 mg, 0.13) in anhydrous THF. The reaction was bubbled with argon gas for 30 min. The reaction was stirred over night at rt. The reaction was diluted with water and extracted with CH_2Cl_2. The organic layer was washed with water, brine, dried under Na_2SO_4, filtered, and concentrated *in vacuo*. Purification via flash chromatography (0 $\rightarrow$ 3% MeOH / CH_2Cl_2) yielded two major products: The O-alkylated product (**6**) (8.6 mg, 0.011 mmol, 11%) and the C-alkylated product (**7**) (9.8 mg, 0.013 mmol, 13%)

Prot-Coel-BeBA(O)

^{1}H-NMR (400 MHz,$CDCl_3$) δ 7.84-7.79 (m, 3H, ArH) 7.56 (d, ^3J = 8.0 Hz, 2H, ArH) 7.33-7.15 (m, 11H, ArH) 7.01 (d, ^3J = 8.0 Hz, 2H, ArH) 4.90 (s, 2H, CH_2) 4.72 (m, 2H, 2xCH) 4.56 (s, 2H, CH_2) 4.11 (s, 2H, CH_2) 2.31 (s, 3H, CH_3CO) 2.27 (s, 3H, CH_3CO) 1.34 (d, ^3J = 6.4 Hz, 6H, 2×CH_3) 1.27 (d, ^3J = 6.4 Hz, 6H, 2×CH_3); ^{13}C-NMR (100 MHz,$CDCl_3$) δ169.42, 169.29, 152.69, 151.59, 151.52, 150.83, 149.18, 137.90, 137.68, 137.07, 136.55, 134.58, 133.14, 132.26, 131.96, 130.05, 129.66, 129.64, 128.17, 127.24, 126.36, 121.84, 121.47, 120.39, 120.35, 108.93, 73.64, 39.31, 32.79, 23.57, 23.52, 23.46, 23.41, 21.08, 21.04. ESIMS: Calc: 779.2961; found: 779.1447 $[M+2H]^+$

List of Publications

1. Full Paper: Development of Luminescent Coelenterazine Derivatives Activatable by β-Galactosidase for Monitoring Dual Gene Expression
   Lindberg, E.; Mizukami, S.; Ibata, K.; Miyawaki, A.; Kikuchi, K.
   Chem. Eur. J. **2013***, in press*

2. Full Paper: Development of Cell-Impermeable Coelenterazine Derivatives
   Lindberg, E.; Mizukami, S.; Ibata, K.; Fukano, T.; Miyawaki, A.; Kikuchi, K.
   Chem. Sci. **2013**, *in press*

3. Communication: Development of Hydrogen Peroxide Activatable Coelenterazine Derivatives
   Lindberg, E.; Mizukami, S.; Kikuchi, K.
   In preparation.

Presentations at International Conferences

1. Poster: Development of Cell-Impermeable Coelenterazine Derivatives
   Lindberg, E.; Mizukami, S.; Kikuchi, K.
   Catalysis and Sensing for Health (CASH 2011) Bath, United Kingdom, February, 2011

2. Poster: Development of Cell-Impermeable Coelenterazine Derivatives
   Lindberg, E.; Mizukami,; Kikuchi, K.
   RIKEN Chemical Biology Symposium "Next Generation Tools for Molecular Target Discovery", Saitama, Japan, 2011

3. Oral: Development of Cell-Impermeable Coelenterazine Derivatives
   Lindberg, E.; Mizukami, S.; Kikuchi, K.
   The 92th Spring Meeting of the Chemical Society of Japan, Kanagawa, Japan, March 2012

Acknowledgements

The author would like to express gratitude to Professor Kazuya Kikuchi for his continuous guidance, support, and encouragement throughout this study. The author expresses his sincere thanks to Dr. Shin Mizukami for his valuable guidance and discussion. The author also expresses his cordial thanks to Dr. Yuichiro Hori for his kind help and useful suggestion.

The author is deeply grateful to Dr. Miyawaki and Dr. Fukano at RIKEN, Saitama and Dr. Ibata at Keio University for their help and support with bioluminescence imaging experiments. Deep thanks also go out to all the members of the Kikuchi laboratory group for their kind help, teaching, and friendship.

The author acknowledges financial support from the Japanese government, MEXT.

Finally, the author appreciates the tremendous support and continuous encouragement from his family and friends.

Osaka, Japan
October, 2013

Eric LINDBERG

Division of Advanced Science and Biotechnology
Department of Material and Life Science
Graduate School of Engineering, Osaka University